PORTABLE MONITORS FOR FLOW INJECTION ANALYSIS WITH POTENTIOMETRIC MULTIPLE ION SENSORS

Telis Dimitrakopoulos
Honours Degree of Bachelor of Science (Monash University, Melbourne, Australia) and
Master of Applied Science (Royal Melbourne Institute of Technology, Melbourne, Australia)

A thesis in fulfilment of the requirements for the Degree of

Doctor of Philosophy in Science

at the

Department of Physical Sciences
School of Science and Technology
University of Tasmania
Launceston Australia

August 1997

"When canoeing against the flow of a stream, one must always paddle harder and harder to propel themselves forward, otherwise you will go backwards and you will never, ever, stay in one single position. Life is no different."

Chung Cheung

To

Lucy Tina Di Benedetto

DECLARATION

I hereby declare that this submission is my own work and that, to the best of my knowledge and belief, it contains no material previously published or written by another person nor material which to a substantial extent has been accepted for the award of any other degree or diploma of a university or other institute of higher learning, except where due acknowledgment is made in the text.

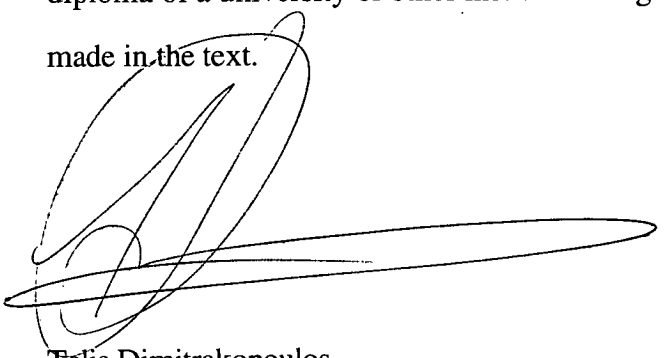

Telis Dimitrakopoulos
Department of Physical Sciences,
University of Tasmania.

25th August, 1997.

This thesis is not to be made available for loan or copying for two years following the date this statement was signed. Following that time the thesis may be made available for loan and limited copying in accordance with the *Copyright Act 1968*.

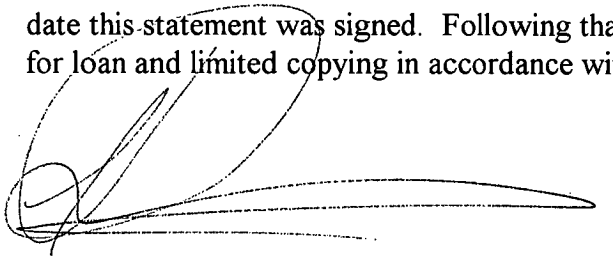

Telis Dimitrakopoulos, 15th July, 1998.

ACKNOWLEDGMENTS

I wish to thank my supervisors Prof. Peter W. Alexander (University of Tasmania) and Prof. D. Brynn Hibbert (University of New South Wales) for their constant encouragement, support and knowledge, and allowing me the freedom to pursue my interests that is presented in this work independently. I wish to thank the Australian Research Council and the University of Tasmania Research Grants Scheme for their financial support for this project and the staff of the Department of Physical Sciences (University of Tasmania) for their friendship, advice and encouragement throughout my candidature.

I would like to thank my entire family in Melbourne for their support and encouragement throughout my life and their unquestionable faith in my abilities. I wish to thank my colleagues, Mr Dusan Losic, Mr Andrew P. Lee and Mrs Fiona G. Beach for their advice, encouragement and friendship. Finally, I extend my warmest gratitude to my fiancee, Ms Lucy Tina Di Benedetto for her overwhelming support, love and encouragement, because without her this work would not have been possible.

SUMMARY

The use of multi-sensing portable monitors is of increasing importance for many applications in modern technology. This thesis reports on the development of a new portable battery-powered flow injection potentiometric (FIP) system suitable for remote-site monitoring that can utilise a range of ion-selective electrodes (ISEs) or arrays of coated-wire electrodes (CWEs) as detectors. A number of different designs were developed and evaluated for a variety of applications.

Portable FIP systems employing: (1) a commercial iodide ISE as a single electrode detector, and (2) a tungsten / tungsten-oxide wire electrode employed as a pH sensor were initially developed. The performance of the iodide electrode exhibited near-Nernstian response over a wide concentration range in the FIP mode. The tungsten / tungsten-oxide electrode exhibited a sub-Nernstian response between the pH range 2 and 11, and was used to determine the pH of various samples in the FIP mode.

Three commercial planar type ISEs (nitrate, potassium and sodium) were arranged in a three-ISE array and used in the portable FIP system. The potassium and sodium ISEs exhibited Nernstian responses, while the nitrate ISE exhibited a near-Nernstian response. The accuracy of the ISE-array was studied and validation of this system was performed with various mineral water samples in the FIP mode.

An eight electrode flow-through cell was developed in a portable FIP system and evaluated in the FIP mode with metallic silver electrodes. These were each anodised with iodide and the responses of the individual electrodes to silver and iodide standard solutions were studied.

Individual photo-cured bisphenol A epoxydiacrylate membrane based CWEs for ammonium, calcium, hydrogen, nitrate and potassium were developed and evaluated using silver wire electrodes in the eight-electrode flow cell described above. Each photo-cured CWE exhibited Nernstian response over a wide concentration range in the steady-state mode and was selective and fast responding taking < 5 seconds to attain 90% of the steady-state value, making them ideal for a multi-CWE arrangement in FIP. These photo-cured CWEs were successfully used to determine the respective ions in various water samples.

Three multi-CWE arrangements employing the photo-cured membranes mentioned above have been investigated in the FIP mode; namely (1) a two sensor array consisting of ammonium and hydrogen CWEs; (2) a four sensor array consisting of calcium, nitrate, potassium CWEs and a Ag/AgCl wire electrode; and (3) a six sensor array consisting of ammonium, calcium, hydrogen, nitrate and potassium CWEs and a Ag/AgCl wire electrode. The multi-CWE arrangements were used to measure the respective ions simultaneously in various water samples in the FIP mode.

LIST OF PUBLICATIONS

Refereed Journal Publications:

1) T. Dimitrakopoulos, P. W. Alexander, D. B. Hibbert, L. Cherkson and J. Morgan, 'A Portable Flow Injection Analyser for use with Ion-Selective Electrodes', Electroanalysis 7, 1118 - 1120, (1995).

2) T. Dimitrakopoulos, P. W. Alexander and D. B. Hibbert, 'Serial Array of ISEs for use in a Portable Battery-Powered Flow Injection Analyser', Electroanalysis 8, 438 - 442, (1996).

3) P. W. Alexander, L. T. Di Benedetto, T. Dimitrakopoulos, D. B. Hibbert, J. C. Nglia, M. Sequeira and D. Sheils, 'Field-Portable Analysers for Monitoring of Air and Water Pollution', Talanta 43, 915 - 925, (1996).

4) P. W. Alexander, T. Dimitrakopoulos and D. B. Hibbert, 'Operational Assessment of a Potentiometric Eight-Sensor Flow cell in a Portable Flow Injection Analyser', Field Analytical Chemistry and Technology 1, 31-37, (1996).

5) P. W. Alexander, T. Dimitrakopoulos and D. B. Hibbert, 'A Photo-Cured Coated-wire Calcium Ion-Selective Electrode for use in Flow Injection Potentiometry', Talanta 44, 1397 - 1405, (1997).

6) P. W. Alexander, T. Dimitrakopoulos and D. B. Hibbert, 'A Photo-Cured Coated-wire Potassium Ion-Selective Electrode for use in Flow Injection Potentiometry', Electroanalysis, in press, (1997).

7) P. W. Alexander, T. Dimitrakopoulos and D. B. Hibbert, 'Photo-cured Ammonium and pH Coated-wire Selective Electrodes used Simultaneously in a Portable Battery-powered Flow Injection Analyser', Electroanalysis, in press, (1997).

8) P. W. Alexander, T. Dimitrakopoulos and D. B. Hibbert, 'Photo-Cured Six-ion Coated-wire Selective Electrode Array used in a Portable Battery-powered Flow Injection Analyser', in preparation.

Conference Publications:

Poster Presentations:

1) T. Dimitrakopoulos, P. W. Alexander, D. B. Hibbert, L. Cherkson and J. Morgan, "A Portable Flow Injection Analyser for use with Ion-Selective Electrodes", 13th Australian Analytical / 4th Environmental Conference Proceedings, Darwin, 1995.

2) P. W. Alexander, T. Dimitrakopoulos and D. B. Hibbert, "A Metallic Tungsten Sensor for On-line Monitoring of pH in a Portable Flow Injection Analyser" to be presented at the 14th Australian Symposium on Analytical Chemistry" to be held in Adelaide, July 1997.

Oral Presentations:

1) P. W. Alexander, L. T. Di Benedetto, T. Dimitrakopoulos, D. B. Hibbert, J. C. Nglia, M. Sequeira and D. Sheils, "Field-Portable Analysers for Monitoring of Air and Water Pollution", 7th International Flow Injection Analysis Conference (ICFIA '95), Seattle, WA, USA, August 1995.

2) T. Dimitrakopoulos, P. W. Alexander and D. B. Hibbert, "Ion-Sensor Array for use in a Portable Flow Injection Analyser", International Chemical Congress of Pacific Basin Societies Conference (PACIFICHEM) Proceedings, Honolulu, 1995.

TABLE OF CONTENTS

Chapter Five: Evaluation and Performance of Various Photo-cured Bisphenol A Epoxydiacrylate based Membrane CWEs.

Chapter One: General Introduction.

1.1 Ion-selective Electrodes (ISEs)

The aim of the work presented in this thesis was to develop and evaluate a portable battery-powered flow injection potentiometric (FIP) system suitable for remote-site monitoring. The portable FIP system developed in this study will employ a range of individual ion-selective electrodes (ISEs) and multi-sensor arrays to determine the feasibility of the system.

An ISE is an electrochemical device that responds directly to changes in ionic activity of a chemical species in solution, where the response is a reversible one. ISEs employ sensing membranes that are selective to particular ions. There are a variety of membrane types for ISEs, which generally fall into three categories: 1) solid (fixed ion-exchange sites) membranes, 2) liquid polymer (mobile ion-exchange sites) membranes and 3) sensitised membranes.

Solid membranes consist of fixed ion-exchange sites that can be either homogeneous or heterogeneous. A homogeneous membrane can be considered as a single crystalline substance or a mixture of substances in one phase. Examples include a crystalline material such as LaF_3 for a fluoride ISE [1] and pressed $Ag_2S/AgCl$ pellets for a chloride ISE [2]. A heterogeneous membrane contains an insoluble crystalline substance dispersed in an inert polymer matrix such as poly(vinyl chloride) (PVC) [3] or silicone rubber [4]. Examples of heterogeneous membranes are AgCl, AgBr and AgI salts dispersed in silicone rubber for chloride, bromide and iodide ISEs, respectively [4].

Liquid polymer membranes contain mobile ion-exchange sites. The polymer base, typically PVC, is required to support the solvent mediator or plasticiser and the electrically charged or neutral electroactive sensor reagent (ionophore) [5,6]. An ion-exchange process occurs between the ionophore in the membrane phase and the determinand in the aqueous phase. The primary role of the plasticiser is to create the ideal environment to facilitate the ion-exchange process.

Sensitised membrane based ISEs include gas-sensing electrodes and biosensors. An example of a simple gas-sensing electrode sensitive to dissolved NH_3 in aquoeus solutions was reported using a glass pH electrode that used dilute ammonium chloride as the internal reference

solution [7]. The detection of the ammonia gas is based on the equilibrium between ammonia and ammonium as follows:

$$NH_3 + H^+ \rightleftharpoons NH_4^+$$

One of the original potentiometric biosensors [8] developed in the early 1970s consisted of coating a Beckman monovalent cationic glass electrode with an enzyme and the resulting ISE responded to the ionic product of the enzymatic reaction. Intially this concept was used to develop an electrode for the determination of amino acids, whereby a coating of L-amino acid oxidase was placed over the glass surface of a monovalent cation glass electrode [8]. This potentiometric biosensor monitors the formation of ammonium ions via the decompositon of the amino acid, which is proportional to the amino acid concentration in the solution.

The electrochemical response of ISEs in a typical electrochemical cell (refer to Figure 1.1) is described by a Nernst type equation (1.1) at 25 °C,

$$E = E' + 59.2/z_i \log_{10}(a_i) \qquad - (1.1)$$

where E = measured potential (mV),

E' = sum of potentials in the electrochemical cell,

z_i = charge of ion i, and

a_i = activity of ion i.

The E' in the above equation (1.1) is a constant potential for a given electrochemical cell illustrated in Figure 1.1, using a conventional configuration ISE (refer to Section 1.2). The components that contribute to E' are the potentials between the ISE's internal electrolyte and the ISE's inner membrane and reference electrode, the potential between the reference electrode and the test solution, and the liquid junction potential created between the reference electrode's internal electrolyte and the test solution.

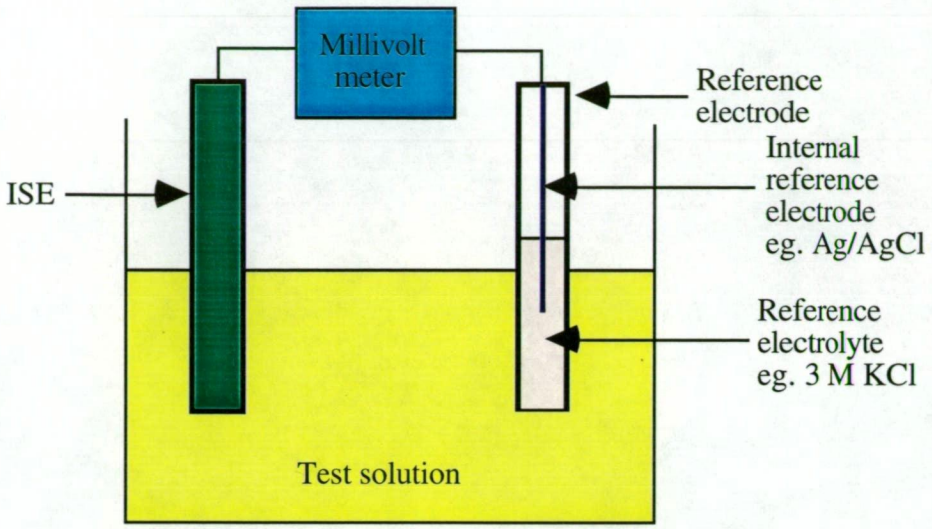

Figure 1.1. A typical electrochemical cell.

The Nernst type equation (1.1) indicates a log-linear response, and a plot of E versus $\log_{10}(a_i)$ will result in a line of slope $59.2/z_i$ mV change per activity decade and a vertical intercept of E'. This slope is referred to as the Nernstian response of an ISE. However, the Nernst equation is inappropriate for measurements of the determinand in a complex matrix containing interfering ions, since interfering (competing) ions will contribute to the measured potential, E. A modification of the Nernst equation (1.1) that allows for the effect of interfering ions is known as the Nicolsky equation (1.2) [9-11],

$$E = E' + 59.2/z_i \log_{10} [a_i + \Sigma k_{ij} \ (a_j)^{z_i/z_j}] \qquad - (1.2)$$

where E, E', z_i and a_i are as defined previously,

k_{ij} = selectivity coefficient for ion i over ion j,

a_j = activity of ion j, and

z_j = charge of ion j.

The consideration of k_{ij} and a_j in the Nicolsky equation (1.2) allows for any contribution to the measured potential, E, of interfering ions present in the test solution.

1.2 Design of Ion-selective Electrodes (ISEs)

There are two types of electrode designs that are generally employed as illustrated in Figure 1.2 and are referred to as 1) conventional and 2) solid-contact design electrodes.

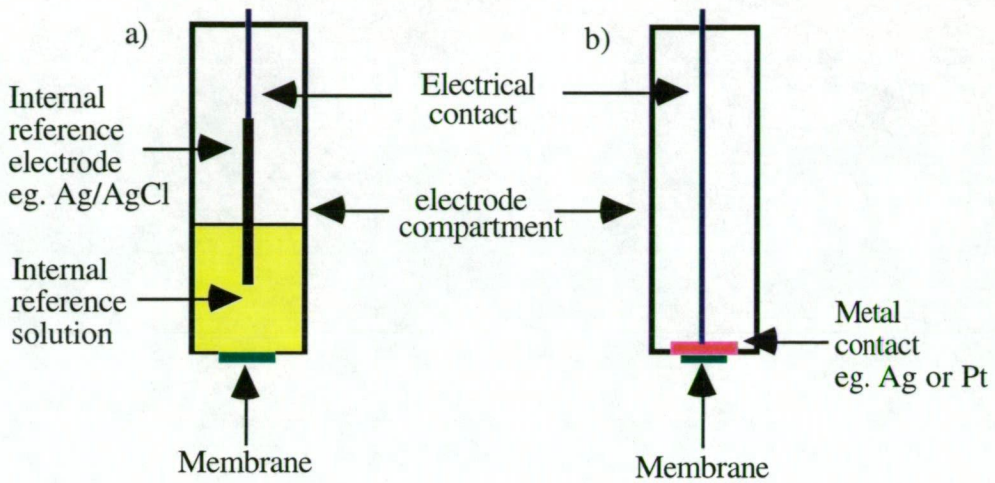

Figure 1.2. a) Conventional and b) Solid-contact design electrodes.

1.2.1 The Conventional Design of ISEs

The conventional design is the traditional electrode assembly that is used in potentiometric measurements. This design contains an internal reference electrode and solution. The internal solution contains a fixed concentration of the determinand, to maintain a constant potential between the internal reference electrode and the inner membrane surface of the ISE. For example, within calcium and potassium ISEs, the internal solutions employed would be 100 mM $CaCl_2$ and 100 mM KCl, respectively. A potential is created when the outer membrane encounters the test solution. According to the Nicolsky equation (1.2), a change in ionic activity (a_i) in the test solution will change the measured potential, E [7,9-11]. A typical conventional cell arrangement for potentiometric measurements using this electrode design is:

Internal reference electrode	Internal reference solution	Ion-selective membrane	Sample solution	External reference electrode

1.2.2 The Solid-contact Design of ISEs

Unlike the conventional design electrode, the solid-contact design does not employ an internal reference electrode and solution. A typical solid-contact electrode cell arrangement is:

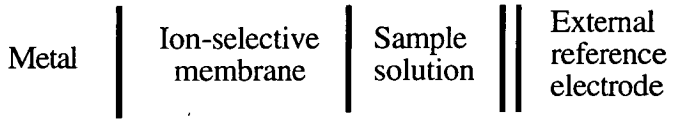

The need to produce both cheaper and miniaturised ISEs has led to the development of the 'coated wire electrode' (CWE) [12-15]. CWEs consist of a liquid polymer membrane that is deposited directly onto a metal wire, such as silver or platinum [12-15] and numerous cation and anion, organic and inorganic CWEs have been studied [12-15].

The solid-contact design has economical advantages over the conventional design relating to the ease of manufacture and miniaturisation [15]. The possibility of the manufacture of microelectrodes (eg 1 to 10 μm diameter) without the added complexity of an internal reference electrode and solution, makes this electrode configuration far more attractive. Microelectrodes are chiefly used for potentiometric measurements in individual cells and intracellular samples [16].

The major disadvantage about liquid polymer membrane based CWEs are that they are renowned for exhibiting electrode drift [15]. It has been suggested that the membrane composition will depend on the extraction constants of the determinand and the interfering (competing) ions present in the sample. The measured potential also depends on the mole fraction of the ionophore in the membrane and any process that alters this, such as water uptake, will change the concentration of the ionophore and lead to an electrode potential drift [15].

An alternative to the CWEs in terms of solid-contact are the ion-selective field effect transistors (ISFETs) [17-21]. The ISFET is simply a selective liquid polymer membrane that is combined with a metal-oxide semiconducting field-effect transistor. A change in ionic activity of the test solution generates an electrical field in the insulating layer, and influences a current flow between the source and the drain [7]. Consequently, the measured drain current is a function of the activity of the determinand [7].

1.3 Liquid Polymer Membrane based ISEs

The development of a reliable calcium ISE based on a liquid polymer membrane was first reported in 1967 [5]. This membrane contained calcium didecyl phosphate as the electrically charged ionophore dissolved in di-n-octyl phenylphosphonate, and this mixture was supported by a cellulose ester filter disc. The electrode design was later improved, becoming the Orion 92-20 model, the first liquid membrane based ISE to be commercially available.

The success of the Orion 92-20 model ISE led to the development of a variety of liquid membrane based ISEs that are selective to metal cations, anions, organic ions and inorganic complexes. A major limitation with the first liquid membranes ISEs was the short operational life-time of one to two weeks. In a different study, PVC was used as an inert polymer matrix to support the electrically charged ionophore and the plasticiser in a liquid polymer membrane based calcium ISE and the operational lifetime was reported to be 18 months [6]. The success of this study, resulted in the popular use of the PVC polymer in commercially available liquid polymer membrane based ISEs.

Components that are necessary for a liquid polymer membrane are: 1) the polymer base, 2) the plasticiser, 3) the ionophore and 4) lipophilic additives. These will be considered individually in the following subsections.

1.3.1 Polymer-based Matrix

The primary role of the polymer base is to support the plasticiser, the ionophore and the lipophilic additives within the membrane. For a polymer base to be useful in a liquid polymer membrane, it needs to be mechanically and chemically stable, be absent of any charged or coordinating sites that may compete with the ion-exchange process between the determinand and the ionophore, and be compatible with respect to the plasticiser and the ionophore [16].

Various polymer bases have been applied to liquid polymer membranes with a varying degree of success. The popular polymer base is PVC, and is employed in most of the commercially available liquid membranes [22]. Other polymer bases that have been used are silicone rubber [23,24], copolymers of poly(bisphenol-A-carbonate) and poly

(dimethyl)siloxane [25], poly(butyl methacrylate) [26], polyurethane [27,28] and poly(decyl methacrylate) [29].

1.3.2 Plasticisers

Plasticisers have two main functions in a liquid membrane. Firstly, the plasticiser is required to lower the glass-transition temperature (Tg) of the polymer, thereby allowing the ionophore mobility within the membrane phase [7,22]. Secondly, the plasticiser needs to create an ideal environment if the ion-exchange process between the ionophore and the determinand is to occur [2,30]. As a result, the selectivity of a liquid membrane based ISE is partly governed by the plasticiser used in some cases and the sensitivity of a liquid membrane based ISE can be affected by the choice of plasticiser [7,31].

A plasticiser must possess certain chemical characteristics for it to be suitable in liquid polymer membranes and they include high lipophilicity, solubility that is compatible with the ionophore and the lipophilic additives, moderate to high viscosity, absent of functional groups that can be either protonated or deprotonated, and chemically inert [32,33]. Examples of the more successful plasticisers used for anion and cation ISEs are chlorobenzene [7], nitrobenzene [7], o-nitrophenyl octyl ether [16], tris(2-ethylhexyl) phosphate [16] dibutyl sebacate [16] and bis(2-ethylhexyl) sebacate [16].

Generally, polar plasticisers such as o-nitrophenyl octyl ether (dielectric constant (ε) = 24.2) are employed in membranes of divalent cation ISEs (eg Ca^{2+}), to increase primary ion selectivity over monovalent cations of similar size (eg Na^{+}), while non-polar plasticisers (eg dibutyl sebacate, $\varepsilon = 4.5$) are used in membranes of monovalent cation ISEs [7]. However, a number of studies have been undertaken with liquid membrane based monovalent cation ISEs that have employed polar plasticisers, such as o-nitrophenyl octyl ether, to improve the ISE's selectivity over interfering monovalent cations [7,31]. As a consequence, the selectivity over some divalent cations was impaired [7]. Liquid membrane based anion ISEs tend to employ polar plasticisers [7].

1.3.3 Classification of Ionophores

There are several types of ionophores that are available for liquid membrane based ISEs. The classification of anion and cation selective ionophores can be subdivided as follows:

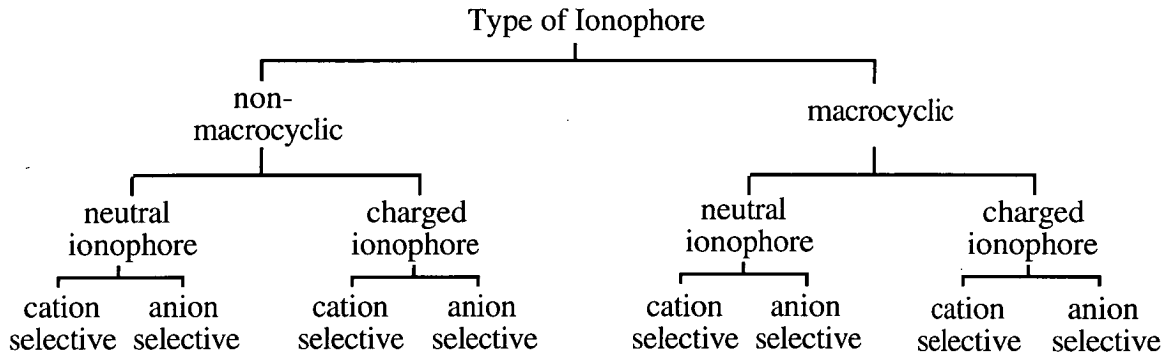

The macrocyclic based ionophores take the form of naturally occurring crown ethers and antibiotics and are found in biological membrane systems [7,16], although there has been considerable work on the synthesis of crown ethers [34]. These ligands are usually electrically neutral and form a stable lipophilic ion-ligand complex within the membrane phase. There are also examples of negatively charged macrocyclic ionophores that have been used in liquid membranes based alkali cation ISEs [16]. Examples of different types of ionophores are presented in Figure 1.3.

The non-macrocyclic ionophores are generally synthetic and are preferred in liquid membranes since they are capable of fast ion-exchange. There are many non-macrocyclic based ionophores for cation selectivity, but they are limited for anion selectivity. The non-macrocyclic ionophores are relatively small in molecular mass, can exhibit excellent selectivity towards their determinand, and are capable of fast ion-exchange. These ionophores imitate the behaviour of naturally occurring ionophores in biological membrane systems. Generally, electrically neutral ionophores are common for cation selectivity [16], although there has also been some success with electrically neutral ionophores for anion selectivity [35-37]. Electrically charged ionophores are plentiful for both anion and cation selectivity and have been widely reported [7].

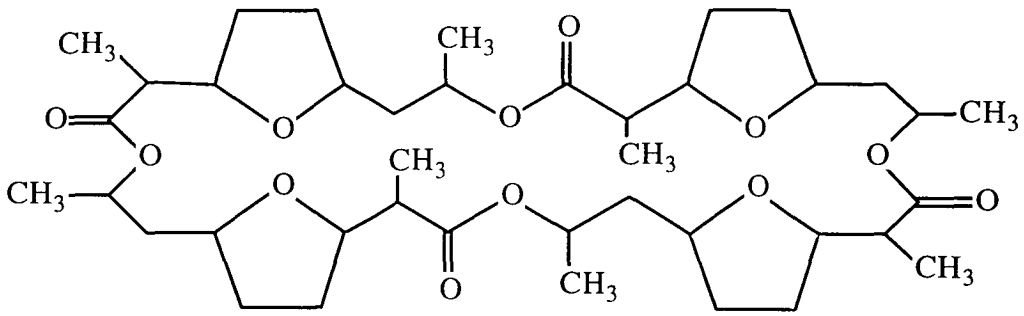

Nonactin

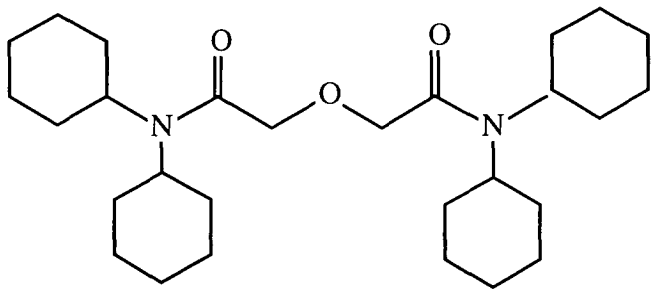

N,N,N',N'-Tetracyclohexyl-3-oxapentanediamide (ETH 129)

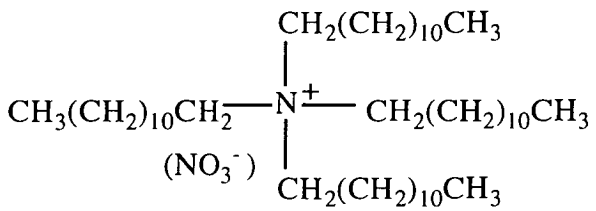

Tetradodecylammonium nitrate

Figure 1.3. A macrocyclic (Nonactin) and non-macrocyclic (ETH 129) as example of electrically neutral ionophore and tetradodecylammonium nitrate as an example of an electrically charged ionophore.

Electrically charged ionophores are generally the determinand salts of hydrophobic organic ions [15] as shown in Figure 1.3. An ion-exchange process occurs between the organic ion (S^-) in the membrane phase and the determinand in the aqueous phase, forming an ion pair association at the aqueous / membrane interface. This ion-exchange behaviour is dependent upon the distribution coefficients of the organic ion and the determinand between the aqueous and membrane phases. A schematic diagram demonstrating the ion pair association at the aqueous / membrane interface for a cation selective liquid membrane is presented in Figure 1.4, whereby BS is the electrically charged ionophore, B'^+ is the determinand.

$$BS_{(membrane)} + B'^{+}_{(aq)} \rightleftharpoons B'S_{(membrane)} + B^{+}_{(aq)}$$

Figure 1.4. Ion-pair association at the membrane-aqueous interface [7].

Electrically neutral ionophores are more common for cation selectivity and are popular with commercially based cation selective electrodes. Generally, electrically neutral ionophores are synthetically made and they form a lipophilic ion-ligand complex that is electrically charged in the membrane phase. A schematic diagram demonstrating this process is presented in Figure 1.5, in Section 1.3.4.

The electrically neutral ionophores require certain characteristics for them to be useful in liquid polymer membranes and they include lipophilicity of both the ionophore and the complex formed in the membrane phase, adequate mobility of the ligand and the ion-ligand complex within the membrane phase, there should be polar and non-polar groups for the coordination site and lipophilic shell respectively, and the ionophore must be flexible to allow for fast exchange between the ion and the ligand [16,38].

As mentioned above, ionophores are mobile in liquid polymer membranes, and the ion-exchange process between the ionophore and the determinand occurs at the membrane / aqueous interface. Therefore, a high concentration of the mobile ionophore is required in the membrane phase of an ISE [7]. In theory, if an intermediate concentration of the mobile ionophore is present in the membrane phase of an ISE, then an equal response between anions

and cations is expected [7]. A low concentration of the mobile ionophore in the membrane phase, would lead to an ISE responding to ions opposite in electrical charge to the determinand.

1.3.4 Lipophilic Additives

When a neutral ionophore coordinates with a metal ion, an overall positive charge is created within the membrane phase. It is important to counterbalance this charge or else the overall positive charge across the membrane will electrostatically attract lipophilic sample anions into the membrane. As a result, a lipophilic sample anion, such as perchlorate, can contribute to the measured potential and lead to non-idealistic electromotive force behaviour of a liquid membrane based ISE [39]. However, this can be overcome by introducing lipophilic additives into liquid membranes.

Lipophilic additives such as sodium tetraphenylborate and potassium tetrakis(p-chlorophenyl) borate are commonly used as ion-balancing reagents, to suppress the interference of sample anions on cation ISEs that are based on electrically neutral ionophores [39]. The bulky tetraphenylborate anion forms anionic sites that overcome the electrostatic attraction of sample anions, and act as an ion-balancing reagent in the membrane once the ligand exchange process occurs [40] as illustrated in Figure 1.5. Additional improvements reported in liquid membrane based ISEs using lipophilic additives are significant selectivity enhancements [41], reduced electrode response time [42] and lower electrical membrane resistance [43].

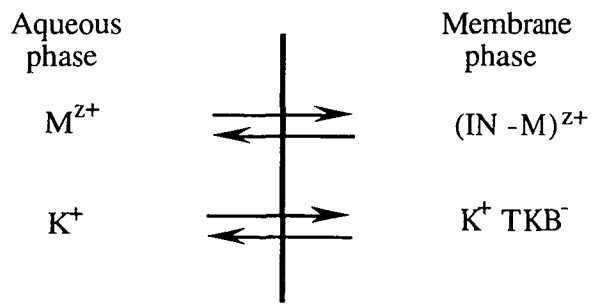

Figure 1.5. Membrane response between a metal ion (M^{z+}) and an electrically neutral ionophore (IN) and the mechanism using potassium tetrakis(p-chlorophenyl) borate (K^+TKB^-) acting as an ion-balancing reagent [40].

1.4 PVC based Liquid Polymer Membranes for ISEs

PVC has been universally accepted as the preferred polymer base for liquid membranes. ISEs that are commercially available are generally PVC based membranes, and Orion Research has a considerable number of commercial cation and anion ISEs available.

As discussed earlier, the PVC based membrane is required to be plasticized to lower the polymer's glass-transition temperature. Generally, the optimum membrane composition is 30% wt/wt PVC base, and 70% wt/wt plasticiser mixture [22]. The plasticiser mixture includes both the ionophore and the lipophilic additive. Usually, the ionophore and the lipophilic additive represent between 1% to 2% wt/wt and 0.1% to 0.5% wt/wt, respectively, of the total membrane composition.

A volatile solvent such as tetrahydrofuran (THF) is used to dissolve the entire membrane composition into a single phase. Drops of this mixture are cast onto a glass plate for a conventional design or directly onto a solid-contact electrode, and allowed to air dry for up to two days to evaporate the THF. This results in a durable and flexible membrane with the ionophore component trapped in a PVC matrix [6]. A major limitation of the PVC membrane is poor adhesion to metallic substrates [26]. This could present a problem with continuous on-line monitoring in terms of the reliability of PVC membrane based ISEs.

1.5 Photopolymerisation of Liquid Polymer Membranes for ISEs.

A novel method for the rapid development of a liquid polymer membrane that is more robust and reliable than the PVC based one has been reported [44-53]. This process involved photo-curing membranes for up to 40 minutes using a low intensity UV mercury vapour lamp. The membrane compositions of these photo-cured membranes were usually 70% wt/wt polymer base and 30% wt/wt plasticiser mixture. The plasticiser mixture contained both the ionophore and the lipophilic additive, which usually contribute between 2% to 6% wt/wt and 0.1% to 0.5% wt/wt, respectively, of the total membrane composition.

The polymer base used in these photo-cured membranes was a 2:1 ratio of bisphenol A epoxy diacrylate, Ebecryl 600 (a copolymer of an epoxy resin and an acrylic acid) and a cross linking acrylate ester, 1,6-hexanedioldiacrylate. The cross linking acrylate behaves as an internal plasticiser, lowering the glass transition temperature of the photo-cured liquid

membrane. As a result, a reduced amount of plasticiser is required in a photo-cured membrane compared to a PVC membrane. In addition, a copolymerisable benzophenone photoinitiator was also required in the photo-cured membrane, in order to initiate the photopolymerisation process and become part of the supporting polymer base. Membranes formed with this technique were more robust and hydrophobic than PVC membranes. Other advantages were good sensitivity, fast response and excellent adhesion to metallic substrates, making photo-cured membranes ideal for flow injection potentiometry (refer to Section 1.6.1) measurements. Photo-cured membrane based ISEs developed at present include calcium [44-47], potassium [48,49], pH [50], nitrate [51], sodium [52] and lithium [53]. Most of these were utilised in the FIP mode.

The major disadvantage with some of the above-mentioned photo-cured membranes, in particular the calcium-selective electrode, was their inability to employ 2-nitrophenyl octyl ether as the plasticiser. Plasticisers of a high dielectric constant, such as 2-nitrophenyl octyl ether (ε = 24.2), are preferred for divalent-selective electrodes since they improve the determinand selectivity over monovalent ions [7]. The nitro group is known to inhibit the photopolymerisation process by acting as a free radical scavenger when using the benzophenone type of photoinitiator [45,49]. However, this can be overcome by introducing a small drop of the 2-nitrophenyl octyl ether plasticiser onto the surface of the photo-cured membrane and allowing it to permeate the membrane [45,52,53]. This procedure improves the response and the selectivity of photo-cured membrane based ISEs, however, there is no control of the amount of plasticiser introduced into the photo-cured membrane.

Recently, there has been a report of a photo-cured nitrate ISE that employed 2-nitrophenyl octyl ether plasticiser in the pre-cured mixture, thereby controlling the amount of plasticiser in the membrane [51]. In this case, photo-curing was made possible by the use of a photoinitiator mixture that contained diaryliodonium chloride and 9,10-phenanthrenequinone in place of the benzophenone initiator, and the photo-curing process was completed in 1 min. This membrane was photo-cured on to a solid-contact electrode and was also photolithographically attached to an ISFET.

1.6 Potentiometric Steady-state Measurements with ISEs

Potentiometric steady-state measurements with ISEs are analytically cumbersome and time consuming. In this mode, it is important for ISEs to achieve complete steady-state in solution in order to develop a reliable calibration curve. A typical ISE is capable of sustaining complete steady-state within 10 minutes at concentrations greater than 1 mM. However, if measurements are required at lower concentrations (< 0.01 mM), then complete steady-state can take between 15 and 30 minutes. Therefore, it becomes time consuming to perform multiple potentiometric measurements and as a result precise data is impractical to obtain with ISEs in the steady-state mode.

1.6.1 Liquid Junction Potentials

Liquid junction potentials occur at the liquid interface between the test and internal reference solution in a typical potentiometric measurement, and can be calculated according to the Henderson equation (1.3) [54].

$$Ej = \frac{RT}{F}\frac{(U_1 - V_1) - (U_2 - V_2)}{(U_1' + V_1') - (U_2' + V_2')} \ln\left(\frac{U_1' + V_1'}{U_2' + V_2'}\right) \qquad -(1.3)$$

where $U = \Sigma\, c_+ \lambda_+$, $V = \Sigma\, c_- \lambda_-$, $U' = \Sigma\, c_+ \lambda_+ |z|$ and $V' = \Sigma\, c_- \lambda_- |z|$

The c_+ and c_- refer to the concentration (mol/L) and λ_+ and λ_- (S cm^2 mol^{-1}) refer to the limiting equivalent conductivity of the cations and the anions, respectively.

The magnitude of the liquid junction potential depends upon the activity and the mobility of the ions present in an electrochemical cell. The presence of a liquid junction potential in an electrochemical cell will introduce uncertainties into the measured potential, E [54]. Therefore, it is desirable to minimise the contribution of the liquid junction potential in a potentiometric measurement and reduce the uncertainty in the measured potential.

To minimise the contribution of liquid junction potential in potentiometric measurements, the following conditions are recommended in the literature:

1) the concentration of the electrolyte background in a given test solution should be higher than the determinand ion [54],

2) the electrolyte background and the internal reference solution should both contain anions and cations of similar mobility [54], and

3) if the activity of an ion, such as the chloride, is kept constant in the test solution, then a second ISE, in this case a chloride ISE, can be employed as a reference electrode, thereby eliminating the liquid junction potential [45,48,55].

1.6.2 Flow Injection Analysis (FIA) with ISEs

FIA is a micro-analysis sampling technique based on the injection of a liquid sample into a moving non-segmented carrier stream [55]. A detector continually monitors the carrier stream and once the injected sample enters the flow cell, an analytical signal is produced that results in a FIA peak.

The combination of FIA with ISEs, or flow injection potentiometry (FIP), reduces the analysis time of potentiometric steady-state measurements as demonstrated in Figure 1.6. A FIP peak can be achieved in less than 30 seconds, so rapid measurements (> 120 injections/hour) and excellent peak height precision (RSD < 3%) are easily achieved. This is accomplished when the flow rate remains constant, allowing for a reproducible transport of the sample zone to the sensing membrane of the ISE. In a well-designed FIP system, the electrode response can be between 80 to 95% of complete steady-state.

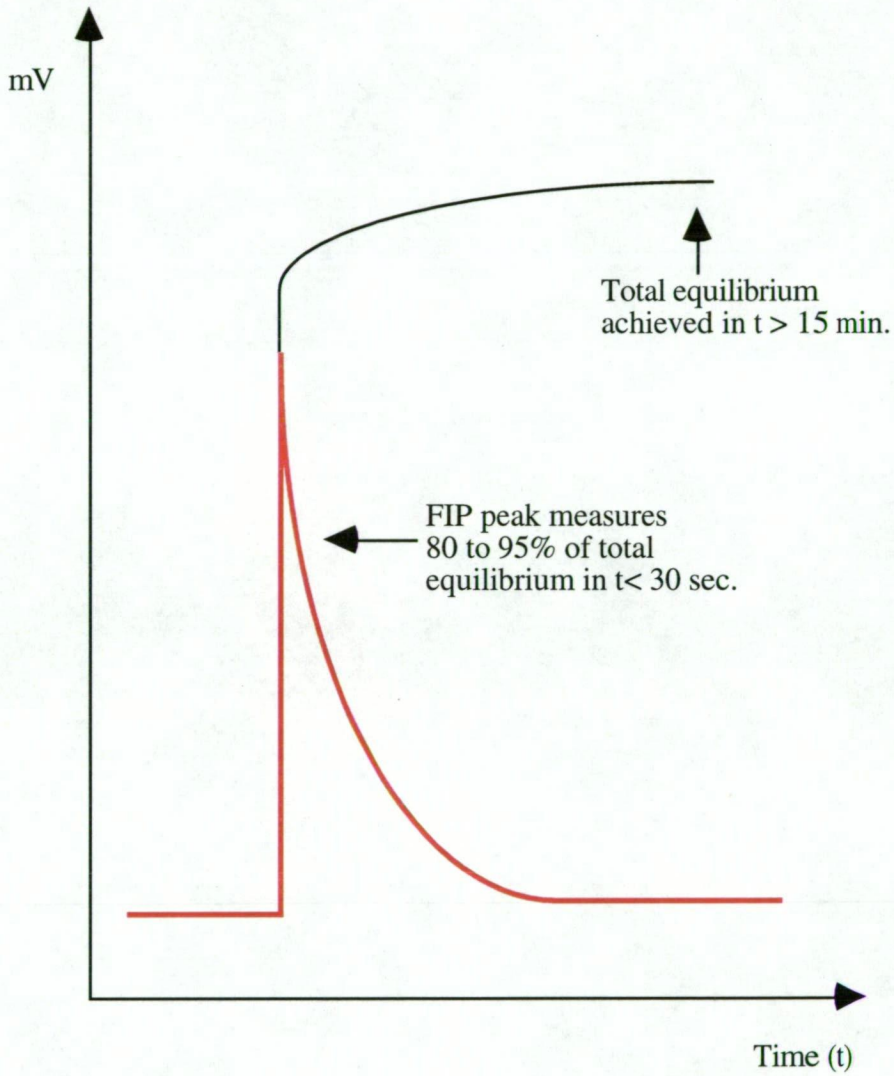

Figure 1.6. FIP versus Equilibrium measurement.

The advantages when using ISEs in the FIP mode [56,57] include;

1) Hydrodynamics responsible for the thickness of the Nernst diffusion layer at the sensing membrane's surface which determines the response time of a given ISE are controlled, resulting in a reproducible potential generation.

2) Liquid junction potential (refer to Section 1.6.1) can be stabilised by the controlled hydrodynamics in the FIP mode, and can be further reduced by employing an appropriate electrolyte solution as the carrier.

3) In the case for homogenous solid membrane based ISEs (refer to Section 1.1) such as a chloride ISE, the selectivity of an ISE can be drastically improved, since the time in which an injected sample zone passes the sensor surface is too short to establish total equilibrium potential for interfering ions. However, improvements in selectivity by this kinetic discrimination of interfering ions for liquid polymer membrane based ISEs are limited.

4) A steady flow of the carrier solution continually cleans the surface of the sensing membrane. Addition of a small amount (< 0.01 mM) of the determinand in the carrier will condition the ISE and improve the response time, selectivity and baseline stability.

5) The capacity to handle small sample volumes (5 to 200 μL), ease of computer automation, economical use of reagents and easy allowance for drifting potential.

Optimising the performance of an ISE to generate rapid measurements in FIP mode requires minimal dispersion between the sample zone and the carrier stream [55]. The dispersion of the sample zone can be minimised by using a large sample size (> 100 μL), fast flow rate (> 1.0 mL/minute), narrow tubing (0.5 to 1.0 mm id), small dead volume in an electrode flow cell, and a short line length between the sample injection valve and the ISE's sensing membrane.

The four main methods employed in introducing the sample zone via a flow cell to the ISE's sensing membrane are illustrated in Figure 1.7 and are as follows:

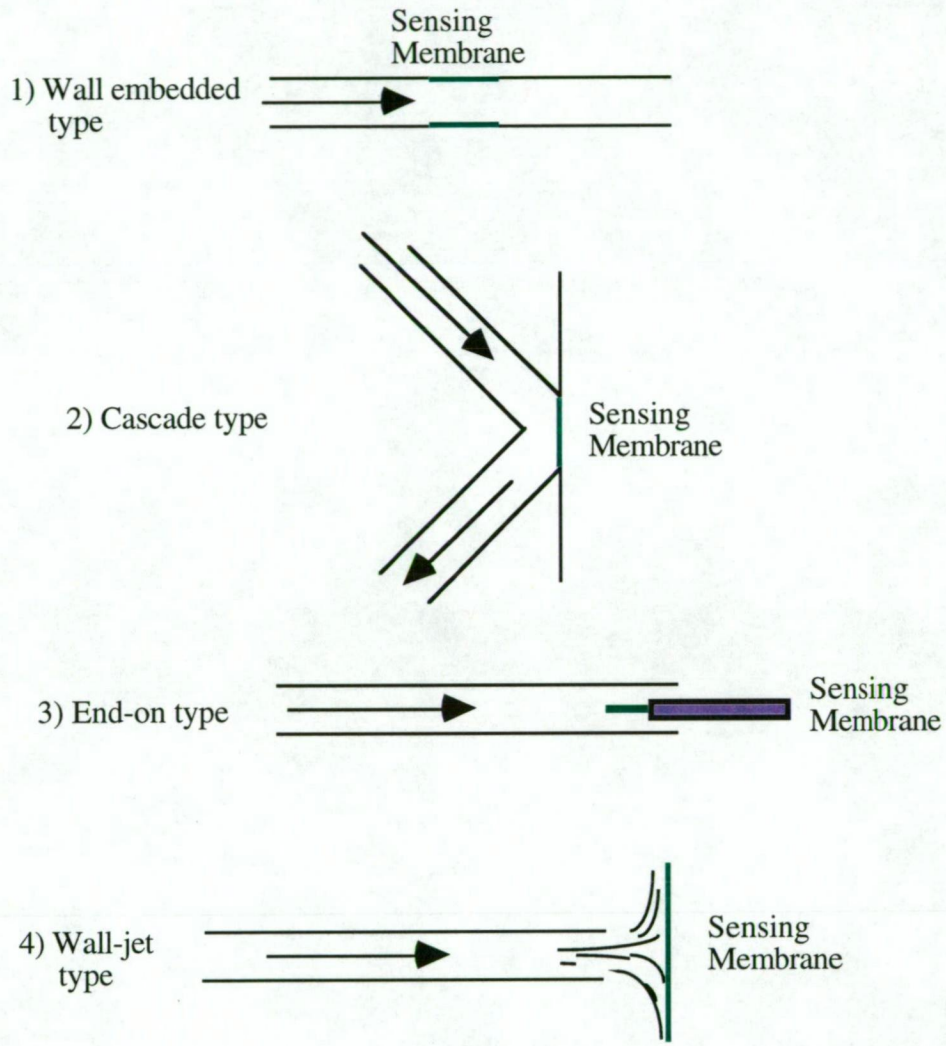

Figure 1.7. The four configurations possible with flow cells; 1) Wall embedded, 2) Cascade, 3) End-on and 4) Wall-jet type; arrows signify the direction of the flow stream.

1) the wall embedded method, whereby the ISE is inserted in the flow channel of a flow cell,

2) the cascade method, whereby the sample zone impinges tangentially to the ISE's membrane,

3) the end-on method, whereby a miniature ISE is positioned centrically at the end of a flow channel, and

4) the wall-jet method, whereby the sample zone impinges perpendicular to the ISE's membrane.

1.7. Multi-sensor Arrays for Multi-ion Determinations

The ability to perform simultaneous multiple ion measurements is extremely attractive since analysis time and expense can be significantly reduced. Employing an array of ion-selective electrodes (ISEs) in the FIP mode, would result in a system that can measure multiple ion species in a sample of interest.

The response of ISE array systems can involve either steady-state [58], FIP [59,60] or batch injection analysis (BIA) [61] measurements. The advantage of a flow through system (FIP and BIA) is that the ISE's signal is a transient one and electrode drift can be corrected. A miniature array of coated-film based ISEs was developed to detect pH, potassium, sodium and calcium ions in aqueous solutions, with a possible low-cost application to clinical analyses [58]. The array of coated-film ISEs was fixed on a polycarbonate sheet. The construction of each of these coated-film based ISEs was achieved by laminating each poly(vinyl chloride) membrane onto a silver substrate. The array of ISEs responded in a Nernstian fashion over a wide concentration range in steady-state measurements.

In a different study, the screen printing of liquid polymer membrane ISEs, such as pH, potassium, ammonium and calcium, has been performed on a multisensing chip [62]. The screen printing technique developed in this study is reproducible and cost effective for mass production. The electrode response of the ISEs on this multisensing chip was 59.3 mV / decade for potassium, 18.0 mV/decade for calcium, 53.4 mV/decade for ammonium, and 79.4 mV/decade for pH over a wide concentration range.

An array of four coated-wire based ISEs has been used in a miniature flow cell design [63] in which the four ISEs and the silver/silver chloride wire reference electrode were placed in separate flow channels that merged down stream. The four ISEs used in this flow cell were

potassium, calcium, nitrate and chloride. This array was used to determine the above-mentioned ions in soil extracts. The entire system incorporating the flow cell, analog-to-digital converter (ADC), computer and peristaltic pump was a desktop instrument.

Research and development in sensor arrays used in the flow injection mode have also been reported using ion-selective field effective transistors (ISFETs) as miniature electrochemical sensors [64-66]. Arrays of ISFETs have been applied to sensing pH, potassium, and calcium ions in aqueous solutions in the FIP mode. Some studies have also included sodium sensors in the above-mentioned array of ISFETs [65].

Recent publications on ISE array systems employ chemometric methods for the optimisation of the individual ISEs in a particular array used in either the steady-state or FIP modes. These statistical methods were used to either improve the selectivity of the individual ISEs in the array or estimate the slope, the selectivity coefficient and the cell constant (E') for each ISE. The statistical methods that have been employed are partial least squares [67], non-linear regression [68], simplex optimisation [60,69] and projection pursuit regression [59,70]. An interesting statistical treatment that is of considerable benefit to the response of ISE arrays is the 'overdetermined' approach to their arrays, for example, eight ISEs were used to measure four different ions in aqueous solution [60].

The application of an array of identical ISEs in the FIP mode has also been applied to determine one ion in solution [71-73] and is referred to as the 'cell-in-series' approach. The advantage of employing several identical ISEs in the cell-in-series approach in an array to measure one ion is improved sensitivity and detection limit in potentiometric detection. In one case, three silver/silver chloride wires used as chloride ISEs were each arranged in separate flow cells and connected in series in a segmented flow analysis system [71]. The detection limit for chloride ions in this arrangement was improved 10-fold.

1.8 Portable Analytical Instrumentation for Remote-site Monitoring

There are numerous types of electrochemical probes [74,75], and some continuous flow and flow injection analysers based on colorimetric measurements reported [76-78] for the analysis of aqueous samples at remote locations. Two recent publications have highlighted the need for portable instrumentation based on flow injection analysis [79] and gas analysers [80]

for the purpose of remote site monitoring. Advances have occurred in many instrumental areas including mass spectrometry, gas chromatography, ion mobility spectrometry, infrared and UV spectroscopy, X-ray fluorescence spectrometry, and laser radar spectroscopy [80].

A field monitor based on a sulfide ISE was used to measure dissolved sulfide in uncontaminated and contaminated ground water [74]. The operation of this sulfide monitor was based on a similar principle to flow injection, but it was powered by a generator which alone would be a limitation in terms of real portability. In-situ monitoring with ISEs for long-term field monitoring has also been reported [79]. However, there has been little research devoted to the development of portable FIP systems that are battery-powered and devoted to field monitoring at remote locations.

1.9 Objectives of this Research

The objectives of the research undertaken were as follows:

1) to evaluate the viability of a portable battery-powered flow injection system employing a single potentiometric detector, in terms of practicability of data acquisition and data storage in such a system as well as the ISE performance under various carrier conditions and sample injection volumes in the FIP mode,

2) to evaluate the viability of employing various commercial planar type ISEs as a sensor array in the above-mentioned portable battery-powered flow injection system,

3) to develop an eight-sensor flow cell that is housed in a portable flow injection analyser that would be practical for remote-site monitoring, and evaluate each individual sensor in terms of the effect of flow rate and sample injection volume has on the electrode slope and peak heights in the FIP mode,

4) to develop photo-cured bisphenol A epoxy diacrylate membrane based CWEs in the eight-sensor flow cell and individually characterise them in terms of selectivity, response time, sensitivity, lifetime, mechanical and electrical integrity in the steady-state and FIP modes, and

5) to apply the photo-cured based CWEs in a multi-sensor array to simultaneously determine these ions in the FIP mode and validate the system with various hydroponic, wastewater and mineral drinking water samples.

In chapter 2, the application of a commercial iodide ISE and a tungsten-oxide wire electrode employed as a pH sensor using a portable battery-powered flow injection analyser is described. Both the performances of the iodide and the tungsten electrodes were evaluated in terms of electrode slope, concentration range and detection limits in the FIP mode. In the case of the tungsten electrode, the validation of this sensor was established using various environmental water and various alcoholic beverage samples in the FIP mode. The effect of sample injection volume and carrier conditions on the performance of these electrodes in the FIP mode will be discussed.

In chapter 3, three commercial planar type ISEs (nitrate, potassium and sodium) arranged in a three-ISE array and employed in a portable battery-powered FIP system is described. The performance of the ISE-array was studied and validation of this system was performed with various mineral water samples in the FIP mode. The effect of carrier conditions on the performance of this ISE-array are discussed.

In the work described in chapter 4, an eight-sensor flow cell in a complete portable battery-powered flow injection system was developed and evaluated in the FIP mode. The silver based sensors were each anodised with iodide and the response of the individual sensors to silver and iodide standard solutions was studied. Evaluation of the multi-sensor flow cell, in terms of effect of varying flow rate and sample injection volume are discussed.

Chapter 5 describes photo-cured epoxydiacrylate based ammonium, calcium, hydrogen, nitrate and potassium CWEs which were developed and individually evaluated using the multi-sensor flow cell described above. Each photo-cured CWE was evaluated in terms of selectivity, response time, sensitivity, lifetime, mechanical and electrical integrity in the steady-state and FIP modes.

Chapter 6 describes the photo-cured based CWEs described above which were employed as a multi-CWE array to determine their respective determinand simultaneously in the FIP mode. This process was evaluated in three parts: 1) the photo-cured ammonium and hydrogen CWEs were used simultaneously in the FIP mode, 2) photo-cured calcium, nitrate, potassium CWEs and a Ag/AgCl wire used as a chloride CWE were used simultaneously in the FIP mode, and 3) combining part 1 and 2, the photo-cured ammonium, calcium, hydrogen, nitrate and potassium CWEs and a Ag/AgCl wire electrode were used simultaneously in the FIP

mode. In parts 1 to 3, the CWE arrays were validated by analysing various water samples in the FIP mode. The choice of carrier and the conditions used for the standard solutions and samples are discussed.

1.9.1 References

1. W. E. Bazzelle, 'Applications of ion-selective electrodes', Analytica Chimica Acta, **54**, 29 - 39, (1971).

2. J. W. Ross, 'Ion-Selective Electrodes', (ed. R. A. Durst) NBS Special Publication No. 314, Washington, (1969).

3. A. Shatkay, 'Ion specific membranes as electrodes in determination of activity of calcium', Analytical Chemistry, **39**, 1056 - 1065, (1967).

4. E. Pungor, 'Theory and application of anions sensitive membrane electrodes', Analytical Chemistry, **39**, 28A, (1967).

5. J. W. Ross, Science, 'Calcium-selective electrode with liquid ion exchanger', **156**, 1378 - 1379, (1967).

6. G. J. Moody, R. B. Oke and J. D. R. Thomas, 'A calcium-sensitive electrode based on a liquid ion exchanger in a poly(vinyl chloride matrix', Analyst, **95**, 910 - 918, (1970).

7. W. E. Morf, 'The Principles of Ion-Selective Electrodes and Membrane Transport', Elsevier Publication Co., New York, (1981).

8. G. G. Guilbault and E. Hrabankova, 'An electrode for determination of amino acids', Analytical Chemistry, **42**, 1779 - 1783, (1970).

9. G. Eisenman, 'Glass Electrodes for Hydrogen and other Cations', Marcel Dekker, New York, (1967).

10. J. Koryta and K. Stulik, 'Ion-Selective Electrodes', 2nd Edition, Cambridge University Press, London, (1983).

11. N. Lakshinarayanaiah, 'Membrane Electrodes', Academic Press, New York, (1976).

12. K. Suzuki, H. Ishiwada, T. Shirai and S. Yanagisawa, 'Coated-wire epoxy-matrix membrane ion-selective electrode', Bunseki Kagaku, **30**, 751 - 754, (1981).

13. H. Freiser, 'Ion-Selective Electrodes in Analytical Chemistry', Vol. 12, ed. H. Freiser, Plenum Press, New York, (1980).

14. R. W. Cattrall, 'Ion-Selective Electrode Methodology', Vol. 1, Chpt. 8, ed. A. Covington, C. R. C. Press, Florida, (1979).

15. R. W. Cattrall and I. C. Hamilton, 'Coated-wire Ion-selective Electrodes', Ion-Selective Electrode Review, **6**, 125 - 172, (1984).

16. D. Ammann, 'Ion-Selective Microelectrodes. Principle, Design and Application', Springler-Verlag, Berlin, (1986).

17. B. Shiramizo, J. Janata and S. D. Moss, 'Ion-selective field effect transistors with hetrogenous membranes', Analytica Chimica Acta, **108**, 161 - 167, (1979).

18. A. Haemmerli, J. Janata and H. M. Brown, 'Ion-selective electrodes for intracellular potassium measurements', Analytical Chemistry, **52**, 1179 - 1182, (1980).

19. U, Oesch, S. Caras and J. Janata, 'Field-effect transistors sensitive to sodium and ammonium ions', Analytical Chemsitry, **53**, 1983 - 1986, (1981).

20. J. Janata, 'Ion-selective field effect transistors, principles and applications in clinical chemistry and biology', Analytical Proceedings, **19**, 65 - 68, (1982).

21. Y. Ohta, S. Shoji, M. Esashi and T. Matsuo, 'Prototype sodium and potassium-sensitive micro ISFETs', Sensors and Actuators, **2**, 387 - 397, (1982).

22. G. J. Moody and J. D. R. Thomas, 'Ion-Selective Electrode Methodology', Vol. 1, Chpt. 7, ed. A. Covington, C. R. C. Press, Florida, (1979).

23. P. Anker, H. B. Jenny, U. Wuthier, R. Aspec, D. Ammann and W. Simon, 'Determination of potassium ion concentration in blood serum with a valinomycin-based silicone rubber membrane of universal applicability to body fluids', Clinical Chemistry, **29**, 1447 - 1448, (1983).

24. I. A. Mostert, P. Anker, H. B. Jenny, U. Oesch, W. E. Morf, D. Ammann and W. Simon, 'Neutral carrier based silicone-rubber membranes for hydrogen, potassium, ammonium and calcium ion selective electrode' Mikrochimica Acta, **1**, 33 - 38, (1985).

25. O. H. LeBlanc and W. T. Grubb, 'Long-lived potassium ion selective polymer membrane electrode', Analytical Chemistry, **48**, 1658 - 1660, (1976).

26. G. J. Moody, J. M. Slater and J. D. R. Thomas, 'Membrane design and photocuring encapsulation of flatpack based ion-sensitive field effect transistors' Analyst, **113**, 103 - 108, (1988).

27. A. Bratov, N. Abramova, J. Muñoz, C. Domínguez, S. Alegret and J. Bartrolí, 'Ion sensor with photocurable polyurethane polymer membrane' Journal of Electrochemical Society, **141**, L111 - L112, (1994).

28. A. Bratov, N. Abramova, J. Muñoz, C. Domínguez, S. Alegret and J. Bartrolí, 'Optimization of photocurable polyurethane membrane composition for ammonium ion sensor', Journal of the Electrochemical Soceity, **144**, 617 - 621, (1997).

29. T. M. Ambrose and M. E. Meyerhoff, 'Charaterization of photopolymerized decyl methacrylate as a membrane matrix for ion-selective electrode', Electroanalysis, **8**, 1095 - 1100, (1996).

30. G. J. Moody and J. D. R. Thomas, 'Selective Ion-selective Electrodes', Merrow, Watford, (1971).

31. E. Lindner, V. V. Cosofret, P. R. Kusy, P. R. Buck, T. Rosatzin, U. Schaller, W. Simon, J. Jeney, K. Toth and E. Pungor, 'Responses of proton-selective solvent polymeric membrane electrodes fabricated from modified PVC membranes', Talanta, **40**, 957 - 967, (1993).

32. A. M. Y. Jaber, G. J. Moody and J. D. R. Thomas, 'Solvent mediator studies on barium ion-selective electrodes based on a sensor of the tetraphenyl borate salt of the barium complex of a nonylphenoxypoly(ethyleneoxy) ethanol', Analyst, **101**, 179 - 186, (1976).

33. G. J. Moody, N. S. Nassory and J. D. R. Thomas, 'Calcium ion-selective electrodes based on calcium bis[di(p-1,1,3,3-tetramethylbutylphenyl)phosphate] sensor and trialkyl phosphate mediators', Analyst, **103**, 68 - 71, (1978).

34. R. L. Solsky, 'Ion-selective electrodes', Analytical Chemistry, **62**, 21R - 33R, (1990).

35. U. Wuthier, P. V. Hung, R. Zuend, D. Welti, R. J. J. Funck, A. Bezegh, D. Ammann, E. Pretsch and W. Simon, 'Tin organic compounds as neutral carriers for anion-selective electrodes', Analytical Chemistry, **56**, 535 - 538, (1984).

36. P. Schulthess, D. Ammann, B. Kräutler, C. Caderas, R. Stepánek and W. Simon, 'Nitrite-selective liquid membrane electrode', Analytical Chemistry, **57**, 1397 - 1401, (1985).

37. D. Siswanta, J. Takenaka, T. Suzuki, H. Sasakura, H. Hisamoto and K. Suzuki, 'Novel neutral anion ionophores based on fluorinated (poly) ether compounds as a sensory molecule for an ion-selective electrode', Chemistry Letters, 195 - 196, (1997).

38. W. Simon and E. Carafoli, 'Design, properties and applications of neutral ionophores', Methods in Enzymology, **56**, 439 - 448, (1979).

39. J. H. Boles and R. P. Buck, 'Anion responses and potential functions for neutral carrier membrane electrodes', Analytical Chemistry, **45**, 2057 - 2062, (1973).

40. T. J. Cardwell, R. W. Cattrall, L. W. Deady and M. Dorkos, 'pH sensitive optodes based on cellulose acetate membranes', 12th Australian Analytical/3rd Environmental Conference Proceedings, Perth, September (1993).

41. W. Simon, D. Ammann, M. Oehme and W. E. Morf, 'Calcium-selective electrodes', Annals New York Academy of Science, **307**, 52 - 70, (1978).

42. E. Lindner, K. Toth, E. Pungor, W. E. Morf and W. Simon, 'Response time studies on neutral carrier ion-selective membrane electrodes', Analytical Chemistry, **50**, 1627 - 1631, (1978).

43. R. A. Steiner, M. Oehme, D. Ammann and W. Simon, 'Neutral carrier sodium ion-selective microelectrode for intracellular studies', Analytical Chemistry, **51**, 351 - 353, (1979).

44. R. W. Cattrall, I. C. Hamilton and P. J. Iles, 'Photocured polymers in ion-selective electrode membranes', Analytica Chimica Acta, **169**, 403 - 406, (1985).

45. T. J. Cardwell, R. W. Cattrall, I. C. Hamilton and P. J. Iles, 'Photocured polymers in ion-selective electrode membranes: Part 2 Calcium electrode for flow injection analysis', Analytica Chimica Acta, **177**, 239 - 242, (1985).

46. T. Dimitrakopoulos, J. R. Farrell and P. J. Iles, 'A photo-cured calcium ion-selective electrode for use in flow injection potentiometry that tolerates high perchlorate levels', Electroanalysis, **8**, 391 - 395, (1996).

47. L. T. Di Benedetto, T. Dimitrakopoulos, J. R. Farrell and P. J. Iles, 'Evaluation of perchlorate tolerant photo-cured calcium selective electrodes for use in flow injection potentiometry', Talanta, **44**, 349 - 356, (1997).

48. T. J. Cardwell, R. W. Cattrall, I. C. Hamilton and P. J. Iles, 'Photo-cured polymers in ion-selective electrode membranes: Part 3 A potassium electrode for flow injection analysis', Analytica Chimica Acta, **204**, 329 - 332, (1988).

49. A. Bratov, N. Abramova, J. Muñoz, C. Domínguez, S. Alegret and J. Bartrolí, 'Photocurable polymer matrices for potassium-sensitive ion-selective electrode membranes', Analytical Chemistry, **67**, 3589 - 3595, (1995).

50. F. R. del Mundo, T. J. Cardwell, R. W. Cattrall, P. J. Iles and I. C. Hamilton, 'An ultraviolet-cured pH-sensitive membrane electrode for use in flow injection analysis', Electroanalysis, **1**, 353 - 356, (1989).

51. C. Dumschat. R. Fromer, H. Rautschek, H. Muller and T. J. Timpe, 'Photolithographically patternable nitrate-sensitive acrylate-based membrane', Analytica Chimica Acta, **243**, 179 - 182, (1989).

52. J. R. Farrell, P. J. Iles and T. Dimitrakopoulos, 'Photocured polymers in ion-selective electrode membranes. Part 5: Photopolymerised sodium sensitive ion-selective electrodes for flow injection potentiometry', Analytica Chimica Acta, **334**, 133 - 137, (1996).

53. J. R. Farrell, P. J. Iles and T. Dimitrakopoulos, 'Photocured polymers in ion-selective electrode membranes. Part 6: Photopolymerised lithium sensitive ion-selective electrodes for flow injection potentiometry', Analytica Chimica Acta, **335**, 111 - 116, (1996).

54. K. Cammann, 'Working with Ion-Selective Electrodes', Springer-Verlag, Berlin, (1979).

55. M. Valcárcel and M. D. Luque De Castro, 'Flow Injection Analysis. Principles and Applications', ed. S. J. Lyle and R. A. Chalmers, Ellis Horwood Ltd., New York, (1987).

56. M. Valcárcel and M. D. Luque De Castro, 'Flow-Through (Bio)Chemical Sensors', Elsevier, Amsterdam, (1994).

57. K. Cammann, 'Flow injection analysis with electrochemical detection', Fresenius Journal of Analytical Chemistry, **329**, 691 - 697, (1988).

58. U. Lemke, K. Cammann, C. Kötter, C. Sundermeier and M. Knoll, 'Multisensor array for pH, K^+, Na^+ and Ca^{2+} measurements based on coated-film electrodes', Sensors and Actuators, **B7**, 488 - 491, (1992).

59. F. J. Sáez de Viteri and D. Diamond, 'Ammonium detection using an ion-selective electrode array in flow injection analysis', Eletroanalysis, **6**, 9 - 16, (1994).

60. D. Diamond and R. J. Forster, 'Robust estimation of selectivity coefficients using multivariate calibration of ion-selective electrode arrays', Analytica Chimica Acta, **276**, 75 - 86, (1993).

61. D. Diamond, J. Lu, Q. Chen and J. Wang, 'Multicomponent batch-injection analysis using an array of ion-selective electrodes', Analytica Chimica Acta, **281**, 629 - 635, (1993).

62. H. D. Goldberg, R. B. Brown, D. P. Liu and M. E. Meyerhoff, 'Screen Printing - A technology for batch fabrication of integrated chemical-sensor arrays', Sensors and Actuarors, **B21**, 171 - 183, (1994).

63. T. J. Cardwell, R. W. Cattrall, P. C. Hauser and I. C. Hamilton, 'A multi-ion sensor cell and data-acquisition system for flow injection analysis', Analytica Chimica Acta, **214**, 359 - 366, (1988).

64. A. U. Ramsing, J. Janata, J. Ruzicka and M. Levy, 'Miniaturization in analytical chemistry - A combination of flow injection analysis and ion-selective field effect transistors for determination of pH, and potassium and calcium ions', Analytica Chimica Acta, **118**, 45 - 52, (1980).

65. A. Sibbald, P. D. Whalley and A. K. Covington, 'A miniature flow-through cell with four-function chemFET intergrated circuit for simultaneous measurements of potassium, hydrogen, calcium and sodium ions', Analytica Chimica Acta, **159**, 47 - 62, (1984).

66. B. H. Van der Schoot, H. H. Van den Vlekkert, N. F. De Rooij, A. Van den Berg and A. Grisel, 'A flow injection analysis system with glass-bonded ISFETs for the simultaneous detection of calcium and potassium ions and pH', Sensors and Actuators, **B4**, 239 - 241, (1991).

67. M. Otto and J. D. R. Thomas, 'Model studies on multiple channel analysis of free magnesium, calcium, sodium and potassium at physiological concentration levels with ion-selective electrodes', Analytical Chemistry, **57**, 2647 - 2651, (1985).

68. K. R. Beebe, D. Uerz, J. Sandifier and B. R. Kowalski, 'Sparingly selective ion-selective electrode arrays for multicomponent analysis', Analytical Chemistry, **60**, 66 - 71, (1988).

69. R. J. Forster and D. Diamond, 'Nonlinear calibration of ion-selective electrode arrays for flow injection analysis', Analytical Chemistry, **64**, 1721 - 1728, (1992).

70. K. R. Beebe and B. R. Kowalski, 'Nonlinear calibration using projection pursuit regression: Application to an array of ion-selective electrodes', Analytical Chemistry, **60**, 2273 - 2278, (1988).

71. D. B. Hibbert, P. W. Alexander, S. Rachmawati and S. A. Caruana, 'Multiple sensor response in segmented flow analysis with ion-selective electrodes', Analytical Chemistry, **62**, 1015 - 1019, (1990).

72. D. B. Hibbert, P. W. Alexander and P. Yatiman, 'Theory of multiple-cell response of redox electrodes', Mikrochimica Acta, **108**, 93 - 101, (1992).

73. J. A. Borzitsky, A. Dvinin, O. M. Petrukhin and Y. I. Urusov, 'Flow cell with double slope factor for potentiometric determination of fluoride at low concentrations', Analyst, **118**, 859 - 861, (1993).

74. J. Gulens, 'A portable monitor for measurement of dissolved sulfide based on the glass/sulfide-selective electrode couple', Water Research, **19**, 201 - 204, (1985).

75. C. E. Reimers, 'An *in situ* microprofiling instrument for measuring interfacial pore water gradients: methods and oxygen profiles from the North Pacific Ocean', Deep Sea Research, **34**, 2019 - 2035, (1987).

76. K. S. Johnson, C. L. Beehler and C. M. Sakamoto-Arnold, 'A submersible flow analysis system', Analytica Chimica Acta, **179**, 245 - 257, (1986).

77. K. S. Johnson, C. M. Sakamoto-Arnold and C. L. Beehler, 'Continuous determination of nitrate concentrations *in situ*', Deep Sea Research, **36**, 1407 - 1413, (1989).

78. N. J. Blundell, A. Hopkins, P. J. Worsfold and H. Casey, 'A portable battery-powered flow injection monitor for the *in situ* analysis of nitrate in natural mineral waters', Journal of Automatic Chemistry, **15**, 159 - 166, (1993).

79. K.N. Andrew, N.J. Blundell, D. Price and P.J. Worsfield, 'Flow injection techniques for water monitoring', Analytical Chemistry, **66**, 917A - 992A, (1994).

80. H. L. C. Meuzelaar, *Ed.*, 'Special Issue on: Field Portable Analytical Instrumentation', Trends in Analytical Chemistry, **13**, 252 - 299, (1994).

Chapter Two: Development and Evaluation of a Portable Flow Injection Potentiometric System.

2.1 Introduction

This chapter is concerned with the development of a portable battery-powered flow injection potentiometric (FIP) system suitable for remote-site monitoring. This portable FIP system was evaluated with a commercial iodide ISE and a tungsten / tungsten-oxide wire electrode used as an example of a miniature pH electrode.

The application of analytical measurements for various anions and cations at remote site locations absent from a main power supply have been possible by the development of hand-held potentiometric monitors suitable for either hydrogen, sodium, potassium or nitrate ions [1,2], as well as submersible colorimetric analysers suitable for a variety of species [3-5]. The Hach Company (Colorado, USA) has commercialised a series of pH, redox and conductivity hand-held meters as well as portable colorimetric analysers and test kits for a wide range of organic and inorganic species that are suitable for remote-site analyses. However, the advantage of ISE measurements compared to colorimetric based analytical methods are that the samples to be analysed do not have to be treated and therefore direct measurements can be performed with little preparation required by the operator. In addition, applying the FIP technique as discussed earlier in Section 1.6.2, has advantages such as the ability to perform rapid measurements (> 120 injections/hour) with high precision, using small sample volumes ($\leq$ 300 μL), low reagent consumption, and easy allowance for electrode drift when calculating peak heights [6]. Therefore the development of a portable FIP system dedicated for remote site monitoring would be of extreme value. Development of other electrochemical based portable instrumentation reported recently include an anodic stripping voltammetry system [7,8] for determining trace metals, a remote electrode operated in the stripping potentiometric mode to measure labile copper in seawater [9] and a remote electrochemical biosensor for monitoring phenolic compounds in untreated river and groundwater samples [10].

Over many years, there has been a great deal of research and development in continuous flow and flow injection type systems using ion-selective electrodes (ISEs) as detectors [11-13]. Examples include the use of ISEs in air-segmented continuous flow analysis applied for the determination of proteins [14], in rapid flow systems for high speed auto-sampling [15], and in

flow injection analysis [16]. There are numerous commercial automated analysers available using ISEs in flow injection potentiometry (FIP) and continuous flow modes [5,16]. However, there has been little research devoted in the development of portable FIP systems employing potentiometric sensors of low weight and low power consumption.

This chapter describes the design and operation of such a portable FIP system that is battery-powered by a 7.2-volt Ni-Cd rechargeable battery pack and is capable of remote-site monitoring. This chapter is in two parts and the evaluation of the portable FIP system was performed using 1) an Orion iodide ISE as an example of a commercial size ISE and 2) a tungsten-oxide wire employed as a miniature hydrogen ion electrode. The tungsten-oxide electrode was used to determine the pH of various alcoholic beverages and various water samples. The carrier conditions required to perform reliable pH measurements in the FIP mode as well as interfering species are discussed.

2.1.1 Metallic Electrodes for Hydrogen Ion Sensors

Non-glass based hydrogen ion electrodes are preferred over glass electrodes for pH measurements where a robust construction is necessary, eg. for clinical, environmental and food monitoring. Sonsequently, considerable research has been reported in this area [17,18]. Metallic based electrodes have several advantages over glass and liquid polymer membrane based electrodes including lower cost, more robust, unlimited operational lifetime and simple manufacture and miniaturisation. The application of metallic electrodes may be better suited in a portable FIP system that is suitable for remote-site monitoring, since there is less chance of breakage during transportation.

Liquid polymer membrane based hydrogen ion electrodes are the most popular form of non-glass electrode developed [17,18]. Initial work in the development of polymer membranes for hydrogen ion electrodes employed plasticised poly (vinyl chloride) as the support polymer and neutrally charged ligands as the electro-active sensor reagent [17.18]. One study reports the fabrication of a non-plasticised poly(vinyl chloride) based membrane for a hydrogen electrode using quinhydrone as the ionophore [19]. The quinhydrone based hydrogen electrode exhibited good mechanical stability and a Nernstian response in the pH range between 3 and 10.

A sodium tungsten bronze based electrode has been shown to respond to the hydrogen ion, but the electrode response was non-linear [20]. The sodium tungsten bronze electrode also exhibited a response to heavy metals such as silver (I) and mercury (II) ions in solution. This study also reported that similar electrode behaviour was observed with lithium tungsten bronze and rubidium tungsten bronze based electrodes.

A hydrogen ion-sensitive field-effect transistor (ISFET) based on aluminium oxide was used successfully in the FIP mode [21]. The hydrogen ISFET exhibited a linear pH range between 2 and 12 and the slope of the sensor was 53 mV change per pH unit. The flow injection system had a sample throughput of 360 injections / hour. In another study, a hydrogen sensitive ISFET based on silicon nitride was applied to FIP measurements employing a nitrate ISE as the reference electrode [22]. The silicon nitride hydrogen ISFET exhibited a Nernstian response and a linear pH range between 1 and 13. In this study, the sample throughput achieved was 140 injections / hour.

Polycrystalline and monocrystalline antimony based electrodes have been proposed for continuous intra-oesophageal pH monitoring as an alternative to a glass microelectrode [23]. The antimony electrodes exhibited a similar drift and electrode response with time when compared to a glass microelectrode in the range pH 1 - 7. The electrode responses of the antimony polycrystalline and monocrystalline electrodes were 54.6 and 55.3 mV change per pH unit, respectively, compared to 61.8 mV change per pH unit for the glass microelectrode. The use of an antimony-based electrode would reduce the cost of such monitoring situations, and the advantages of employing a robust non-glass electrode in continuous monitoring of patients are obvious.

In a different study, an antimony/antimony-oxide electrode was used as a hydrogen sensor in the FIP mode employing a wall-jet flow cell design [24]. A sub-Nernstian response of -42.1 mV change per pH unit was observed over a pH range between 1.6 and 12.0. In this study the antimony/antimony-oxide electrode was used to successfully determine the acidity in coke and vinegar samples in the FIP mode.

Other metal electrodes that exhibit a response to pH change have been used as potentiometric enzyme electrodes by modifying the electrode surface [25-27]. Such electrode materials used were antimony [26], iridium oxide [25,26] and ruthenium oxide [25] and were used to measure various enzymes by monitoring the enzyme substrate as the hydrolysis

decreases the pH at the electrode surface. Enzymes determined with such metal / metal oxide electrodes were urea [26], chymotrypsin [25] and trypsin [25].

2.2 Experimental

2.2.1 Materials

The following reagents were used as received from the suppliers: sodium acetate (BDH, General Purpose Reagent), sodium chloride (BDH, AnalaR), potassium iodide (BDH, AnalaR), sodium dihydrogen phosphate (BDH, AnalaR), di-sodium tetraborate (BDH, AnalaR), tri-sodium citrate (BDH, AnalaR) and tris(hydroxymethyl)methylamine (BDH, AnalaR). Ultrapure water (Barnstead Ultrapure water systems, 18.0 MΩ cm) was used throughout this study.

Standard potassium iodide solutions were prepared by serial dilution from a stock solution (100 mM potassium iodide). A universal pH buffer stock solution containing 10 mM sodium dihydrogen phosphate, 2.5 mM di-sodium tetraborate and 7 mM trisodium citrate (all BDH, AnalaR) was prepared. pH standards were prepared daily by diluting the stock solution 10 fold and the pH was adjusted with either 100 mM HCl or NaOH. An Activon pH glass combination electrode and pH / mV meter (model AS209) was used to determine the pH of the prepared universal pH buffer solutions.

The tungsten wire used was 0.25 mm in diameter, 99.95% pure and was obtained from Goodfellow (England). The silver wire used as the reference electrode was 0.5 mm in diameter, 99.99% pure and was obtained from Aldrich (Australia). Tank water and seawater samples were used for freshwater fish and crayfish breeding, respectively and were provided by the Dept. of Aquaculture. River water samples were collected on site from the Derwent river and the Tamar river. The alcohol samples were purchased from the local liquor stores.

2.2.2 Electrode Preparation and Conditioning of the Orion Iodide ISE

An Orion cyanide ISE (94-06) based on a pressed Ag_2S/AgI solid state membrane was used as an iodide ISE throughout this study. This iodide ISE was polished using a Struers polishing unit (Dap-V) fitted with a 12 mm diameter PVC disk and a polishing cloth (DP- Mol). A 3 μm diamond particle spray (DP-Spray HQ) and a Struers lubricant (DP-Lubricant Red HQ) was used to clean and polish the surface of the iodide ISE on the polishing unit, until a mirror finish was achieved. Prior to use, the polished iodide ISE was conditioned in a 0.1 mM potassium iodide solution overnight.

2.2.3 Design of the Portable Flow Injection System

A general diagram of the portable flow injection system is given in Figure 2.1. The flow injection system consisted of components developed in-house and constructed in a carry-case. The light-weight carry case (30 x 25 x 8 cm) was used for portability, and housed the flow injection manifold (either a septum injection port described previously [15] or a Rheodyne (5020) injection valve fitted with a 200 μL sample loop), a potentiometric flow cell, an eight channel analog-to-digital converter (ADC) and a peristaltic pump both powered with a battery-pack of six Ni-Cd rechargeable 1.2 volt batteries. Total weight was 1.8 kg.

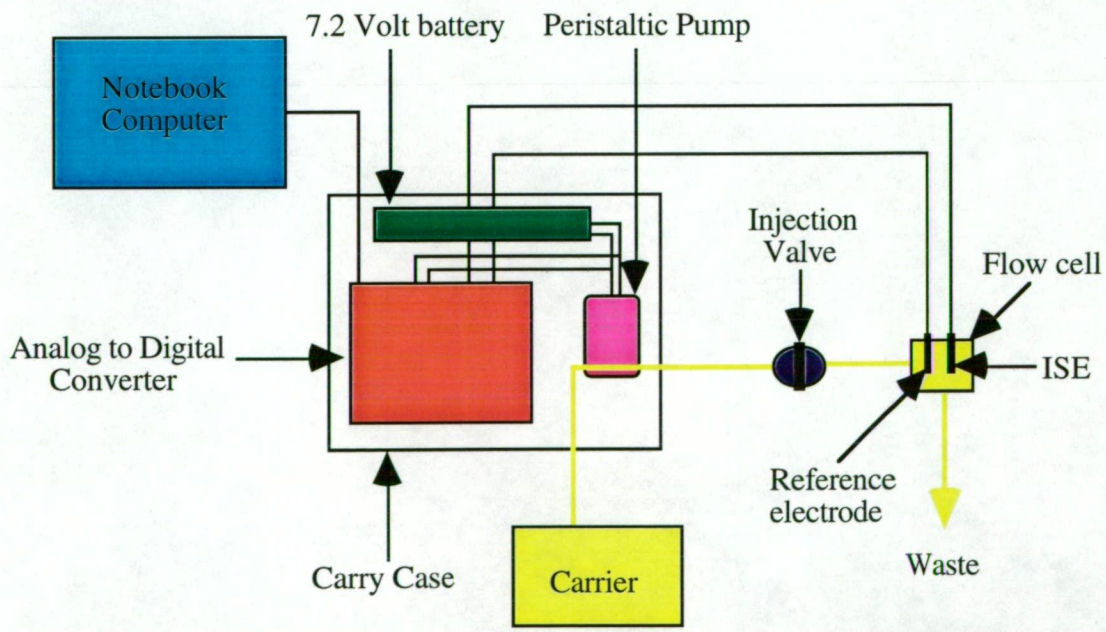

Figure 2.1. A schematic diagram of the portable FIP system developed in this study.

The 2-channel peristaltic pump (Alitea-AB, Model OEM-S2) was obtained from A.I. Scientific Pty Ltd (Australia). The ADC was an eight channel with 12-bit resolution with a serial output at 9600 baud rate, 2 stop bits, zero parity, and with cable connection to a RS232 port in a Macintosh 145B Powerbook computer. The ADC was built at the chemistry workshops at the University of Tasmania and a block diagram and circuit design are both presented in Appendix 1.

2.2.4 Potentiometric Measurement Procedure

Steady-state potential measurements were made with the Orion iodide ISE and the tungsten-oxide wire electrode versus an Orion double junction reference electrode (Ag/AgCl / saturated AgCl // 10% KNO_3) in stirred solutions. The data acquisition program called 'Satod' © Version 1.46 was written by Dr J. Morgan (University of New South Wales, Sydney, Australia) in Think C for a Macintosh Powerbook 145B computer. The acquired digital data were displayed in real time millivolt readings plotted as a function of time and were saved as text files. A software package called 'IGOR PRO' (AD Instruments) was used for data analysis and graphical representation of the data. The ion activities were calculated using the Debye-Hückel equation [28] and used to determine the concentration of the determinand.

A program called MacCurve Fit © Version 0.7 was used to calculate the electrode slope, the E' and the standard deviations (95% confidence) of a given electrode in either steady-state or FIP modes. This program was written and supplied by Dr Kevin Raner (CSIRO, Division of Chemicals and Polymers, Victoria, Australia).

2.2.5 Iodide Measurements in the FIP mode

A wall-jet flow cell design for the commercial ISE (typically 12 mm in diameter) and a Ag/AgCl reference electrode built into the cell is given in Figure 2.2. The iodide standards were introduced manually into the flow stream via the septum injection port, using a 250 µL Hamilton HPLC syringe. The flow rate was 13.0 mL/minute through a single channel and the sample injected volume was 100 µL. Potassium iodide standards injected were in the concentration range from 0.001 mM to 10 mM in various carriers. In all FIP measurements, the ionic background of the injected iodide standards matched the carrier solution employed.

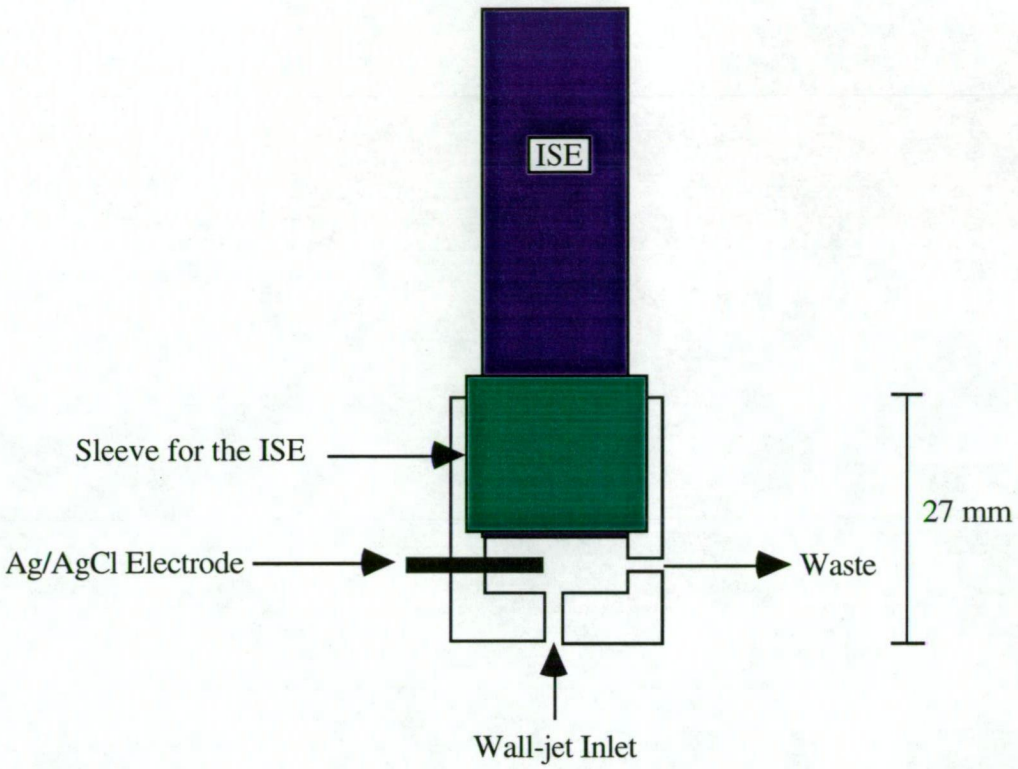

Figure 2.2. Diagram of the wall-jet flow cell used with the Orion iodide ISE.

2.2.6 pH Measurements in the FIP mode

The tungsten-oxide wire electrode was used in a flow-through cell illustrated in Figure 2.3. The flow rate was between 1.8 - 3.2 mL/min through a single channel. The samples and standards were introduced into the carrier stream manually using a Rheodyne (5020) injection valve fitted with a 200 µL sample loop. The tungsten wire was conditioned in 1.0 M KOH solution overnight, prior to use. When not in use, the tungsten wire electrode was stored in a 1.0 M KOH solution.

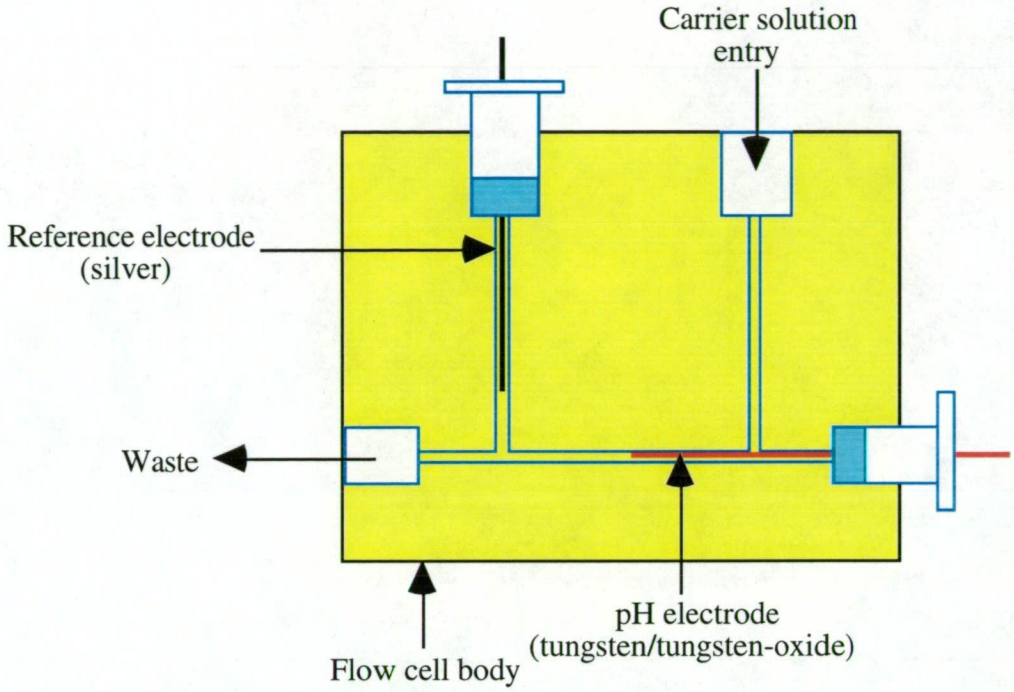

Figure 2.3. The flow cell used for the tungsten-oxide wire electrode.

2.3 Results and Discussion

The battery-powered FIP system developed in this study can be operated in a totally portable manner with low power consumption using six 1.2 Volt Ni-Cd rechargeable battery-pack to run both the analog-to-digital converter and the peristaltic pump. Up to three hours operation was possible before recharging was required, the notebook computer being powered by its own internal Ni-Cd rechargeable battery pack, allowing real time plotting of data at remote locations away from conventional laboratories. The portable FIP system was designed to accommodate commercial ISEs (typically 12 mm in diameter), hence making a variety of determinations possible with the large range of ISEs available, as well as employing miniature electrodes. The following sections describe the performance of an Orion iodide ISE and a tungsten-oxide wire electrode sensitive to hydrogen ions that were both applied in the portable FIP system.

2.3.1 Response Performance of the Orion Iodide ISE

The iodide ISE exhibited a Nernstian response of -59.1 ± 0.9 mV change per activity decade and a log-linear range between 0.001 mM and 100 mM in the steady-state mode. In the FIP mode, the peak heights recorded when using 100 mM acetate as the carrier exhibited a near-Nernstian response of -53.8 ± 2.1 mV change per activity decade, a log-linear range of between 0.005 mM and 10 mM iodide and the smallest iodide concentration detected was 0.001 mM iodide in the FIP mode. Figure 2.4 shows the peak heights recorded with iodide concentrations ranging from 0.001 mM to 10 mM in a 100 mM sodium acetate background carrier. The peak heights observed for the iodide ISE were 90% of the steady state response.

FIP data were also recorded when employing Ultrapure water as the background carrier solution. The peak heights using the iodide ISE exhibited a higher than Nernstian response of -67.8 mV change per activity decade. Similar hyper-Nernstian response has been reported for other silver iodide based iodide-selective electrodes when conditioned in distilled water [14]. The response data of the iodide ISE in various carriers are presented in Table 2.1. Interfering ions such as acetate that are present in the background of the potassium iodide solutions also respond at the Ag_2S/AgI membrane, leading to the observed lower electrode slope [15]. By contrast, the absence of interfering ions in the background carrier leads to the observed higher electrode slope of the iodide ISE in the FIP mode.

The baseline observed for the iodide ISE in this portable FIP system continually drifted in an ultrapure water as the carrier. Improvement was observed in 100 mM sodium acetate carrier, where the ISE drift was negligible. However, baseline drift in the FIP mode has little effect on calibrations since modelling was not employed. The data processing was used to account for any drift when manually calculating peak heights.

Employing 100 mM sodium chloride as the carrier significantly lowers the electrode slope of the iodide ISE to -48.1 mV change per activity decade, and a slightly narrower log-linear range between 0.01 mM to 10 mM iodide was observed when compared to 100 mM sodium acetate and Ultrapure water as the carriers. Table 2.1 summarises these data. Clearly, the chloride ions present in the background of the potassium iodide solutions add to the response of the Ag_2S/AgI membrane, and this behaviour would lead to the reduced electrode.

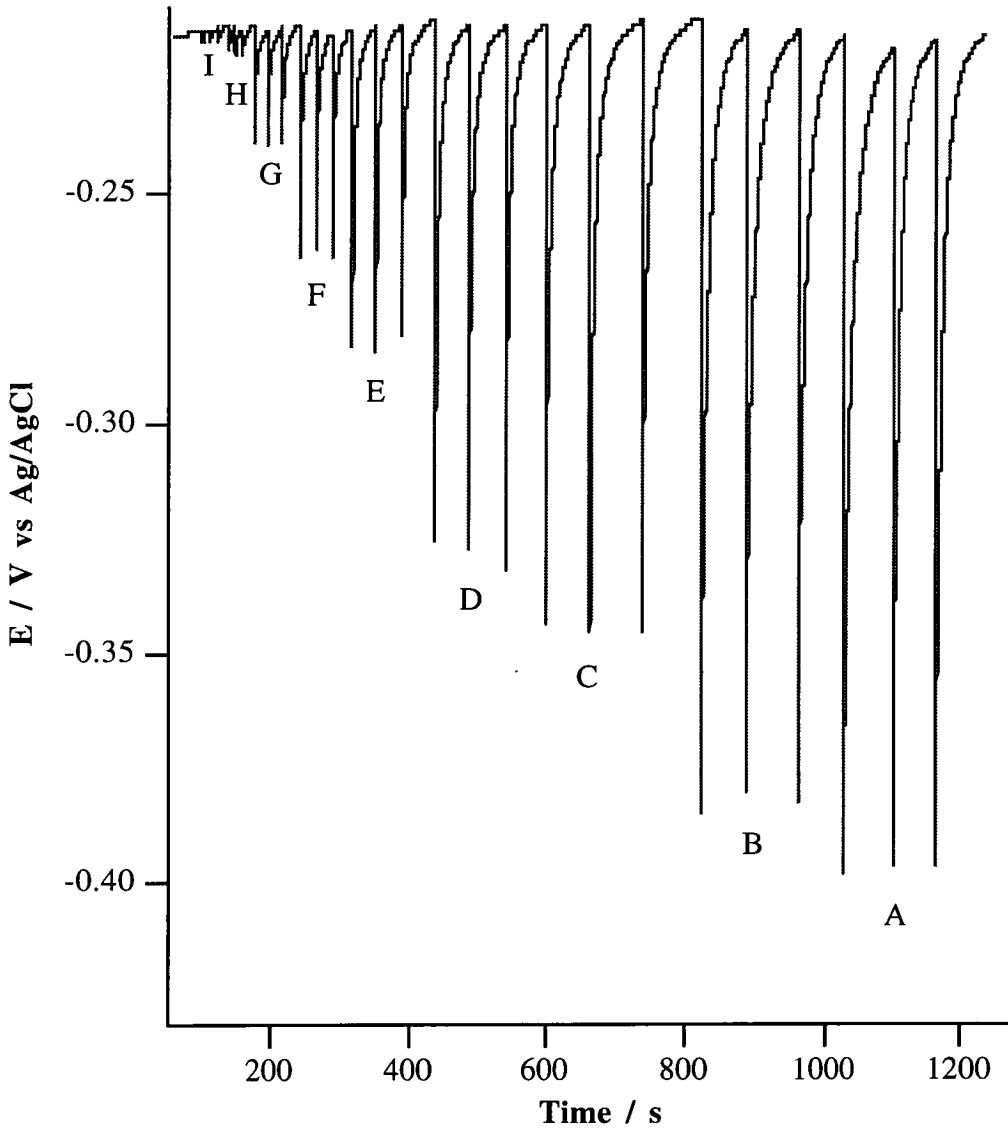

Figure 2.4. Typical FIP response observed for the Iodide ISE in the portable FIP system; A = 10 mM, B = 5 mM, C = 1 mM, D = 0.5 mM, E = 0.1 mM, F = 0.05 mM, G = 0.01 mM, H = 0.005 mM and I = 0.001 mM iodide solutions all in a 100 mM sodium acetate ionic background and sample volume = 100 µL.

slope observed [15]. The baseline drift observed with the 100 mM sodium chloride was negligible, similar to that observed with a 100 mM sodium acetate background.

Table 2.1. The response behaviour observed for the iodide ISE in the portable FIP system employing various carrier solutions.

Carrier	Electrode slope (S.D) / mV/decade	log-linear range / mM
Ultrapure water	-67.8 (1.7)	0.005 to 10
100 mM sodium acetate	-53.8 (2.1)	0.005 to 10
100 mM sodium chloride	-48.1 (2.3)	0.01 to 10

Table 2.2 shows data for sample throughput rates observed for the iodide ISE with the various carriers employed in the portable FIP system. The data indicates that very fast sampling throughput can be achieved in the portable monitor with rates in the range from 73 to 330 injections per hour, depending on the iodide concentration and the carrier employed. The high throughput observed when using Ultrapure water carrier was the opposite to what was expected.

Table 2.2. Sample throughput (injections / hour) observed for the iodide ISE with different carriers in the portable FIP monitor

	Sample Throughput Rates (injection/hour) in Various Carriers		
Iodide standard	Ultrapure water	100 mM Sodium Acetate	100 mM Sodium Chloride
10 mM KI	210	73	103
1 mM KI	223	78	116
0.1 mM KI	262	132	137
0.01 mM KI	330	225	196

The reproducibility of the iodide ISE response in the portable FIP system was determined from 19 replicate injections of 1 mM potassium iodide standard in 100 mM sodium acetate background into the flow stream. The relative standard deviation of the peak heights determined for these replicate injections was found to be 2.1 %.

2.3.2 pH Response of the Tungsten / Tungsten-oxide Coated Wire Electrode

The appearance of the tungsten wire electrode after conditioning in 1.0 M KOH (refer to experimental Section 2.2.6) was a dark brown/blue colouration, suggesting that an oxide layer was formed on the surface of the tungsten wire. The likely form of the tungsten oxide was either tungsten dioxide (WO_2) which is brown or di-tungsten pentoxide (W_2O_5) which is blue. The mechanisms for the observed pH response by the tungsten oxide coated wire electrode have been reported [32], and the following half-cell reactions (equations 2.1 and 2.2) have been proposed as follows:

$$WO_2 + 4H^+ + 4e \rightleftharpoons W + 2H_2O \qquad (2.1)$$

$$W_2O_5 + 2H^+ + 2e \rightleftharpoons 2WO_2 + H_2O \qquad (2.2)$$

Therefore, a Nernstian one electron slope for the pH response of the tungsten-oxide wire electrode was expected.

The tungsten oxide coated wire exhibited a sub-Nernstian electrode slope of 44.8 ± 0.5 mV change per pH unit over the pH range of 2.2 to 11.0 in the steady-state mode. In a different study, a similar electrode slope was observed for an antimony/antimony oxide electrode response for pH in the FIP mode [24]. It was suggested that the possible reason for the observed sub-Nernstian response exhibited by the tungsten oxide electrode could be due to the interference by dissolved oxygen that was present in the universal pH buffer solutions [29]. Performing the same pH potentiometric measurements with tungsten oxide electrode in a closed system where the dissolved oxygen was removed from the universal pH buffer solutions by bubbling nitrogen gas, resulted in an improved electrode slope of 56.0 ± 0.9 mV change per pH unit over the same pH range mentioned above in the steady-state mode, as shown in Figure 2.5.

It is clear that the removal of dissolved oxygen improves the electrode response of the tungsten oxide coated wire electrode to pH in the steady-state mode. Regardless of the interference that dissolved oxygen has on the tungsten oxide coated wire electrode, the observed electrode response was linear in the pH range 2.2 and 11.0 and a slope of 44.8 mV change per pH unit is analytically useful provided that the oxygen concentration is constant.

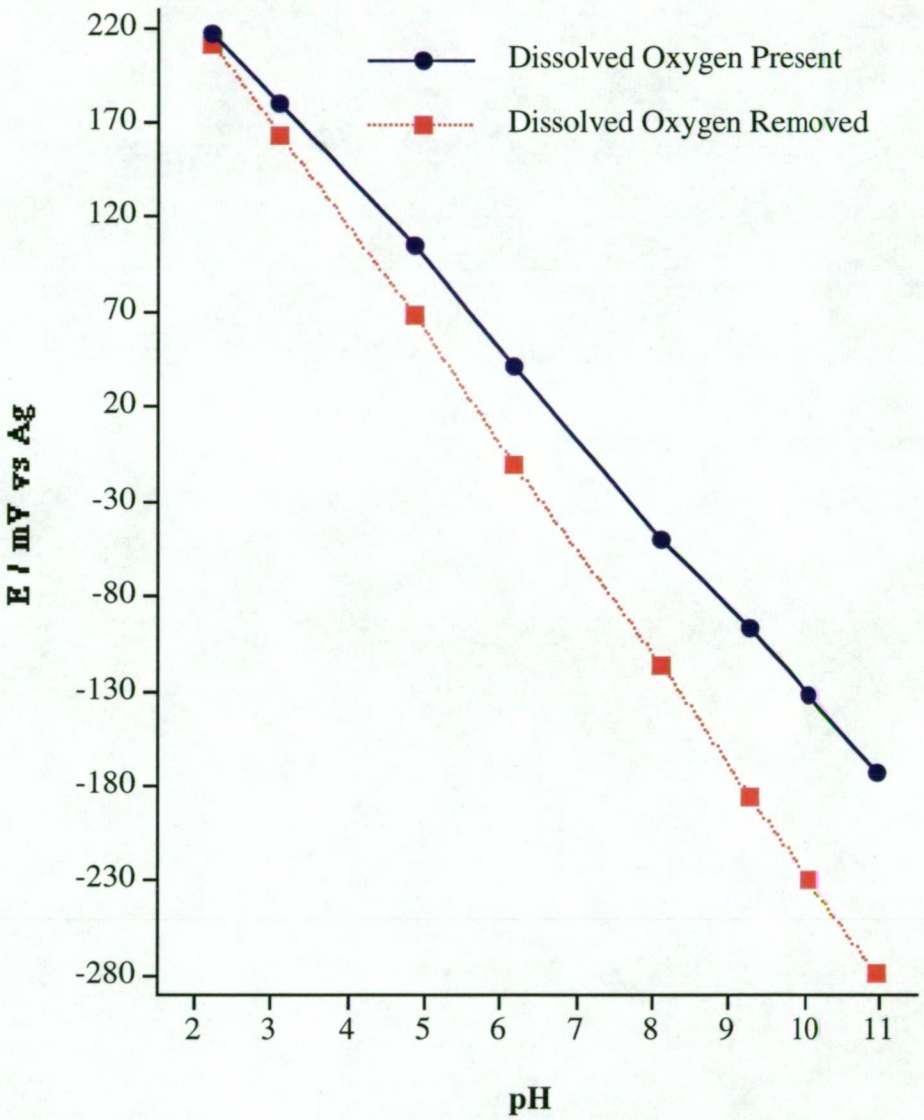

Figure 2.5. Effect of dissolved oxygen absent and present in universal pH buffer solutions has on the pH response of the tungsten oxide coated wire electrode in the steady-state mode.

2.3.3 Criteria for Performing Reliable pH Measurements in FIP

As shown in recent studies [6,30-32], performing reliable pH measurements in FIP requires three main conditions to be met. Firstly, the dispersion of the injected sample zone needs to be minimised for the peak height to be a true measure of the sample's pH and this can be achieved by minimising the distance between the injection valve and the detector [6]. Secondly, the buffer capacity of the injected sample must be at least 10 times greater than the carrier, otherwise the ΔpH between the carrier and the injected sample as a result of dispersion will be large and the pH measurement will be incorrect [6]. In addition recent work has concluded that minimised dispersion is aided when employing a carrier at pH close to 7.0. If a sample of low buffering capacity is to be measured for pH in the FIP mode, then increasing the sample volume (eg. 150 μL to 300 μL) will counter the effect of the carrier stream buffer as well as minimise the dispersion of the sample zone [6]. Thirdly, the pH difference between the carrier and the sample should not be too large and within 2 pH units, unless the sample is known to have a high buffer capacity [31].

2.3.4 The Performance of the Tungsten / Tungsten-oxide Coated Wire Electrode in FIP

The carrier used for pH measurements in the FIP mode was the universal buffer pH 7.20, and the tungsten oxide wire exhibited an electrode slope of 42.4 ± 0.9 mV change per pH unit over the range pH 2.2 to 11.0, and typical peak heights are presented in Figure 2.6. No attempt was made to remove dissolved oxygen presented in the pH buffer solution employed since it would not be practical in a portable FIP system and the observed 42.4 mV change per pH unit was analytically useful.

The peak heights observed represent 95% of the steady-state value and the peak widths observed were 5 seconds. Injecting pH standards 3.10 and 2.23 resulted in a reproducible negative response after the positive response corresponding to the hydrogen ion, as shown in Figure 2.6. The reason for the observed negative response is not clear, but it could be due to an interaction between the injected sample zone and the silver reference wire employed. However this argument is speculation.

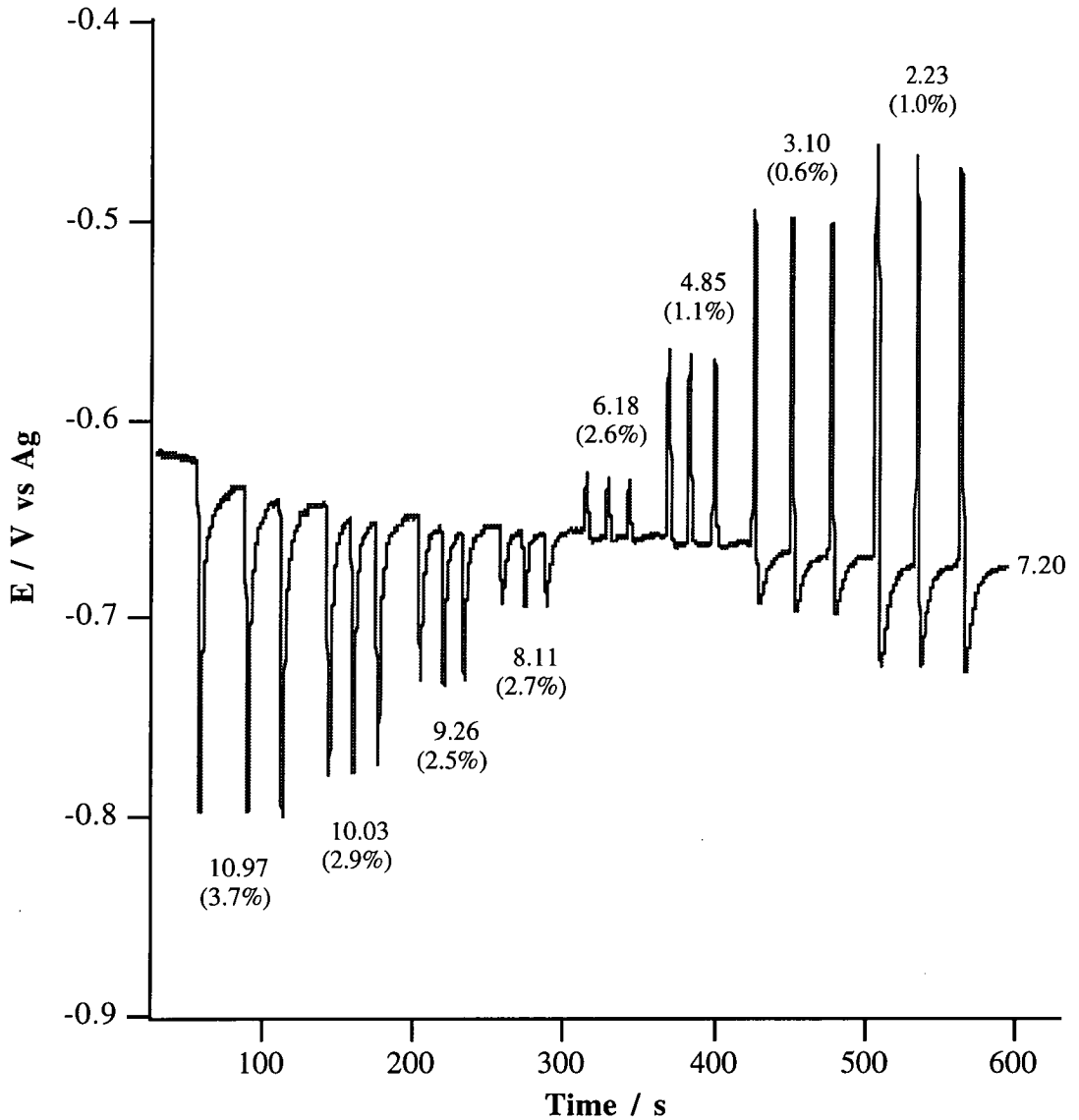

Figure 2.6. Typical FIP response observed for the tungsten oxide electrode to pH changes. Sample injection volume was 200 µL and flow rate was 2.8 mL/min and carrier was pH 7.20 universal buffer. Percentages in parentheses refer to peak height precision.

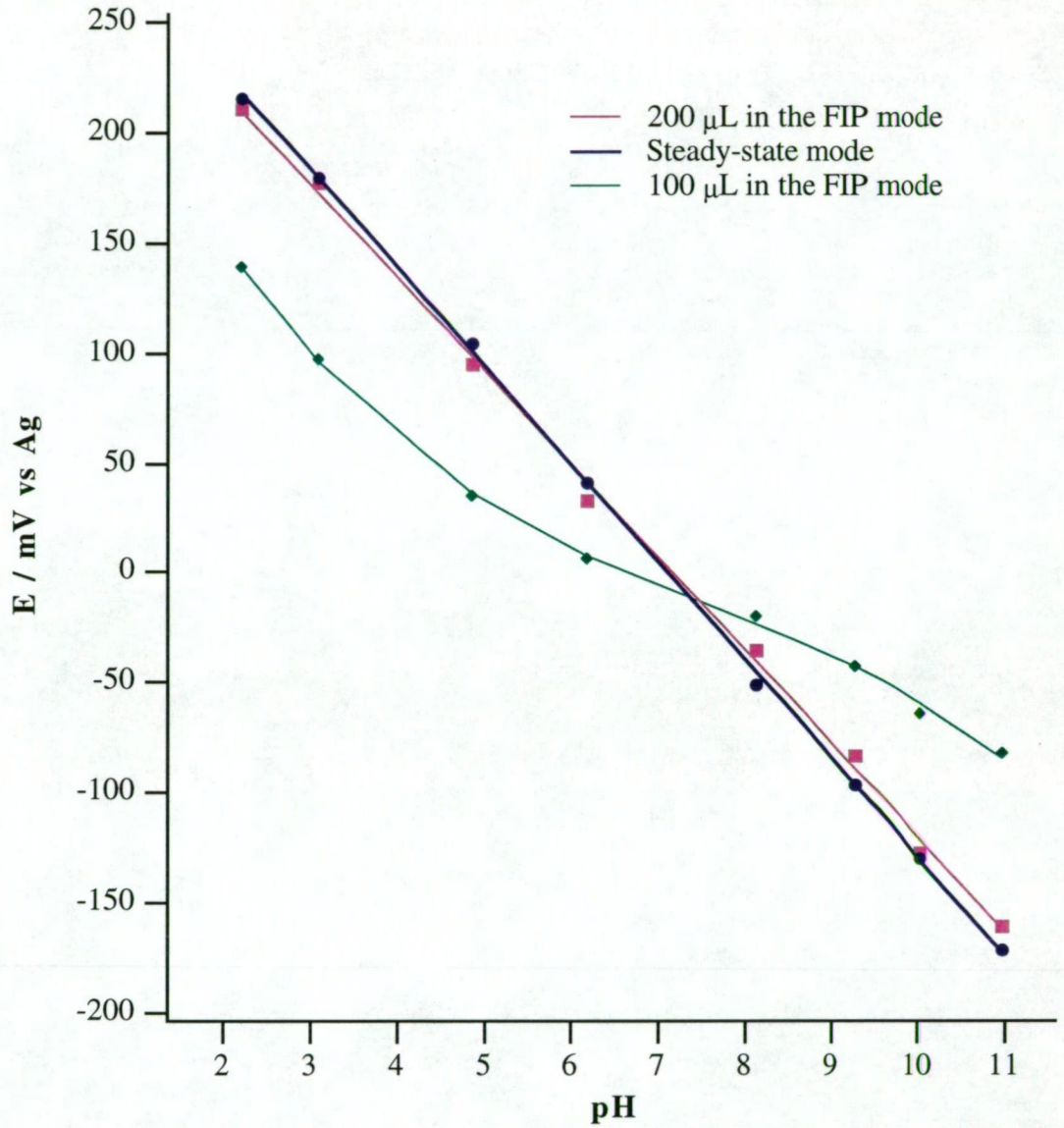

Figure 2.7. Comparison of the calibration plot of the pH electrode (tungsten oxide) in steady-state and FIP modes with different sample volumes. Carrier used for the FIP measurements was universal pH buffer pH 7.20 and flow rate was 2.8 mL/minute.

The tungsten oxide electrode thus exhibited a fast response and minimal dispersion of the injected sample zone was achieved in the FIP mode. A baseline drift of 5 mV / hour was observed with the tungsten oxide wire, however, an electrode drifting in the FIP mode has little effect on calibrations since data processing can account for this when calculating peak heights. Calibration plots of the response of the tungsten oxide coated wire electrode to pH standards injected into universal pH 7.20 buffer carrier are presented in Figure 2.7.

Lowering the sample volume from 200 to 100 μL resulted in a non-linear calibration plot over the pH range between 2.2 and 11.0 (Figure 2.7). Reducing the injected sample volume increases the dispersion leading to a significant change of the true pH of the sample zone [6,30], in agreement with recent studies [6]. In addition, the influence of the carrier's buffer capacity was considerably greater on the 100 μL sample volume than on the 200 μL sample volume in the FIP mode.

2.3.5 Interferences on the Tungsten/Tungsten-oxide Electrode Response

In previous studies, tungsten based electrodes have exhibited a response towards alkali and transition metal ions in solution [20,34]. The common ions present in beverages and environmental bodies of water are potassium and sodium ions. The tungsten oxide electrode exhibited a response to potassium and sodium ions in the FIP mode. Therefore, to determine the pH of water samples such as tank water, river and seawater it would be necessary to correct for any cation response other than hydrogen, by introducing the interfering cation into the carrier stream.

Figure 2.8 shows the effect of increasing the sodium chloride concentration in a 100 mM tris(hydroxymethyl)methylamine (TRIS) solution (pH = 9.10) has on the peak height. In this case the carrier was 0.1 mM citric acid at pH 3.3 and contained no sodium chloride. The presence of 10 mM sodium chloride in the 100 mM TRIS solution (pH = 9.10), significantly reduces the peak height by 15 mV compared to the TRIS solutions containing 1 mM sodium chloride and no sodium chloride (both pH = 9.10). This would obviously result in an inaccurate pH measurement if the interfering ions in samples were not matched in the pH standards used and the carrier stream. Similar behaviour was observed when replacing sodium chloride with sodium nitrate, which eliminates chloride ion interference to the silver reference contributing this observation.

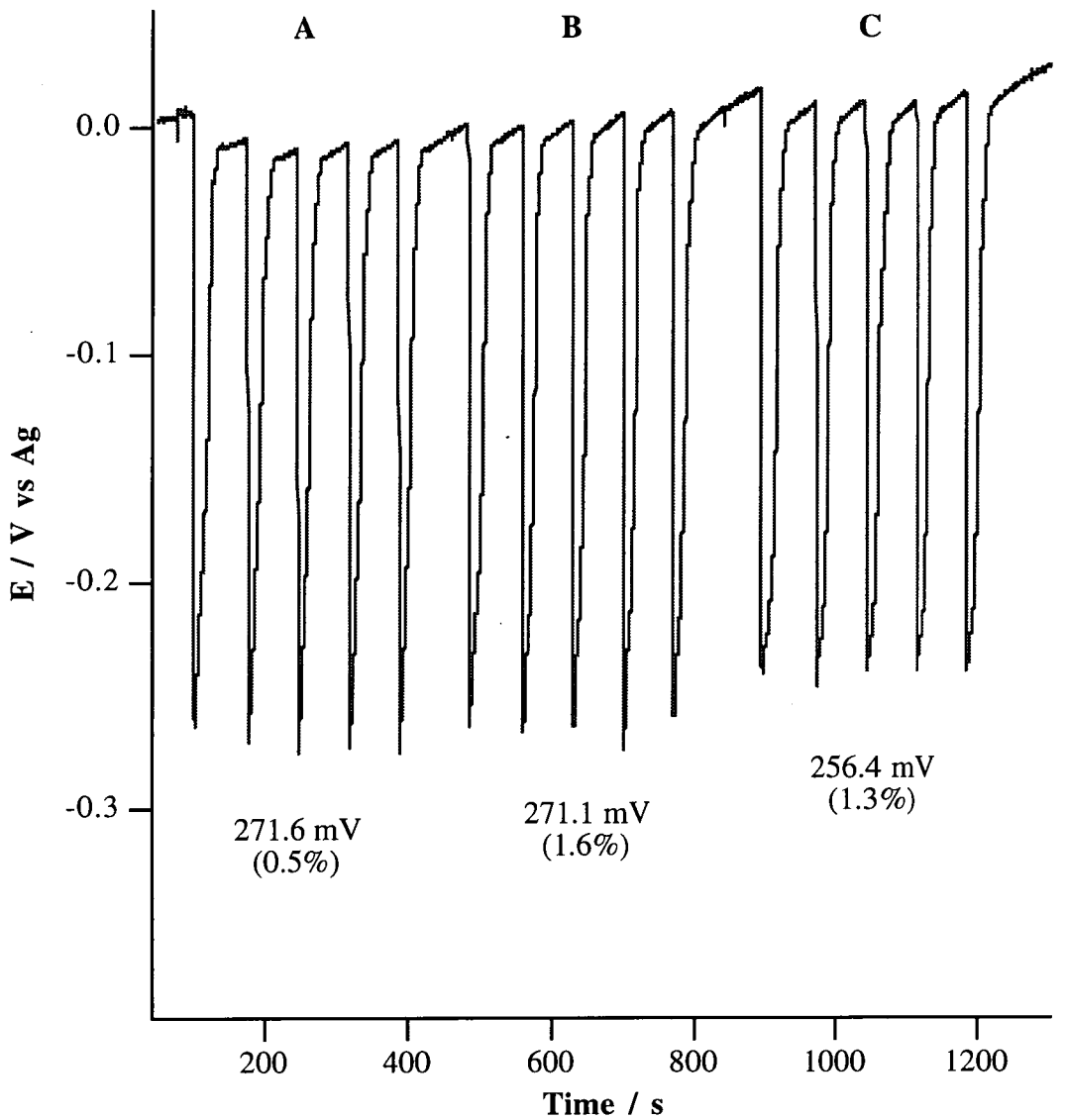

Figure 2.8. Effect of increasing NaCl has on the pH response using 100 mM TRIS solutions containing (**A**) nil NaCl, (**B**) 1 mM NaCl, and (**C**) 10 mM NaCl all pH = 9.10; carrier was 0.1 mM citric acid (pH = 3.3), flow rate = 1.8 mL/minute and sample volume = 200 µL. Percentages in parentheses are RSD for peak height precision.

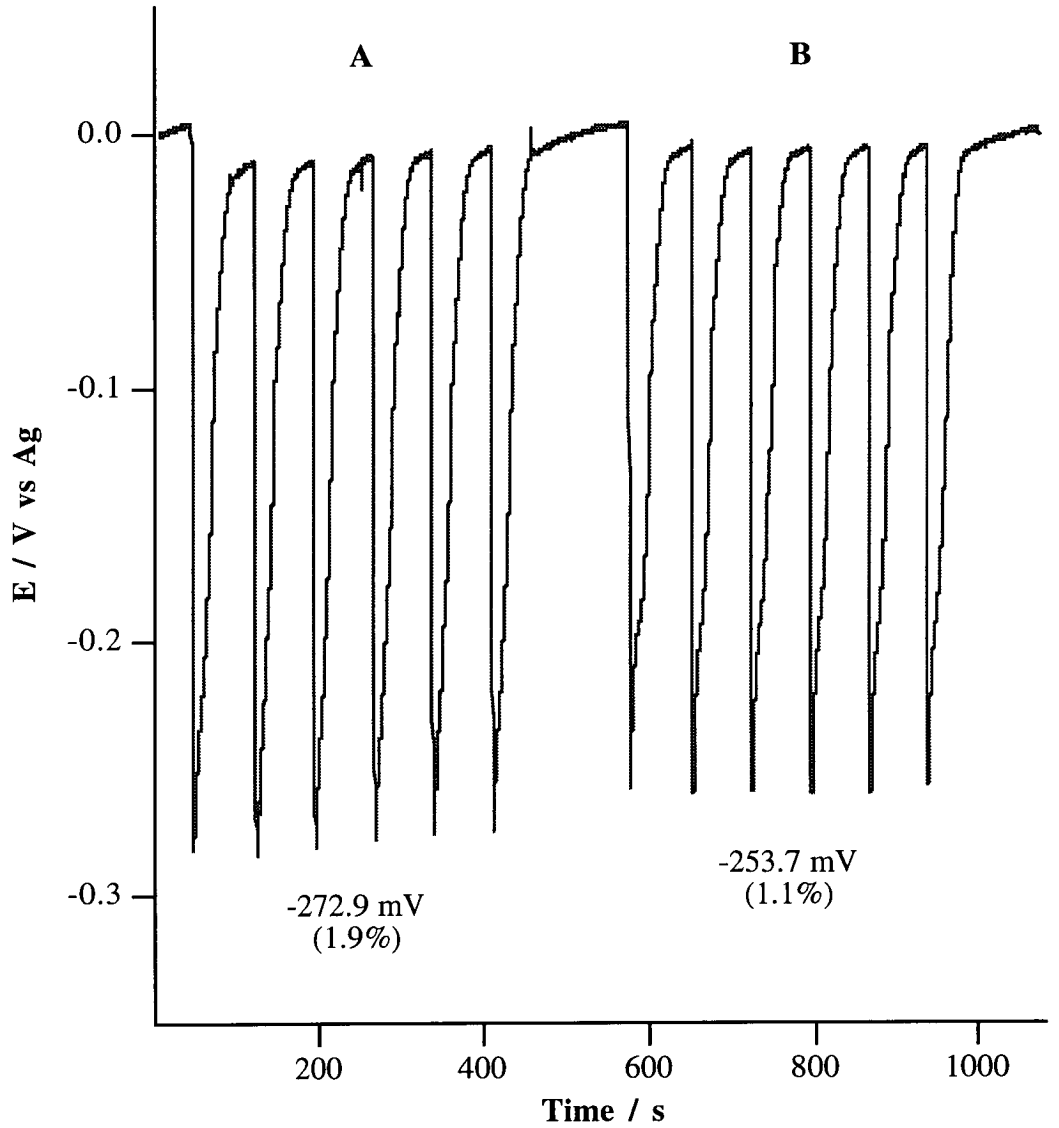

Figure 2.9. Effect of increasing ascorbic acid has on the pH response using 100 mM TRIS solutions containing (**A**) nil ascorbic acid and (**B**) 1 mM ascorbic acid both pH = 9.10 in the FIP mode; carrier was 0.1 mM citric acid (pH = 3.3), flow rate = 1.8 mL/minute and sample volume = 200 µL. Percentages in parentheses refer to RSD for peak height precision.

Similarly, the presence of reducing agents in the sample can also affect the pH response. Figure 2.9 exhibits the effect of ascorbic acid has on the peak height of the 100 mM TRIS solution at pH 9.10. In this case, the addition of 1 mM ascorbic acid in the 100 mM TRIS solution (pH = 9.10) resulted in a 20 mV reduction in the peak heights.

2.3.6 Determination of the pH of Alcoholic Samples

Various alcoholic beverages were analysed using the portable pH FIP system. As described previously [6,30], it is important that the buffer capacity of the carrier solution be at least 10 times lower than the samples so that minimal dispersion is maintained. Alcoholic beverages such as wine, port, low alcohol beers and regular beers were analysed for pH in the FIP mode. These beverages have a high salt content, and therefore the ionic strengths of these samples were high. It was found that the pH 7.20 universal buffer as a carrier was adequate and approximated the ionic strength of these alcoholic beverages for the determination of pH. The pH results obtained with the portable pH system were in good agreement with glass electrode measurements as shown in Table 2.3.

Table 2.3. Determined pH of Various Alcoholic Beverages.

Sample	pH (FIP)[a]	pH (Glass Electrode)
Red wine	3.23	3.21
Port	3.49	3.56
Light Beer	4.09	4.15
Normal Beer	4.05	4.09

a - Carrier was universal pH buffer (pH = 7.20), flow rate was 3.1 mL/min and sample volume was 200 µL.

2.3.7 Determination of the pH of Aqueous Samples

A practical problem encountered with potentiometric pH measurements of low ionic strength aqueous samples, such as tank water and river water, is the accuracy of the result. The main contribution to errors in potentiometric pH measurements arise when neglecting liquid junction potentials [35], inorganic salts present and the ionic strength [36] of these samples.

To determine the pH of water samples, such as tank water and river water in the FIP mode, requires a carrier with a significantly lower buffer capacity than that of the samples

[6,30]. In addition, the dispersion of the injected sample zone needs to be minimised. Table 2.4 summarises the pH of various water samples determined by FIP and a glass electrode. In this study, the carrier used to determine the pH of tank water and river water was 10 mM NaCl / 0.01 mM sodium tetraborate (pH = 9.40). The 10 mM NaCl in the carrier was necessary to match the ionic strength of the water samples, namely the river and tank water samples. Performing pH measurements with these water samples without the NaCl present in the carrier resulted in an inaccurate result, due to the additional response to interfering ions present in these water samples. Therefore, to determine accurate pH measurements of water samples in the FIP mode, it is crucial that interfering ions are corrected by including these ions in the carrier. The pH measurements determined for the tank water and the river water samples were in good agreement with glass electrode measurements as shown in Table 2.4.

Table 2.4. Determined pH of Various Water Samples (n = 3).

Sample	pH in FIP (RSD)[a]	pH Glass Electrode
Tank water	8.10 (2.1 %)[b]	8.04
Tamar river	7.76 (1.5 %)[b]	7.81
Derwent river	7.85 (1.1 %)[b]	7.87
Seawater	8.05 (2.3 %)[c,d]	8.04[d]

a - RSD values denotes the precision of the peak heights.
b - Carrier was 10 mM NaCl / 0.01 mM $Na_2B_4O_7$ (pH = 9.40), flow rate was 3.2 mL/min and sample volume was 200 µL.
c - Carrier was 600 mM NaCl / 0.01 mM $Na_2B_4O_7$ (pH = 9.53), flow rate was 1.8 mL/min and sample volume was 200 µL.
d - Corrected for liquid junction potential.

To determining the pH of seawater which has a high ionic strength, it was necessary to correct for the high sodium content in this sample, since the sodium ion is by far the most abundant ion in seawater. In the FIP mode, the most suitable carrier used for the pH measurement of seawater was 600 mM NaCl / 0.01 mM sodium tetraborate (pH = 9.53). It was also necessary to correct for the liquid junction potentials for both the glass electrode and the tungsten wire electrode using the Henderson equation [35] for the results to agree.

2.4 Conclusion

The above results show that the FIP system described can be operated in a totally portable manner with low power consumption using six 1.2 Volt Ni-Cd rechargeable battery-pack to run the analog-to-digital converter and the peristaltic pump for up to three hours before recharging was required. The use of a notebook computer allows for real time plotting of data at remote locations away from conventional laboratories. This was demonstrated with the application of an Orion iodide ISE as an example of a commercial ISE and the tungsten oxide pH electrode used with the portable FIP system described.

The electrode response observed for the iodide ISE in the FIP mode exhibited near-Nernstian to super-Nernstian response depending on the carrier and ionic background employed. The optimum log-linear range observed in the FIP mode was between 0.005 mM and 10 mM. The FIP response observed for the iodide ISE represents 80% of the steady-state value and performance exhibited was analytically useful for remote-site monitoring.

The tungsten oxide coated wire electrode was applied to the portable FIP system as an example of a miniaturised pH electrode. The tungsten oxide coated wire electrode exhibited a sub-Nernstian response of 44.8 ± 0.5 mV change per pH unit over a pH range between 2.2 and 11.0 in the steady-state mode. It was shown that the presence of dissolved oxygen in the universal pH buffer solutions was the reason for the sub-Nernstian response of the tungsten oxide electrode. The tungsten oxide coated wire electrode exhibited a fast response and the FIP response represented 95% of the steady-state value.

The tungsten oxide coated wire electrode is more robust, easily miniaturised and is a low cost alternative in comparison with a glass or liquid polymer membrane based electrode. However, for accurate pH measurements in the FIP mode, it was important to account for interferences from other cations and reducing agents present in the sample of interest.

2.5 References

1. Horiba Ltd (Japan), 'Cardy Na^+, K^+ and NO_3^- Ion Meter', Bulletin: HRE-1127A, (1994).

2. Horiba Ltd (Japan), 'Compact pH meter, TWINpH', Bulletin: HRE-1138A, (1994).

3. K. S. Johnson, C. M. Sakamoto-Arnold and C. L. Beehler, 'Continuous determination of nitrate concentrations in situ', Deep-Sea Research, **36**, 1407 - 1413, (1989).

4. K. S. Johnson, C. L. Beehler, and C. M. Sakamoto-Arnold, 'A submersible flow analysis system', Analytica Chimica Acta, **179**, 245 - 257, (1986).

5. K. N. Andrew, N. J. Blundell, D. Price and P. J. Worsfold, 'Flow injection techniques for water monitoring', Analytical Chemistry, **66**, 917A - 922A, (1994).

6. J. Ruzicka and E. H. Hansen, 'Flow Injection Analysis', 2nd ed., John Wiley and Sons, New York, (1987).

7. A. M. Bond, D. L. Luscombe, S. N. Tan and F. L. Walter, 'A battery-powered, microprocessor controlled, programmable function generator for field-based stripping voltammetry with conventional and microsized electrodes', Electroanalysis, **2**, 195 - 202, (1990).

8. G. Williams and C. D'Silva, 'Hand-held instrumentation for environmental monitoring', Analyst, **119**, 187 - 190, (1994).

9. J. Wang, N. Foster, S. Armalis, D. Larson, A. Zirino and K. Olsen, 'Remote stripping electrode for in situ monitoring of labile copper in the marine environment', Analytica Chimica Acta, **310**, 223 - 231, (1995).

10. J. Wang and Q. Chen, 'Remote electrochemical biosensor for field monitoring of phenolic compounds', Analytica Chimica Acta, **312**, 39 - 44, (1995).

11. J. Koryta, 'Theory and applications of ion-selective electrodes', Analytica Chimica Acta, **206**, 1 - 48, (1988).

12. R. L. Solsky, 'Ion-selective electrodes', Analytical Chemistry, **62**, 21R - 33R, (1990).

13. H. Hara, N. Ishio and K. Takahashi, 'High speed potentiometric analyzer equipped with an ion-selective electrode detector', Analytica Chimica Acta, **281**, (1993) 45.

14. P.W. Alexander and G.A. Rechnitz, 'Automated protein determination with ion-selective membrane electrodes', Analytical Chemistry, **46**, 860 - 865, (1974).

15. P.W. Alexander and P. Seegopaul, 'Rapid-flow continuous analysis with ion-selective electrode', Analytical Chemistry, **52**, 2403 - 2406, (1980).

16. M. Valcarcel and M. D. Luque de Castro, 'Flow Injection Analysis: Principles and Applications', Ellis Horwood: Chichester, UK, 1987.

17. P. Schulthess, Y. Shijo, H. V. Pham, E. Pretsch, D. Ammann and W. Simon, 'Hydrogen-ion-selective liquid polymer electrode based on tridodecylamine as neutral carrier', Analytica Chimica Acta, **131**, 111 - 116, (1981).

18. U. Oesch, Z. Brzozka, A. Xu, B. Rusterholz, G. Suter, H. V. Pham, D. H. Welti, D. Ammann, E. Pretsch and W. Simon, 'Design of neutral hydrogen ion carriers for solvent polymeric membrane electrodes of selected pH range', Analytical Chemistry, **58**, 2285 - 2289, (1986).

19. C. Aquinobinag, P. J. Pigram, R. N. Lamb and P. W. Alexander, 'Surface studies of quinhydrone pH sensors', Analytica Chimica Acta, **291**, 65, (1994).

20. M. A. Wechter, H. R. Shanks, G. Carter, G. M. Ebert, R. Guglielmino and A. F. Voigt, 'Use of metal tungsten bronze electrodes in chemical analysis', Analytical Chemistry, **44**, 850 - 853, (1972).

21. S. Alegret, J. Alonso, J. Bartroli, J. Domenech, N. Jaffrezic-Renault and Y. Duvault-Herrera, 'Flow-through pH-ISFET detector for flow injection analysis', Analytica Chimica Acta, **222**, 373 - 377, (1989).

22. S. Alegret, J. Bartroli, C. Jimenez-Jorquera, M. del Valle, C. Dominguez, J. Esteve and J. Bausells, 'Flow-through pH-ISFET and reference-ISE as intergrated detector in automated FIA determinations', Sensors and Actuators, **B7**, 555 - 560, (1992).

23. W. P. Geus, A. J. P. M. Smout, J. C. Kooiman, C. B. H. W. Lamers and J. W. Geus, 'Glass and antimony electrode for long term pH monitoring - A dynamic in vitro comparison', European Journal of Gastroenterology and Hepatology, **7**, 29 - 35, (1995).

24. M. D. Capelato, A. M. dos Santos, O. Fatibello-Filho and R. Gama, 'Flow injection potentiometric determination of coke acidity and acetic acid content in vinegar using an antimony electrode', Analytical Letters, **29**, 711 - 724, (1996).

25. D. C. Roberts, J. A. Osborn and A. M. Yacynych, 'Proteolytic enzyme modified metal-oxide electrodes as potentiometric sensors', Analytical Chemistry, **58**, 140 - 144, (1986).

26. P. W. Alexander and J. P. Joseph, 'Coated-metal enzyme electrode for urea determination', Analytica Chimica Acta, **131**, 103 - 109, (1981).

27. R. M. Iannilleo and A. M. Yacynych, 'Urea sensor based on iridium dioxide electrodes with immobilised urease', Analytica Chimica Acta, **146**, 249 - 253, (1983).

28. D. A. Skoog and D. M. West, 'Fundamentals of Analytical Chemistry', CBS Publishings, 4th edn., Japan, (1982), p 118.

29. M. Trojanowicz, Private Communication, University of Warsaw, Poland (1995).

30. C. Hongbo, E. H. Hansen and J. Ruzicka, 'Evaluation of critical parameters for measurement of pH by flow injection analysis: Determination of pH in soil extracts', Analytica Chimica Acta, **169**, 209 - 220, (1985).

31. P. C. Hauser, T. J. Cardwell, R. W. Cattrall, S. S. Tan and I. C. Hamilton, 'Measurtements of pH by flow injection over a wide dynamic range with PVC/neutral carrier electrodes', Analytica Chimica Acta, **221**, 139 - 146, (1989).

32. F. R. del Mundo, T. J. Cardwell, R. W. Cattrall, P. J. Iles and I. C. Hamilton, 'An ultraviolet-cured pH-sensitive membrane electrode for use in flow injection analysis', Electroanalysis, **1**, 353 - 356, (1989).

33. 'CRC Handbook of Chemistry and Physics', 59th edn., R. C. Weast Ed., CRC Press Inc., Florida, page D-195, (1978).

34. Z. Chen, PhD Thesis, University of New South Wales, (1994).

35. R. G. Bates, 'Determination of pH, Theory and Practice', John Wiley and Sons, 2nd ed., New York, (1973).

36. B. A. Woods, J. Ruzicka, G. D. Christian, N. J. Rose and R. J. Charlson, 'Measurement of rain-water pH by optosensing flow injection analysis', Analyst, **113**, 301 - 306, (1988).

Chapter Three: Application of an Array of Commercial ISEs with the Portable Flow Injection Potentiometric System.

3.1 Introduction

This chapter was aimed at developing and evaluating a three-ion-selective electrode (ISEs) array with the portable FIP system described in Chapter two. The three ISEs used in the described arrayed were commercial planar designed sensors and were chosen for their small size and were relatively inexpensive compared to other commercially available ISEs.

Employing an array of ISEs in a flow through technique, such as flow injection potentiometry (FIP), results in a system that can measure multiple ion species in a sample of interest. Additional advantages are excellent peak height precision (typically < 3%), fast sample throughput rate (> 120 injections/hr) and the use of small sample volumes (≤ 300 μL) [1]. Converting this technology into a portable battery-powered FIP system employing an array of ISEs as detectors would allow the operator to conduct FIP measurements at remote site locations, and observe the response of each ISE simultaneously in real time.

Recent publications on ISE array systems employ chemometric methods for the optimisation of the individual ISEs in a particular array. These statistical methods were used to either improve the selectivity of the individual ISEs in the array or estimate the slope, the selectivity coefficient and the cell constant (E') for each ISE. The statistical methods that have been employed are partial least squares [2], non-linear regression [3], simplex optimisation [4,5] and projection pursuit regression [6,7]. An interesting statistical treatment which is of considerable benefit to the response of ISE arrays is the 'over-determined' approach to their arrays, for example, where eight ISEs were used to measure four different ions in aqueous solution [5]. Although the above mentioned statistical treatments are useful, they are impractical for portable FIP systems using ISE array detectors that are dedicated for remote-site monitoring. Therefore, it is a desirable that the ISEs to be used in an array for a portable FIP system are selective enough to avoid interference with a range of interfering ions present in both standards and samples.

A miniature array of coated-film based ISEs was developed to detect pH, potassium, sodium and calcium ions in aqueous solutions, with a possible low-cost application to clinical

analyses in the steady-state mode [8]. The array of coated-film ISEs were fixed on a polycarbonate sheet. The construction of each of these coated-film based ISEs was achieved by laminating each poly(vinyl chloride) membrane onto a silver substrate. The array of ISEs responded in a Nernstian fashion over a wide concentration range in steady-state measurements.

Screen printing technology has been applied to the development of liquid polymer membrane based miniature electrodes onto a multisensing chip, namely ammonium, calcium, hydrogen and potassium [9]. The screen printing technique developed in this report was reproducible and cost effective for mass production. Typical electrode response observed for the sensors on this multisensing chip were 59.3 mV / decade for potassium, 18.0 mV/decade for calcium, 53.4 mV/decade for ammonium, and 79.4 mV/pH unit for hydrogen over a wide pH range in the flow injection mode.

A miniature flow cell design containing four coated-wire based electrodes has been developed [10], in which the four ISEs and the silver/silver chloride wire reference electrode were placed in separate flow channels that merged down stream. The four CWEs used in this flow cell were potassium, calcium, nitrate and chloride and were used to determine the above-mentioned ions in soil extracts. The entire system, incorporating the flow cell, an analog-to-digital converter (ADC), computer and peristaltic pump relying on mains power supply, was used as a desktop instrument . However, the flow cell design could be incorporated into a portable FIP system. The identical miniature flow cell was also used to measure the hydrogen ion over a pH range was between 1 - 13 using two different PVC based hydrogen electrodes, whereby the pH range of each electrode overlapped [11]. Along with hydrogen ion they also determined calcium and potassium ions simultaneously in the FIP mode.

Research and development in sensor arrays used in the flow injection mode have also been reported using ion-selective field effective transistors (ISFETs) as miniature electrochemical sensors [12-15]. Arrays of ISFETs have been applied to sensing pH, potassium, and calcium ions in aqueous solutions in the FIP mode [12,14]. Some studies have also included sodium sensors in the above-mentioned array of ISFETs [13]. A recent study reported on a continuous flow system employing an ammonium, hydrogen, calcium and nitrate

sensor array on an ISFET and was applied successfully for on-line monitoring of various water samples, such as, sea, river and tap water samples [15].

Although there have been advances with multi-analyte potentiometric measurements, there seems to be no reported papers on portable battery-powered FIP systems for potentiometric multi-ion determinations with low weight and power consumption. The main objective of the work presented in this chapter was to determine the feasibility of multi-ion determination of three selected ions simultaneously, in this case with available commercial planar-type electrode sensors for potassium, sodium, and nitrate using the portable FIP system described in the previous chapter. The reliability of this portable FIP system was evaluated by determining nitrate, sodium and potassium levels in natural mineral water samples, as an example of a remote-site monitoring system and the FIP results were compared with other analytical methods such as atomic absorption spectrometry and polarography.

3.2 Experimental

3.2.1 Materials

The following reagents were used as received: potassium nitrate (BDH, AnalaR), sodium nitrate (BDH, AnalaR), calcium chloride (BDH, AnalaR) and magnesium sulfate (BDH, AnalaR). Ultrapure water (Barnstead Ultrapure water systems, 18.0 MΩ cm) was used throughout this work. The standard potassium, sodium and nitrate solutions were prepared by serial dilution from a stock solution containing 100 mM potassium nitrate and sodium nitrate mixture.

3.2.2 Design of the Ion-selective Electrode Array Flow-through Cell

The nitrate, sodium and potassium ISEs were planar type sensors, each with their own inbuilt reference electrode were purchased from Horiba Ltd (Japan) and were the only electrodes available commercially in this design [16]. The sensing membranes of the nitrate, sodium and potassium ISEs were PVC based, however, the compositions of each liquid polymer membrane were unknown. It was assumed that these planar electrodes employed the more popular ionophores, such as valinomycin for the potassium ISE, N,N',N"-triheptyl-N,N',N"-trimethyl-4,4',4"-propylidynetris(3-oxabutyramide), (ETH 227) for the sodium ISE,

and tetradodecylammonium nitrate for the nitrate ISE. The three planar type ISEs were positioned in a serial arrangement in a flow-through cell, whereby the carrier solution can travel over the surface of the sensing membranes in turn. A schematic diagram of the electrode flow cell design housing the three planar type ISEs in a serial arrangement is given in Figure 3.1.

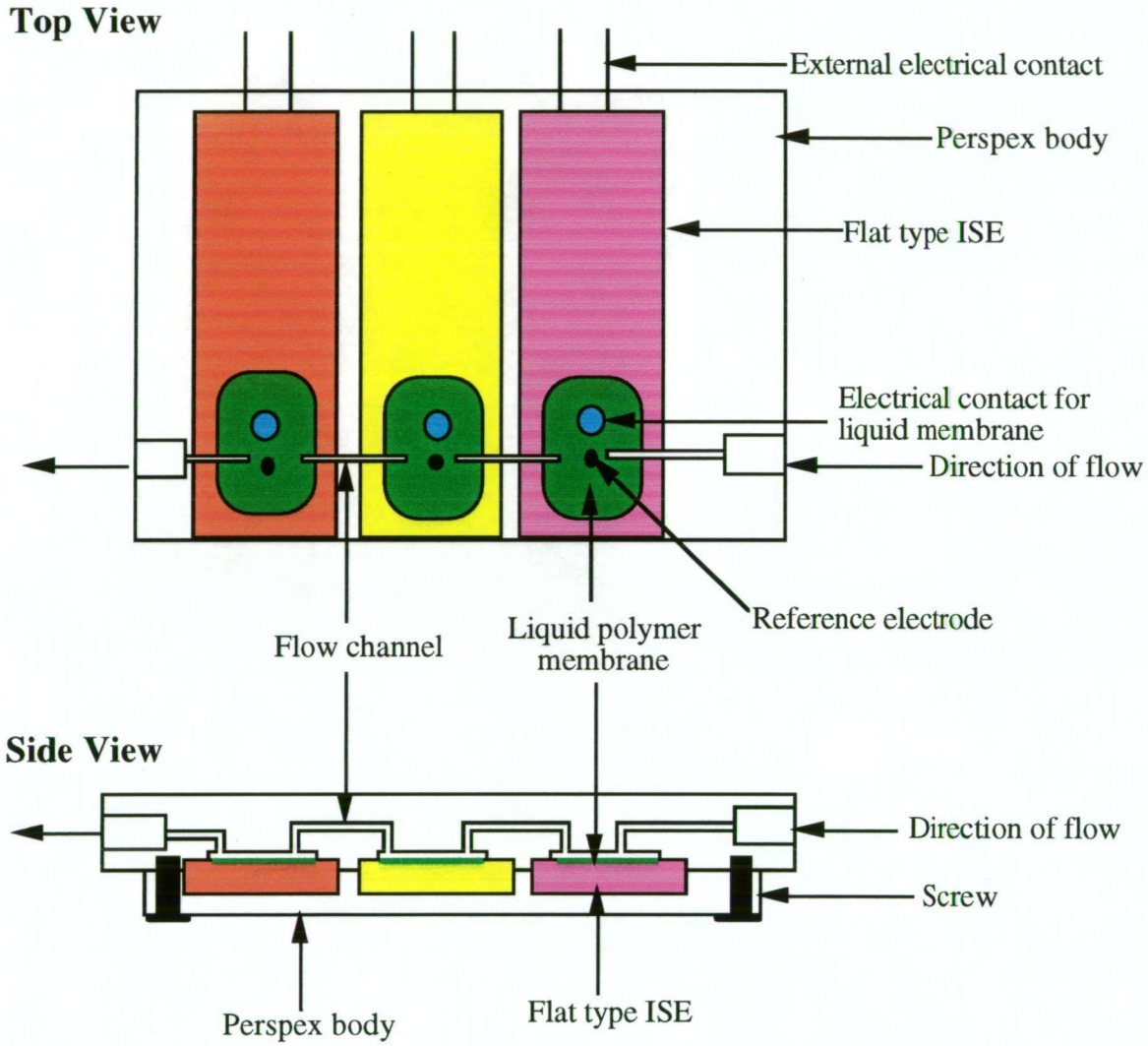

Figure 3.1. A diagram of the flow-through cell that housed the planar type nitrate, potassium and sodium ISE array.

3.2.3 Potentiometric Measurement Procedure

The ISE array flow cell illustrated in Figure 3.1 was used with the portable FIP system described in Section 2.2.3. The peristaltic pump was at a fixed speed and the flow rate was 6.8 mL/minute through a single flow channel. The injection volume of the samples and

standards were 200 μL. The injected standards and samples were introduced manually into the carrier solution using a Rheodyne 5020 injection valve.

The ionic activity calculations, data acquisition program, the data analysis and graphical representation of the data procedures described earlier in Chapter two, Section 2.2.4 were employed in the work described in this chapter. The acquired digital data were displayed in real time millivolt readings plotted as a function of time and were saved as text files. A program called MacCurve Fit © Version 0.7 was used to calculate the electrode slope, the E' and the standard deviations (95% confidence) of a given electrode in either steady-state or FIP modes.

3.2.4 Water Samples and Validation Methods

The natural mineral water samples use to validate the 3 ISE array system were Mt Franklin and Deep Spring Water, commonly available in Australian supermarkets. The natural mineral water samples were injected into the portable FIP system as received in an Ultrapure water carrier. The nitrate, sodium and potassium mixed standards contained 1 mM calcium chloride as the background to match the natural mineral water samples.

Validation of the sodium and potassium FIP results were performed using a Varian 1100 atomic absorption spectrometer (AAS). A Metrohm 647 VA Stand polarograph was used to compare the nitrate ion FIP results. In this instance, the nitrate ion present in each sample was converted to o-nitrophenol [17].

3.3 Results and Discussion

3.3.1 Response of the Nitrate, Sodium and Potassium ISEs in the Steady-state mode

The sodium and potassium ISEs both exhibited Nernstian responses of 61.2 ± 1.0 and 60.9 ± 1.1 mV change per activity decade using pure sodium nitrate and potassium nitrate solutions, respectively in the steady-state mode. The log-linear ranges observed for both ISEs were between 0.01 mM and 100 mM and the detection limits were 0.005 mM and 0.003 mM for the potassium and sodium ISEs, respectively. The nitrate ISE exhibited a sub-Nernstian response of -52.1 ± 1.1 mV change per activity decade using pure sodium nitrate solutions in the steady-state mode. The log-linear range was between 0.1 mM and 100 mM and a detection

limit of 0.001 mM. Figure 3.2 presents the calibration plots for the nitrate, sodium and potassium ISE in the steady-state mode.

The sodium and potassium ISEs both exhibited fast responses each taking < 5 seconds to achieve 90% of the steady-state value, therefore making both ISEs suitable for FIP measurements. The nitrate ISE exhibited a fast response taking < 7 seconds to achieve 90% of the steady-state value. A typical step change response observed simultaneously for the nitrate, potassium and sodium ISE array is presented in Figure 3.3. Figure 3.4 presents the selectivity coefficients determined for the nitrate, sodium and potassium ISEs using the matched potential method [18].

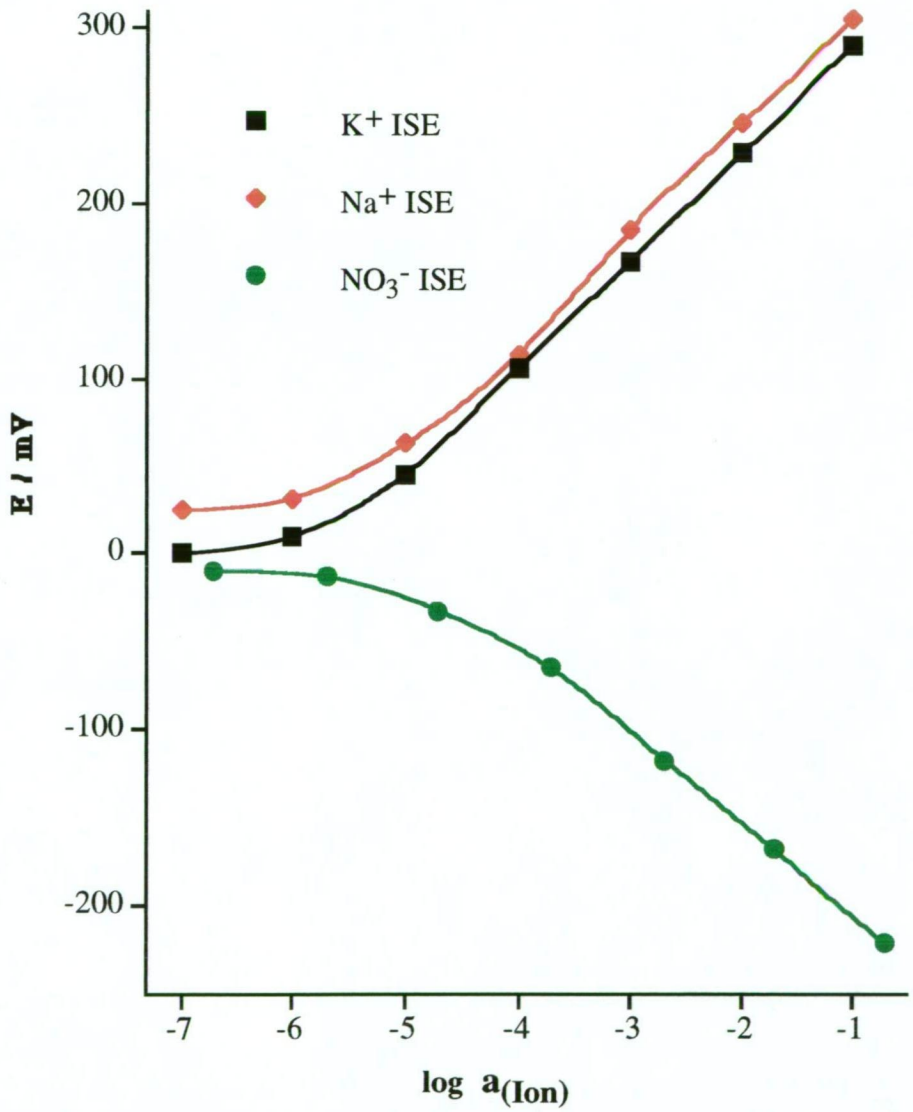

Figure 3.2. Calibration curves for the nitrate, potassium and sodium ISEs simultaneously using mixed $NaNO_3$ and KNO_3 solutions in the steady-state mode.

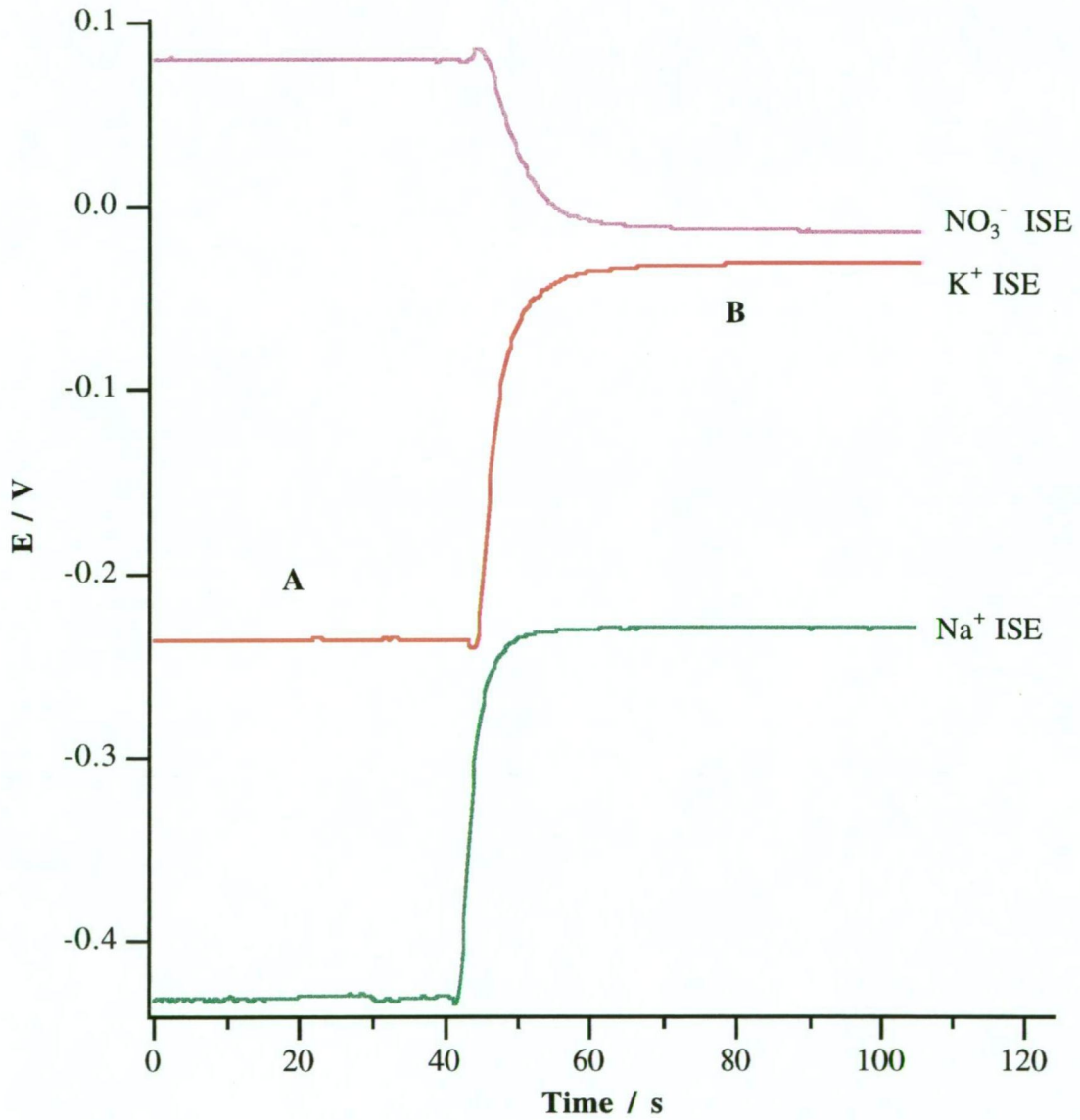

Figure 3.3. The step change response curves for the nitrate, potassium and sodium ISE array from 0.01 mM (**A**) to 10 mM (**B**) $NaNO_3$ - KNO_3 solution mixtures. The response curves are relative potentials.

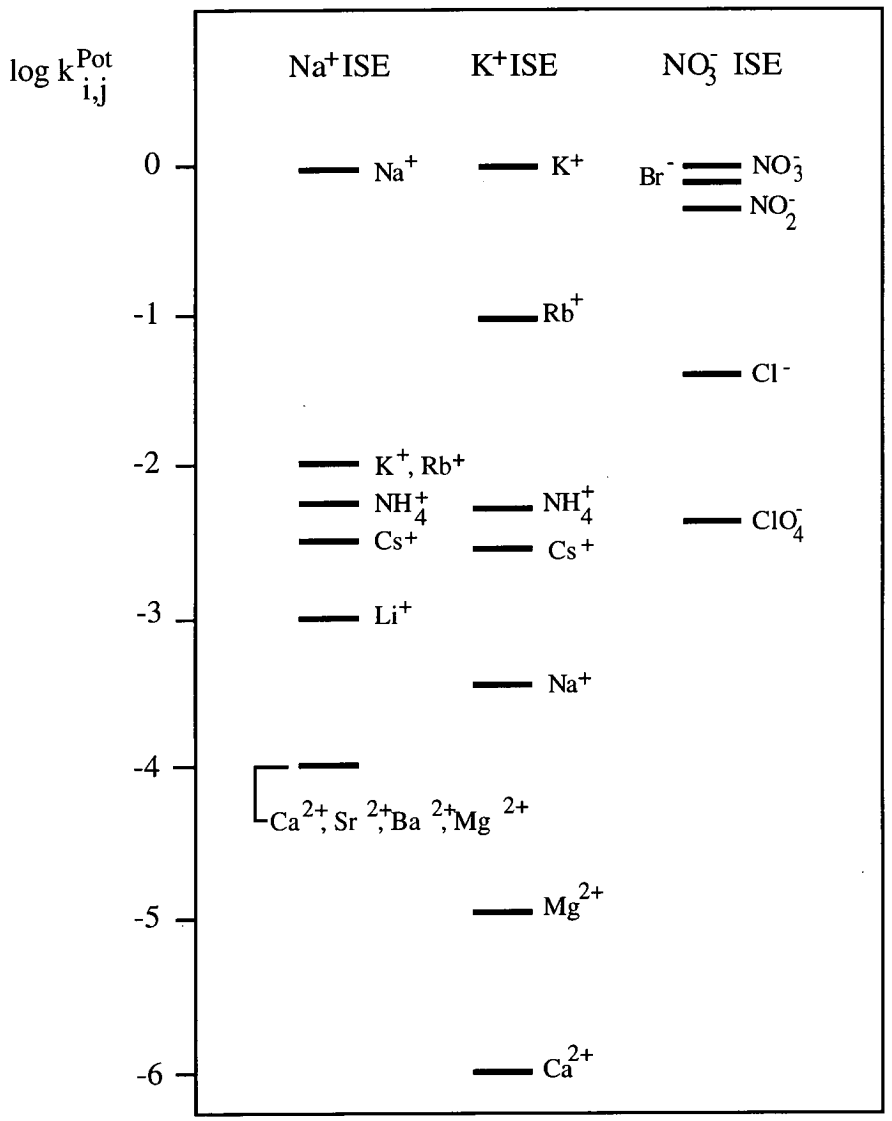

Figure 3.4. The selectivity coefficients determined for the nitrate, potassium and sodium ISEs; i = determinand and j = interfering ion.

3.3.2 FIP Response of the Nitrate, Sodium and Potassium ISE array

With continuous use the operational time of the portable FIP system was 3 hours, while intermittent usage for short time periods allows an operator to conduct numerous remote-site measurements of bodies of environmental water over an entire day before recharging is necessary. The main advantage of applying a multiple ISE array in this portable FIP system, was the data acquisition of each ISE can be observed simultaneously and stored on the notebook computer at remote-site locations. This was useful for monitoring the response of each ISE for samples/standards, as well as being a useful diagnostic tool for the performance of the system.

The results of using the portable FIP system with the ISE array are described below for the individual sensors used. It was determined that the optimum carrier to be used for the ISE array was 7 mM lithium acetate in the FIP mode. Figure 3.5 show the typical FIP response using the portable FIP system in a 7 mM lithium acetate carrier background. The nitrate ISE exhibited a sub-Nernstian response of -43.4 ± 0.1 mV change per activity decade and a log-linear range of between 0.2 mM and 20 mM using a 7 mM lithium acetate carrier in the FIP mode. The potassium and sodium ISEs in the serial array arrangement both exhibited a Nernstian response of 60.6 ± 3.4 and 60.0 ± 2.2 mV change per activity decade, respectively using the 7 mM lithium acetate background. The optimum log-linear range observed for the potassium and sodium ISEs were between 0.01 mM and 10 mM using either an ultrapure water or a 7 mM lithium acetate background in the FIP mode. The baseline drift observed for the ISE array was about 2 mV/hour in either an Ultrapure water or a lithium acetate carrier. It is important to note that the impact of baseline drift of ISEs in the flow injection mode is negligible on calibrations since data processing can account for any drift when calculating peak heights.

For simultaneous multi-analyte determinations with ISEs, the choice of ionic background is of major importance, since the components of the carrier solutions may interfere with the analyte ions. A range of carriers were employed with this ISE array system and the electrode performance of each ISE in the array is summarised in Table 3.1.

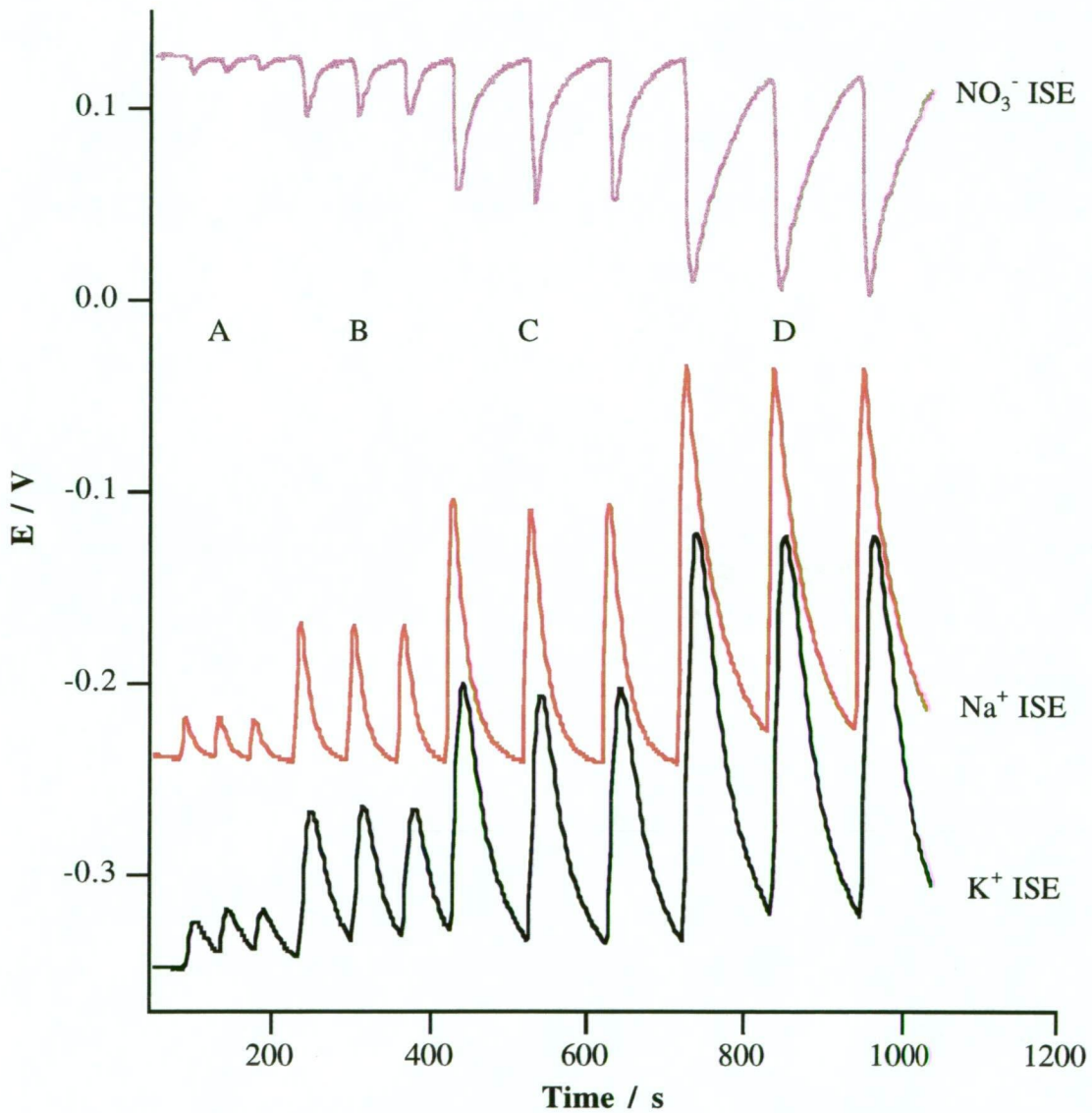

Figure 3.5. Typical FIP response observed for the nitrate, sodium and potassium ISE array using a 7 mM lithium acetate background carrier. A) 0.01 mM KNO_3 and $NaNO_3$, B) 0.1 mM mM KNO_3 and $NaNO_3$, C) 1 mM KNO_3 and $NaNO_3$ and D) 10 mM KNO_3 and $NaNO_3$.

It is clear from the data presented in Table 3.1 that employing either a 50 mM $MgSO_4$ or 1 mM $CaCl_2$ ionic background resulted in a reduced electrode slope for the nitrate, potassium and sodium ISEs and the log-linear range was narrowed 10 fold for all ISEs in the FIP mode. In the case of the nitrate ISE employing the ultrapure water carrier resulted in an electrode slope of -31.2 ± 2.0 mV change per activity decade, although the optimum log-linear range was observed which was between 0.1 mM and 10 mM in the FIP mode.

Table 3.1. Response behaviour of each ISE in the array with various carriers in FIP mode.

	Electrode Slope (S.D), mV/ decade	Log-linear range, mM	Detection limit, mM
Nitrate ISE			
Ultrapure water	-31.2 (2.0)	0.2 to 20	0.02
1 mM $CaCl_2$	-29.1	2 to 20	0.63
7 mM $LiCH_3COO$	-43.4 (0.1)	0.2 to 20	0.009
50 mM $MgSO_4$	-33.9	2 to 20	0.5
Sodium ISE			
Ultrapure water	49.9 (1.9)	0.01 to 10	0.0079
1 mM $CaCl_2$	52.0 (0.9)	0.1 to 10	0.05
7 mM $LiCH_3COO$	60.0 (2.2)	0.01 to 10	0.0023
50 mM $MgSO_4$	42.4 (2.6)	0.1 to 10	0.0014
Potassium ISE			
Ultrapure water	53.0 (1.5)	0.01 to 10	0.025
1 mM $CaCl_2$	47.0 (2.5)	0.1 to 10	0.032
7 mM $LiCH_3COO$	60.6 (3.4)	0.01 to 10	0.004
50 mM $MgSO_4$	42.2 (3.2)	0.1 to 10	0.072

3.3.3 Analysis of Natural Mineral Water Samples

To analyse the natural mineral water samples, it was important to correct for any chloride interference for the nitrate ISE in this serial array and was accomplished by employing an ultrapure water carrier and the mixed potassium, sodium and nitrate standards contained 1 mM calcium chloride, to match the chloride levels in the natural mineral water samples for the nitrate determinations as labelled on the mineral water bottles. This approach was successful and reliable FIP results for nitrate, sodium and potassium levels were easily obtained simultaneously with this ISE array, and the results are given in Table 3.2. The carrier

employed was Ultrapure water since the ionic strength of the mineral water samples were low. The FIP results were in agreement when compared to AAS measurements for the potassium and sodium ions and polarography for the nitrate ions, as shown in Table 3.2.

Table 3.2. Results of the natural mineral water analysis.

Sample	Determinand	Concentration (mg / L)		
		FIP array (RSD)	Standard method	Labelled value
Mt Franklin	Potassium	1.6 (4.9%)	1.0[a]	1.0
Mineral water	Sodium	9.4 (1.1%)	11.5[a]	14.0
	Nitrate	10.5 (2.4%)	11.2[b]	c
Deep Spring	Potassium	3.5 (4.6%)	4.5[a]	5.1
mineral water	Sodium	62.1 (2.4%)	59.8[a]	69.0
	Nitrate	7.4 (5.4%)	6.8[b]	c

a - AAS, b - polarography, c - not available.

3.4 Conclusion

The results in this chapter demonstrate the possibilities of multi-ion determinations in portable FIP system. The three ion sensors selected were chosen because of easy commercial availability in the planar design. The portable ISE array system was used successfully to determine nitrate, sodium and potassium levels simultaneously in natural mineral water samples, as an example of an environmental body of water at remote-site locations. It was demonstrated that optimisation was required to select the best carrier composition and an appropriate background for the mixed nitrate, sodium and potassium standards to minimise the response by interfering ions on the ISEs employed for the FIP measurements at remote-site locations. One of the main problems in an array of ISEs in the FIP mode is finding a suitable carrier composition that will have a negligible interference on the ISE array. The use of selective ISEs in the FIP array allows the operator to conduct rapid simultaneous determinations of nitrate, sodium and potassium in aqueous samples, employing a low cost data acquisition system. Furthermore, the ISE array can be operated in a totally portable manner in the FIP mode, whereby fast and precise data can be obtained in a short time span suitable for remote-site monitoring.

3.5 References

1. M. Valcarel and M. D. Luque De Castro 'Flow Injection Analysis. Principles and Applications', ed. S. J. Lyle and R. A. Chalmers, Ellis Horwood Ltd., New York, (1987).

2. M. Otto and J. D. R. Thomas, 'Model studies on multiple channel analysis of free magnesium, calcium, sodium and potassium at physiological concentration levels with ion-selective electrodes', Analytical Chemistry, **57**, 2647 - 2651, (1985).

3. K. R. Beebe, D. Uerz, J. Sandifier and B. R. Kowalski, 'Sparingly selective ion-selective electrode arrays for multicomponent analysis', Analytical Chemistry, **60**, 66 - 71, (1988).

4. R. J. Forster and D. Diamond, 'Nonlinear calibration of ion-selective electrode arrays for flow injection analysis', Analytical Chemistry, **64**, 1721 - 1728, (1992).

5. D. Diamond and R. J. Forster, 'Robust estimation of selectivity coefficients using multivariate calibration of ion-selective electrode arrays', Analytica Chimica Acta, **276**, 75 - 86, (1993).

6. K. R. Beebe and B. R. Kowalski, 'Nonlinear calibration using projection pursuit regression: Application to an array of ion-selective electrodes', Analytical Chemistry, **60**, 2273 - 2278, (1988).

7.. F. J. Sáez de Viteri and D. Diamond, 'Ammonium detection using an ion-selective electrode array in flow injection analysis', Eletroanalysis, **6**, 9 - 16, (1994).

8. U. Lemke, K. Cammann, C. Kötter, C. Sundermeier and M. Knoll, 'Multisensor array for pH, K^+, Na^+ and Ca^{2+} measurements based on coated-film electrodes', Sensors and Actuators, **B7**, 488 - 491, (1992).

9. H. D. Goldberg, R. B. Brown, D. P. Liu and M. E. Meyerhoff, 'Screen Printing - A technology for batch fabrication of intergrated chemical-sensor arrays', Sensors and Actuarors, **B21**, 171 - 183, (1994).

10. T. J. Cardwell, R. W. Cattrall, P. C. Hauser and I. C. Hamilton, 'A multi-ion sensor cell and data-acquisition system for flow injection analysis', Analytica Chimica Acta, **214**, 359 - 366, (1988).

11. T. J. Cardwell, R. W. Cattrall, P. C. Hauser, S. S. Tan and I. C. Hamilton, 'Measurement of pH by flow injection over a wide dynamic range with PVC / neutral carrier electrodes', Analytica Chimica Acta, **221**, 139 - 146, (1989).

12. A. U. Ramsing, J. Janata, J. Ruzicka and M. Levy, 'Miniaturization in analytical chemistry - A combination of flow injection analysis and ion-selective field effect transistors for determination of pH, and potassium and calcium ions', Analytica Chimica Acta, **118**, 45 - 52, (1980).

13. A. Sibbald, P. D. Whalley and A. K. Covington, 'A miniature flow-through cell with four-function chemFET intergrated circuit for simultaneous measurements of potassium, hydrogen, calcium and sodium ions', Analytica Chimica Acta, **159**, 47 - 62, (1984).

14. B. H. Van der Schoot, H. H. Van den Vlekkert, N. F. De Rooij, A. Van den Berg and A. Grisel, 'A flow injection analysis system with glass-bonded ISFETs for the simultaneous detection of calcium and potassium ions and pH', Sensors and Actuators, **B4**, 239 - 241, (1991).

15. C. Jiménez, I. Marqués and J. Bartrolí, 'Continuous-flow system for on-line water monitoring using back-side contact ISFET-based sensors', Analytical Chemistry, **68**, 3801 - 3807, (1996).

16. Horiba Ltd (Japan), 'Cardy Na^+, K^+ and NO_3^- Ion Meter', Bulletin: HRE-1127A, (1994).

17. Methrom Application Bulletin, 'Polargraphic nitrate determination in water, soil and plant extracts, vegetables juices, meat and sausage products, fertilizer, liquid manure, etc, No. 70/1e, Metrohm, Herisau, Swtzerland, (1992).

18. Y. Umezawa, K. Umezawa and H. Sato, 'Selectivity coefficients for ion-selective electrodes: Reccommended methods for reporting $K_{A,B}$ values (Technical Report)', Pure and Applied Chemistry, **67**, 507 - 518, (1996).

Chapter Four: Evaluation of an Eight-sensor Flow Cell in a Portable Flow Injection Potentiometric System.

4.1 Introduction

As discussed previously in Chapter three, there has been considerable work in the development of multi-electrode systems in either flowing streams, such as flow injection potentiometry (FIP) [1-8] or steady-state [9,10] measurements. However, employing potentiometric measurements in the FIP mode is more advantageous than the steady-state mode, in terms of fast sample throughput rate (>120 injection/hour), use of small sample volumes (≤ 300 μL), high peak height precision, economical use of reagents and a drifting electrode can be corrected when measuring peak heights [11].

Four coated-wire electrodes have been used in a miniature flow cell design [4] in which the four ISEs and the silver/silver chloride wire reference electrode were placed in separate flow channels that merged down stream. The miniature flow cell described in this study was applied to a desktop instrument. The four CWEs used in this flow cell were potassium, calcium, nitrate and chloride. In a different study, a flow cell arrangement containing six commercial ISEs was applied in the FIP mode [12]. The six ISEs were selective towards calcium, bicarbonate, chloride, nitrate, potassium and sodium and this multi-electrode system was used to analyse various drinking water samples.

A recent study applied quite a different application for a multi-electrode system where a single analyte was monitored in an arrangement known as the 'cell-in-series' approach [13-17]. Arrays of up to six identical ISEs have been used to determine one analyte in the FIP mode. The major advantages of employing cells-in-series with identical electrodes were the improvements in sensitivity and in detection limits compared to a single electrode system. This approach has been used successfully for measurements of cyanide [16], chloride [13], fluoride[15] and nitrate [17] ions.

This chapter reports on the design and evaluation of an eight-electrode flow-through cell that is housed in a portable battery-powered flow injection system. Silver wires were employed as electrodes in the flow-through cell where each silver wire was anodised with iodide. The electrode response to silver and iodide standard solutions was used to evaluate the performance

of the flow cell design in terms of electrode slope and log-linear range using various flow rates and sample volumes.

4.2 Experimental

4.2.1 Materials

All reagents were used as received from the suppliers: silver nitrate (Aldrich), potassium iodide (BDH, AR) and sodium acetate (BDH, AR). The silver and the iodide standard solutions were prepared by serial dilution from a stock solution of 100 mM silver nitrate and 100 mM of potassium iodide. Ultrapure water (Barnstead Ultrapure water systems, 18.0 MΩ cm) was used throughout this study.

4.2.2 Design of the Portable Flow Injection Potentiometric System

The flow injection system consisted of components developed in-house and constructed in a carry-case, and photographs of the entire system are given in Figure 4.1. The carry-case consisted of a battery-pack containing six Ni-Cd rechargeable 1.2 volt batteries; a 2-channel peristaltic pump (Model OEM-S2) obtained from A. I. Scientific Pty Ltd (Australia); a modified Rheodyne 5020 injection valve controlled by a small motor that controls the switching from the load to the inject position in 0.5 seconds via a switch located outside the case; and an analog-to-digital converter described in Chapters two and three. The weight of the entire system was 2.1 kg.

A)

B)

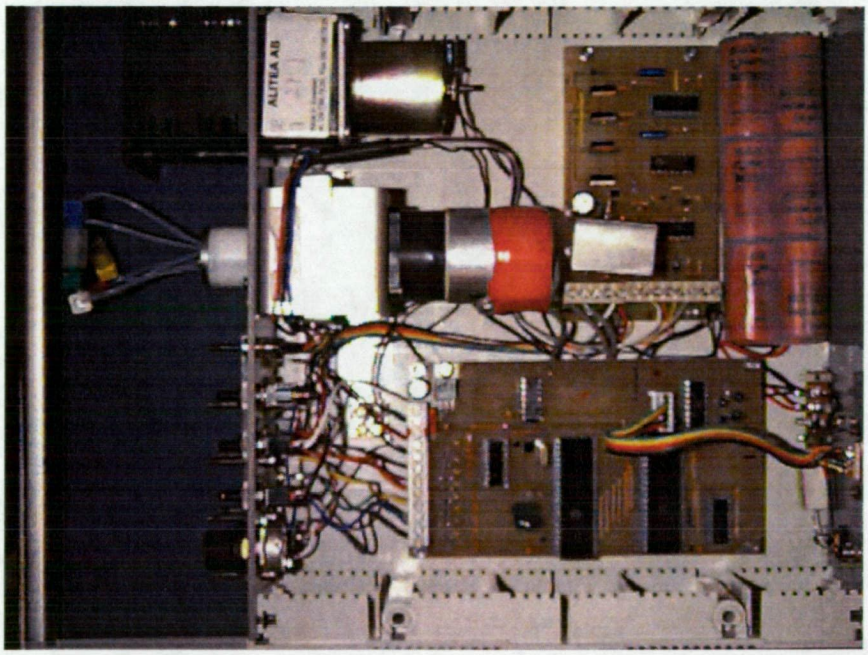

Figure 4.1. A) The portable battery-powered FIP system employing the eight electrode flow cell connected to a notebook computer used for data acquisition. B) Internal electronic circuitry of the portable FIP system developed in this study.

4.2.3 Flow Injection Measurement Procedure

The portable FIP system described above was used at flow rates varying between 1.5 to 2.8 ml/min through 2 channels, one for the reference electrode and the other for the eight electrodes. The flow ratio between the carrier and the reference streams through the multi-sensor flow cell was set at 1:1. The silver and iodide standard solutions were introduced manually to fill the sample loop using the modified Rheodyne (5020) injection valve described above, fitted with sample volumes ranging between 100 to 250 μL. The carrier and reference streams used for all flow injection measurements was 100 mM sodium acetate, and in the case of silver ion measurements, 0.01 mM AgCl was added to the 100 mM sodium acetate carrier. Prior to use, the eight silver based electrodes were conditioned in a 100 mM sodium acetate / 0.1 mM silver iodide solution overnight.

The ionic activity calculations, data acquisition program, data analysis and graphical representation of the data procedures described earlier in Chapter two, Section 2.2.4 were employed in the work described in this chapter. A program called MacCurve Fit © Version 0.7 was used to calculate the electrode slope, the E' and the standard deviations (95% confidence) of a given electrode in either steady-state or FIP modes.

4.3 Results and Discussion

4.3.1 Design of the Multi-electrode Flow Cell

As shown in previous studies, the appropriate design of a miniature multi-sensor flow cell requires the wall-embedded configuration [11], whereby, the sensor is positioned in the flow channel and the injected sample zone flows over the surface of the electrode. This arrangement allows several sensors to be positioned in a single flow stream, whereby, a single injected sample zone can contact each of the measuring electrodes while maintaining limited dispersion. A schematic diagram of the eight-electrode flow cell design is given in Figure 4.2.

The position of the reference electrode could be chosen either downstream from the sensors or in a differential arrangement, where the reference electrode is contained in a separate flow channel that merges downstream with the multi-sensor channel. Studies have shown that the differential approach in potentiometric flow-through cells leads to improved precision [18] and a negligible liquid junction potential at the merging point, due to rapid hydrodynamic mixing [19].

A)

B)

C)

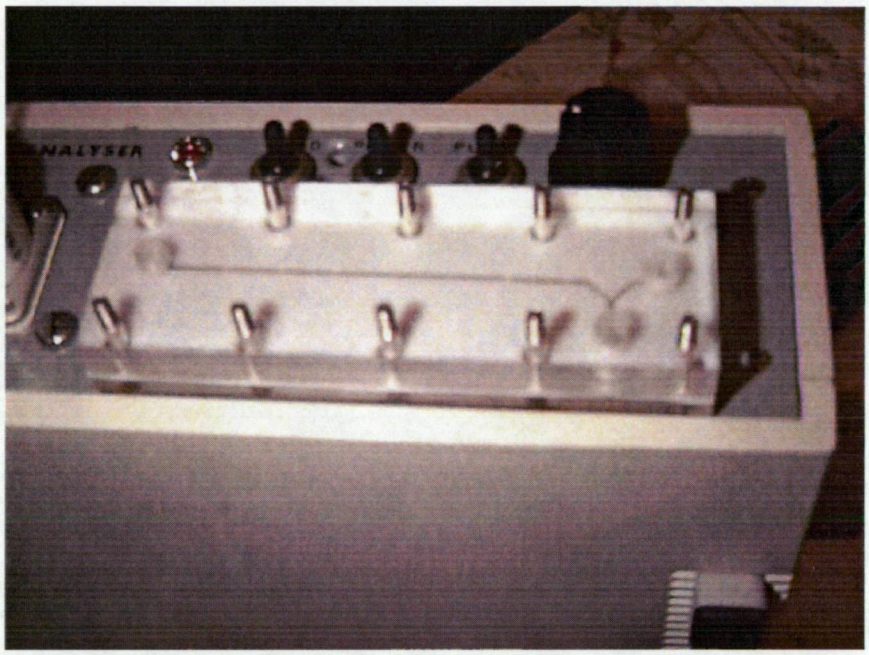

D)

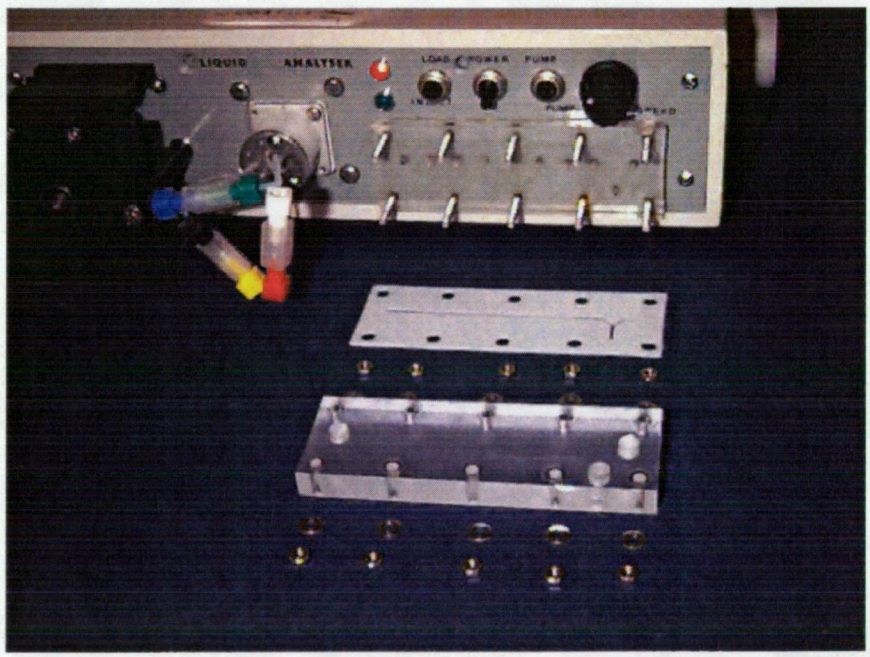

Figure 4.2. Illustration of the assembly of the eight-electrode flow-through cell design. A) The eight silver electrodes inbuilt in the lower poly(methyl methacrylate) block; B) the teflon gasket positioned over the lower poly(methyl methacrylate) block; C) the top poly(methyl methacrylate) body positioned over the gasket and D) the entire assembly of the eight electrode flow cell contained in the lower poly(methyl methacrylate) body, the gasket and upper poly(methyl methacrylate) body.

For this reason, the differential arrangement was employed in the multi-sensor flow cell design presented in this study. Employing identical concentration and composition of the carrier and the reference solutions would also minimise liquid junction potentials [19]. In case identical carrier and reference solutions can not be employed, the electrolytes should be equitransferrent [20].

Streaming potentials are common with potentiometric measurements employing flow-through cells [21,22]. Baseline oscillations as large as 3 mV have been observed and relate to the revolution of the peristaltic pump [23]. To minimise any streaming potentials, low flow rate and electrolyte concentration ≥ 10 mM were to be used for the carrier and the reference streams [23]. The multi-electrode flow cell evaluated in this study did not exhibit any streaming potential effects and was the subject of studies on factors affecting the electrode behaviour of the eight electrodes.

4.3.2 Effect of Dispersion on the Peak Heights and Peak Widths

Typical FIP responses observed for the silver iodide electrodes to silver ions using the eight electrode flow cell in the portable FIP system in real time are presented in Figure 4.3, while Figure 4.4 show the silver ion FIP response, where the baselines were offset. Figures 4.5 and 4.6 show the iodide ion FIP response in real time and the baseline offsets, respectively. The silver electrode connected to channel 7 was in close proximity to the sample injection valve whereas channel 0 was the furthest away.

A general reduction in the peak height was observed as the injected sample zone travelled from the channel 7 to the channel 0 sensor. The observed peak heights from each of the eight electrodes for a particular injected sample zone varied by up to 11%, due to the increasing dispersion of the sample zone pumped through the flow channel. The reproducibility of the silver electrodes was determined with eight replicate injections of a 10 mM potassium iodide standard in a sodium acetate background in the flow stream. The relative standard deviation (RSD) of the peak heights determined for each of the eight electrodes was between 1.7% and 3.3%.

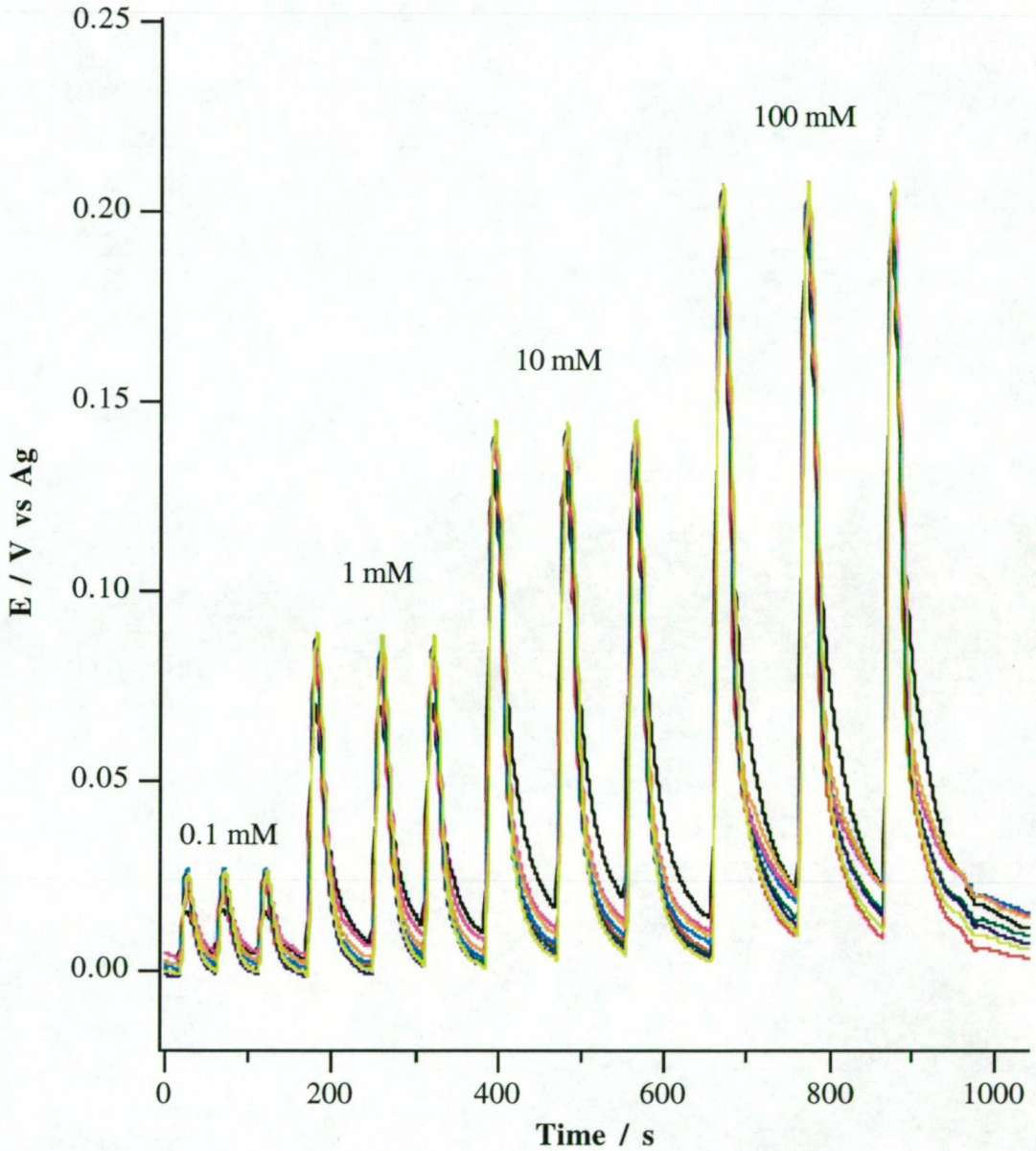

Figure 4.3. Typical FIP silver ion response for each electrode in the eight-electrode flow cell design displayed in real time. Sample volume = 200 µL and total flow rate = 2.2 mL/minute. Carrier and reference streams were 100 mM sodium acetate containing 0.01 mM silver chloride.

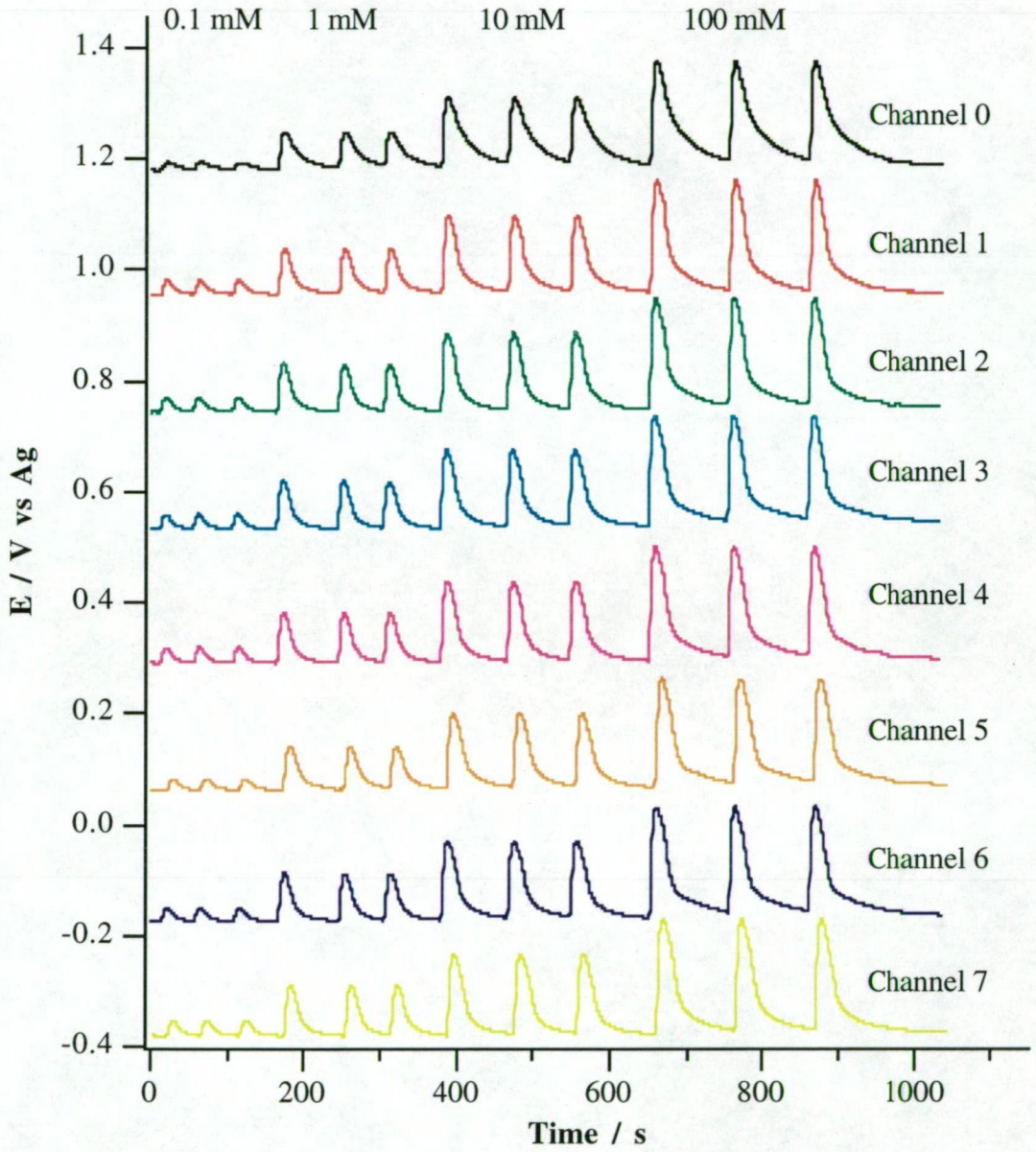

Figure 4.4. FIP response shown in Figure 4.3 where the baselines were offset.

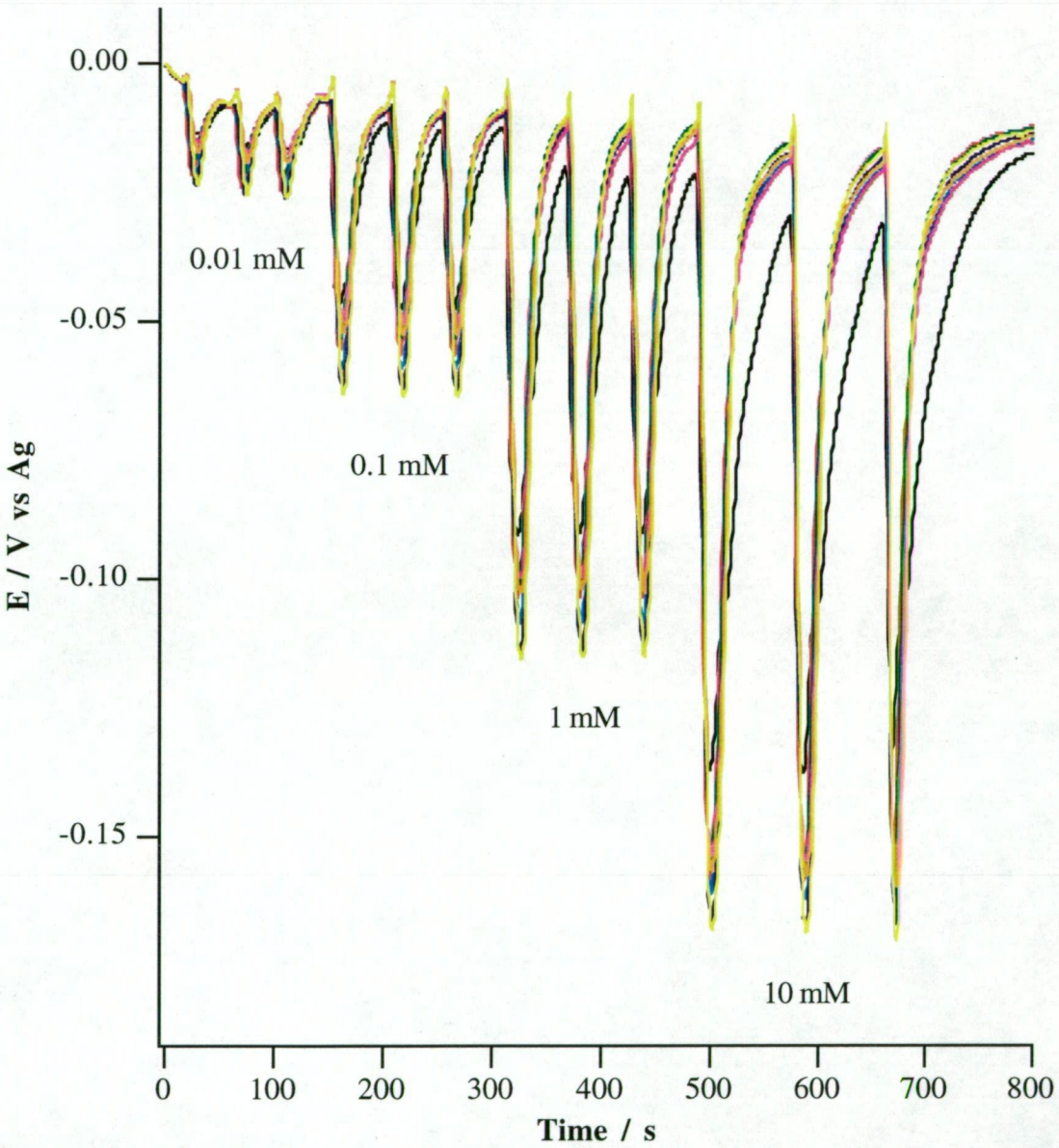

Figure 4.5. Typical FIP iodide ion response for each electrode in the eight-electrode flow cell design displayed in real time. Sample volume = 200 µL and total flow rate = 2.2 mL/minute. Carrier and reference streams were 100 mM sodium acetate.

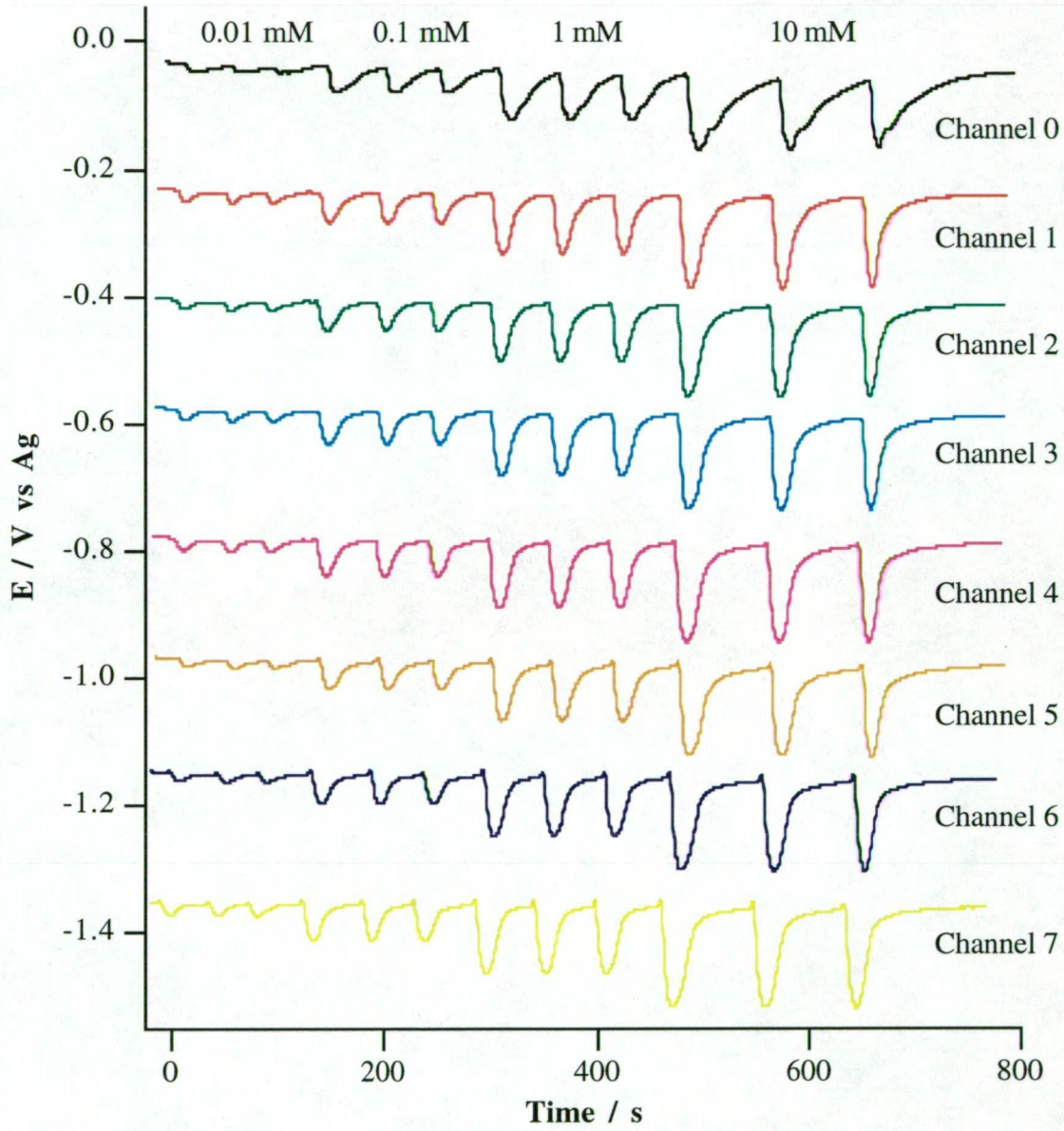

Figure 4.6. FIP response shown in Figure 4.5 where the baselines were offset.

The flow injection peaks recorded simultaneously for each electrode exhibited a response width ranging from 30 - 100 seconds, depending on the concentration injected and the position of each sensor in the flow channel. As shown in Figures 4.3 and 4.5 for the response observed for silver and iodide ions, respectively, peak widths increased from channel 7 to channel 0 as the distance travelled by the injected sample zone increased. Clearly, this suggests that dispersion of the injected sample zone has increased as it approaches the flow channel outlet. Increasing the concentration of the injected sample zone and decreasing the flow rate also resulted in increasing peak widths.

4.3.3 Effect of Dispersion on the Electrode Slopes

4.3.3.1 Silver Ion Response in the FIP mode

The size of the injected sample zone used in this study ranged between 100 and 250 µL. The silver ion responses observed for the eight measuring electrodes all exhibited a log-linear range of between 0.1 - 100 mM using a 100 mM sodium acetate background in the FIP mode, regardless of the sample volume employed. The electrode slopes of each of the eight electrodes varied with the sample volume used, as shown in Table 4.1. Figure 4.7 shows comparative calibration curves of the silver ion response observed for the eight electrodes in the FIP mode.

Table 4.1. The effect of varying the injection sample volumes has on the electrode slopes (mV/decade) of the eight electrode responses to silver ions in the FIP mode; total flow rate was 2.2 mL/minute and the background was 100 mM sodium acetate with 0.01 mM silver chloride.

Electrode channel	Injection volume			
	100 µL	150 µL	200 µL	250 µL
0	44.6 ± 1.4	53.0 ± 2.0	56.2 ± 1.9	57.0 ± 1.5
1	49.1 ± 1.5	59.5 ± 0.2	58.5 ± 1.3	58.5 ± 1.6
2	50.7 ± 0.3	57.7 ± 1.0	56.4 ± 1.1	56.1 ± 0.9
3	50.7 ± 0.3	56.7 ± 1.6	56.2 ± 1.3	55.9 ± 1.0
4	52.1 ± 0.6	59.2 ± 1.1	57.7 ± 1.4	56.3 ± 0.7
5	52.9 ± 1.0	57.6 ± 0.2	58.0 ± 0.4	56.3 ± 0.5
6	53.1 ± 0.8	57.9 ± 1.1	57.4 ± 1.4	55.6 ± 0.7
7	53.3 ± 0.9	60.5 ± 1.1	58.9 ± 1.6	57.2 ± 1.2
Mean, (RSD)	50.8 (5.3%)	57.8 (3.7%)	57.4 (1.7%)	56.6 (1.5%)

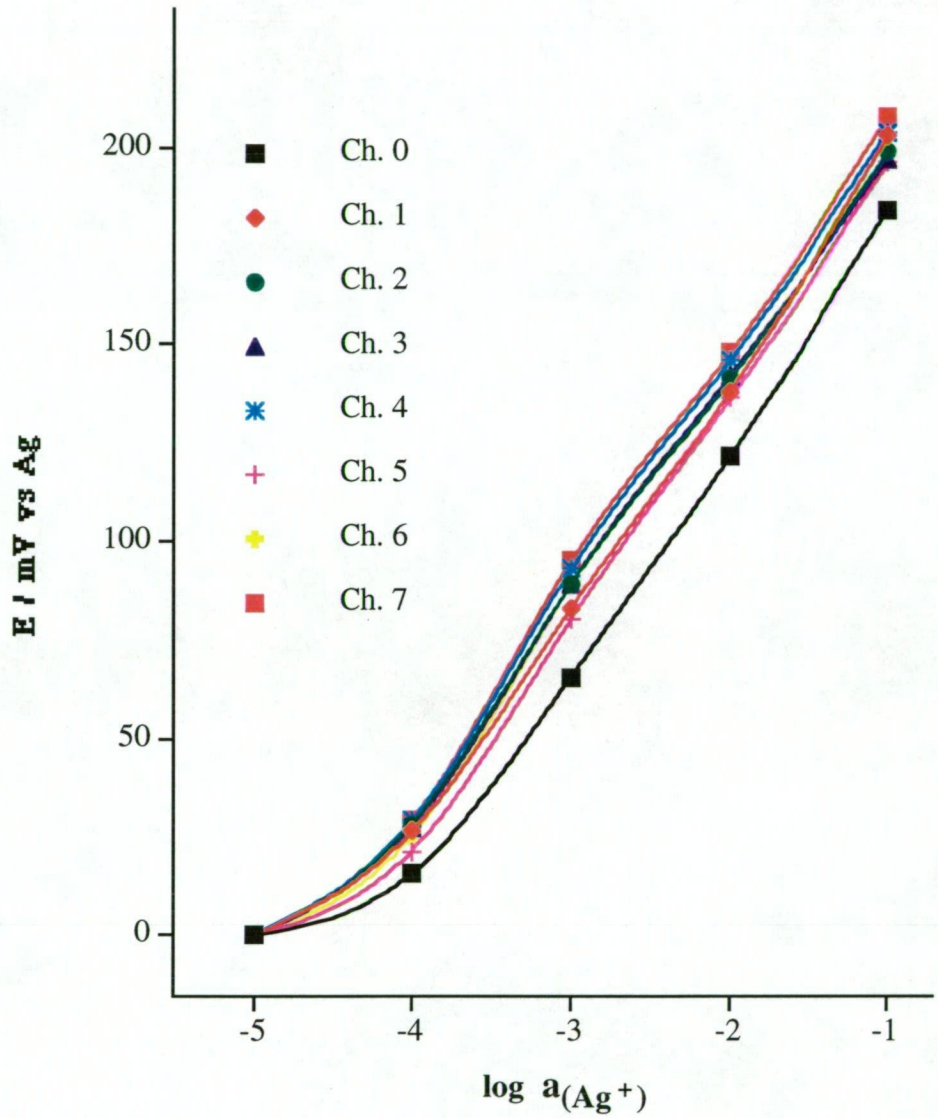

Figure 4.7. Comparative calibration curves for the eight Ag/AgI electrodes (Ch. 0 to Ch. 7) response to $AgNO_3$ solutions in the FIP mode employing a 200 µL sample injection volume with a total flow rate of 2.2 mL/minute.

Clearly, the lower the sample volume used, the lower the electrode slope observed, due to the increased dispersion of the sample zone. Using 100 µL sample volume, the RSD of the electrode slopes of the eight measuring electrodes was 5.3 %. As the sample volume increased the RSD of the electrode slopes observed for the eight electrodes decreased as shown in Table 4.1. Increasing the sample volume resulted in a similar electrode slope for the silver ion responses of each of the eight electrodes in the FIP mode.

It was found that 200 µL was the optimum sample volume to be employed with the potentiometric flow cell presented in this study. The mean electrode slope observed for the eight silver ion responses was 57.4 ± 1.0 mV per activity decade using the optimum injection sample volume of 200 µL. The RSD for the mean electrode slopes was 1.7%. Varying the flow rate between 1.5 and 2.8 ml/minute had a negligible effect on the electrode slope of the eight electrodes.

4.3.3.2 Iodide Ion Response in the FIP mode

The iodide ion responses observed under similar conditions to the silver ion response (flow rate, injected sample volume and ionic background) were clearly sub-Nernstian in the FIP mode, ranging from 36.3 - 50.9 mV per activity decade using the optimum sample volume of 200 µL, as shown in Table 4.2. Figure 4.8 illustrates the comparative calibration curves for the iodide ion response. A log-linear range of between 0.1 - 10 mM was observed regardless of the sample volume employed.

Table 4.2. The effect of varying the injection sample volumes has on the electrode slopes (mV/decade) of the eight electrode responses to iodide ions in the FIP mode; total flow rate was 2.2 mL/minute and the background was 100 mM sodium acetate.

Electrode channel	Injection volume			
	100 µL	150 µL	200 µL	250 µL
0	30.8 ± 0.9	35.3 ± 2.4	36.3 ± 0.9	37.9 ± 0.7
1	39.2 ± 3.0	50.5 ± 0.7	48.3 ± 2.0	49.3 ± 0.3
2	42.5 ± 2.6	49.7 ± 0.3	48.3 ± 1.5	51.3 ± 1.0
3	44.5 ± 0.5	47.5 ± 1.0	46.9 ± 0.2	47.7 ± 0.2
4	46.5 ± 0.5	48.6 ± 1.7	49.8 ± 0.6	49.4 ± 1.1
5	44.3 ± 1.3	48.2 ± 0.2	48.7 ± 0.5	50.9 ± 0.7
6	49.4 ± 2.1	50.9 ± 0.5	50.5 ± 0.3	49.7 ± 0.9
7	51.2 ± 0.2	50.5 ± 1.0	50.9 ± 1.2	51.8 ± 0.7
Mean, (RSD)	43.6 (13.7%)	47.7 (10.1%)	47.5 (9.3%)	48.5 (8.6%)

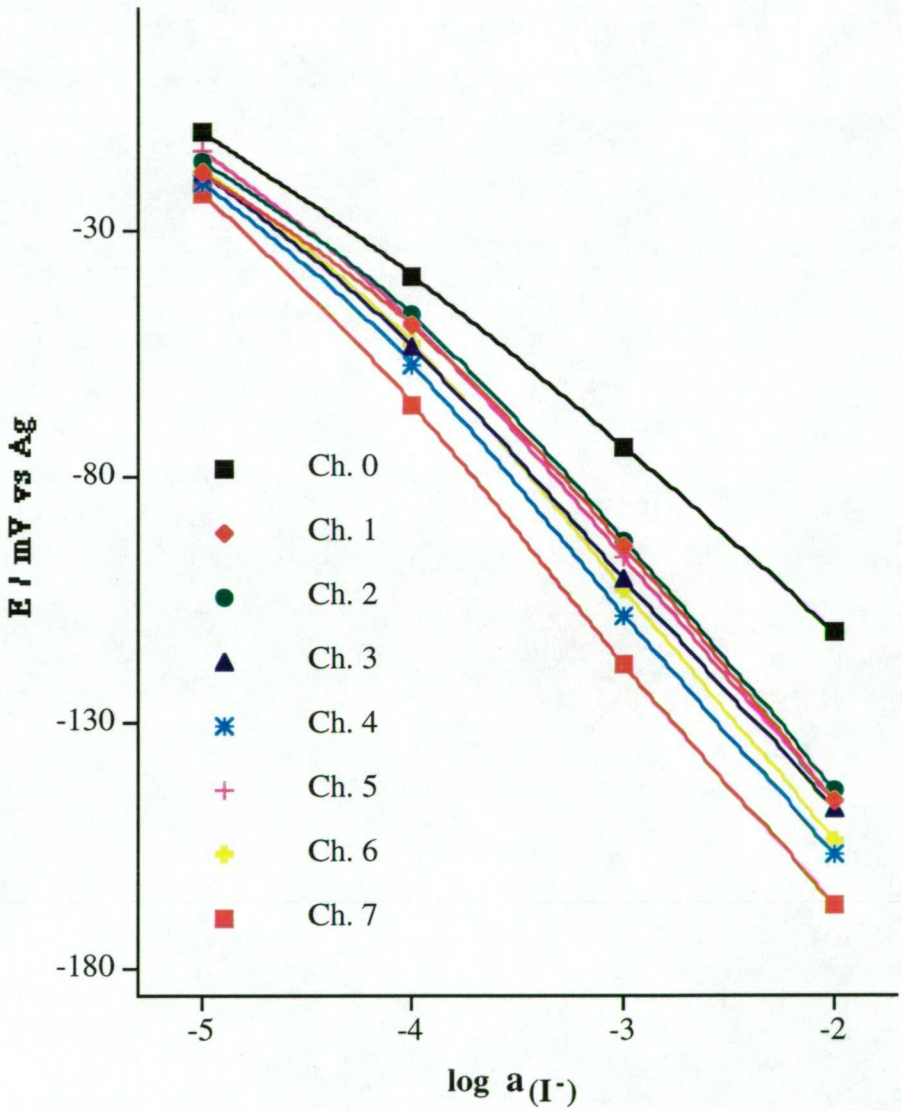

Figure 4.8. Comparative calibration curves for the eight Ag/AgI electrodes (Ch. 0 to Ch. 7) response to KI solutions in the FIP mode employing a 200 µL sample injection volume with a total flow rate = 2.2 mL/minute.

The sub-Nernstian iodide responses observed for the silver electrodes are likely to be due either to the slower response of the electrodes to iodide, the interference of the acetate background or the complexation processes occurring at the surface of the silver electrodes. The latter can be represented as follows:

$$Ag^{+} + 2I^{-} \rightleftharpoons AgI_2^{-}$$

The formation of the diiodo silver(I) complex at the surface of the metallic silver electrode would significantly reduce the electrode response leading to the observed sub-Nernstian response. The surface of the silver electrodes had changed to yellow when in contact with the iodide solutions. After prolonged exposure to light, a black appearance was observed, which clearly suggests the formation of the diiodo silver (I) complex at the surface of the silver electrodes.

The mean electrode slope observed for the eight iodide ion responses was 47.5 ± 4.4 mV per activity decade, and the RSD was 9.3% using the optimum sample volume of 200 µL. Table 4.2 summarises these data. The higher RSD observed for the iodide response was largely contributed to the electrode slope observed for channel 0 electrode. Excluding the channel 0 response would result in a mean electrode slope of 49.1 ± 1.3 mV per activity decade; corresponding to a RSD of 2.7%. Increasing the sample volume from 200 to 250 µL results in a similar electrode response for the channel 0 electrode, and eliminates dispersion as the sole reason for the observed lower electrode slopes.

The likely reason for the irregular response observed for the channel 0 sensor could be a combination of the following; (i) the interference of the acetate background and the diiodo silver (I) complexation at the surface of this electrode, (ii) a slower response to the iodide ion compared to the other 7 sensors and (iii) the increased dispersion of the injected sample zone.

4.3.4 Cells-in-Series Approach for the Silver Ion and the Iodide Ion Response in the FIP mode

An alternative approach to improve the sensitivity and detection limit of the ISEs is to employ the cells-in-series approach [13-17] to the eight identical electrodes in this portable FIP system. The main advantages, such as an increased sensitivity and improved detection limits for a single analyte, can be applied for a single anion or cation. To illustrate this example, the eight silver ion and the eight iodide ion FIP responses discussed above, were each added using the 'IGOR PRO' package, as presented in Figures 4.9 and 4.10, respectively.

The detection limit was also improved in cases where random noise is a major limitation, since the increase in signal to the square root of the noise ratio is proportional to the square root of the number of cells in series [13,14]. A five fold improvement in the detection limit was calculated for the silver ion and the iodide ion responses were 0.045 mM and 0.004 mM, respectively. These aspects would be invaluable for environmental monitoring at remote site locations, where improved sensitivity over a single cell measurement may offer the above advantages.

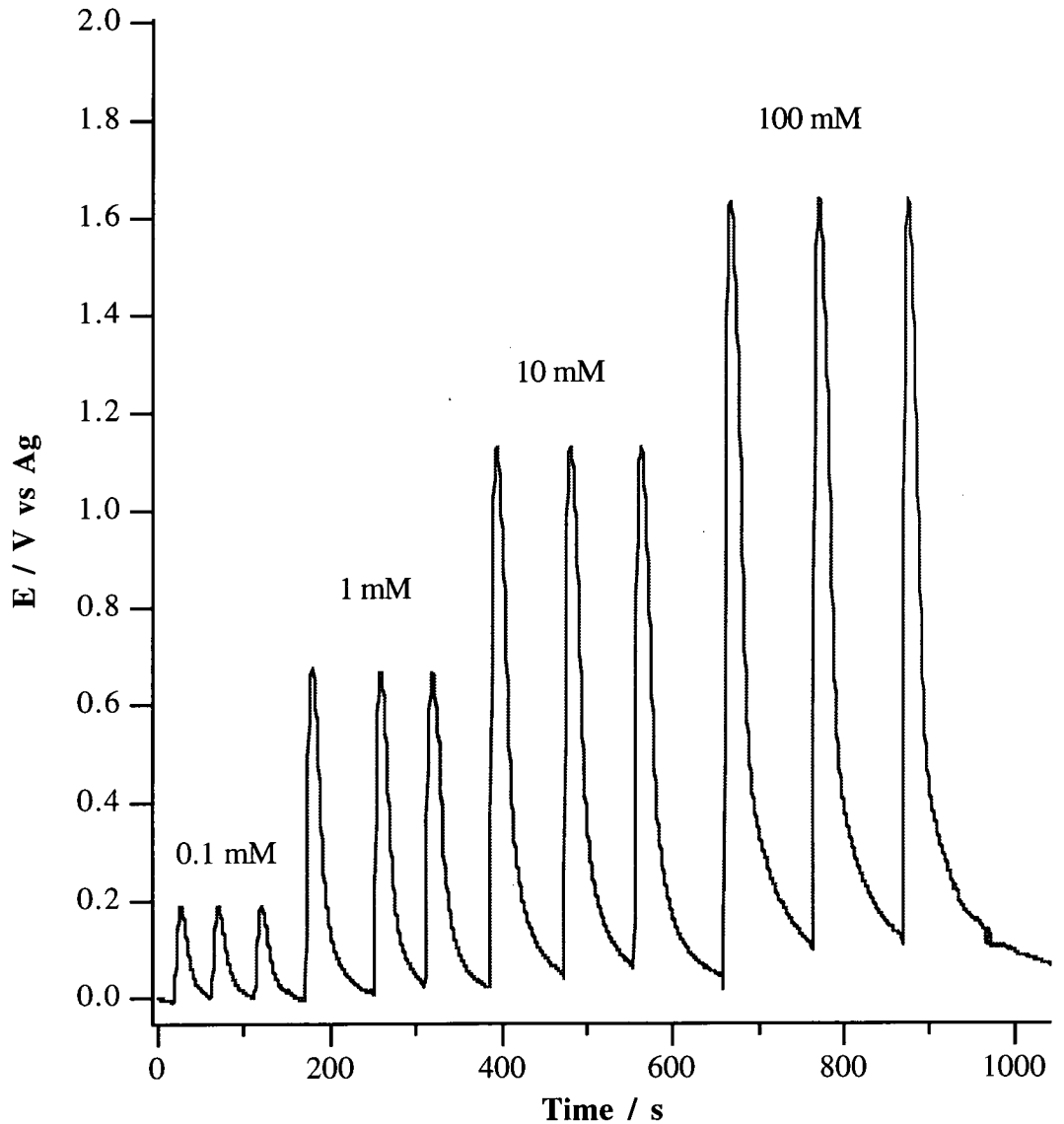

Figure 4.9. The cell-in-series approach applied to the FIP response to the silver ion.

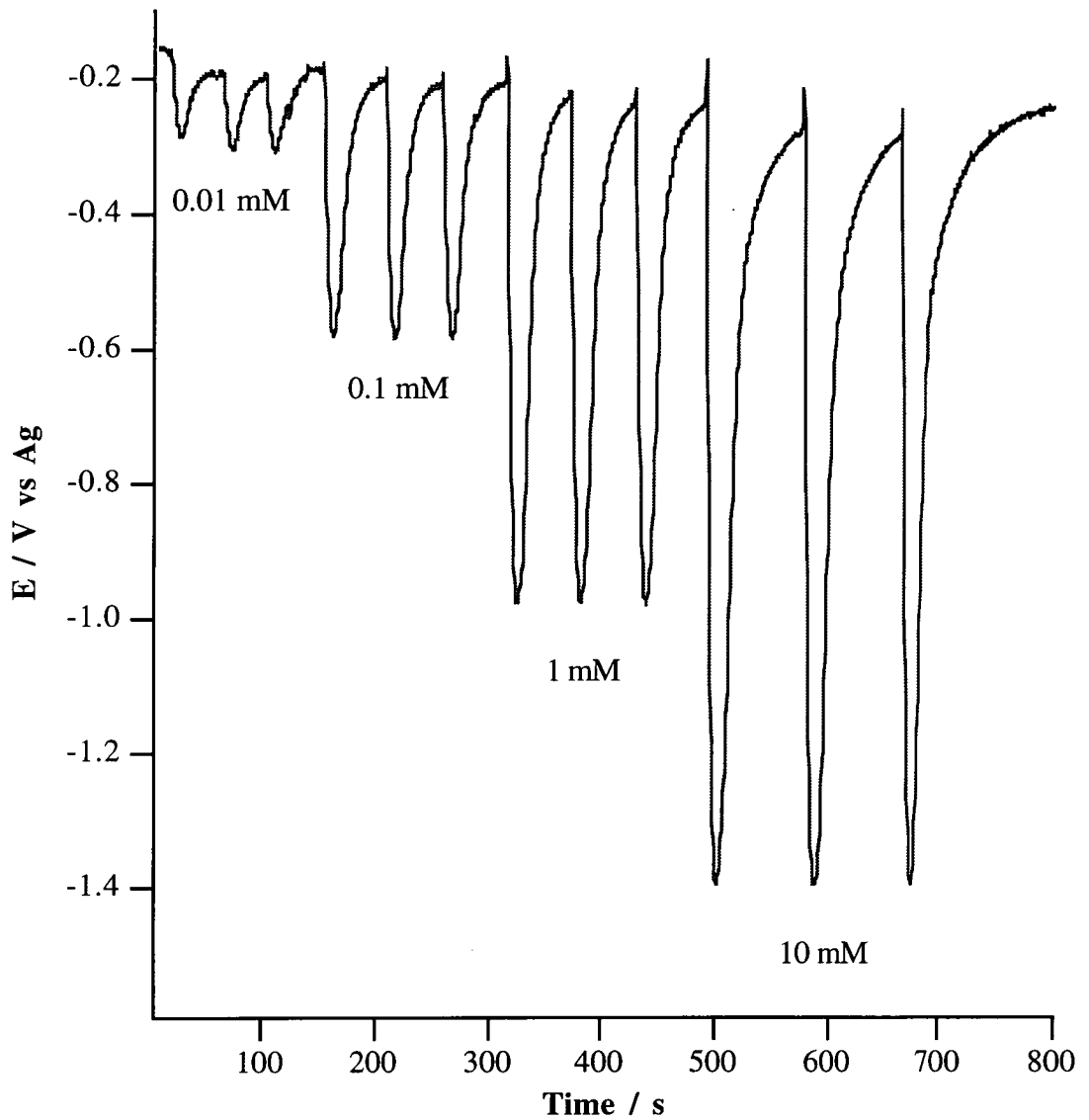

Figure 4.10. The cell-in-series approach applied to the FIP response to the iodide ion.

4.4 Conclusion

There are numerous applications that could be utilised with the multi-sensor flow cell used in the portable flow injection system for remote site monitoring. The design of the analog-to-digital converter employed in this portable system should allow for liquid polymer membranes selective to different analytes to be applied to each silver substrate. Hence, high resistance electrodes with liquid membranes > 10 MΩ resistance could be used in the flow injection mode. However, the main obstacle to be overcome with this approach is the choice of the carrier solution to be used for FIP measurements, such that the sensitivity and selectivity of the liquid membrane based sensors is not affected.

The eight-electrode flow cell used in the portable FIP system provides peak heights of high precision and reproducible electrode slopes for the response to silver and, to a certain extent, iodide ions. The optimum injection volume determined for this eight-electrode flow cell was 200 µL. The possibility of either applying eight different sensors or employing the cells-in-series approach makes this portable FIP system a highly attractive analytical instrument for remote site monitoring.

4.5 References

1. A. U. Ramsing, J. Janata, J. Ruzicka and M. Levy, 'Miniaturization in analytical chemistry - A combination of flow injection analysis and ion-selective field effect transistors for determination of pH, and potassium and calcium Ions', Analytica Chimica Acta, **118**, 45 - 52, (1980).

2. A. Sibbald, P. D. Whalley and A. K. Covington, 'A miniature flow-through cell with four-function chemFET integrated circuit for simultaneous measurements of potassium, hydrogen, calcium and sodium ions', Analytica Chimica Acta, **159**, 47 - 62, (1984).

3. J. F. Van Staden, 'Electrodes in series. Simultaneous flow injection determination of chloride and pH with ion-selective electrodes', Analyst, **111**, 1231 - 1234, (1986).

4. T. J. Cardwell, R. W. Cattrall, P. C. Hauser and I. C. Hamilton, 'A multi-ion sensor cell and data-acquisition system for flow injection analysis', Analytica Chimica Acta, **214**, 359 - 366, (1988).

5. B. H. Van Der Schoot, H. H. Van Den Vlekkert, N. F. De Rooij, A. Van Den Berg and A. Grisel, 'A flow injection analysis system with glass-bonded ISFETs for the simultaneous detection of calcium and potassium ions and pH', Sensors and Actuators, **B4**, 239 - 241, (1991).

6. R. J. Forster and D. Diamond, 'Nonlinear calibration of ion-selective electrode arrays for flow injection analysis', Analytical Chemistry, **64**, 1721 - 1728, (1992).

7. F. J. Sáez de Viteri and D. Diamond, 'Determination and application of ion-selective electrode model parameters using flow injection and simplex optimization', Analyst, **119**, 749 - 758, (1994).

8. F. J. Sáez de Viteri and D. Diamond, 'Ammonium detection using an ion-selective electrode array in flow-injection analysis', Electroanalysis, **6**, 9 - 16, (1994).

9. K. Beebe, D. Verz, J. Sandifer and B. Kowalski, 'Sparingly selective ion-selective electrode arrays for multicomponent analysis', Analytical Chemistry, **60**, 66 - 71, (1988).

10. U. Lemke, K. Cammann, C. Kötter, C. Sundermeier and M. Knoll, 'Multisensor array for pH, K^+, Na^+ and Ca^{2+} measurements based on coated-film electrodes', Sensors and Actuators, **B7**, 488 - 491, (1992).

11. J. Ruzicka and E. H. Hansen, 'Flow Injection Analysis', John Wiley and Sons, New York, 2nd ed., (1988).

12. K. Cammann, 'Flow injection analysis with electrochemical detection', Fresenius Journal of Analytical Chemistry, **329**, 691 - 697, (1988).

13. D. B. Hibbert, P. W. Alexander, S. Rachmawati and S. A. Caruara, 'Multiple sensor response in segmented flow analysis with ion-selective electrodes', Analytical Chemistry, **62**, 1015 - 1019, (1990).

14. D. B. Hibbert, P. W. Alexander and P. Yatiman, 'Theory of multiple-cell response of redox electrodes', Mikrochimica Acta, **108**, 93 - 101, (1992).

15. J. A. Borzitsky, A. Dvinin, O. M. Petrukhin, Y. I. Urusov, 'Flow cell with double slope factor for potentiometric determination of fluoride at low concentrations', Analyst, **118**, 859 - 861, (1993).

16. D. Shiels, P. W. Alexander and D. B. Hibbert, 'A multicell potentiometric detector for environmental analysis', **Proc. 11th Aust. Symp. on Analytical Chemistry,** Hobart, pg 121 - 123, (1991).

17. J. C. Ngila, D. B. Hibbert and P. W. Alexander, 'Response amplification of multiple coated-wire ion-selective electrodes for flow analysis based on nitrate doped poly(pyrrole)', **Proc. 13th Aust. Symp. on Analytical Chemistry,** Darwin, pg AS45-1 - AS45-2, (1995).

18. R. Wawro and G. A. Rechnitz, 'Split crystal ion selective membrane electrodes', Analytical Chemistry, **46**, 806 - 808, (1974).

19. K. Cammann, 'Working with Ion-Selective Electrodes', Springer-Verlay, Berlin, (1979).

20. E. Metzger, R. Dohner and W. Simon, 'Lithium/Sodium ion concentration ratio measurements in blood serum with lithium and sodium ion selective liquid membrane electrodes', Analytical Chemistry, **59**, 1600 - 1603, (1987).

21. P. Van Den Winkel, J. Mertens and D. L. Massart, 'Streaming potentials in automatic potentiometric systems', Analytical Chemistry, **46**, 1765 - 1768, (1974).

22. T. K. Christopoulos and E. P. Diamandis, 'Flow-through units for solid-state, liquid and PVC matrix membrane ion-selective electrodes to minimise streaming potentials', Analyst, **112**, 1293 - 1298, (1987).

23. P. C. Hauser, 'Aspects of the use of Ion-Selective Electrodes in Flow Injection Analysis', Ph.D. Thesis, Latrobe University, (1988).

Chapter Five: Evaluation and Performance of Various Photo-cured Bisphenol A Epoxydiacrylate based Membrane CWEs.

5.1 Introduction

PVC has been universally accepted as the preferred polymer base for liquid membranes, and is employed in numerous commercially available ion-selective electrodes (ISEs). However, the manufacture of PVC membranes poses a disadvantage that arises from the solvent used in the casting procedure which can take up to two days, producing a liquid membrane that is durable and flexible, but exhibits poor adhesion to solid-contact electrodes [1] and consequently is unreliable in a continuous flowing stream as demonstrated in previous studies [1,2].

An alternative method for the rapid manufacture of liquid polymer membranes that are more robust than the PVC based membranes has been reported [1,3-15] and involves a photopolymerisation process. The photopolymerisation process involves the UV-curing of a bisphenol A epoxydiacrylate based membrane that is cross linked with an acrylate ester and initiated by a benzophenone photoinitiator for up to 40 minutes using an ultra-violet mercury vapour lamp. Other photo-curable polymers used in sensing membranes for ISEs include poly(methyl methacrylate) [1], polyurethane [3,4] and poly (decyl methacrylate) [5]. Membranes formed with the photo-curing technique are mechanically stronger and more hydrophobic than PVC membranes, due to lower amount of plasticiser required in these photo-cured membranes and exhibit excellent adhesion properties to solid-contact electrodes. Other advantages of photo-cured membranes include good sensitivity and fast response, making these membrane based electrodes ideal for FIP measurements and compatible with microelectronic technology enabling the production of miniature sensing devices.

Photo-cured membranes for ISEs that have been developed to-date include ammonium [3,4], calcium [1,6-9], lithium [10], nitrate [11], hydrogen [12], potassium [13,14] and sodium [15], most of which were applied to FIP measurements. Most of these photo-cured membrane based ISEs have been employed in the FIP mode and used to determine the respective primary ion in variety of environmental and drinking water samples [7-

10,12,13,15]. Generally, the FIP results obtained for these photo-cured ISEs were in good agreement with comparative analytical methods.

An interesting study involving a photo-cured calcium ISE which was based on the calcium bis[4-(1',1',3',3'-tetramethylbutyl)phenyl]phosphate ionophore and the potassium tetrakis(4-chlorophenyl)borate lipophilic additive exhibited an excellent tolerance to high levels of perchlorate in the FIP mode [8,9], compared to other reported calcium ISEs [6,7]. The photo-cured calcium ISE was successfully used to determine total calcium levels in nitric/perchloric acid digested milk samples in the FIP mode. However, this photo-cured calcium membrane based ISE experienced severe interferences from barium and zinc ions. The zinc ion interference of the photo-cured calcium ISE has been observed with other calcium ISEs based on similar phosphate ester based ionophores [16].

A modification to the above-mentioned UV-curing procedure was laser curing acrylate based membranes [17,18] that exclude the need for a photoinitiator. Membranes prepared with this technique were firstly spin coated to reduce the thickness of the membrane and then exposed to a XeCl excimer laser (0.35 W cm^{-2}, λ = 308 nm) for 10 seconds at a frequency of 60 Hz. Membranes produced were robust, hydrophobic, sensitive and fast responding making them ideal for FIP measurements. Laser cured membrane ISEs that have been developed to-date are potassium [17] and tetrachloroaurate(III) [18].

Plasticisers of a high dielectric constant, such as 2-nitrophenyl octyl ether (ε = 24.2), are preferred for divalent-selective electrodes since they improve the determinand selectivity over monovalent ions [19]. The major disadvantage with some of the above-mentioned photo-cured membranes, in particular the calcium-selective electrode, was their inability to employ 2-nitrophenyl octyl ether as the plasticiser. The nitro group is known to inhibit the photopolymerisation process by acting as a free radical scavenger when using the benzophenone type of photoinitiator [7,10,11,14,15]. This can be overcome by introducing a small drop of the 2-nitrophenyl octyl ether plasticiser onto the surface of the photo-cured membrane and allowing it to permeate into the membrane [7,10,15]. This procedure improves the response and the selectivity of photo-cured membrane based ISEs, however, there is no control of the amount of plasticiser introduced into the photo-cured membrane.

Recently, there has been a report of a photo-cured nitrate ISE that employed 2-nitrophenyl octyl ether plasticiser in the pre-cured mixture, thereby controlling the amount of plasticiser in the membrane [11]. In this case, photo-curing was made possible by the use of a photoinitiator mixture that contained diaryliodonium chloride and 9,10-phenanthrenequinone, and the photo-curing process was completed in 1 minute. This membrane was photo-cured on to a solid-contact electrode and was also photolithographically attached to an ion-sensitive field effect transistor.

This chapter reports on the electrode performance of a variety of photo-cured bisphenol A epoxy diacrylate based ammonium, calcium, hydrogen, nitrate and potassium CWEs in the steady-state and FIP modes and determines their suitability in an multi-electrode array in terms of selectivity against interfering ions. Each photo-cured membrane based CWE was coated onto one of the silver electrodes in the eight-electrode flow cell described in Chapter four. The photo-cured CWEs were then individually characterised in terms of electrode slope, selectivity, response time, mechanical and electrical integrity, and applicability in the FIP mode.

5.2 Experimental

5.2.1 Materials

All reagents were used as received from the suppliers: ammonium chloride, calcium chloride, potassium chloride, potassium nitrate and lithium acetate (all BDH, AnalaR). Stock solutions ranging between 0.01 mM and 100 mM of determinand as the chloride salt were prepared by serial dilution. In the case of pH measurements, universal pH buffer solutions described in Section 2.2.1 were prepared daily. Ultrapure water (Barnstead Ultrapure water systems, 18.0 MΩ cm) was used throughout this work.

The polymer matrix of the photo-cured membrane prepared in this study consisted of Ebecryl 600 (bisphenol A epoxydiacrylate) and Uvecryl P36 (benzophenone based initiator) were donated by UCB Chemical Sector (Belgium), and 1,6-hexanedioldiacrylate was obtained from Anchor Chemicals Australia Pty. Ltd. The initiator used in the photo-cured membranes was a mixture of 9,10-phenanthrenequinone and diphenyliodonium chloride, both obtained from Fluka. The lipophilic additives used were potassium tetrakis(4-chlorophenyl)borate (KClTPB) and ammonium tetrakis(4-chlorophenyl)borate (TAClTPB), both obtained from

Fluka. The ionophores used were nonactin for ammonium, N,N,N',N'-tetracyclohexyl-3-oxapentane diamide (ETH 129) for calcium, N,N-dioctadecylmethylamine for hydrogen, 2,2'-bis[3,4-(15-crown-5-)-2-nitrophenylcarbamoxymethyl]tetradecane (BME-44) for potassium were all obtained from Fluka. The nitrate (TDA-NO_3) ionophore was prepared from tetradodecylammonium bromide, which was obtained from Fluka, and converted to the nitrate salt by a solvent extraction procedure. The plasticisers used were dioctyl phenylphosphonate (DOPP) which was obtained from Aldrich, while bis(2-ethylhexyl) phthalate (BEHP) and o-nitrophenyl octyl ether (NPOE) were both obtained from Fluka.

5.2.2 Preparation of the CWEs

The constituents of a pre-cured membrane were each weighed into a small glass vial with a screw cap. Pre-cured membranes were then ultrasonically mixed for 3 hours and then, using thin nylon brushes, were each applied directly onto a 1.0 mm in diameter Ag wire embedded in the eight electrode flow cell described in Chapter four (Figure 4.1). The photo-curing of membranes were performed using a Phillips UV lamp (250 W, $\lambda = 300$ nm) under a nitrogen atmosphere for up to 5 minutes, and all membranes produced were hard and transparent. A small carton box (75 mm X 120 mm X 75 mm) was used as a nitrogen chamber and positioned over the eight-electrode flow cell and covered by a sheet of polyethylene as shown in Figure 5.1, forcing the air out through the bottom of the nitrogen box. In the case of the calcium CWE, the photo-curing process was performed in the open atmosphere. The resultant photo-cured membrane CWEs were washed with a 10% (V/V) ethanol solution and ultrapure water for 5 minutes and then conditioned in a 10 mM of the determinand solution overnight prior to any measurements.

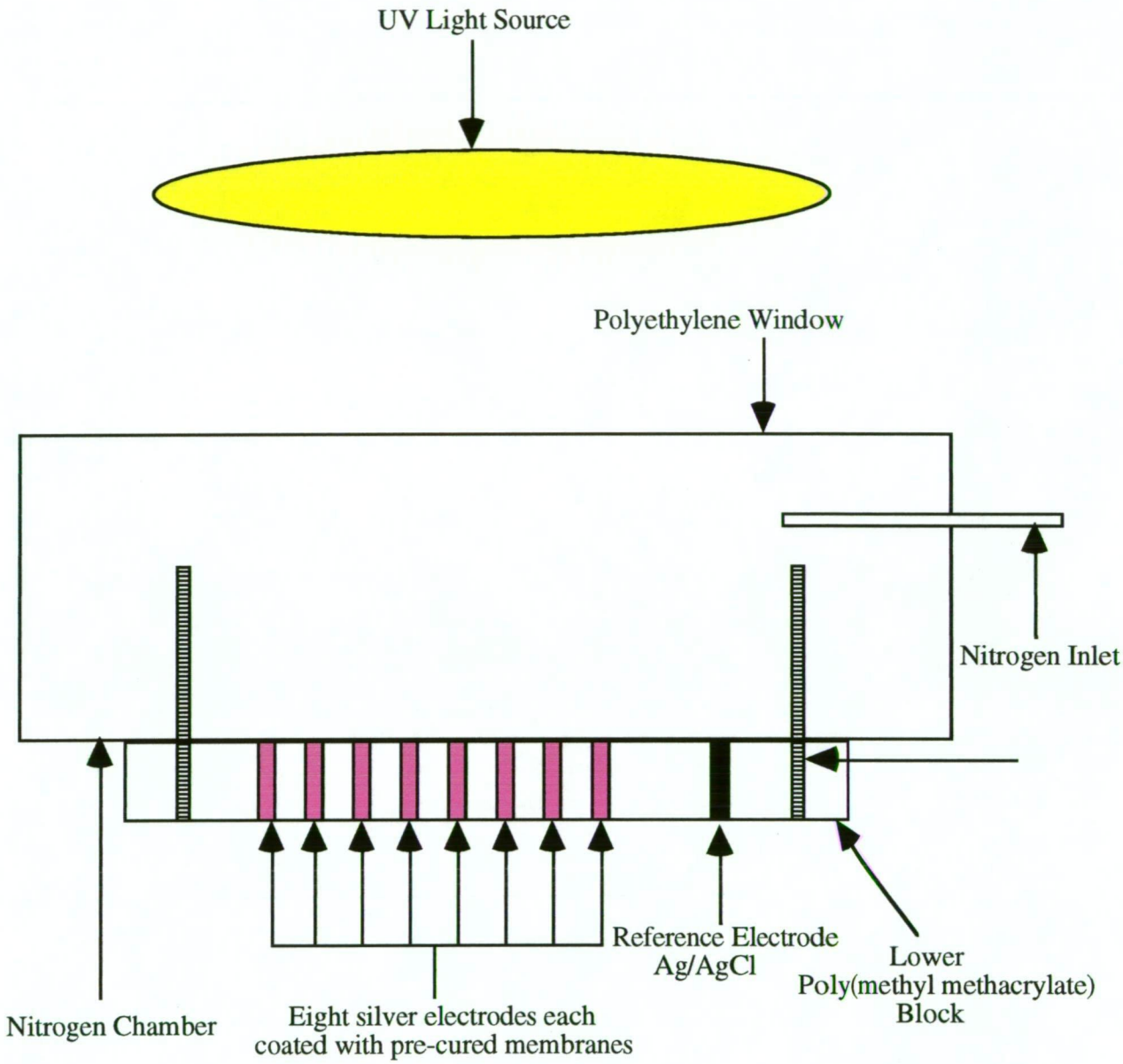

Figure 5.1. The nitrogen chamber box positioned over the eight-electrode flow cell used to photo-cure membranes based CWEs.

5.2.3 Potentiometric Measurement Procedure

Steady-state and FIP measurements were performed for each individual photo-cured membrane based CWE using one of the silver electrodes in the eight-electrode flow cell (Figure 4.2). Steady-state measurements were performed by continuously pumping each standard solution into the flow channel containing the photo-cured electrodes. The reference solution used was 10 mM potassium chloride with all steady-state measurements. In the FIP mode, the reference solution employed was lithium acetate which exhibited a stable reference potential during the course of this study. The FIP measurements were performed by injecting a fixed sample volume into a carrier solution that travels over the surface of the photo-cured membrane. The injection sample volume used throughout this work was 200 µL. The selectivity coefficients for the CWEs were determined using the matched potential method [22] in the steady-state mode.

In the steady-state and FIP modes, electrode potentials were acquired using an analog-to-digital converter similar to that described in Chapter two, Section 2.2.3 (refer to Appendix 1), and were displayed in real time and saved on a Macintosh Powerbook 145B computer. A program called MacCurve Fit © Version 0.7 was used to calculate the electrode slope, the E' and the standard deviations (95% confidence) of a given electrode in either steady-state or FIP modes, as described in Chapter two, Section 2.2.4.

5.2.4 Comparative Analytical Methods

A Varian SpectrAA-300 atomic absorption spectrometer was used to compare the calcium and potassium FIP results. A Pye Unicam SP6-300 UV/Vis spectrophotometer equipped with a flow-through cuvette suitable for flow injection was used to determine ammonium as the salicylic acid analog of indophenol blue [20] to compare the ammonium FIP results, while the chloride FIP result was compared to a UV/Vis spectrophotometric method in the flow injection mode as described previously [21]. The nitrate FIP result was compared to an ion chromatography method using a Millipore Waters IC-Pak A column (50 mm x 4.6 mm, 10 µm) and conductivity detector (Model 430).

5.3 Results and Discussion

The photo-cured membranes for ammonium, calcium, hydrogen (pH), nitrate and potassium CWEs presented in this chapter were all optimum membrane compositions for the potentiometric measurement of their respective determinand in the steady state mode and each type of CWE is discussed in turn. The proposed photo-cured CWEs were characterised in terms of electrode slope, selectivity, response time, mechanical and electrical integrity with a view to determining their suitability in a CWE array. The performance characteristics of each CWE were tested in the FIP mode and each were used to analyse a variety of water samples for their respective determinand.

5.3.1.1 The Calcium CWE

Two photo-cured calcium membranes (Ca1 and Ca2) prepared for this work exhibited the most promising response to pure calcium chloride solutions in the steady-state mode. The membrane compositions (pre-curing) prepared for this work are given in Table 5.1.

Table 5.1. Pre-cured calcium membrane compositions investigated.

Membrane Components	Ca1 (wt/wt %)	Ca2 (wt/wt %)	Ca3 (wt/wt %)	Ca4 (wt/wt %)
KClTPB	—	—	0.9	1.0
TAClTPB	1.8	1.5	—	—
ETH 129	1.4	1.4	1.3	1.4
9,10-phenanthrenequinone	0.5	0.8	0.7	0.6
diphenyliodonium chloride	0.5	0.8	0.7	0.6
BEHP	10.4	—	11.9	—
NPOE	10.4	21.7	11.9	22.9
HDDA	25.0	24.6	24.2	24.5
Ebecryl 600	50.0	49.2	48.4	49.0

The Ca1 and Ca2 CWEs exhibited an electrode slope of 27.7 ± 0.6 and 28.8 ± 0.7 mV change per activity decade, respectively in pure calcium chloride solution. The log-linear ranges observed for the Ca1 and Ca2 CWEs were between 0.01 mM and 10 mM with a detection limit of 0.001 mM in pure calcium chloride solutions in the steady-state mode. The time taken for Ca1 and Ca2 CWEs to achieve 90% steady-state was 5 seconds for each making

these photo-cured membranes ideal for FIP measurements. The observed baseline drifts for the Ca1 and Ca2 CWEs were about 5 mV / week, and both calcium CWEs were stored in 100 mM calcium chloride solution when not in use and were still operational after 3 months.

The interesting feature of the Ca1 and Ca2 membrane compositions was that they both employed the tetradodecyl ammonium tetrakis(4-chlorophenyl) borate lipophilic additive as the anion suppressing agent. The Ca3 and Ca4 CWEs were each similar to the Ca1 and Ca2 membrane compositions respectively, however, they employed the potassium tetrakis(4-chlorophenyl) borate lipophilic additive, as shown in Table 5.1. The Ca3 and Ca4 CWEs both exhibited inferior responses to pure calcium chloride solutions in the steady-state mode compared to the Ca1 and Ca2 CWEs. Calibration curves for the four types of calcium CWEs are presented in Figure 5.2. It is important to note that the absence of anion suppressing agents in these photo-cured calcium membranes results in electrodes that respond to sample anions, such as chloride and was likely due to the formation of the positively charged calcium-ionophore complex in the membrane phase which electrostatically attracts sample anions, as discussed in Chapter one, Section 1.3.4. There are two main reasons for the poor performance exhibited by the Ca3 and Ca4 CWEs: 1) the potassium tetrakis(4-chlorophenyl) borate lipophilic additive did not sufficiently reduce the membrane resistance of the Ca3 and Ca4 CWEs and 2) the potassium ion in the Ca3 and Ca4 membranes was exchanging with the ETH 129 ionophore. Consequently, this could have resulted in the observed non-idealistic response of the Ca3 and Ca4 CWEs.

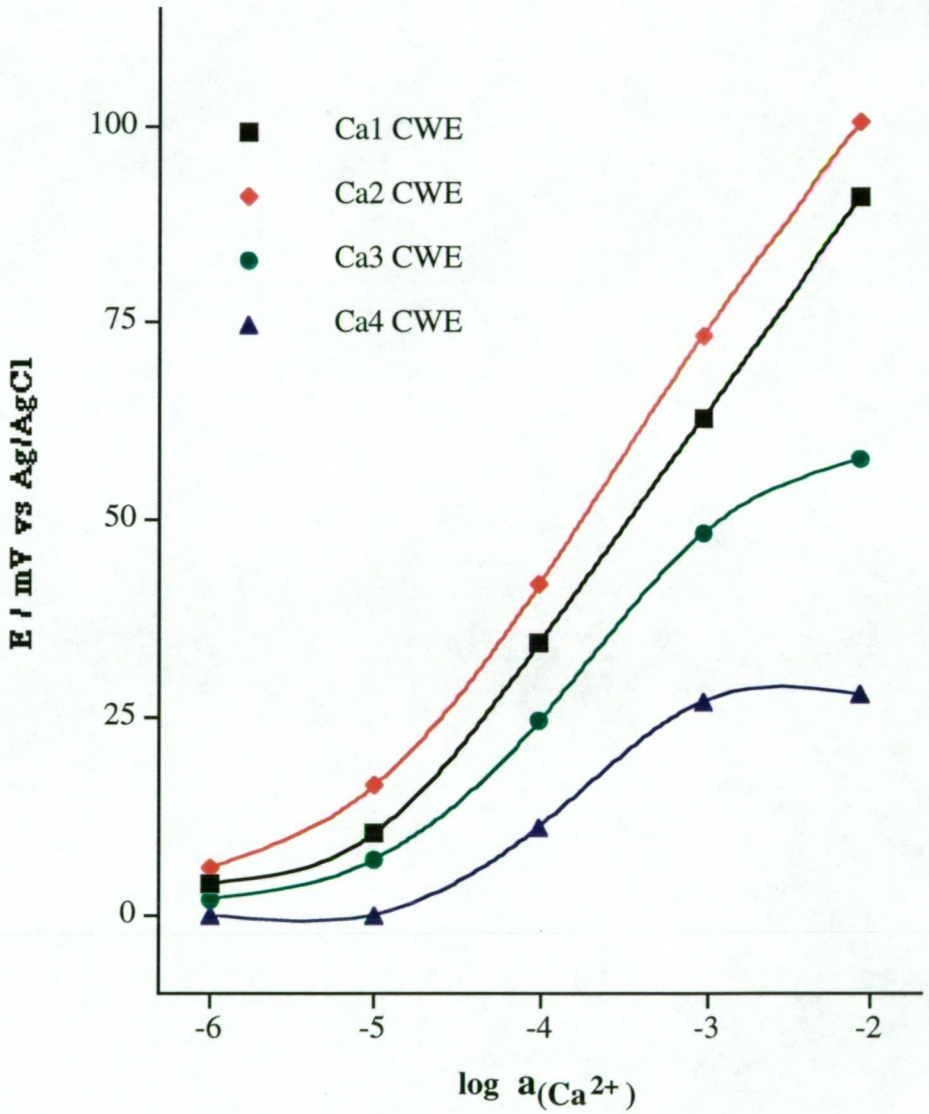

Figure 5.2. Calibration curve observed for the photo-cured (Ca1 - Ca4) calcium CWEs in the steady-state mode in pure calcium chloride solutions.

5.3.1.2 Selectivity of Ca1 and Ca2 CWEs

The selectivity coefficients for the Ca1 and Ca2 CWEs were determined using the matched potential method [22]. Figure 5.3 shows the selectivity coefficients for the photo-cured Ca1 and Ca2 CWEs and a previously reported PVC based calcium ISE employing the same ionophore. The study reporting the PVC calcium ISE employed the separate solution method to calculate their selectivity coefficients and caution needs to be stressed when comparing selectivity coefficients that were determined using two different methods.

The Ca2 CWE was generally more selective against interfering ions than the Ca1. Generally, polar plasticisers such as NPOE having a high dielectric constant ($\varepsilon = 24.2$) are used in liquid polymer membranes of divalent cation ISEs in order to increase the selectivity of the determinand ion over monovalent cations [19]. The plasticiser mixture employed for the Ca1 membrane consisted of 50% BEHP ($\varepsilon = 4.2$) and 50 % NPOE, while the plasticiser used for the Ca2 membrane was NPOE alone as shown in Table 5.1. Since the overall polarity of the Ca1 membrane was lower than that of the Ca2 membrane, the inferior selectivity observed for the Ca1 CWE was expected.

The observed selectivities over the magnesium ion for the Ca1 and Ca2 based CWEs were inferior to a previously reported PVC membrane for calcium employing the same ionophore [23]. The Ca1 and Ca2 CWEs experienced severe interference from the hydrogen ion, but this was not detrimental to the calcium ion response. The Ca2 CWE exhibited adequate selectivity over sodium, potassium and magnesium ions for calcium FIP measurements in a range of water samples. However, the pH of the standards and samples must be the same, in order to correct for hydrogen ion interference.

Figure 5.4 shows the calibration plot for the Ca2 CWE measured in the steady-state mode with solutions of different pH. Using a 10 mM sodium acetate buffer at pH = 5.5, there was a negligible response to calcium ions. In 10 mM sodium acetate buffer at pH 7.0 and in 10 mM sodium hydrogen carbonate buffer at pH 8.3, the electrode slopes were 22.5 ± 0.9 and 24.5 ± 0.5 mV per activity decade, respectively, and the observed log-linear range was between 0.5 mM and 10 mM calcium in the steady-state mode. Clearly, to perform reliable potentiometric measurements with this CWE, the pH must be ≥ 7.0 and there must be a pH match between the standards and the samples as discussed above.

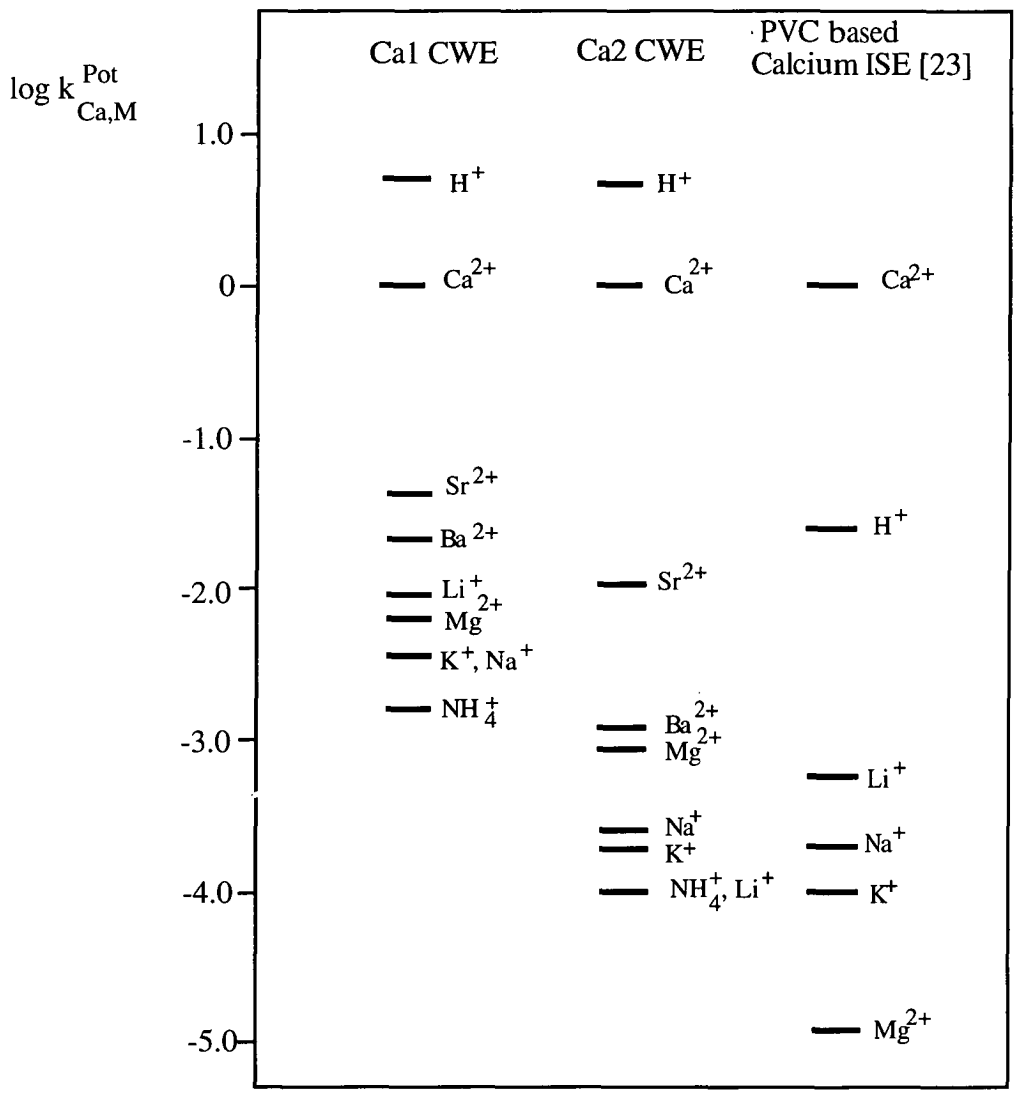

Figure 5.3. The selectivity coefficients for the photo-cured Ca1 and Ca2 CWEs compared to previously reported PVC based calcium ISE.

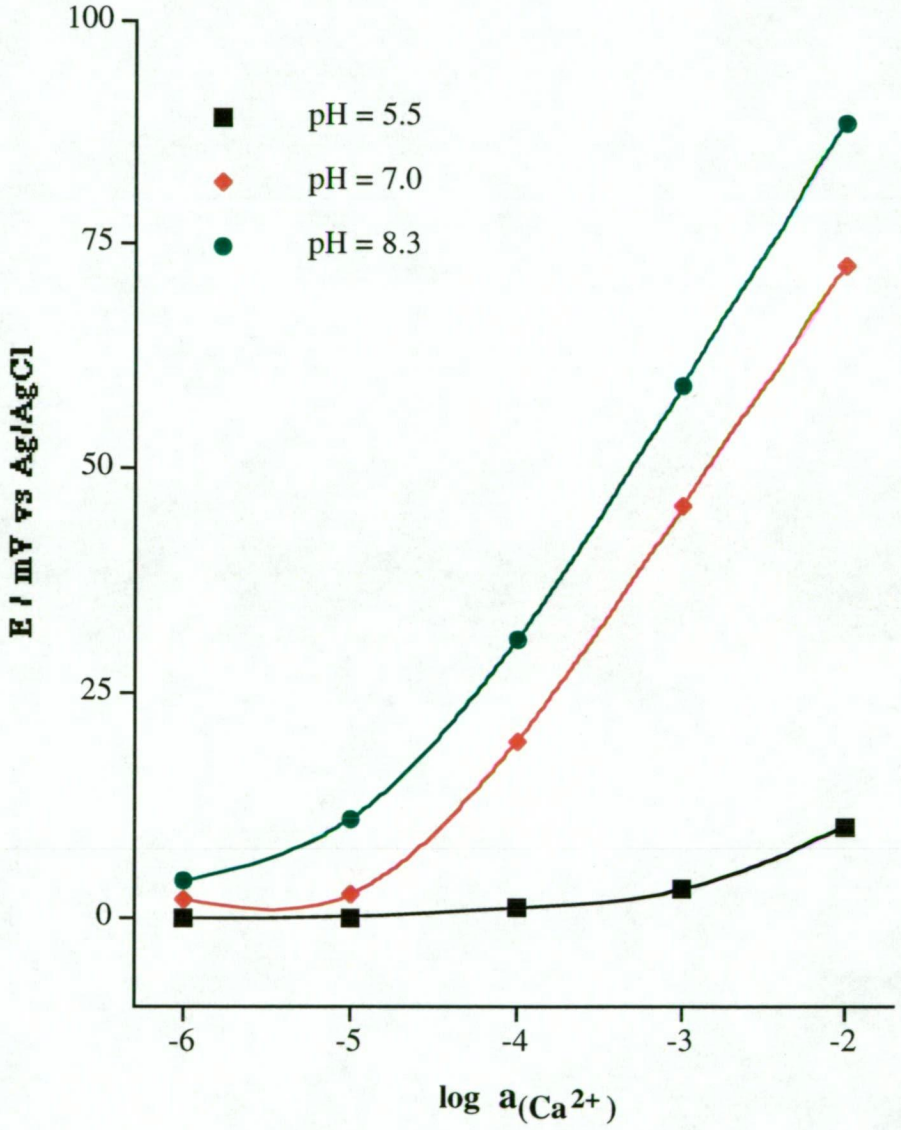

Figure 5.4. Calibration curves observed for the photo-cured Ca2 CWE in the steady-state mode with calcium chloride solutions in 10 mM sodium acetate buffer at pH 5.5 and pH 7.0, and 10 mM sodium hydrogen carbonate buffer at pH 8.3.

There are three possible reasons for the hydrogen interference experienced by the Ca1 and Ca2 CWEs; 1) the epoxyacrylate membrane exhibited some pH sensitivity, 2) the lipophilic additive (tetradodecyl ammonium tetrakis(4-chlorophenyl) borate) was sensitive to pH, or 3) the ETH 129 ionophore (refer to Chapter one, Figure 1.3) was degraded after exposure to the UV radiation. Each point will be discussed in turn.

There have been numerous photo-cured epoxyacrylate based anion and cation-selective electrodes employing various ionophores and plasticisers (including NPOE), and none of these membranes have experienced any hydrogen interference [6-10,12,13,15]. A blank photo-cured membrane of similar composition to the Ca2 membrane, but without the ETH 129 ionophore, exhibited no hydrogen ion response. It is therefore unlikely that the epoxydiacrylate polymer base and the lipophilic additive, tetradodecyl ammonium tetrakis(4-chlorophenyl) borate, contributed to the pH interference shown in this study This eliminates the photo-cured epoxyacrylate polymer base for contributing to any pH interference of the Ca1 and Ca2 CWEs and the tetradodecyl ammonium tetrakis(4-chlorophenyl) borate additive.

In a previous study, oven-curing (90°C for 30 minutes) of a silicon rubber based calcium CWE which contained the ETH 129 ionophore resulted in an electrode response that was sub-Nernstian due to degradation of the ionophore [24]. In a different study, the room-temperature curing of a plasticised silicon rubber membrane employing the ETH 129 ionophore produced a calcium CWE that was comparable with PVC based calcium ISEs [25].

A PVC calcium CWE based on the ETH 129 ionophore and the potassium tetrakis (4-chlorophenyl)borate lipophilic additive was prepared as described previously [23] was prepared and evaluated. The PVC based calcium CWE exhibited Nernstian response and exhibited no hydrogen interference. Then the PVC based calcium CWE was exposed to UV radiation under the same conditions as the Ca1 and Ca2 CWEs. The PVC based calcium CWE exhibited a significant hydrogen ion interference similar to that observed for the Ca1 and Ca2 CWEs. Clearly, UV-curing of liquid polymer membranes containing the ETH 129 ionophore above room temperature results in a calcium electrode that shows some inferior electrochemical properties when compared to any liquid polymer membrane prepared at room temperature. Therefore, it is believed that some degradation of the ETH 129 ionophore occurs on UV curing which raises the temperature of the membrane above room temperature and that this leads to the

observed pH interference. The excellent selectivity observed against monovalent ions suggests that the extent of degradation is not great.

5.3.1.3 FIP Measurements with the Ca2 CWE

Typical peaks observed for four photo-cured Ca2 CWEs in the FIP mode are presented in Figure 5.5 after baseline offsetting for each response. The photo-cured Ca2 CWE was fast responding, exhibited excellent adhesion to the silver substrate and was mechanically strong, thus making it ideal for FIP measurements. The carrier was 10 mM sodium hydrogen carbonate buffer (pH = 8.3) and at no stage did the calcium ion precipitate out of solution. The precision of triplicate peak heights range between 1.0% and 4.0% (RSD). The mean electrode slope observed for the four Ca2 CWEs was 25.4 ± 0.4 mV change per activity decade which demonstrates the reproducible manufacture of the Ca2 membrane. The log-linear range observed for the Ca2 CWE was between 0.5 mM and 10 mM and the detection limit was 0.01 mM of calcium using a 10 mM sodium hydrogen carbonate ionic background in the FIP mode. The FIP response observed for the Ca2 CWE was 85 % of the steady-state response. The deterioration of the observed log-linear range and detection limit of the Ca2 CWE in the FIP mode compared to the steady-state mode was due to initial slow response of the electrode at low concentrations, dispersion of the injected sample zone and the slight interference by the sodium ion present in the ionic background.

To demonstrate the reliability of the Ca2 CWE in the FIP mode, three types of water samples were analysed for their calcium content: (1) with low levels of calcium ions that would be near the detection limit of the Ca2 CWE (Tap water), (2) with similar levels of calcium and magnesium ions (Summit Mineral Water), and (3) with a higher calcium level than that of magnesium (Evian Mineral Water). Table 5.2 presents the results of the water analysis which were in agreement with AAS measurements.

Table 5.2. Calcium determination of various water samples by FIP and AAS, (n = 3).

Water sample	Ca2 ISE mg/L (RSD)	AAS mg/L (RSD)	Labelled mg/L
Evian mineral water	71.2 (2.1%)	78.2 (0.3%)	78
Summit mineral water	16.0 (4.1%)	15.2 (0.3%)	18
Tap water	5.3 (4.2%)	5.6 (0.2%)	1 - 5*

* Expected range

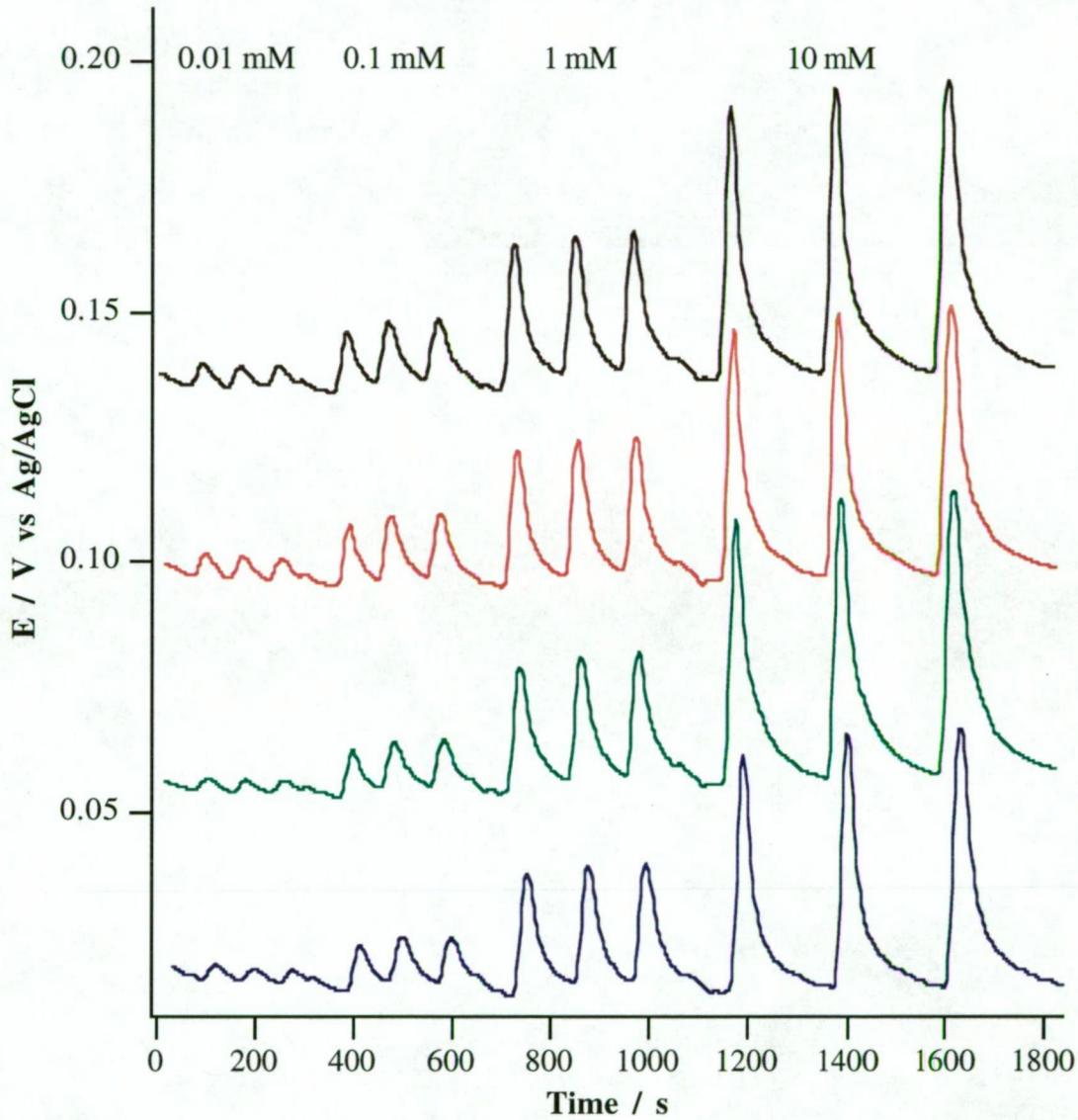

Figure 5.5. Typical peak height responses observed for 4 photo-cured Ca2 CWEs, carrier stream was 10 mM sodium hydrogen carbonate (pH = 8.3) and reference stream was 10 mM sodium chloride, total flow rate was 2.5 mL/minute, and the sample volume was 200 µL.

5.3.2.1 The Ammonium CWE

The optimum membrane composition for the photo-cured ammonium CWE is given in Table 5.3. The photo-cured ammonium sensor exhibited a Nernstian response of 59.4 ± 0.6 mV change / activity decade over a concentration range between 0.01 mM and 10 mM with a detection limit of 0.001 mM with pure ammonium chloride solutions in the steady-state mode. Figure 5.6 shows the calibration curve for the ammonium CWE. The photo-cured ammonium CWE exhibited a negligible response to hydrogen ions for $2.0 < pH < 10.0$ and a negligible electrode drift of < 2 mV / day, was observed. The ammonium CWE was still operational after 4 weeks. The time taken for the photo-cured ammonium CWE to attain 90% of steady-state response was typically 5 seconds making this electrode ideal for FIP measurements.

Table 5.3. Optimum pre-cured membrane composition used for the ammonium CWE

Membrane Components	NH_4 CWE (wt/wt %)
KClTPB	1.6
Nonactin	5.3
9,10-phenanthrenequinone	0.4
diphenyliodonium chloride	0.4
Uvecryl P36	—
2-nitrophenyl octyl ether	23.5
bis(2-ethylhexyl)phlalate	—
HDDA	34.4
Ebecryl 600	34.4

In this study, the plasticiser found to produce the most responsive ammonium electrode was NPOE, producing photo-cured membranes that were hard and transparent exhibiting excellent adhesion to the metal substrate. Photopolymerisation of the ammonium membrane employing nitro containing plasticiser, such as NPOE, was accomplished using, an initiator of a mixture containing equal amounts of 9,10-phenanthrenequinone and diphenyliodonium chloride [11]. Photo-cured ammonium membrane based sensors employing either BEHP or DOPP produced cloudy membranes suggesting an incompatibility between the constituents of the membranes and consequently failed to respond to the determinand.

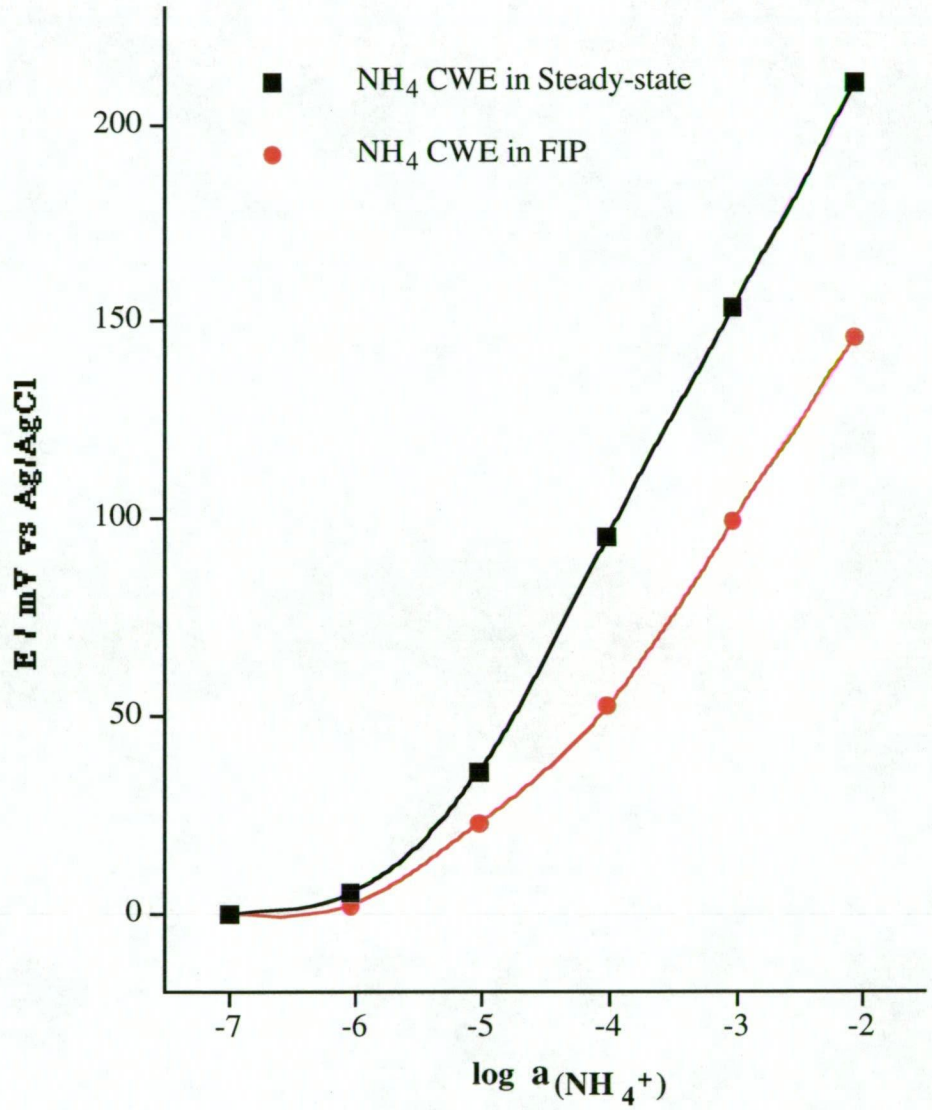

Figure 5.6. Calibration curves for the photo-cured ammonium CWE using pure NH_4Cl solutions in the steady-state compared to the FIP response. Sample volume = 200 µL, flow rate = 1.3 mL/minute and the carrier and reference streams were 3 mM lithium acetate.

The ideal polymer base for the photo-cured ammonium membrane contained equal amounts of epoxydiacrylate and 1,6-hexanediol diacrylate. Increasing the amount of epoxydiacrylate in the polymer base to twice that of 1,6-hexanediol diacrylate, resulted in an ammonium sensor that exhibited a near-Nernstian response of 58.0 ± 0.9 mV change / activity decade and a log-linear range between 0.01 mM and 100 mM. However, the response time for this electrode was poor, requiring 30 seconds to attain 90% of the steady-state value (compared to 5 seconds for the optimum CWE).

5.3.2.2 Selectivity of the Ammonium CWE

The selectivity coefficients for the ammonium CWE were determined using the matched potential method [22]. The selectivity coefficients determined for the ammonium CWE are presented in Figure 5.7, and are compared to the selectivity coefficients for PVC and photo-cured polyurethane based ammonium electrodes reported in previous studies. The photo-cured ammonium CWE generally exhibited superior selectivity when compared to the previously reported PVC based ammonium ISE, that employed the NPOE plasticiser [26] and a photo-cured polyurethane based ammonium sensor [3]. In particular, an improvement was achieved with the selectivity of the determinand against the interference of potassium ions, which has been a limitation in previous studies.

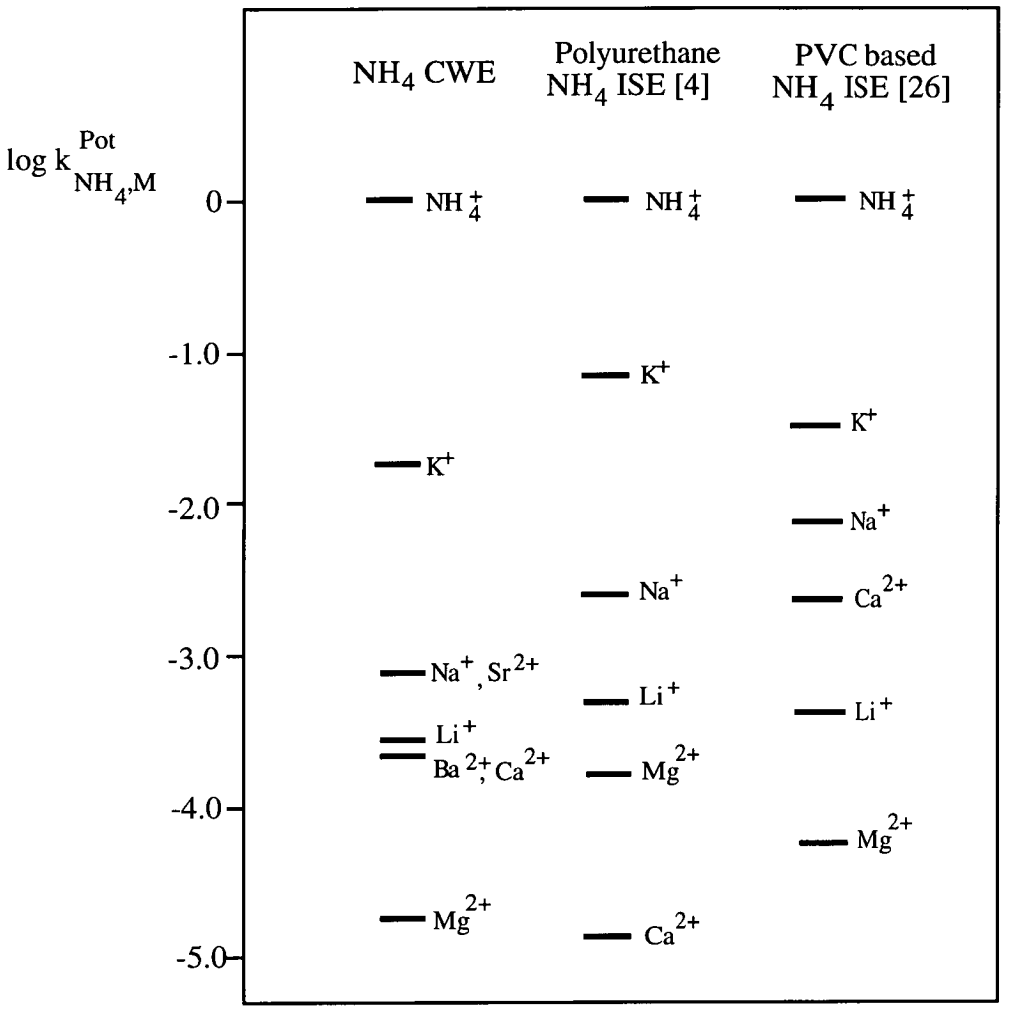

Figure 5.7. Selectivity coefficients determined for the ammonium CWE compared to previously reported polyurethane and PVC based ammonium sensors.

5.3.2.3 The Ammonium CWE in the FIP mode

Typical flow injection peaks observed for the photo-cured ammonium CWE are presented in Figure 5.8 demonstrating the reproducibility of the peak heights observed. There was some baseline drift observed when high concentrations were injected. However, in the FIP mode there is little effect on calibrations since data processing can account for any drift when calculating peak heights for calibration plots. The photo-cured ammonium CWE exhibited a near-Nernstian slope of 49.2 ± 1.0 mV change / activity decade using a 3 mM lithium acetate ionic background in the FIP mode. The sub-Nernstian response observed for the ammonium CWE in the FIP mode is typical of other photo-cured sensors [10,13,15] and was due to the initial slow response of the photo-cured membrane and the dispersion of the injected sample zone. However, the FIP response observed represents about 85% of the steady-state response and provides adequate analytical sensitivity. A calibration curve for the ammonium CWE in the FIP mode is given in Figure 5.6. The log-linear range observed was between 0.01 mM and 10 mM and a sample throughput of up to 180 injections / hour was easily achieved.

To determine the reliability of the ammonium CWE in the FIP mode, hydroponic nutrient sample and waste water samples obtained from a local greenhouse grower were analysed for their ammonium content. The potassium content of the hydroponic nutrient and waste water solutions was determined by AAS measurements and was found to be 265.4 and 312.2 mg/L, respectively. Table 5.4 presents the results of the ammonium water analysis and are in agreement with UV/Vis spectrophotometry in the flow injection mode, thus demonstrating the accuracy of the ammonium CWE and the good selectivity observed against interfering ions such as potassium in the FIP mode.

Table 5.4. Determination of ammonium levels in hydroponic nutrient and waste water samples (n = 3) in the FIP mode. RSD values quote the peak height precision.

Water sample	NH_4 CWE in FIP, mg/L (RSD)	UV / Vis (NH_4^+), mg/L (RSD)
Hydroponic Nutrient Sample	31.8 (1.5%)	29.5 (1.3%)
Waste water Sample	36.5 (1.9%)	37.4 (1.1%)

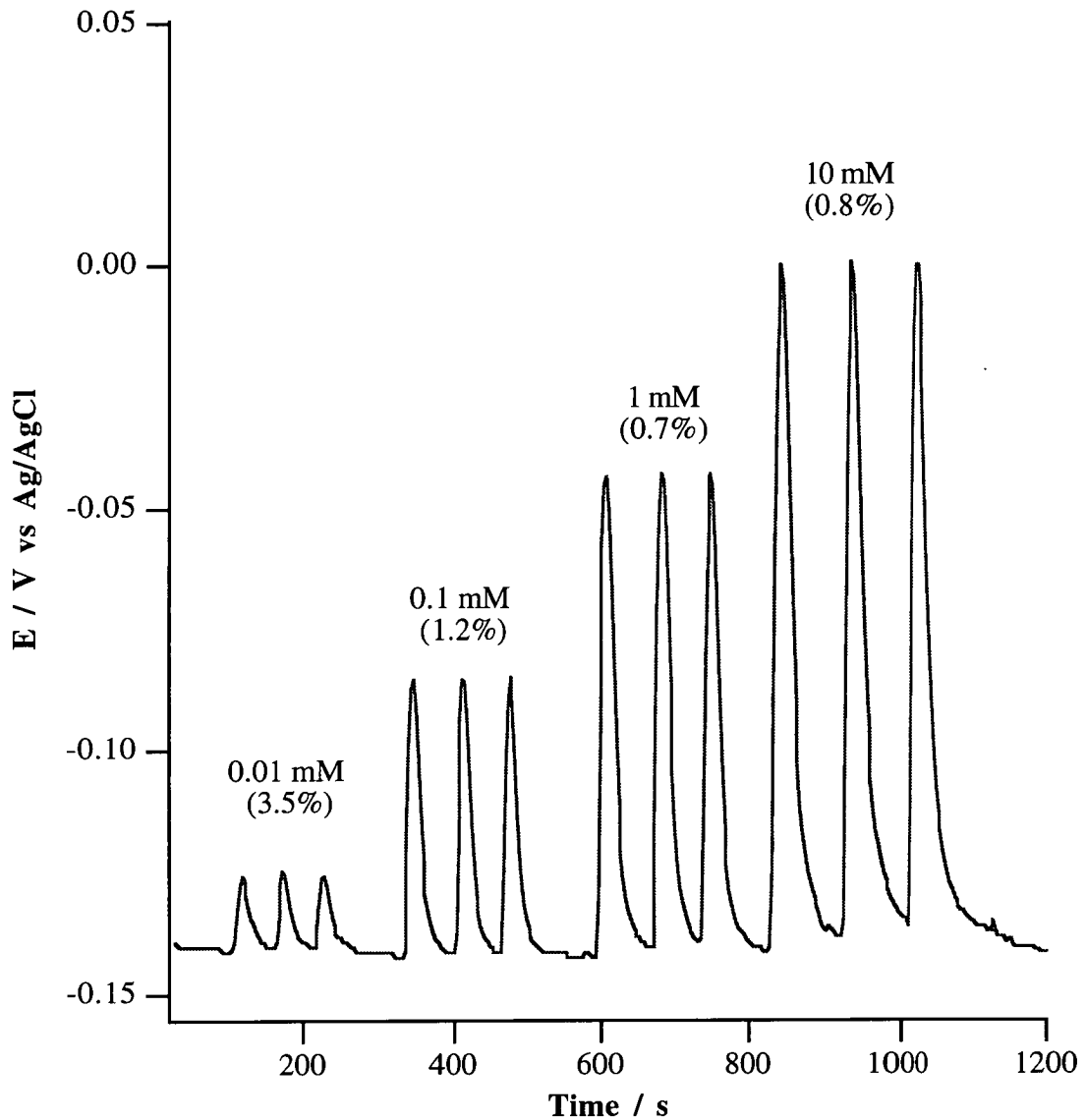

Figure 5.8. Typical peak heights observed for the photo-cured ammonium CWE in the FIP mode. Injection sample volume was 200 µL, total flow rate was 1.3 mL/minute and the carrier and reference streams were both 3 mM lithium acetate.

5.3.3.1 The Hydrogen CWE

Two photo-cured hydrogen CWEs (pH1 and pH2 CWEs) prepared with different plasticisers (BEHP and NPOE) were found to exhibit near-Nernstian response to pH. Their membrane compositions are given in Table 5.5.

Table 5.5. Optimum pre-cured membrane compositions used for the pH CWEs

Membrane Components	pH1 (wt/wt %)	pH2 (wt/wt %)
KClTPB	1.8	1.6
N,N-dioctadecylmethylamine	5.3	5.2
9,10-phenanthrenequinone	—	0.5
diphenyliodonium chloride	—	0.5
Uvecryl P36	5.3	—
2-nitrophenyl octyl ether	—	23.2
bis(2-ethylhexyl)phlalate	23.2	—
HDDA	32.2	34.5
Ebecryl 600	32.2	34.5

The pH1 CWE exhibited near-Nernstian response of 55.10 ± 0.8 mV change / pH unit, while the pH2 CWE exhibited a slightly lower electrode slope of 53.5 ± 0.4 mV change / pH unit, both over a pH range between 4.0 and 11.0. Typical calibration plots for the pH1 and pH2 CWEs are presented in Figure 5.9. Each membrane was hard and transparent and exhibited excellent adhesion to the silver substrate. The response time for both the pH1 and pH2 CWEs to attain 90% of steady-state response was typically 3 seconds, making these pH sensors suited for FIP measurements. The pH1 and pH2 CWEs exhibited a negligible electrode drift of < 2 mV / day and were still operational after 4 weeks.

A recently reported PVC-based hydrogen electrode with the ionophore N,N-dioctadecylmethylamine exhibited a linear response over a pH range between 3.0 and 11.0 [27]. The somewhat shorter pH range observed for the photo-cured pH1 and pH2 CWEs may arise from the restriction of the mobility of the ionophore in the epoxydiacrylate polymer base. However, the linear pH ranges of the pH1 and pH2 CWEs were greater than a previously reported photo-cured hydrogen membrane electrode that was based on the tridodecylamine ionophore which exhibited a pH linear range between 5.0 and 10.0 [12].

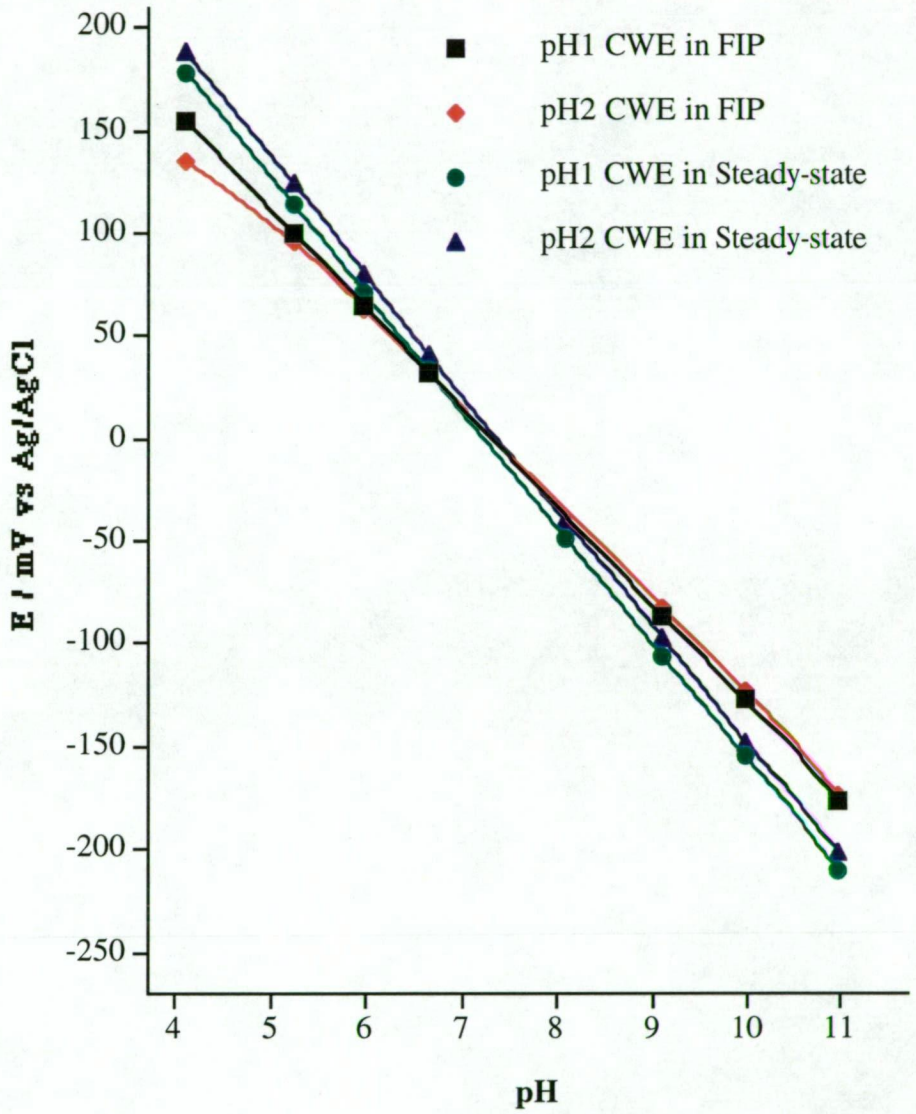

Figure 5.9. Comparison of calibration curves for the photo-cured pH1 and pH2 CWEs using universal pH buffer solutions in the steady-state and FIP modes.

In agreement with a previous report of a photo-cured pH electrode [12], the optimum ratio of epoxydiacrylate to 1,6-hexanediol diacrylate in the polymer base was 1:1. Increasing the amount of the epoxydiacrylate polymer in the membrane composition to a 2:1 ratio resulted in pH sensors that were very slow in responding and had a non-Nernstian response, regardless of the plasticiser employed. The poor response characteristics observed when increasing the amount of the epoxydiacrylate was due to a greater restriction in mobility for the ionophore in the membrane phase, making the ionophore incompatible with this polymer mixture.

5.3.3.2 Selectivity for Hydrogen Ion (pH) CWEs

The selectivity coefficients for the photo-cured pH CWEs were determined using the fixed interference method [28]. The selectivity coefficients for the pH1 and pH2 CWEs are presented in Table 5.5, and are compared to the selectivity coefficients reported for PVC based sensors in previous studies. The selectivity exhibited by the pH1 CWE was generally superior compared to the pH2 CWE and a previously reported PVC based pH ISE [27] employing the same ionophore.

Table 5.5. Selectivity coefficients determined for the pH1 and pH2 CWEs and previously reported PVC based pH ISEs.

$\log k^{Pot}_{(H, M)}$	$M = Na^+$	$M = K^+$	$M = Li^+$	$M = Ca^{2+}$	$M = Mg^{2+}$
Photo-cured pH1 CWE	-10.9	< -11.0	< -11.0	-10.8	-10.5
Photo-cured pH2 CWE	-10.3	-10.2	-10.1	-10.2	-10.2
PVC based pH ISE [27]	-10.3	-10.0	—	-10.6	—

5.3.3.3 Hydrogen Ion (pH) CWEs in the FIP mode

As shown in previous studies [21, 29], the buffer capacity of the injected sample zone must be at least 10 times greater than that of the carrier, otherwise there will be sufficient mixing and consequent alteration of the pH of the injected sample zone, resulting in an inaccurate result. To minimise the dispersion of the injected sample zone it is also important to minimise the pH difference between the injected sample and the carrier in order to attain reliable pH measurements in the FIP mode. The carrier fulfilling these requirements and used in this study was 3 mM lithium acetate with pH between 7.5 and 6.5.

The photo-cured pH1 and pH2 CWEs each exhibited a near-Nernstian slope of 50.2 ± 0.4 and 46.2 ± 1.0 mV change / pH unit, respectively in the FIP mode using a 3 mM lithium acetate (pH = 7.30) carrier solution. Figure 5.10 shows typical FIP responses for the pH1 and pH2 CWEs and the calibration curve is presented in Figure 5.9. The linear response of the pH1 CWE was between pH 4.0 and 11.0 in the FIP mode and the linear range was similar to that observed in the steady-state mode. The FIP response observed for the pH1 CWE was about 90% of the steady-state value and provides adequate analytical sensitivity.

The pH2 CWE exhibited a reduced pH range between pH 4.5 and pH 11.0 in the FIP mode compared to the steady-state response, as shown in Figure 5.9. The FIP response observed for the pH2 CWE represented 85% of the steady-state response. The reduction of the linear range observed for this sensor in the FIP mode was likely due to interference from the lipophilic sample anions present in the universal pH buffer solutions. In previous studies, it has been shown that liquid polymer membranes employing polar plasticisers were more susceptible to anion interference than membranes using non-polar plasticisers [19]. Therefore, it may be concluded that the pH2 CWE experienced interference from sample anions since NPOE plasticiser employed had a high dielectric constant (ε = 24.2) and was more polar than the BEHP plasticiser (ε = 4.2) used for the pH1 CWE.

To determine the accuracy of the pH1 and pH2 CWEs in the FIP mode, a hydroponic nutrient solution obtained from a local greenhouse grower and a natural mineral water sample were analysed for their pH value. Table 5.6 presents the FIP results of the water analysis showing good agreement with a pH glass electrode.

Table 5.6. Determination of pH in hydroponic nutrient and natural mineral water samples (n = 3) in the FIP mode. RSD values quote the peak height precision.

Water sample	pH1 CWE, (RSD)	pH2 CWE, (RSD)	pH (Glass)
Hydroponic Nutrient Sample	4.88 (1.7%)	4.89 (2.0%)	4.84
Deep Spring Mineral Water	6.12 (1.8%)	6.11 (1.9%)	6.15

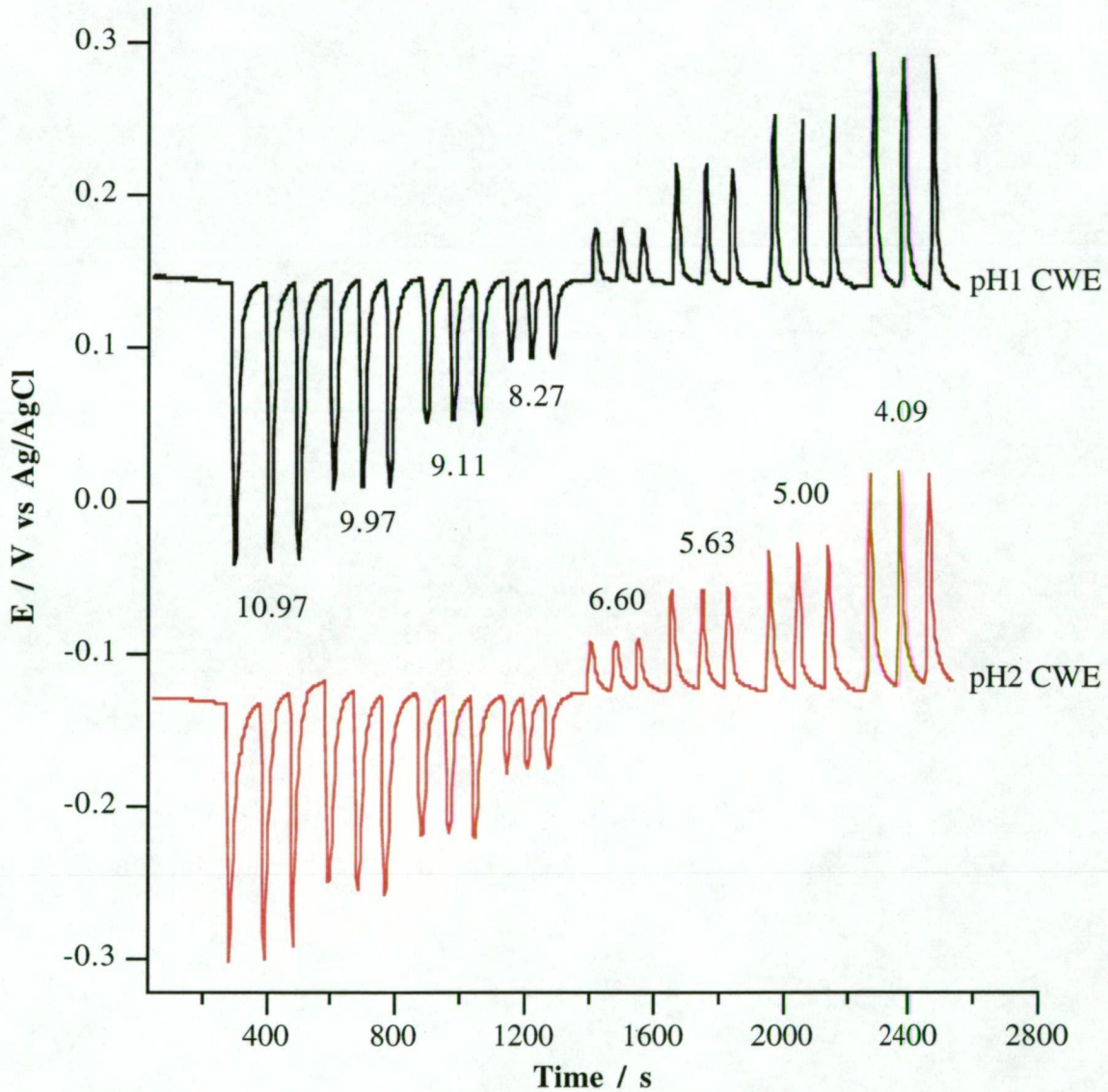

Figure 5.10. Typical peak heights observed for the photo-cured pH1 and pH2 CWEs in the FIP mode. Injection sample volume was 200 μL, total flow rate was 1.6 mL/minute and the carrier and reference streams were both 3 mM lithium acetate (pH = 7.30).

5.3.4.1 The Potassium CWE

Two photo-cured potassium based CWEs (K1 and K2 CWEs) were prepared and evaluated and their respective membrane compositions are presented in Table 5.7.

Table 5.7. Optimum pre-cured membrane compositions used for the potassium CWEs

Membrane Components	K1 (wt/wt %)	K2 (wt/wt %)
KClTPB	1.2	0.9
TAClTPB	0.6	1.0
BME-44 Ionophore	4.3	4.9
9,10-phenanthrenequinone	0.4	0.4
diphenyliodonium chloride	0.4	0.4
NPOE	12.7	26.3
BEHP	12.7	—
HDDA	22.8	22.0
Ebecryl 600	45.7	44.1

The electrode response observed for the K1 and the K2 CWEs were both Nernstian over a log-linear range between 0.01 mM and 100 mM in pure potassium chloride solutions in the steady-state mode. Comparative calibration curves for the photo-cured K1 and K2 CWEs in the steady-state mode is given in Figure 5.11. The K1 and K2 CWEs exhibited a negligible response to hydrogen ions between $3.0 < pH < 10.0$.

All the photo-cured potassium membranes prepared were transparent and mechanically strong suggesting that the ionophore, plasticiser and lipophilic additives were all compatible with the polymer mixture, consisting of Ebecryl 600 and 1,6-hexanedioldiacrylate, that was used in this study. A negligible electrode drift (< 2 mV / day) for the K2 CWE and a more significant drift of > 10 mV/day was observed for the K1 CWE. The photo-cured K1 and K2 CWEs were both stored in a 10 mM potassium chloride solution when not in use. The operational lifetime observed for the K1 ISE was limited to less than 3 weeks, while the K2 ISE was still operational after 4 months with little observable change to the Nernstian response and log-linear range. The time taken for the photo-cured K1 and K2 CWEs to achieve 90% of complete steady-state were both 5 seconds making both CWEs ideally suited for FIP measurements.

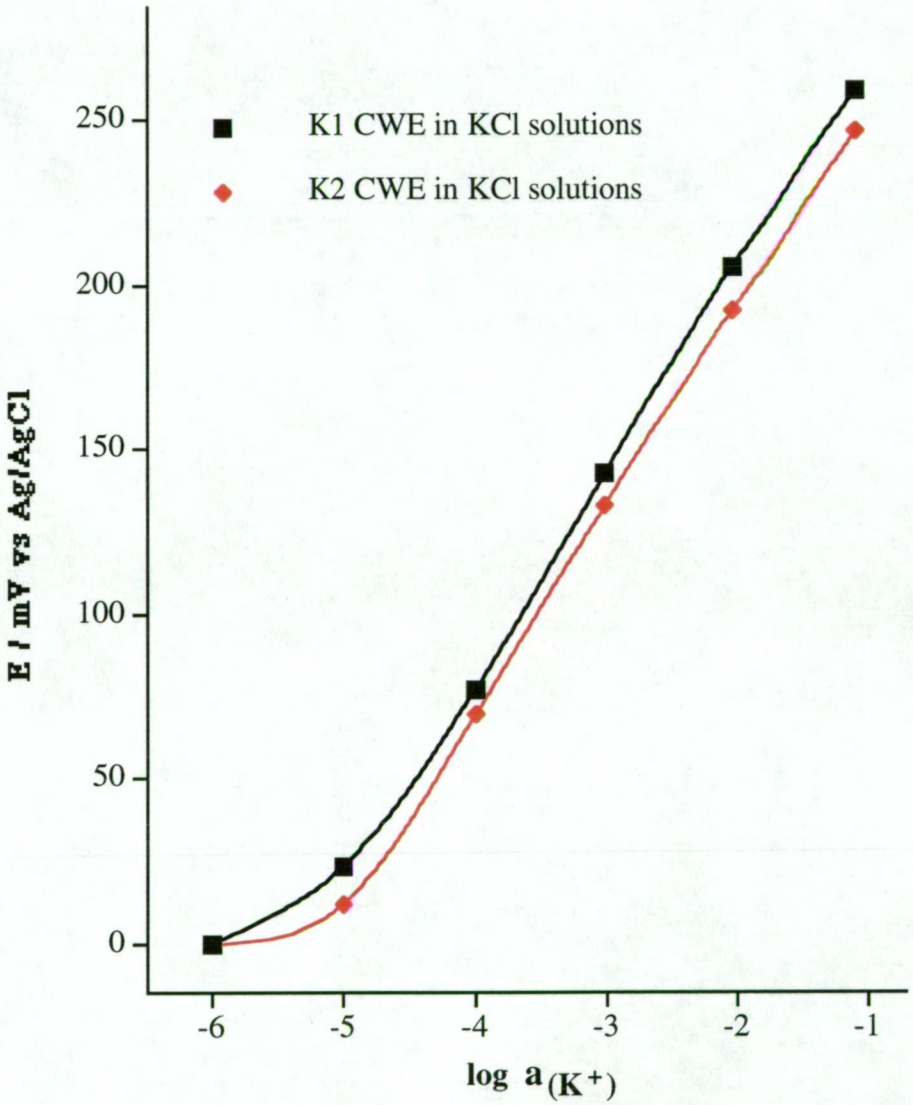

Figure 5.11. Calibration curves for the photo-cured K1 and K2 CWEs using pure KCl solutions in the steady-state mode.

5.3.4.2 Anion Interferences

Figure 5.12 shows the effect on the calibration curve for the K1 and K2 CWEs when pure potassium nitrate standard solutions were used instead of potassium chloride solutions. The K1 and K2 CWEs exhibited electrode slopes between 57 and 60 mV change per activity decade with pure potassium nitrate solutions, however, the log-linear range was reduced to 0.01 mM and 10 mM compared to the log-linear range observed with pure potassium chloride solutions. The observed nitrate interference for the K1 and K2 CWEs at the upper concentration was due to the use of the NPOE plasticiser in the photo-cured membranes, and the greater lipophilicity of the nitrate ion compared to the chloride ion as predicted by the Hofmeister lipophilic anion series [19].

Previous studies have demonstrated that anion interference observed for liquid polymer membrane based ISEs is more evident for a polar plasticiser, such as NPOE, compared to the use of non-polar plasticisers [19]. The severity of the anion interference is also dependent on the lipophilicity of the anion, that is, the greater the lipophilicity of the anion, the greater the penetration of the anion into the liquid membrane, consequently, the greater the interference exerted upon the cation selective membrane at higher concentration, usually > 10 mM [19].

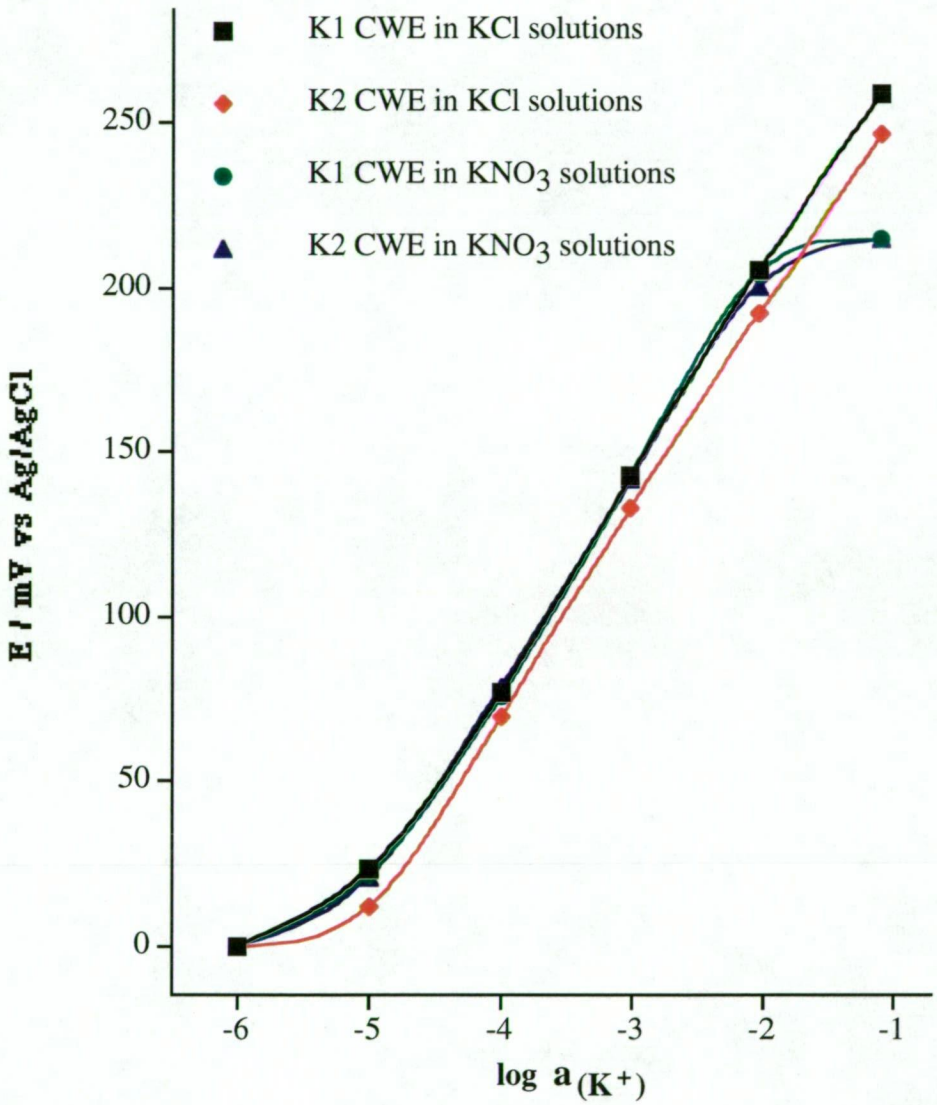

Figure 5.12. Comparison of the calibration curves for the photo-cured K1 and K2 CWEs using pure KCl and KNO_3 solutions in the steady-state mode.

5.3.4.3 Selectivity for K1 and K2 CWEs

The selectivity coefficients for the photo-cured K1 and K2 CWEs are presented in Figure 5.13 and were determined using the matched potential method [22]. Clearly, the K2 CWE had exhibited similar selectivity properties to that of a previously reported PVC based potassium electrode [30] and was also superior compared to the K1 CWE. The K1 and K2 CWEs exhibited selectivity superior to that of previously reported photo-cured potassium electrode based on the valinomycin ionophore [13]. The K2 CWE and the previously reported PVC based potassium ISE both employed the NPOE plasticiser. It is unusual for monovalent cation-selective electrodes based on liquid polymer membranes to employ polar plasticisers such as NPOE as suggested by previous work [19], however, there have been many monovalent cation based ISEs that employ such plasticisers and perform satisfactorily.

In previous studies, it has been demonstrated that the BME-44 ionophore in PVC based membranes exhibits improved selectivity when NPOE plasticiser was employed compared to using a non-polar plasticiser such as bis(1-butylphenyl)adipate [30]. In this study, similar selectivity behaviour was observed for the photo-cured K1 CWE which contained a 50% BEHP and 50% NPOE plasticiser mixture compared to the K2 CWE which solely used the NPOE plasticiser. The polarity of the photo-cured K1 CWE would have been lower compared to the K2 CWE, and consequently the more superior selectivity was observed for the K2 CWE as shown in Figure 5.13.

It is unusual that an improved selectivity was observed for monovalent selective electrodes when polar plasticiser were employed. Independently, this study using photo-curable diacrylate based membranes and a previous study using conventional PVC based membranes with the BME-44 ionophore demonstrated that improved selectivity for these potassium sensors over both monovalent and divalent interfering ions were observed when employing NPOE compared to the use of less polar plasticisers such as BEHP in this study and bis(1-butylpentyl)adipate in the previous study. However, the disadvantage of using the NPOE plasticiser with the BME-44 ionophore in photo-curable membrane presented in this work and PVC membranes in a previous study [30] is that lipophilic anion interference is more prevalent.

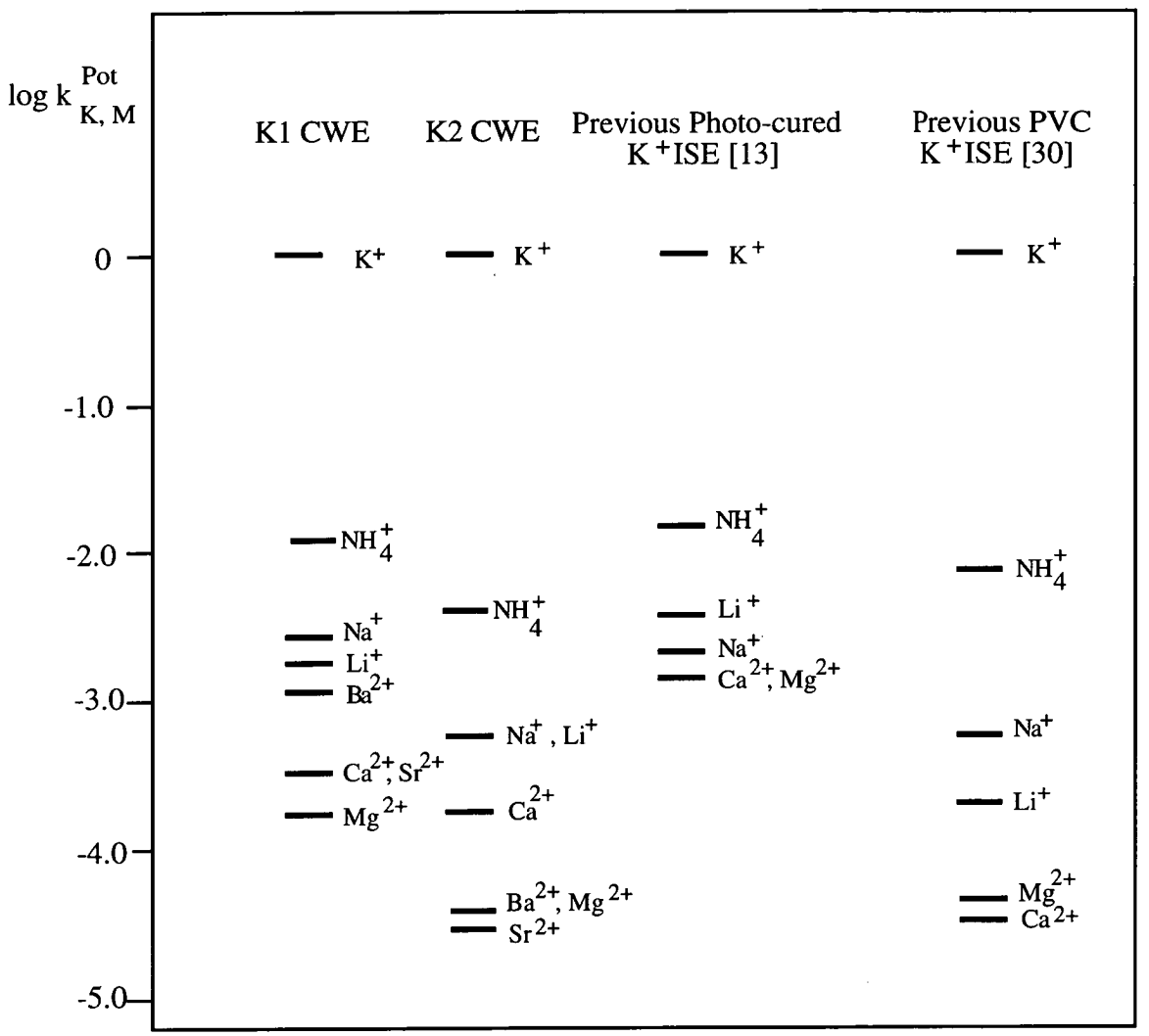

Figure 5.13. Selectivity co-efficients for the K1 and K2 CWEs compared to a previously reported photo-cured potassium ISE [13] using valinomycin ionophore and a PVC based potassium ISE [30] using the BME-44 ionophore.

5.3.4.4 FIP Measurements for the K1 and K2 CWEs

The photo-cured K1 and K2 CWEs each exhibited a near-Nernstian slope of 47.4 ± 1.1 and 48.2 ± 0.9 mV change per activity decade using a 10 mM lithium acetate ionic background, respectively in the FIP mode. The lower than Nernstian response observed for the K1 and K2 CWEs in the FIP mode is typical of other photo-cured potassium CWEs [13] and was due to the initial slow response of the CWE and the dispersion of the injected sample zone. However, the FIP response observed with the K1 and K2 CWEs represents 80% of the steady-state response and provides with adequate analytical sensitivity. The log-linear range observed was between 0.01 mM and 10 mM and a sample throughput rate of up to 180 injections / hour. Typical flow injection peaks observed for the photo-cured K1 and K2 CWEs are presented in Figure 5.14 and high reproducibility of the peak heights was observed. Significant electrode drifting was observed with the K1 CWE compared to the K2 CWE, however, baseline drift in the FIP mode has little effect on calibrations since data processing can account for any drift when calculating peak heights.

The photo-cured K1 and K2 CWEs were used to determine the potassium content of various water samples in the FIP mode, and the results are presented in Table 5.8. The water analysis results were in good agreement with AAS, however, the relative error observed for photo-cured K2 CWE demonstrates that this CWE was more reliable than the K1 CWE. The superior results observed for the water analysis with the K2 CWE in the FIP mode was likely due to the improved selectivity compared to the K1 CWE.

Table 5.8. Determination of potassium in various water samples (n = 3) in the FIP mode. RSD values quote the peak height precision.

Water Sample	K1 CWE in FIP, mg/L (RSD)	K2 CWE in FIP, mg/L (RSD)	AAS, mg/L	Labelled, mg/L
Tap water	0.48 (4.9%)	0.43 (6.0%)	0.45	0 - 2*
Charlton's Mineral Water	3.07 (2.2%)	2.55 (2.2%)	2.00	1.5
Deep Spring Mineral Water	2.72 (1.8%)	2.31 (2.3%)	2.57	5.0
Summit Mineral Water	13.70 (1.7%)	13.59 (0.9%)	12.82	18.0

* Expected range

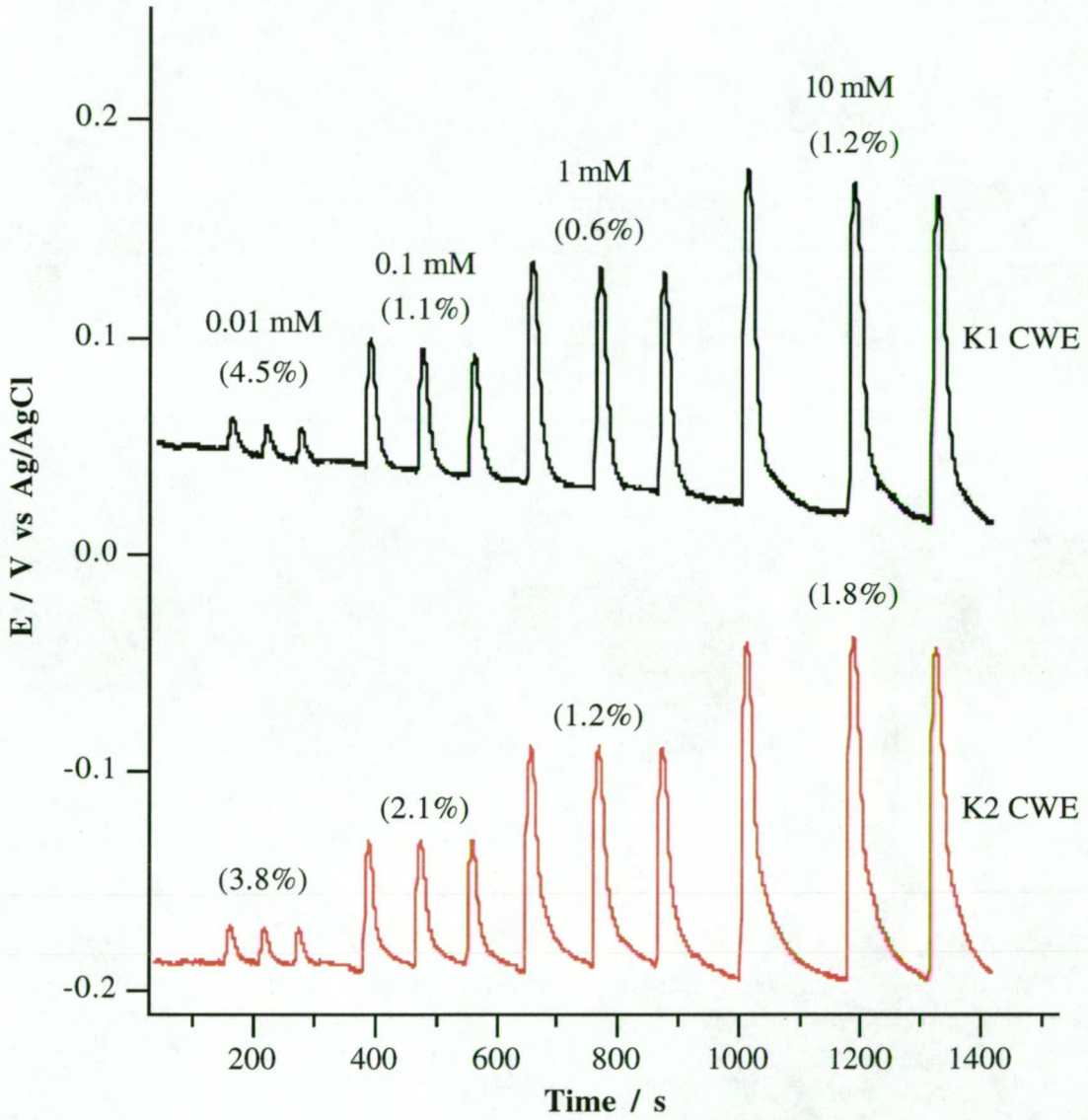

Figure 5.14. Typical peaks observed for the photo-cured K2 and K3 ISEs in the FIP mode. Injection sample volume was 200 μL, total flow rate was 1.8 mL/minute and the carrier and reference streams were both 10 mM lithium acetate. Relative standard deviations are given in parentheses.

5.3.5.1 The Nitrate CWE

The optimum membrane composition for the photo-cured nitrate CWE is given in Table 5.9. The photo-cured nitrate CWE exhibited Nernstian responses of -59.5 ± 0.8 mV change per activity decade with the log-linear range between 0.01 mM and 100 mM using pure potassium nitrate solutions in the steady-state mode. Figure 5.15 shows the calibration curve for the nitrate CWE. The photo-cured nitrate CWE exhibited a negligible response to hydrogen ions for 2.0 < pH < 10.0, and a negligible electrode drift, typically < 5 mV / day, was observed. The time taken for the photo-cured nitrate CWE to attain 90% of steady-state response was typically 5 seconds making this CWE ideal for FIP measurements.

Table 5.9. Optimum pre-cured membrane composition used for the nitrate CWE

Membrane Components	NO_3 CWE (wt/wt %)
TDA-NO_3 Ionophore	5.0
9,10-phenanthrenequinone	0.6
diphenyliodonium chloride	0.6
2-nitrophenyl octyl ether	21.8
HDDA	24.0
Ebecryl 600	48.0

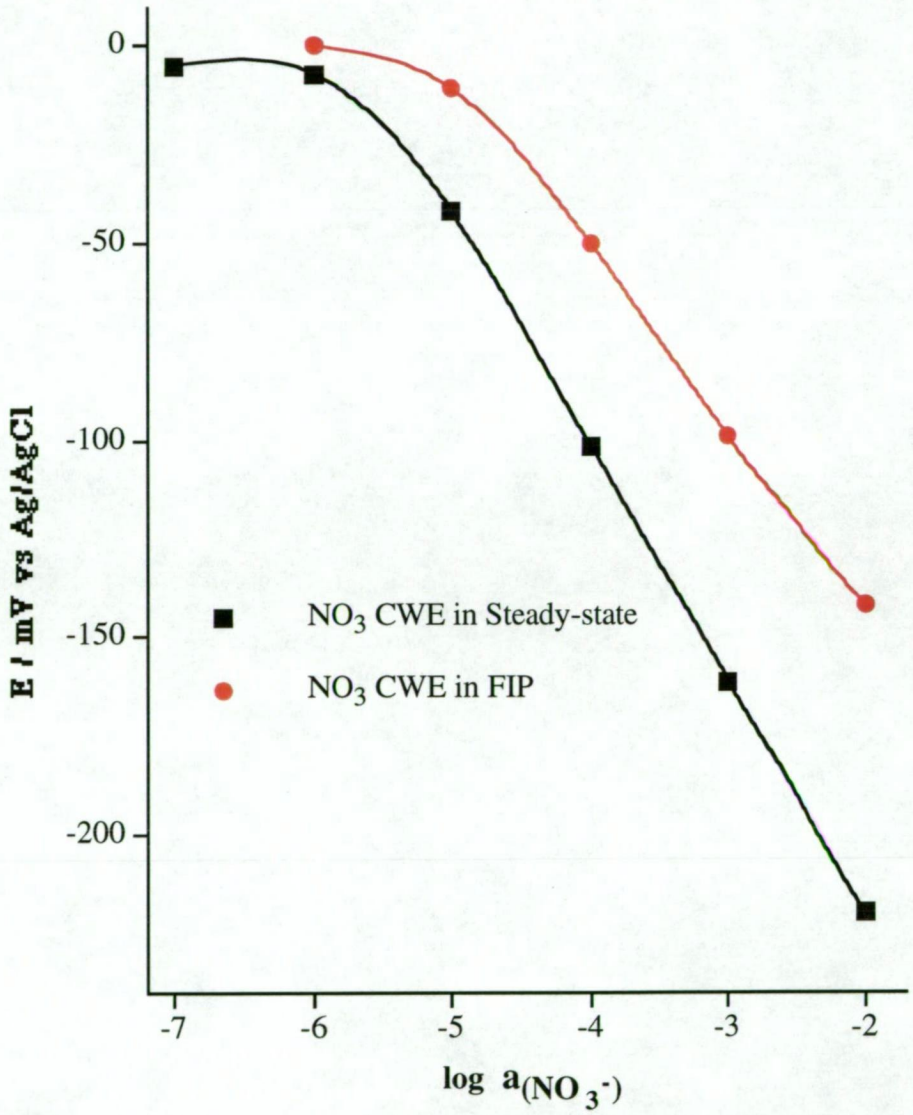

Figure 5.15. Calibration curves for the photo-cured nitrate CWE using pure KNO_3 solutions in the steady-state compared to the FIP response. Sample volume = 200 µL, flow rate = 1.9 mL/minute and the carrier and reference streams were 3 mM lithium acetate.

5.3.5.2 Selectivity of the Nitrate CWE

The selectivity coefficients for the nitrate CWE were determined using the matched potential method [22]. The selectivity coefficients determined for the nitrate CWE are presented in Figure 5.16, and are compared to the selectivity coefficients for an Orion (No. 92-07) nitrate ISE and a photo-cured acrylate based nitrate ISE reported in previous studies that was based on the tributyloctadecylphosphonium-nitrate ionophore [11]. The selectivity exhibited by the nitrate CWE compared favourably against the Orion nitrate ISE and the previously reported photo-cured nitrate ISE. The nitrate CWE exhibited excellent selectivity against common interfering ions, including chloride, making this CWE very suitable for potentiometric measurements in the presence of moderate chloride levels, and no chloride corrections would be required.

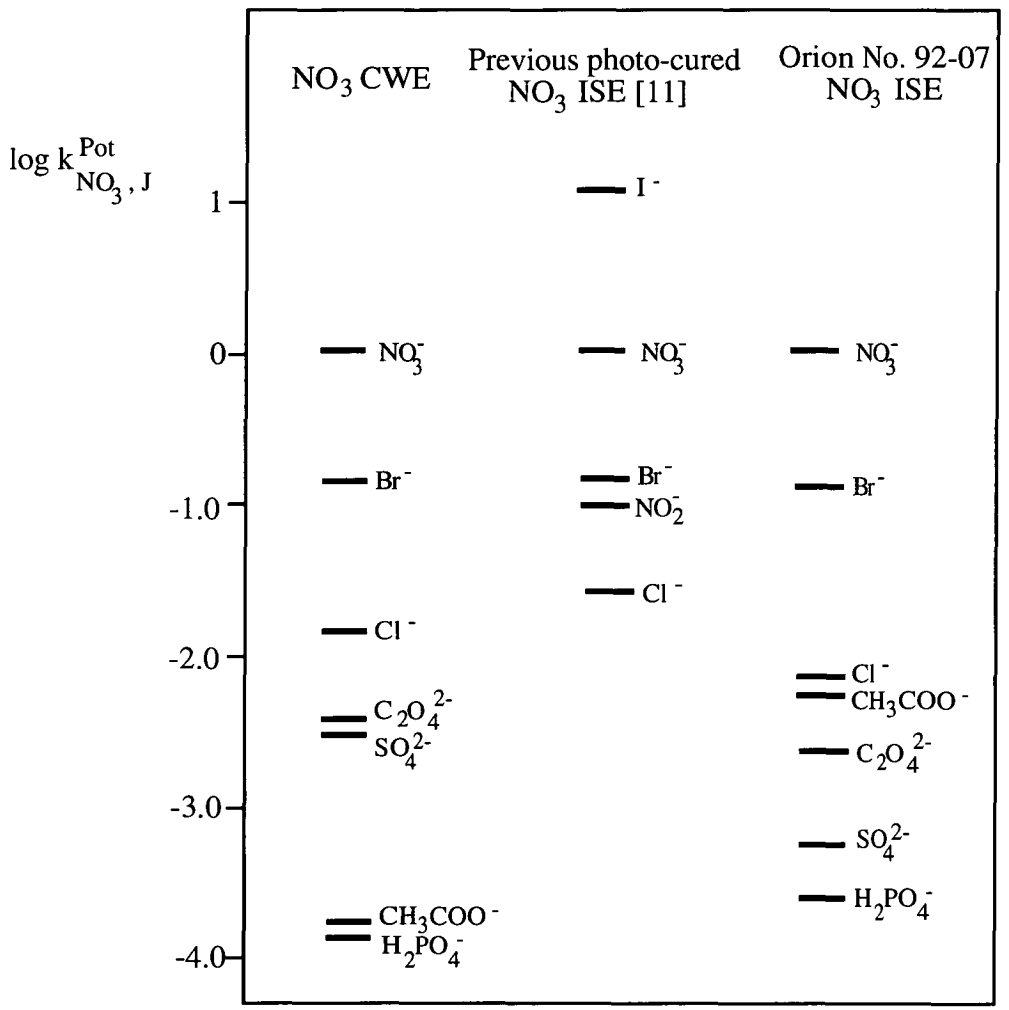

Figure 5.16. Selectivity coefficients determined for the nitrate CWE compared to an Orion (No. 92-07) nitrate ISE and a previously reported photo-cured nitrate ISE.

5.3.5.3 The Nitrate CWE in the FIP mode

The nitrate CWE exhibited a near-Nernstian response of -46.4 ± 0.6 mV per activity decade and a log-linear range between 0.1 mM and 10 mM using a 3 mM lithium acetate ionic carrier in the FIP mode. The lowest detected standard was 0.01 mM nitrate solution. Typical flow injection peaks observed for the photo-cured nitrate CWE are presented in Figure 5.17 demonstrating the high reproducibility of the peak heights observed. There was some baseline drift observed, however, in the FIP mode there is little effect on calibrations since data processing can account for any drift when calculating peak heights for calibration plots.

The less than Nernstian response observed for the nitrate CWE in the FIP mode is typical of other photo-cured electrodes [10,13,15] and was due to the initial slow response of the photo-cured membrane and the dispersion of the injected sample zone. However, the FIP response observed represents about 80% of the steady-state response and provides adequate analytical sensitivity. A calibration curve for the nitrate CWE in the FIP mode is given in Figure 5.15.

The reliability of the nitrate CWE in the FIP mode was determined by the analysis of various water samples for their nitrate content. Table 5.10 presents the results of the nitrate water analysis and were in agreement with ion chromatography. The chloride content of these water samples were also determined using a UV/Visible spectrophotometric method in the flow injection mode described previously [21]. The nitrate CWE exhibited reliable analysis in the FIP mode whereby the presence of chloride was up to 20 times more than nitrate.

Table 5.10. Determination of nitrate in various water samples (n = 3) in the FIP mode. RSD values quote the peak height precision.

Water Sample	NO_3 CWE in FIP, mg/L (RSD)	IC (NO_3^-), mg/L	Chloride content, mg/L (RSD)
Tap water	2.1 (2.5%)	2.2	17.1 (2.0%)
Deep Spring Mineral Water	3.7 (2.8%)	3.2	86.1 (1.1%)
Summit Mineral Water	10.4 (1.9%)	11.2	59.2 (1.2%)

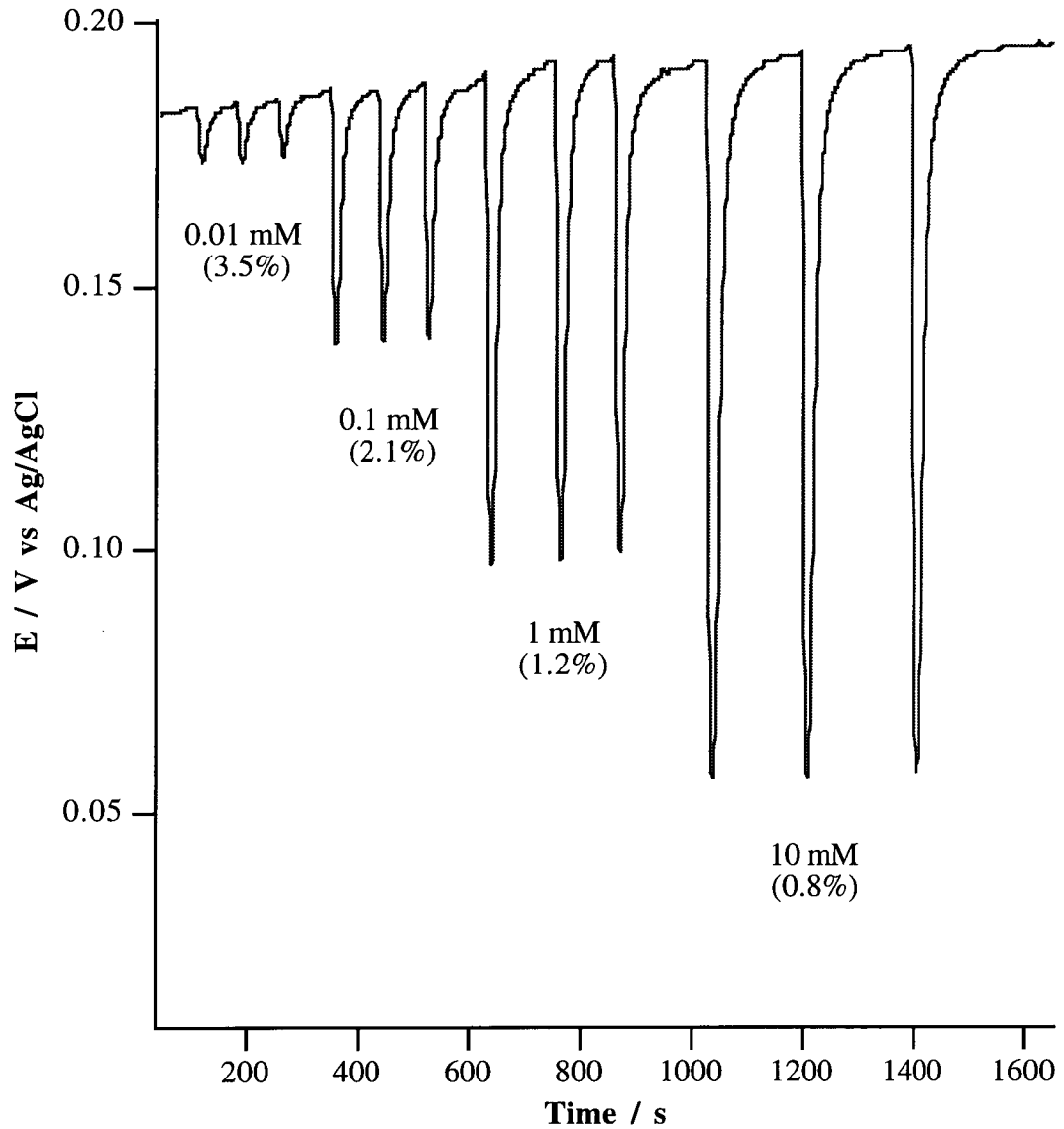

Figure 5.17. Typical FIP response observed for the photo-cured nitrate CWE. Sample injection volume = 200 μL, total flow rate = 1.9 mL/minute and the carrier and reference streams were both 3 mM lithium acetate.

5.4 Conclusion

The photo-cured membranes prepared in this work exhibited excellent adhesion to the silver substrate making them reliable in flow-through systems. The photo-cured ammonium, hydrogen (pH1), potassium (K2) and nitrate CWEs exhibited reliable response to their respective determinand in the steady-state and FIP modes, each using one of the eight silver electrodes in the multi-electrode flow cell described in Chapter four. The selectivity exhibited by each of these CWEs suggests that these photo-cured CWEs could be applied to a multi-sensor array that would not require any mathematical corrections. The reliability of these CWEs in the FIP mode was demonstrated by the analysis of various water samples for their respective determinand, giving good agreement with comparative analytical methods. Lithium acetate carrier solutions were employed for each of the above-mentioned CWEs in the FIP mode, and will be the obvious choice as a carrier when employing these CWEs in a multi-sensor arrangement.

The photo-cured calcium CWE based on the ETH 129 ionophore exhibited excellent response to calcium ions in the steady-state mode however, the selectivity for calcium against some interfering ions was poor compared to a previously reported PVC version. A major disadvantage was the interference exhibited by hydrogen ions, and consequently needed to be corrected by matching the pH of the sample and standards for reliable calcium FIP measurements can be achieved. It is believed that the exposure of UV radiation degraded the ETH 129 ionophore, resulting in the calcium CWE poor selectivity against hydrogen. As a result, pH measurements could not be achieved simultaneously with the calcium CWE based on the ETH 129 ionophore.

5.5 References

1. G. J. Moody, J. M. Slater and J. D. R. Thomas, 'Membrane design and photocuring encapsulation of flatpack based ion-sensitive field effect transistors', Analyst, **113**, 103 - 108, (1988).

2. S. Ufer and K. Cammann, 'Ion-sensitive field-effect transistor with improved membrane adhesion', Sensors and Actuators, **B7**, 572- 575, (1992).

3. A. Bratov, N. Abramova, J. Muñoz, C. Domínguez, S. Alegret and J. Bartrolí, 'Ion sensor with photocurable polyurethane polymer membrane' Journal of Electrochemical Society, **141**, L111 - L112, (1994).

4. A. Bratov, N. Abramova, J. Muñoz, C. Domínguez, S. Alegret and J. Bartrolí, 'Optimization of photocurable polyurethane membrane composition for ammonium ion sensor', Journal of the Electrochemical Soceity, **144**, 617 - 621, (1997).

5. T. M. Ambrose and M. E. Meyerhoff, 'Charaterization of photopolymerized decyl methacrylate as a membrane matrix for ion-selective electrode', Electroanalysis, **8**, 1095 - 1100, (1996).

6. R. W. Cattrall, I. C. Hamilton and P. J. Iles, 'Photocured polymers in ion-selective electrode membranes', Analytica Chimica Acta, **169**, 403 - 406, (1985).

7. T. J. Cardwell, R. W. Cattrall, I. C. Hamilton and P. J. Iles, 'Photocured polymers in ion-selective electrode membranes: Part 2 Calcium electrode for flow injection analysis', Analytica Chimica. Acta, **177**, 239 - 242, (1985).

8. T. Dimitrakopoulos, J. R. Farrell and P. J. Iles, 'A photo-cured calcium ion-selective electrode for use in flow injection potentiometry that tolerates high perchlorate levels', Electroanalysis, **8**, 391 - 395, (1996).

9. L. T. Di Benedetto, T. Dimitrakopoulos, J. R. Farrell and P. J. Iles, 'Evaluation of perchlorate tolerant photo-cured calcium selective electrodes for use in flow injection potentiometry', Talanta, **44**, 349 - 356, (1997).

10. J. R. Farrell, P. J. Iles and T. Dimitrakopoulos, 'Photocured polymers in ion-selective electrode membranes. Part 6: Photopolymerised lithium sensitive ion-selective electrodes for flow injection potentiometry', Analytica Chimica Acta, **335**, 111 - 116, (1996).

11. C. Dumschat. R. Fromer, H. Rautschek, H. Muller and T. J. Timpe, 'Photolithographically patternable nitrate-sensitive acrylate-based membrane', Analytica Chimica Acta, **243**, 179 - 182, (1989).

12. F. R. del Mundo, T. J. Cardwell, R. W. Cattrall, P. J. Iles and I. C. Hamilton, 'An ultraviolet-cured pH-sensitive membrane electrode for use in flow injection analysis', Electroanalysis, **1**, 353 - 356, (1989).

13. T. J. Cardwell, R. W. Cattrall, I. C. Hamilton and P. J. Iles, 'Photo-cured polymers in ion-selective electrode membranes: Part 3 A potassium electrode for flow injection analysis', Analytica Chimica Acta, **204**, 329 - 332, (1988).

14. A. Bratov, N. Abramova, J. Muñoz, C. Domínguez, S. Algret and J. Bartrolí, 'Photocurable polymer matrices for potassium-sensitive ion-selective electrode membranes', Analytical Chemistry, **67**, 3589 - 3595, (1995).

15. J. R. Farrell, P. J. Iles and T. Dimitrakopoulos, 'Photocured polymers in ion-selective electrode membranes. Part 5: Photopolymerised sodium sensitive ion-selective electrodes for flow injection potentiometry', Analytica Chimica Acta, **334**, 133 - 137, (1996).

16. R. W. Cattrall and I. C. Hamilton, 'Coated-wire Ion-selective Electrodes', Ion-Selective Electrode Review, **6**, 125 - 172, (1984).

17. T. J. Cardwell, R. W. Cattrall, I. C. Hamilton and P. J. Iles, 'Photo-cured polymers in ion-selective electrode membranes: Part 4 An ultraviolet laser cured membrane for potassium', Analytica Chimica Acta, **219**, 135 - 140, (1989).

18. P. J. Iles, PhD Thesis, 'Ion-selective electrodes: their fabrication and response characteristics', Latrobe University, (1992).

19. W. E. Morf, 'The Principles of Ion-Selective Electrodes and Membrane Transport', Elsevier Publication Co., New York, (1981).

20. Perstorp Analytical Environmental Methodology 'Total Kjeldahl Nitrogen (P/N 002054)' Doc. No. 002060, (1994).

21. J. Ruzicka and E. H. Hansen, "Flow Injection Analysis", John Wiley and Sons, New York, 2nd ed., (1988).

22. Y. Umezawa, K. Umezawa and H. Sato, 'Selectivity coefficients for ion-selective electrodes: Reccommended methods for reporting $K_{A,B}$ values (Technical Report)', Pure and Applied Chemistry, **67**, 507 - 518, (1996).

23. U. Schefer, D. Ammann, E. Pretsch, U. Oesch and W. Simon, 'Neutral carrier based Ca^{2+} -selective electrode with detection limit in sub-nanomolar range', Analytical Chemistry, **58**, 2282 - 2285, (1986).

24. H. D. Goldberg, R. B. Brown, D. P. Liu and M. Meyerhoff, 'Screen printing - A technology for the batch fabrication of itergrated chemical-sensor arrays', Sensors and Actuators, **B21**, 171 - 183, (1994).

25. B. K. Oh, C. Y. Kim, H. J. Lee, K. L. Rho, G. S. Cha and H. Nam, 'One-component room temperature vulcanizing-type silicone rubber-based calcium-selective electrodes', Analytical Chemistry, **68**, 503 - 508, (1996).

26. M. S. Ghauri and J. D. R. Thomas, 'Evaluation of an ammonium ionophore for use in poly(viyl chloride) membrane ion-selective electrodes: Solvent mediator effects', Analyst, **119**, 2323 - 2326, (1994).

27. H. L. Wu and R. Q. Yu, 'A PVC membrane pH-sensitive electrode based on methyldioctadecylamine as neutral carrier', Talanta, **34**, 577 - 579, (1987).

28. R. P. Buck and E. Lindner, 'Recommendations for nomenclature of ion-selective electrodes (IUPAC Recommendations 1994)', Pure and Applied Chemistry, 66, 2527 - 2536, (1994).

29. C. Hongbo, E. H. Hansen and J. Ruzicka, 'Evaluation of critical parameters for measurement of pH by flow injection analysis: Determination of pH in soil extracts', Analytica Chimica Acta, **169**, 209 - 220, (1985).

30. E. Lindner, K. Tóth, J. Jeney, M. Horváth, E. Pungor, I. Bitter, B. Ágai, L. Töke, 'Novel bis(crown ether)-based potassium sensor for biological applications', Mikrochimica Acta, **1**, 157 - 168, (1990).

Chapter Six: Evaluation Of Photo-Cured Epoxydiacrylate Based Multi-CWE Arrays For Use In A Portable Flow Injection Potentiometric System.

6.1 Introduction

As described in the previous chapters, the advantages of employing an array of CWEs in a FIP arrangement results in a system that can measure multiple ion species simultaneously in a sample of interest. Additional advantages of FIP discussed previously include excellent peak height precision (typically < 3%), fast sample throughput rate (> 120 injections/hour), use of small sample volumes (≤ 300 μL) and as demonstrated in the previous chapters, the ability to incorporate a FIP system in a portable battery-powered system employing either single or multi-ISE arrangements as detectors. Therefore, the work presented in this chapter concentrates on the application of an array of photo-cured membrane based CWEs in the portable FIP system described in Chapter four.

Previous studies on polymer based ISE array systems have involved electrodes prepared with the PVC based liquid polymer membranes in either steady-state [1] or FIP modes [2]. ISFETs [3-5] and solid contact type ISEs [6] have been used as multi-electrode arrays and typically employ PVC based membranes as the sensing membranes. However, a major disadvantage of applying PVC based membranes onto metallic substrates was the poor adhesion usually exhibited by these membranes, and they are commonly unreliable in a continuous flowing stream, as demonstrated in previous studies [7,8]. Alternative liquid polymer membrane materials investigated include silicone rubber [9], polysiloxane [10] and polyurethane [11] in order to improve the adhesion properties on solid surfaces. An interesting approach to improve the adhesive properties of PVC membranes onto solid surfaces was achieved by introducing hydroxylated-PVC into the PVC matrix [12]. This approach has also been performed with polyurethane based membranes with some success [13].

The work presented in this chapter applies some of the photo-cured membrane based CWEs described and evaluated in Chapter five, namely ammonium, hydrogen, nitrate and potassium CWEs as well as a previously reported photo-cured calcium membrane based on calcium bis[4-(1',1',3',3'-tetramethylbutyl) phenyl]phosphate as the ionophore and including

potassium (4-chlorophenyl) borate as lipophilic additive [14,15], and a silver/silver chloride wire used as a chloride CWE in an array of CWEs. The work presented in this chapter is in three parts; 1) the photo-cured ammonium and hydrogen CWEs used simultaneously in the FIP mode, 2) photo-cured calcium, nitrate, potassium CWEs and a Ag/AgCl wire chloride CWE used simultaneously in the FIP mode, and 3) combining part 1 and 2, the photo-cured ammonium, calcium, hydrogen, nitrate and potassium CWEs and a Ag/AgCl wire electrode used simultaneously in the FIP mode are described. In all three parts, the FIP measurements of the respective determinand for various environmental and drinking water samples using the described CWE array are performed and the FIP results compared to other analytical methods.

6.2 Experimental

All reagents were used as received from the suppliers: ammonium chloride, ammonium nitrate, calcium chloride, potassium nitrate and lithium acetate (all BDH, AnalaR). Stock solutions ranging between 0.01 mM and 100 mM of ammonium chloride, ammonium nitrate, calcium chloride and potassium nitrate were each prepared by serial dilution. A universal pH buffer stock solution containing 10 mM sodium dihydrogen phosphate, 2.5 mM di-sodium tetraborate and 7 mM trisodium citrate (all BDH, AnalaR) was prepared.

The mixed ammonium chloride-pH standards were prepared daily by diluting the appropriate stock solution 10 fold and the pH was adjusted with either 100 mM HCl or NaOH. An Activon pH glass combination electrode and pH / mV meter (model AS209) were used to determine the pH of the mixed ammonium chloride-pH standards. The mixed calcium chloride - potassium nitrate standard solutions were prepared by serial dilution from a stock solution of 100 mM calcium chloride and potassium nitrate.

The mixed ammonium nitrate - calcium chloride - potassium nitrate - pH buffer standard solutions were prepared daily by diluting the appropriate stock solution 10 fold and the pH adjusted with either 50 mM H_2SO_4 or 100 mM NaOH. The pH of the prepared ammonium nitrate - calcium chloride - potassium nitrate - pH buffer standards solutions was monitored with the Activon pH glass electrode set-up described above. Ultrapure water (Barnstead Ultrapure water systems, 18.0 MΩ cm) was used throughout this work.

The materials used for the photo-cured liquid polymer membrane based ammonium, hydrogen, nitrate and potassium CWEs that were used in this work have been described in Chapter five, Section 5.2.1. The photo-cured calcium CWE membrane used in this work was based on dioctylphenyl phosphonate (DOPP) as the plasticiser and calcium bis[4-(1',1',3',3'-tetramethylbutyl) phenyl]phosphate (CaTBPP) as the ionophore.

The preparation and manufacture of the photo-cured membrane based CWE has been described in Chapter five, Section 5.2.2. A silver / silver chloride based CWE was prepared by electrochemically anodising one of the silver wire electrodes in the eight electrode flow cell described in Chapter four (Figure 4.1) using a 7.2 Volt battery-pack and a platinum wire as the cathode while circulating a 100 mM potassium chloride solution through the multi-electrode flow cell. The steady-state and FIP measurement procedures employed in this work were similar to that described in Chapter five, Section 5.2.3.

The ionic activities, data acquisition program, the data analysis and graphical representation of the data procedures described earlier in Chapter two, Section 2.2.4 were employed in the work described in this chapter. The acquired digital data were displayed in real time millivolt readings plotted as a function of time and were saved as text files. A program called MacCurve Fit © Version 0.7 was used to calculate the electrode slope, the E' and the standard deviations (95% confidence) of a given electrode in either the steady-state or FIP modes.

Comparative analytical methods described in Chapter five, Section 5.2.4 were used to validate the analysis of various water samples for the three CWE array systems described in this chapter. In the case of comparing the calcium FIP results in this chapter, Section 6.3.3.2, a commercial calcium ISE (Model No. ASE502) that was obtained from Activon (Sydney, Australia) used in a wall-jet flow cell previously described [16] was used to validate the calcium CWE FIP result.

6.3 Results and Discussion

The design of the ADC employed in the portable FIP system allows for liquid polymer membranes of up to 100 MΩ resistance as discussed in Chapter four. The portable FIP system consisting of the ADC and a 4 channel peristaltic pump were both powered by a six Ni-Cd

rechargeable 1.2 Volt battery-pack, which allowed the system to be used continuously for up to 6 hours before recharging was required. The acquired data from each of the eight silver electrodes can be simultaneously displayed on a notebook computer. The notebook computer can operate for up to 3 hours before recharging is required and was the limiting factor for this portable FIP system.

The following sections describe the application of the photo-cured based CWEs evaluated and described in Chapter five as well as a silver/silver chloride CWE and a calcium CWE based on a previously reported photo-cured membrane [14] as a multi-CWE array to determine their respective determinand simultaneously in the FIP mode. The photo-cured membranes employed in this study exhibited excellent adhesion properties to the metal substrates making them ideal for flow-through systems and were each clear and transparent in appearance after 8 weeks of use.

6.3.1 Application of Ammonium and Hydrogen (pH1) CWEs Simultaneously in the Steady-state and FIP modes

As described in Chapter two Section 2.3.3, performing reliable pH measurements in the FIP mode, the buffer capacity of the injected sample zone must be at least 10 times higher than the carrier [17,18], otherwise the sample will be diluted sufficiently and alter the pH of the injected sample zone, resulting in an inaccurate result. Employing larger sample volumes (up to 300 μL) in the FIP will minimise the effect of the buffer capacity of the carrier stream has on the injected sample zone [17,18]. It was also important to minimise the pH difference between the injected sample and the carrier in order to attain reliable pH measurements in the FIP mode. Therefore, to measure pH accurately in the FIP mode, the carrier must be close to pH 7.0 in order to minimise the dispersion of the injected sample zone.

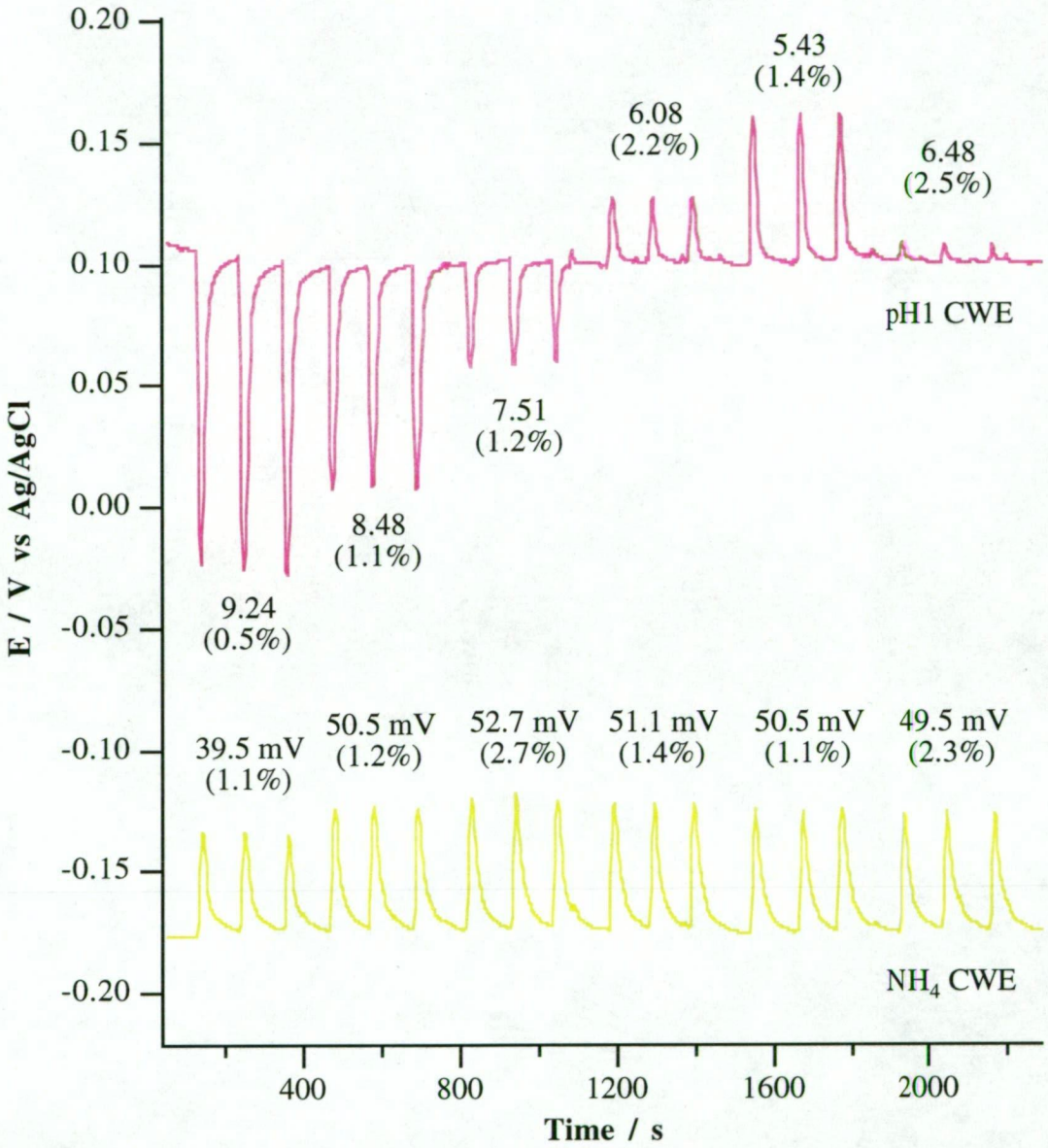

Figure 6.1. Effect of varying pH in a series of 0.1 mM NH_4Cl solutions has on the response of the ammonium CWE. Carrier and reference streams were 3 mM lithium acetate (pH = 6.70), sample volume was 200 µL and total flow rate was 1.5 mL/minute. Relative standard deviations of peak heights are given in parentheses.

However, performing ammonium and pH measurements simultaneously in the FIP mode, requires a restriction on the pH range to be used in conjunction with the ammonium ion standards. The carrier must accommodate both the ammonium and pH1 CWEs so that the optimum FIP performance for both CWEs can be maintained. The upper pH limit is pH 8.5 to avoid an equilibrium shift to ammonia. This was confirmed when injecting a series of 0.1 mM ammonium chloride standards with pH values between 5.4 and 9.2 in the FIP mode, as shown in Figure 6.1. Figure 6.1 demonstrates the effect of varying the pH of 0.1 mM ammonium chloride solutions has on the ammonium CWE response in the FIP mode. A significant reduction in the peak height was observed when the pH was > 8.5.

Figure 6.2 shows the calibration curves for the ammonium and pH1 CWEs determined simultaneously in the steady-state mode using mixed ammonium chloride - pH solutions. The ammonium CWE exhibited a near-Nernstian response of 58.1 ± 0.8 mV change per activity decade and the pH1 CWE exhibited an electrode slope of 55.7 ± 0.9 mV change per pH unit between the pH range 8.2 < pH < 4.9, simultaneously in the steady-state mode. The log-linear range exhibited by the ammonium CWE was between 0.01 mM and 10 mM.

Typical FIP responses for the ammonium and pH1 CWEs when used simultaneously with the above mentioned conditions are presented in Figure 6.3. The electrode slope observed for the ammonium CWE was 49.6 ± 0.6 mV change per activity decade over a log-linear range between 0.1 mM and 10 mM, while the pH1 CWE exhibited an electrode slope of 49.8 ± 0.1 mV change per pH unit between the pH range of 4.9 and 8.2 used simultaneously in the FIP mode.

The lithium acetate carrier used in these FIP measurements contained 0.005 mM ammonium chloride and was included to improve the baseline stability and response time and automatically conditions the ammonium CWE. The simultaneous FIP response exhibited by the ammonium and pH1 CWEs represents up to 85% of the steady-state response. Comparative calibration curves for the ammonium and pH1 CWEs in the steady-state and FIP modes are presented in Figure 6.2.

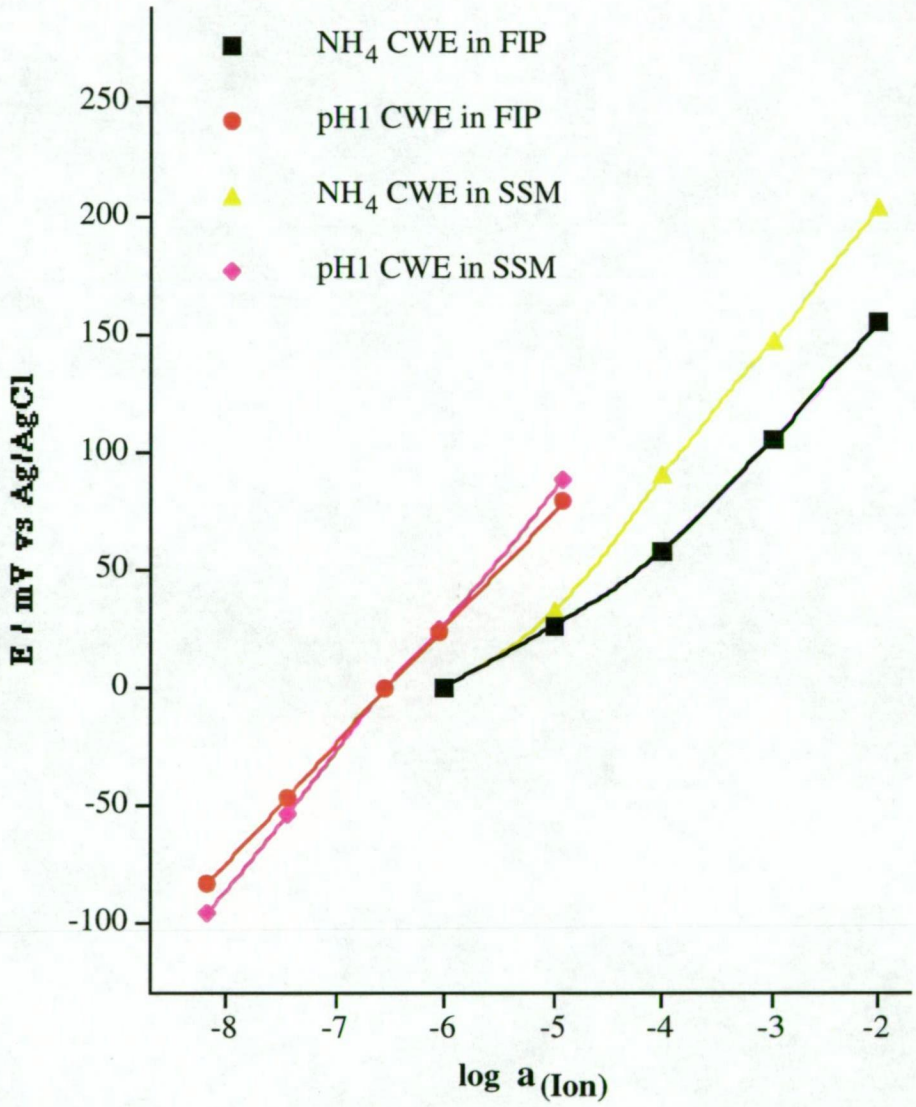

Figure 6.2. Comparative calibration curves for the ammonium and pH1 CWEs used simultaneously in the steady-state (SSM) and FIP modes.

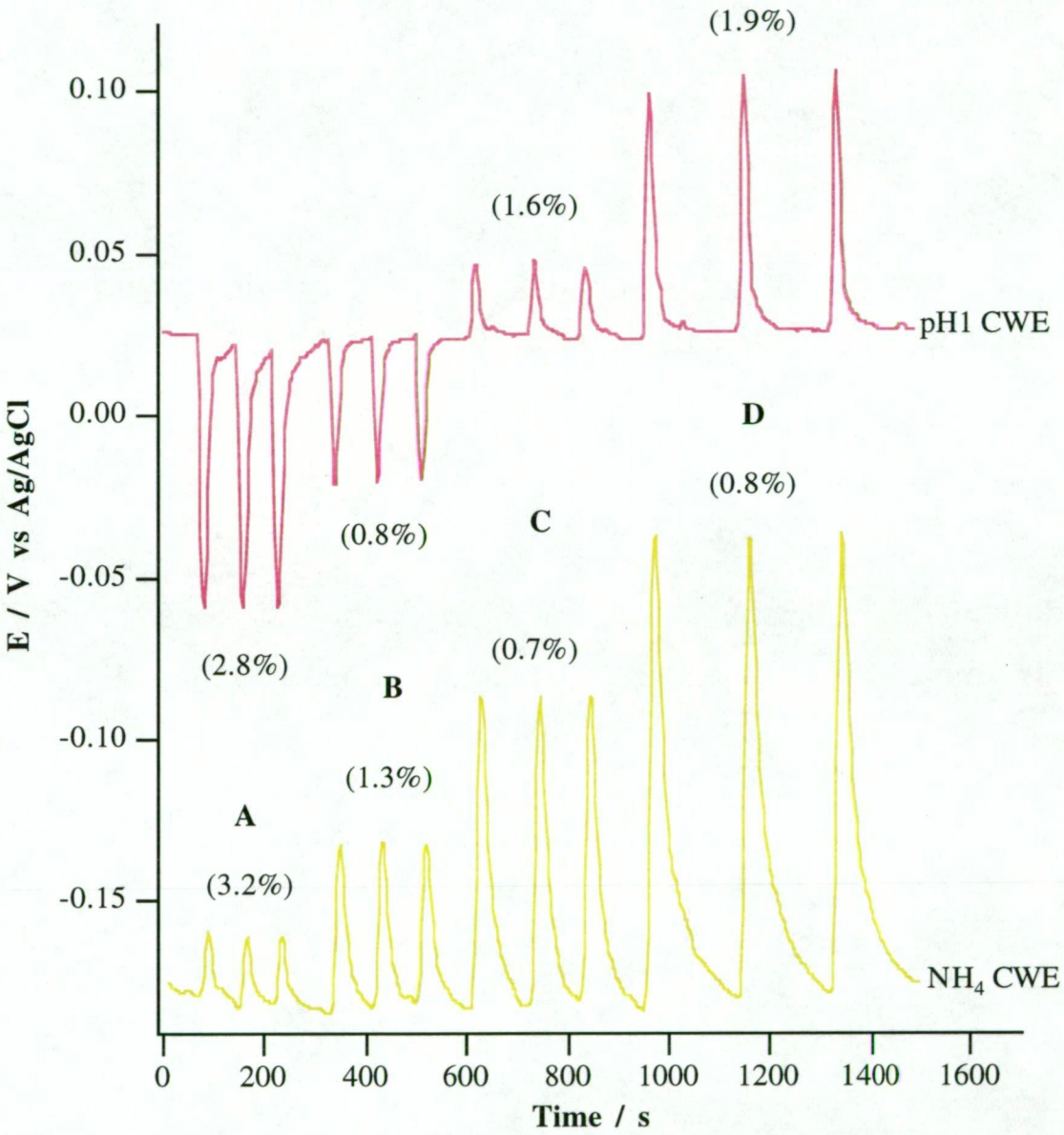

Figure 6.3. Typical simultaneous FIP responses observed for the photo-cured ammonium and pH1 CWEs. Injection sample volume = 200 µL, total flow rate = 1.5 mL/min and the carrier and reference streams were both 3 mM lithium acetate (pH = 6.55) with 0.005 mM NH_4Cl. Relative standard deviations of peak heights are given in parentheses. A = 0.01 mM NH_4Cl - pH 8.19, B = 0.1 mM NH_4Cl - pH 7.45, C = 1 mM NH_4Cl - pH 6.05 and D = 10 mM NH_4Cl - pH 4.91.

A series of hydroponic and waste water samples obtained from a local greenhouse grower were used to validate the performance of the ammonium - hydrogen CWEs system in the FIP mode. Three hydroponic nutrient samples and two waste water samples were analysed for their ammonium and pH levels in the FIP mode. These data are summarised in Table 6.1. Validation of the simultaneous FIP measurements of ammonium and pH was demonstrated with various hydroponic nutrient and waste-water samples and the results were in good agreement with comparative analytical methods. Clearly, the simultaneous application of the photo-cured ammonium and pH1 CWEs demonstrates reliable potentiometric measurements in the FIP mode, providing that certain chemical conditions are met.

Table 6.1. Simultaneous FIP determinations of ammonium and pH levels in various water samples. RSD (n = 3) values quote the peak height precision of the CWEs for each sample.

Water Sample	NH_4 CWE in FIP, mg/L (RSD%)	UV/Vis (NH_4^+), mg/L (RSD%)	pH1 CWE in FIP, (RSD%)	pH (Glass)
Nutrient solution 1	31.4 (2.3)	28.9 (1.1)	4.74 (1.9)	4.77
Nutrient solution 2	33.8 (2.2)	34.0 (2.2)	4.72 (1.3)	4.76
Nutrient solution 3	32.4 (1.8)	30.8 (2.3)	5.71 (2.2)	5.68
Waste-water 1	31.0 (1.9)	28.4 (1.5)	4.00 (1.1)	3.97
Waste-water 2	36.7 (1.7)	37.7 (0.9)	5.25 (1.3)	5.26

6.3.2 Application of Calcium, Chloride, Nitrate and Potassium CWEs Simultaneously in the Steady-state and FIP modes

Photo-cured membrane based calcium, nitrate and potassium CWEs were used in the multi-CWE system along with a silver/silver chloride CWE as a chloride electrode. The membrane composition of the photo-cured potassium (K2) and nitrate CWEs are given in Chapter five, Tables 5.7 and 5.9 respectively. The photo-cured calcium membrane based CWEs used in this work have been described and evaluated in previous studies [14,15] and the membrane composition is presented in Table 6.2.

Table 6.2. Composition of the pre-cured calcium membrane mixture prepared in this work.

Membrane Components	Ca5 (wt/wt %)
KClTPB	0.5
CaTBPP Ionophore	6.1
Uvecryl P36	5.3
DOPP	20.9
HDDA	22.4
Ebecryl 600	44.8

Figure 6.4 presents the calibration curves for the Ca5, chloride, nitrate and K2 CWE array determined simultaneously in the steady-state mode using mixed calcium chloride - potassium nitrate solutions. The photo-cured nitrate CWE exhibited Nernstian responses of -59.5 ± 0.8 mV change per activity decade with the log-linear range between 0.01 mM and 10 mM in the steady-state mode. The photo-cured Ca5 CWE exhibited a hyper-Nernstian response of 33.1 ± 0.5 mV change per activity decade and a log-linear range between 0.01 mM and 10 mM in the steady-state mode. The chloride CWE exhibited a near-Nernstian response of -55.0 ± 0.5 mV change per activity decade over a log-linear range 0.02 mM and 20 mM in the steady-state mode. Detection limits for the calcium and nitrate CWEs were 0.005 mM for their respective determinand, while the chloride CWE was 0.02 mM. The photo-cured K2 CWE exhibited a Nernstian response of 58.3 ± 0.8 mV change per activity decade over a log-linear range between 0.01 mM and 10 mM in the presence of both chloride and nitrate ions.

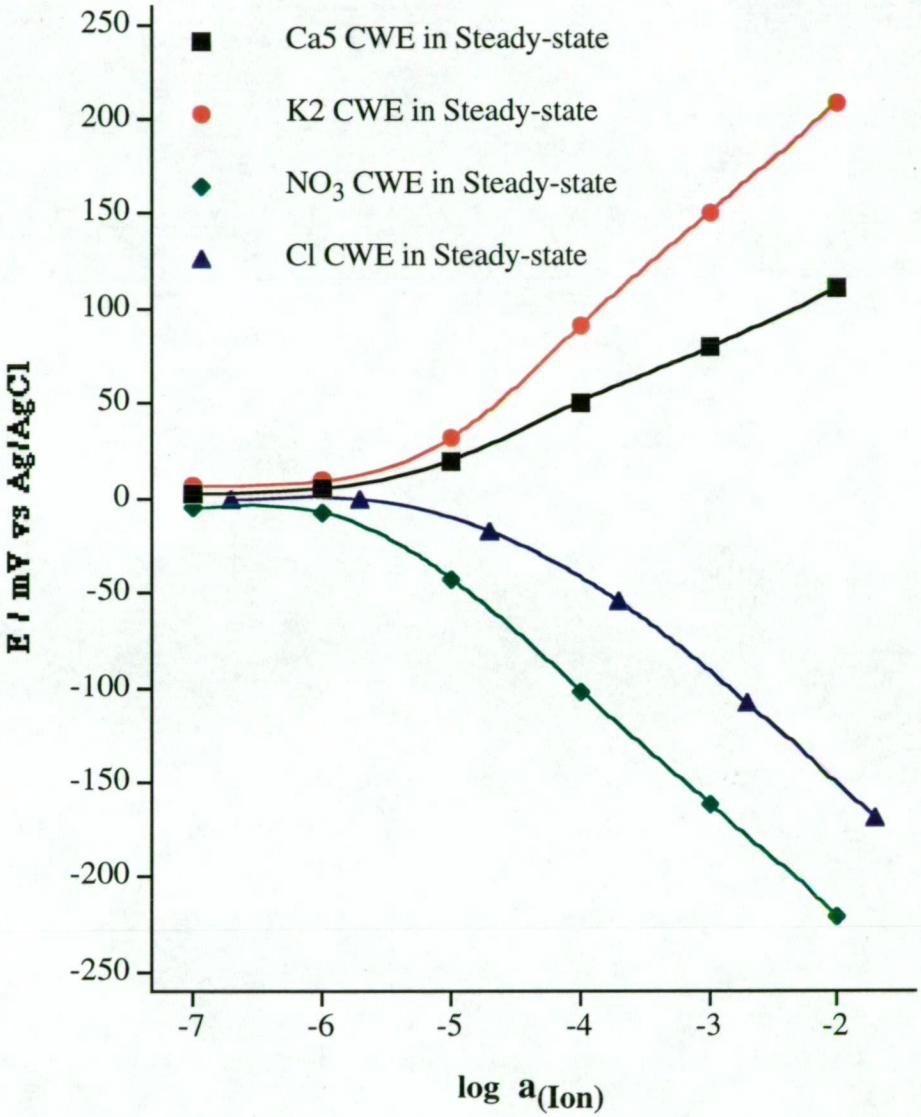

Figure 6.4. Typical calibration curves observed for the Ca5, chloride, nitrate and K2 CWE array simultaneously in the steady-state mode.

A typical FIP response observed simultaneously for the CWE array is presented in Figure 6.5. As discussed above, the ideal carrier was 3 mM lithium acetate that contained 0.0005 mM calcium chloride and potassium nitrate. It has been demonstrated that the presence of a small amount of the determinand (< 0.01 mM) in the carrier solution will automatically condition a given ISE and improvements in the responsiveness, baseline stability and a greater sample throughput rate have been achieved [20]. For this reason, the carrier solution contained 0.0005 mM of the determinand for each CWE used in the multi-sensor flow-through cell. The reference solution employed with the multi-CWE FIP measurements was identical to that of the carrier in order to minimise any liquid junction potential contributing to the potentiometric measurement, which has been observed in previous studies [19]. The FIP response presented in Figure 6.5 clearly demonstrates baseline stability and sample throughput rate of up to 180 injections / hour, for each CWE depending on the concentration injected. There was some potential drifting observed for each of the CWE, however, in the FIP mode baseline drifting has little effect on calibrations since data processing can account for any drifting when calculating peak heights.

In the FIP mode, the chloride CWE exhibited an electrode slope of -47.7 ± 1.1 mV per activity decade over a log-linear range between 0.2 mM and 20 mM. Therefore, the peak heights observed for the chloride CWE represent 80 % of the steady-state value. The nitrate CWE exhibited a near-Nernstian response of -45.4 ± 1.8 mV per activity decade and a log-linear range between 0.1 mM and 10 mM in the FIP mode. The lowest detectable concentration in the FIP mode for the chloride and nitrate CWEs were both 0.02 mM and 0.01 mM, respectively.

The Ca5 CWE exhibited a near-Nernstian slope of 26.1 ± 0.4 mV per activity decade over a log-linear range between 0.1 mM and 10 mM and a detection limit of 0.01 mM in the FIP mode. The K2 CWE exhibited a near-Nernstian response of 48.6 ± 0.5 mV change per activity decade over a log-linear range between 0.1 mM and 10 mM. Figure 6.6 presents the calibration curves for the multi-CWE array in the FIP mode. The lowest detected concentration in the FIP mode for both the Ca5 and K2 CWE was 0.01 mM.

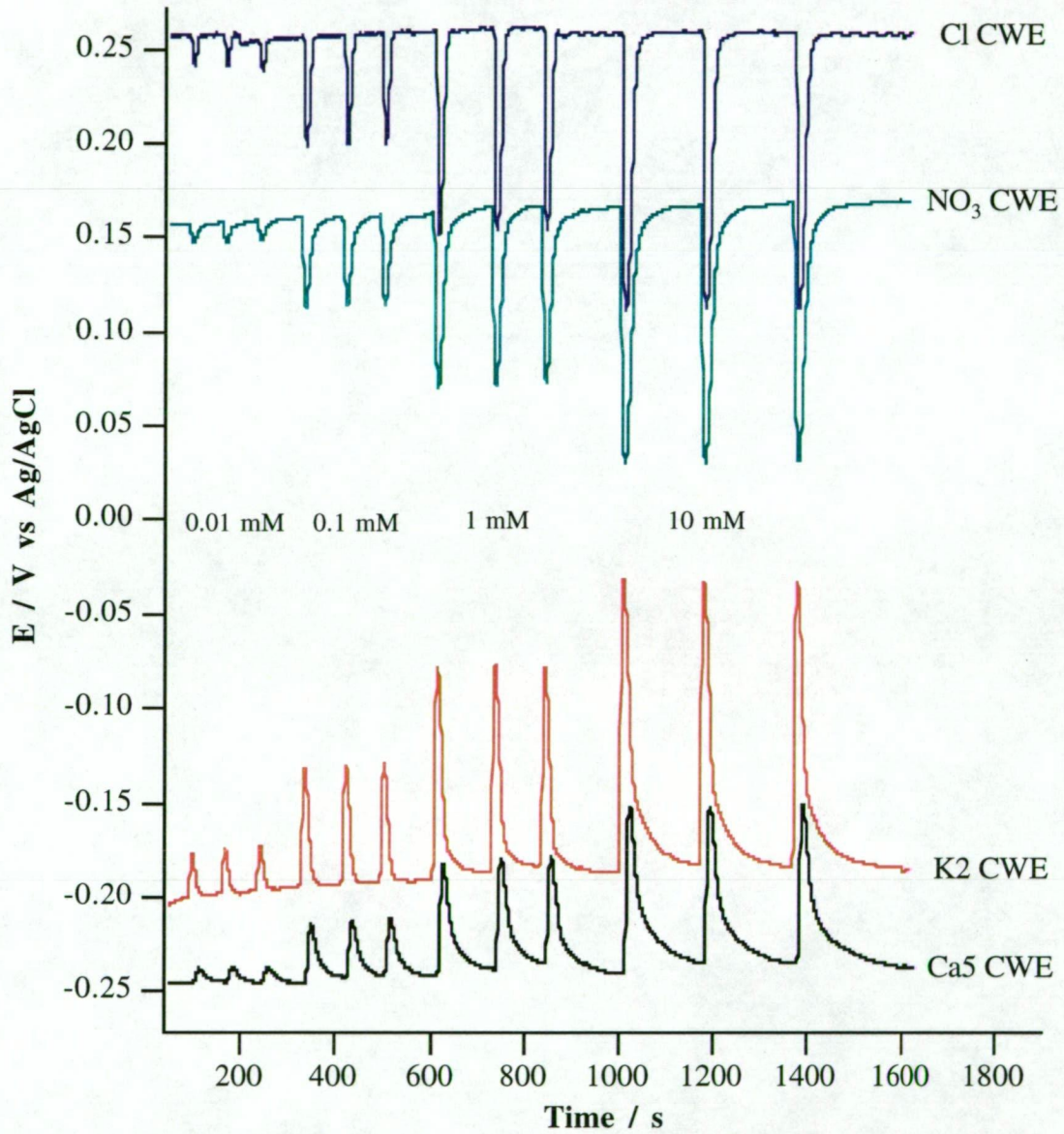

Figure 6.5. Typical peak heights observed for the chloride (Ag/AgCl) CWE and the photo-cured Ca5, nitrate and K2 CWEs in the FIP mode. Injection sample volume was 200 µL, total flow rate = 1.5 ml/min and the carrier and reference streams were both 3 mM lithium acetate containing 0.0005 mM KNO_3 and $CaCl_2$.

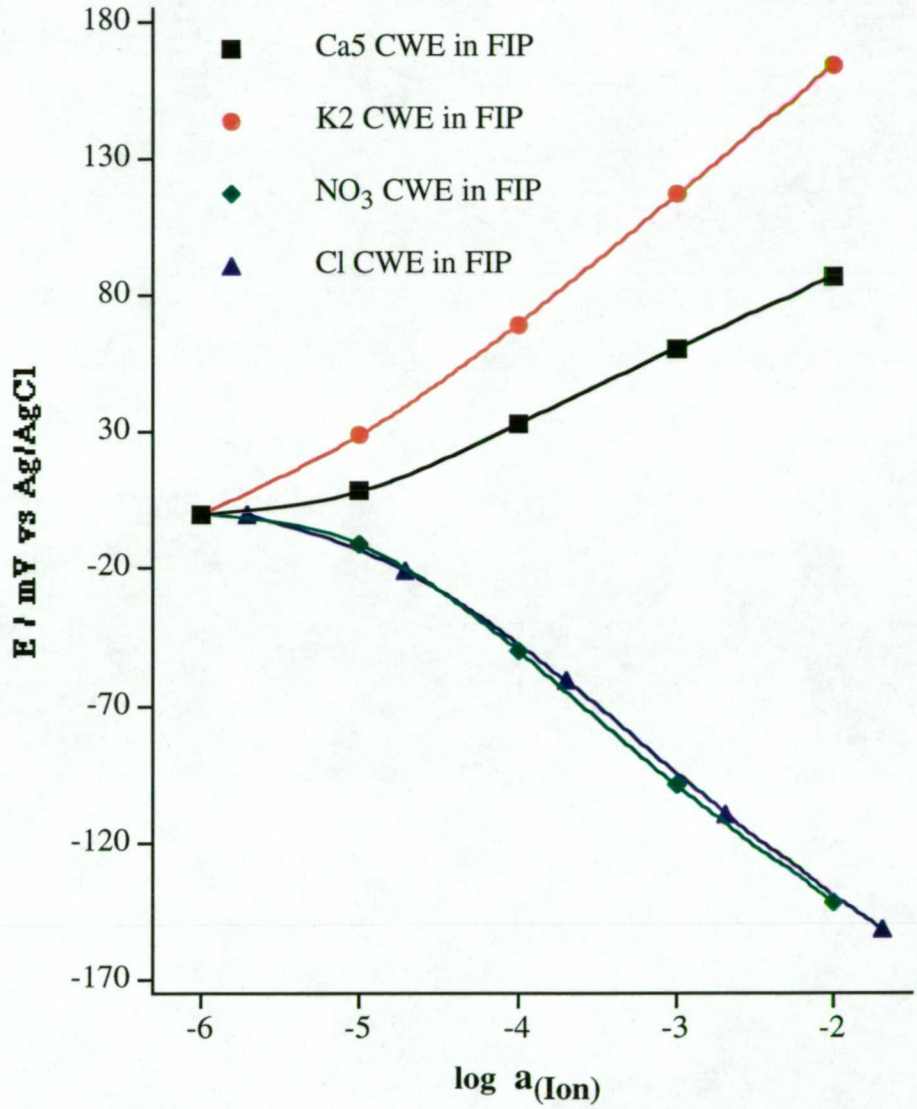

Figure 6.6. Typical calibration curves observed for the Ca5, chloride, nitrate and K2 CWE array in the FIP mode.

The lower than Nernstian response observed for the Ca5, chloride, nitrate and K2 CWEs in the FIP mode was typical of other photo-cured ISEs [21-23] and was due to the initial slow response time of the CWEs and the dispersion of the injected sample zone. However, the FIP response observed for the four-CWE array represents at least 80% of the steady-state value and provides adequate analytical sensitivity.

Various environmental and drinking water samples were simultaneously analysed for their calcium, chloride, nitrate and potassium ion levels using the portable FIP system and the results are presented in Table 6.3. The FIP results are in good agreement with standards analytical methods. Clearly, each CWE employed in the electrode-array demonstrated excellent selectivity and consequently reliable analysis in the FIP mode.

Table 6.3 Analysis of calcium, potassium, chloride and nitrate ions in various water samples, (n=3).

Water Samples	Ca measurement, mg/L (RSD%)		K measurement, mg/L (RSD%)		Cl measurement, mg/L (RSD%)		NO_3 measurement, mg/L (RSD%)	
	FIP	AAS	FIP	AAS	FIP	UV/Vis	FIP	IC
Tap Water	5.2 (1.2)	5.6	0.51 (3.2)	0.45	16.9 (0.5)	17.1	2.1 (2.5)	2.2
Deep Spring MW	3.8 (1.5)	3.9	2.3 (1.8)	2.6	85.1 (1.5)	86.1	3.7 (2.8)	3.2
Summit MW	15.0 (1.6)	15.2	13.3 (0.9)	12.8	64.6 (1.1)	59.2	10.4 (1.9)	11.2
Dove Lake	1.4 (3.6)	1.7	0.52 (2.1)	0.52	7.5 (3.2)	8.3	0.35 (3.5)	0.30

MW = Mineral water

6.3.3 Application of the Ammonium, Calcium, Chloride, Hydrogen, Nitrate and Potassium CWE Array

6.3.3.1 Steady-state Measurements

Figure 6.7 presents the calibration curves for the photo-cured ammonium, Ca5, chloride, pH1, nitrate and K2 CWE array determined simultaneously using mixed ammonium nitrate - calcium chloride - potassium nitrate - pH solutions in the steady-state mode. The photo-cured calcium CWE exhibited a hyper-Nernstian response of 30.8 ± 0.4 mV change per activity decade and a log-linear range between 0.01 mM and 100 mM, while the chloride CWE exhibited a near-Nernstian response of -53.9 ± 0.5 mV change per activity decade over a log-

linear range 0.02 mM and 200 mM in the steady-state mode. Detection limits for the calcium and chloride CWEs were 0.001 mM calcium chloride for their respective determinand. The ammonium and K2 CWEs exhibited electrode slopes of 57.4 ± 1.1 and 58.6 ± 0.8 mV change per activity decade, respectively over a log-linear range of between 0.01 mM and 10 mM and a detection limit of 0.001 mM. The nitrate CWE exhibited an electrode slope of -56.7 ± 0.4 mV change per activity decade and a log-linear range between 0.2 mM and 20 mM. The pH1 CWE exhibited a near-Nernstian response of -55.9 ± 0.7 mV change / pH unit over a pH range between 5.0 and 8.2 in the steady-state mode. The response times observed for the ammonium, Ca5, chloride, pH, nitrate and K2 CWEs to attain 90% of steady-state response were typically between 3 to 5 seconds, making all these electrodes ideally suited for FIP measurements simultaneously.

The pH profiles of each of the photo-cured CWEs exhibited in a mixed 10 mM calcium chloride - potassium nitrate solution are presented in Figure 6.8. No ammonium ion was present in the solution since the response in the alkaline region (pH > 8.5) would be dominated by the equilibrium shift to ammonia and would not be a true representation of the pH independent range of the ammonium CWE. A universal pH independent range between 4.5 and 10.0 exist for the ammonium, Ca5, chloride, nitrate and K2 CWEs. However, the pH range of the mixed standard solutions containing ammonium nitrate, potassium nitrate and calcium chloride needs to be restricted between pH 4.5 and 8.5 for two main reasons: 1) standard solutions with < pH 4.5 will result in an erroneous result for the Ca5 CWE and 2) the mixed standards solutions need to be < pH 8.5 to avoid the equilibrium shift from the ammonium ion to ammonia as the result of the increasing hydroxide ion level.

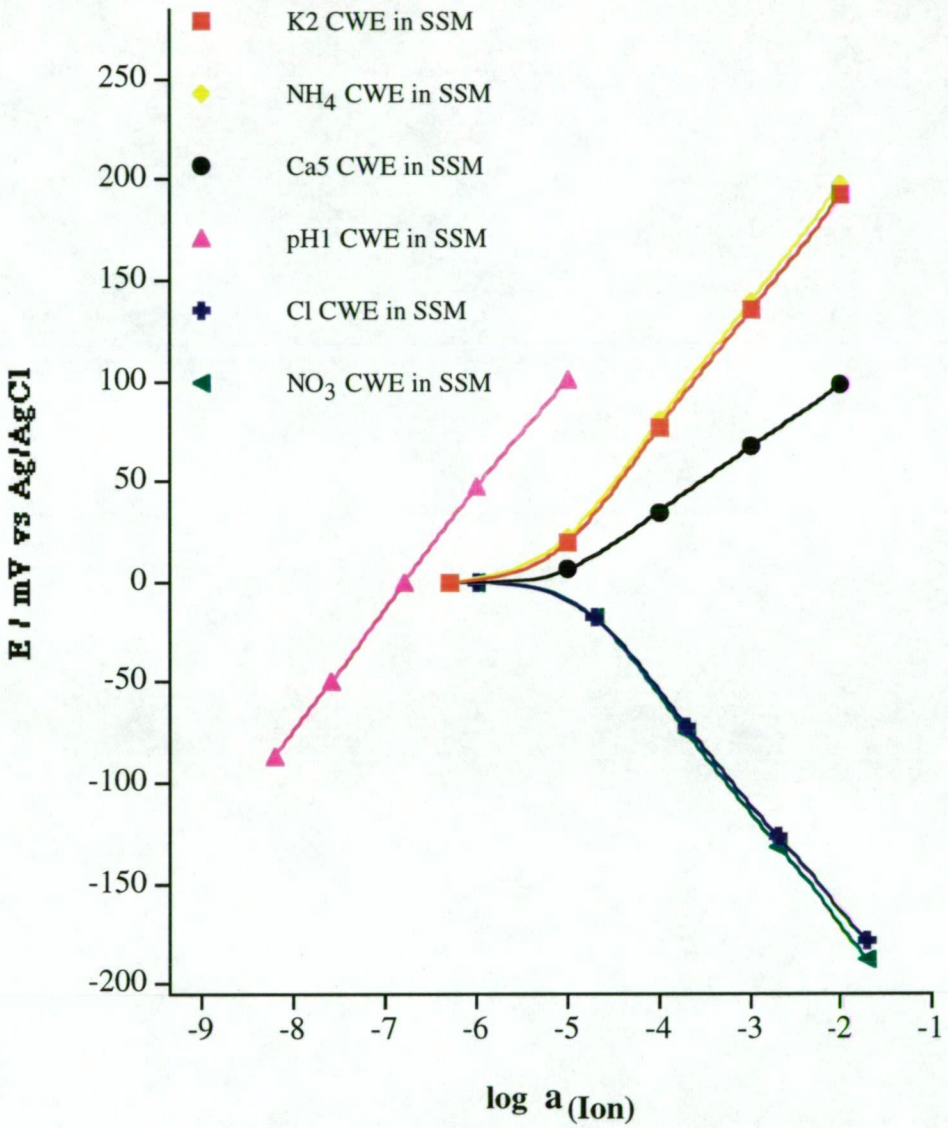

Figure 6.7. Calibration curves exhibited simultaneously for the photo-cured ammonium, Ca5, pH1, nitrate and K2 CWE and chloride CWE in the steady-state mode (SSM).

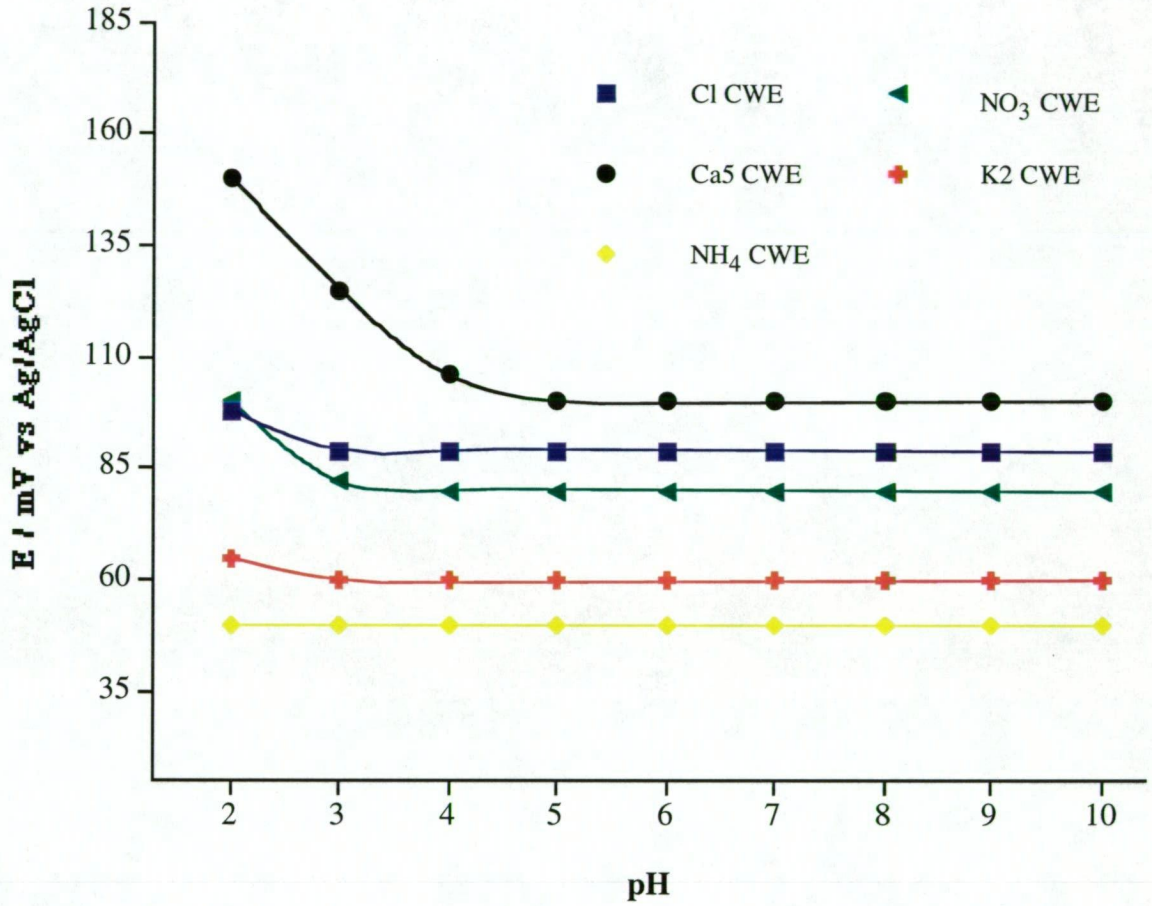

Figure 6.8. pH profile of the ammonium, Ca5, chloride, nitrate and K2 CWEs in a mixed 10 mM KNO_3-$CaCl_2$ solution.

6.3.3.2 FIP Measurements

Typical FIP responses observed for the six-CWE array simultaneously are presented in Figure 6.9. In the FIP mode, the ammonium and K2 CWEs each exhibited a near-Nernstian response of 49.2 ± 1.0 mV and 48.7 ± 0.6 mV change per activity decade, respectively and a log-linear range between 0.1 mM and 10 mM in the FIP mode. The chloride and nitrate CWEs exhibited near-Nernstian responses between -46.5 ± 0.8 mV and -49.5 ± 0.7 mV change per activity decade, respectively and a log-linear range between 0.2 mM and 20 mM in the FIP mode. The photo-cured pH1 CWE exhibited near-Nernstian slope of 49.9 ± 0.6 mV change per pH unit over a pH range between pH 8.2 and pH 5.0 in the FIP mode. The Ca5 CWE exhibited a near-Nernstian slope of 25.8 ± 0.4 mV per activity decade over a log-linear range between 0.1 mM and 10 mM in the FIP mode.

The FIP response observed with the CWE array represents at least 80% of the steady-state response and provides adequate analytical sensitivity. The FIP response presented in Figure 6.9 clearly demonstrates baseline stability and sample throughput rate of up to 180 injections / hour, for each CWE depending on the concentration injected. Figure 6.10 presents the calibration curves for the multi-CWE array in the FIP mode.

Validation of the six-CWE array in the portable battery-powered FIP system was demonstrated by determining the determinand content in various water samples that included hydroponic nutrient solutions and waste-water samples obtained from a local greenhouse grower and a bottled spring mineral water sample. It was necessary to injected a 100 mM ammonium nitrate standard in order to bracket the nitrate ion level in the hydroponic and waste-water samples. The FIP results are presented in Table 6.4 and are in good agreement with comparative analytical methods. The results presented in Table 6.4 demonstrate the reliability and selectivity of each of the six CWE for their respective determinand employed simultaneously in the CWE-array system in the FIP mode.

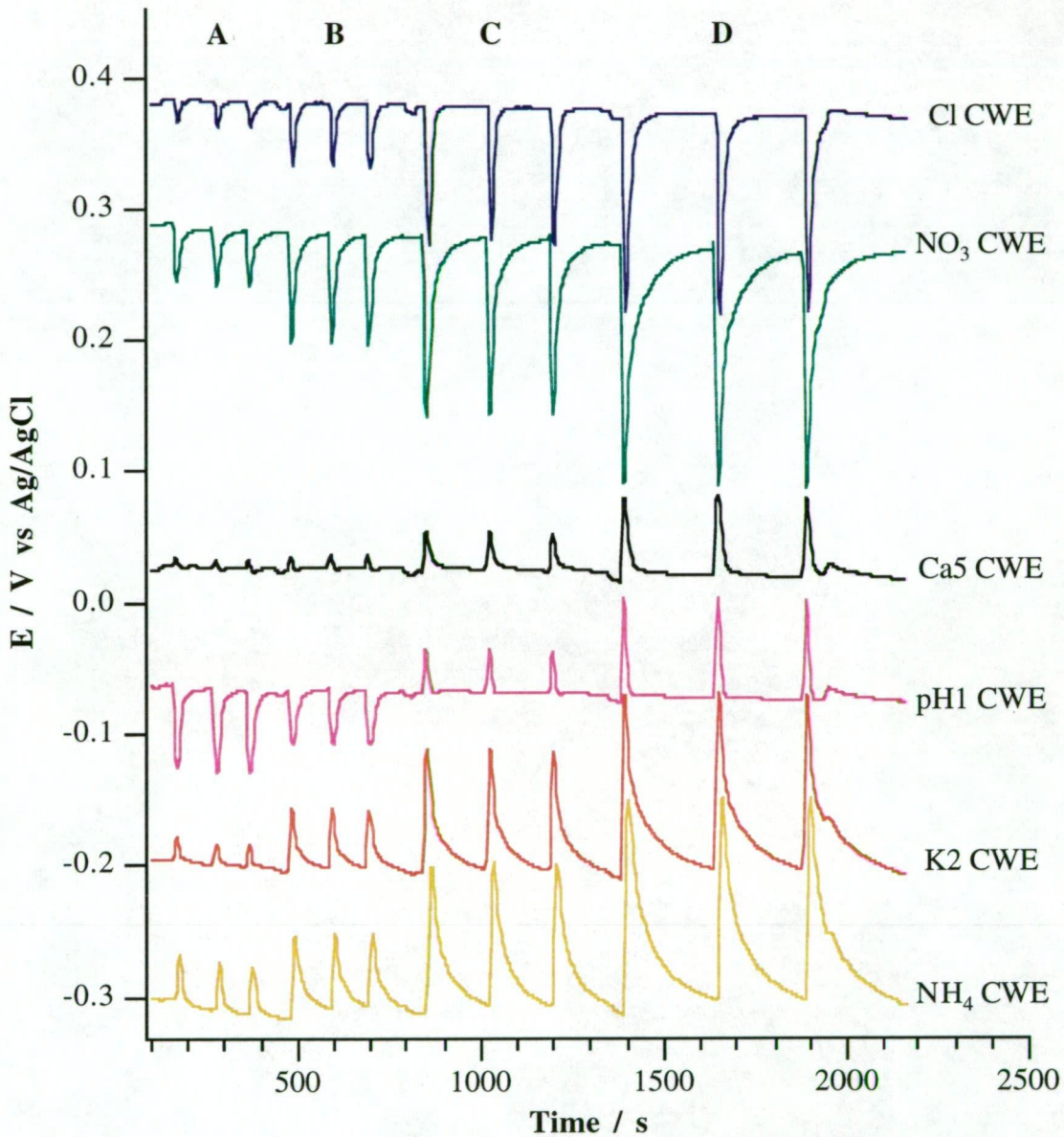

Figure 6.9. Typical simultaneous FIP response for the photo-cured ammonium, Ca5, pH1, nitrate and K2 CWE and a chloride CWE in the FIP mode. Sample injection volume = 200 µL and the total flow rate = 1.6 mL/min and carrier was 3 mM lithium acetate (pH = 6.79) containing 0.0005 mM NH_4NO_3-KNO_3-$CaCl_2$; A = 0.01 mM NH_4NO_3-KNO_3-$CaCl_2$-pH 8.21; B = 0.1 mM NH_4NO_3-KNO_3-$CaCl_2$-pH 7.58; C = 1 mM NH_4NO_3-KNO_3-$CaCl_2$-pH 5.97 and D = 10 mM NH_4NO_3 -KNO_3-$CaCl_2$-pH 5.01.

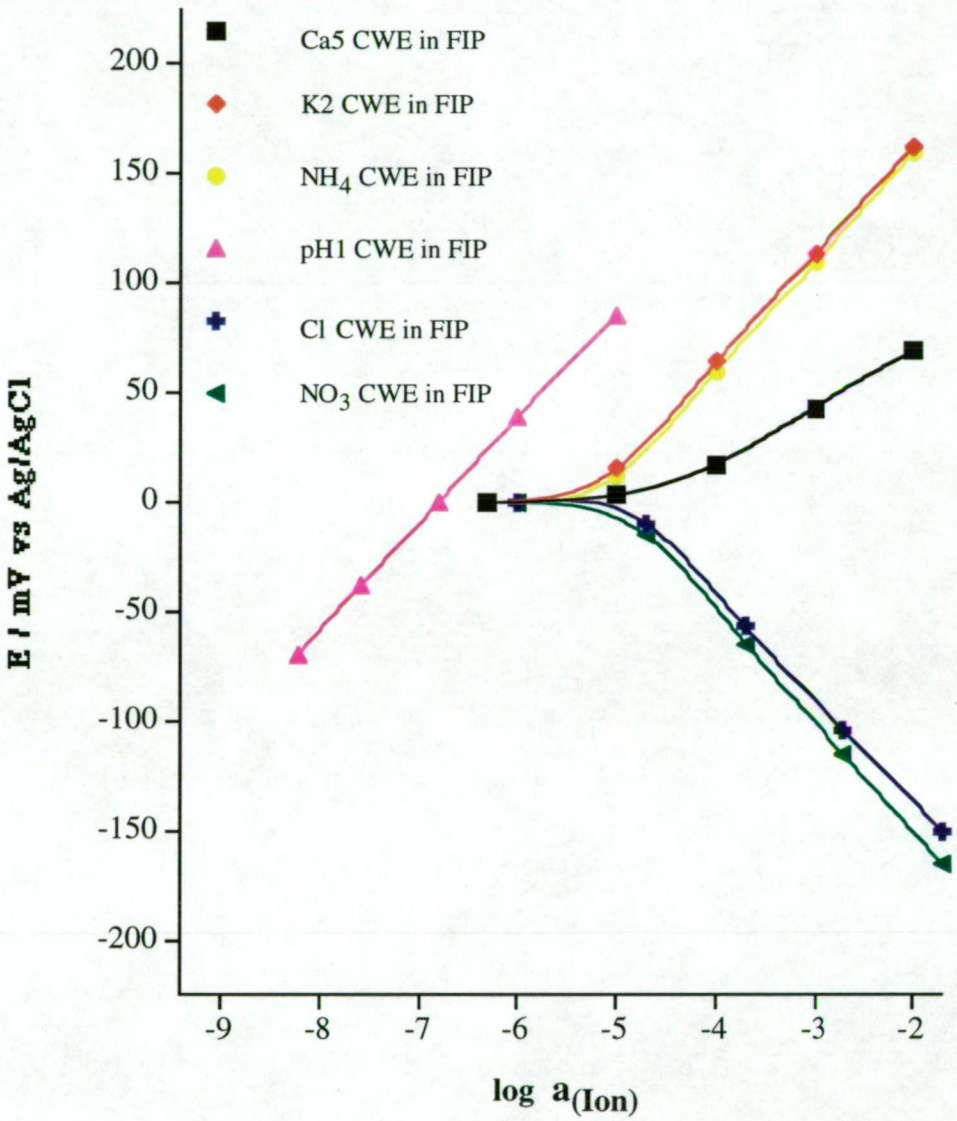

Figure 6.10. Calibration curves exhibited simultaneously for the photo-cured ammonium, Ca5, pH1, nitrate and K2 CWEs and a Ag/AgCl wire based chloride CWE in the FIP mode. Sample injection volume = 200 µL and the total flow rate = 1.6 mL/min and carrier was 3 mM lithium acetate (pH = 6.79) containing 0.0005 mM NH_4NO_3-KNO_3-$CaCl_2$.

Table 6.4. Determination of ammonium, calcium, chloride, pH, nitrate and potassium ions simultaneously in FIP for water samples (n = 3).

Water Sample	NH_4, mg/L (RSD%)		Ca, mg/L (RSD%)		pH (RSD%)	
	FIP	UV/Vis	FIP[a]	FIP[b]	FIP	pH (glass)
Hydroponic solution 1	26.4 (1.3)	24.2 (2.1)	175.0 (1.2)	169.7 (1.6)	4.88 (1.1)	4.84
Hydroponic solution 2	26.4 (1.1)	23.2 (1.7)	166.0 (1.4)	165.3 (1.1)	5.23 (1.5)	5.25
Waste solution 1	29.1 (1.1)	29.1 0.9)	184.3 (2.1)	178.3 (1.5)	4.84 (0.6)	4.81
Waste solution 2	27.0 (0.9)	29.5 (0.9)	166.2 (1.7)	170.9 (2.1)	5.24 (2.2)	5.28
Deep Spring mineral water	0.8 (1.9)	0.7 (2.1)	125.0 (0.9)	121.4 (1.1)	6.11 (2.7)	6.15

Water Sample	K, mg/L (RSD%)		Cl, mg/L (RSD%)		NO_3, mg/L (RSD%)	
	FIP	AAS	FIP	UV/Vis	FIP	IC
Hydroponic solution 1	269.1 (1.3)	264.0	18.4 (1.2)	17.2 (1.0)	1995.1 (1.1)	1999
Hydroponic solution 2	269.5 (1.0)	267.6	20.9 (1.4)	18.9 (0.7)	1515.0 (1.5)	1591.7
Waste solution 1	315.1 (1.4)	310.7	24.2 (2.3)	23.8 (1.5)	2118.0 (1.6)	2110.1
Waste solution 2	269.1 (1.9)	264.9	21.1 (1.7)	19.4 (1.1)	1385.0 (2.3)	1367.2
Deep Spring mineral water	2.6 (2.6)	2.6	18.5 (2.9)	20.6 (1.8)	5.8 (2.9)	5.9

a - Ca CWE used in the array, b - Commercial Ca ISE used in wall-jet flow cell [16].

6.4 Conclusion

The electronic design of the portable battery-powered FIP system allowed for multiple photo-cured membrane based CWEs of up to 100 MΩ resistance to be used simultaneously in potentiometric measurements. This work has demonstrated the reliability of photo-cured epoxydiacrylate membrane based CWE used in a multi-electrode system for FIP measurements. The main advantages of photo-cured epoxydiacrylate membranes include an increased mechanical strength, improved adhesion to metal substrates and faster manufacturing time (< 5 minutes) compared to the traditional PVC membranes (2 days), making photo-cured membranes more suitable for flow-through systems.

Three multi-CWE arrangements were presented in this chapter, namely the ammonium - pH1 CWE array, the Ca5 - chloride - nitrate - K2 CWE array, and the ammonium - Ca5 -

chloride -pH1 - nitrate - K2 CWE array. Each performed reliably in the FIP mode and accurate analyses of various environmental and drinking water samples was demonstrated. The FIP results obtained with the multi-CWE arrangements were in good agreement with comparative analytical methods. The ideal carrier and ionic background for all three multi-CWE arrangements was found to be 3 mM lithium acetate. In the case where the pH1 CWE was employed in a multi-electrode array system, the pH of the carrier required to be close to the pH 7.0 to minimise the dispersion of the injected sample zone.

The FIP response observed for each of the photo-cured CWE used in each of the three multi-CWE arrangements represented up to 85% of the steady-state value, making each of the CWE array system analytically useful. In each of the multi-CWE arrangements presented in this work, the lithium acetate carrier contained a small amount of the determinand ion (usually 0.0005 mM) in order to automatically condition each of the CWE as well as maintaining a stable baseline, and consequently improve the responsiveness of each of the photo-cured based CWE.

The excellent selectivity demonstrated by each of the photo-cured CWEs eliminated the need for chemometric type corrections to be applied to each of the multi-CWE arrangements which was an additional advantage of the described FIP system. Therefore, the multi-CWE arrangements used in the portable FIP system described in this work could practically be applied to field measurements at remote locations. An operator would simply need to calibrate the portable FIP system with standard solutions and then test samples on site and store the acquired data on the notebook computer, and then move onto the next site and repeat the procedure. The advantage of the data acquisition program (Satod © Ver. 1.46) used in this work is that it can present each electrode potential from a given CWE array simultaneously on the notebook's screen and therefore an operator can also monitor the performance of each CWE employed in the field, acting as a diagnostic tool.

6.5 References

1. U. Lemke, K. Cammann, C. Kötter, C. Sundermeier and M. Knoll, 'Multisensor array for pH, K^+, Na^+ and Ca^{2+} measurements based on coated-film electrodes', Sensors and Actuators, **B7**, 488 - 491, (1992).

2. F. J. Sáez de Viteri and D. Diamond, 'Determination and application of ion-selective electrode model parameters using flow injection and simplex optimization', Analyst, **119**, 749 - 758, (1994).

3. A. U. Ramsing, J. Janata, J. Ruzicka and M. Levy, 'Miniturization in analytical chemistry - A combination of flow injection analysis and ion-sensitive field transistors for determination of pH, and potassium and calcium Ions', Analytica Chimica Acta, **118**, 45 - 52, (1980).

4. A. Sibbald, P. D. Whalley and A. K. Covington, "A miniature flow-through cell with four-function CHEMFET integrated circuit for simultaneous measurements of potassium, hydrogen, calcium and sodium ions', Analytica Chimica Acta, **159**, 47 - 62, (1984).

5. H. D. Goldberg, R. B. Brown, D. P. Liu and E. Meyerhoff, 'Screen printing: A technology for the batch fabrication of integrated chemical-sensor arrays', Sensors and Actuators, **B21**, 171 - 183, (1994).

6. T. J. Cardwell, R. W. Cattrall, P. C. Hauser and I. C. Hamilton, 'A multi-ion sensor cell and data acquisition system for flow injection analysis', Analytica Chimica Acta, **214**, 359 - 366, (1988).

7. G. J. Moody, J. M. Slater and J. D. R. Thomas, 'Membrane design and photocuring encapsulation of flatpack based ion-sensitive field effect transistors', Analyst, **113**, 103 - 108, (1988).

8. S. Ufer and K. Cammann, 'Ion-sensitive field-effect transistor with improved membrane adhesion', Sensors and Actuators, **B7**, 572- 575, (1992).

9. E. Malinowska, V. Oklejas, R. W. Hower, R. B. Brown and M. E. Meyerhoff, 'Enhanced electrochemical performance of solid-state ion sensors based on silicon rubber membranes', Sensors and Actuators, **B33**, 161 - 167, (1996).

10. P. D. van der Wal, M. Skowronska-Ptasinska, A. van den Berg, P. Bergveld, E. J. R. Sudhölter and D. Reinhoudt, 'New membrane materials for potassium-selective ion-sensitive field-effect transistors', Analytica Chimica Acta, **231**, 41 - 52, (1990).

11. A. Bratov, N. Abramova, J. Muñoz, C. Domínguez, S. Alegret and J. Bartrolí, 'Ion sensor with photocurable polyurethane polymer membrane', Journal of Electrochemical Society, **141**, L111 - L112, (1994).

12. G. S. Cha, D. Liu, M. E. Meyerhoff, H. C. Cantor, A. R. Midgley, H. D. Goldberg and R. B. Brown, 'Electrochemical performance, biocompatibility and adhesion of new polymer matrices for solid-state ion sensors', Analytical Chemistry, **63**, 1666 - 1672, (1991).

13. R. W. Hower, J. H. Shin, G. S. Cha, R. K. Meruva, M. E. Meyerhoff and R. B. Brown, 'New solvent system for the improved electrochemical performance of screen-printed polyurethane membrane-based solid-state sensors', Sensors and Actuators, **B33**, 168 - 172, (1996).

14. T. Dimitrakopoulos, J. R. Farrell and P. J. Iles, 'A photo-cured calcium ion-selective electrode for use in flow injection potentiometry that tolerates high perchlorate levels', Electroanalysis, **8**, 391 - 395, (1996).

15. L. T. Di Benedetto, T. Dimitrakopoulos, J. R. Farrell and P. J. Iles, 'Evaluation of perchlorate tolerant photo-cured calcium selective electrodes for use in flow injection potentiometry', Talanta, **44**, 349 - 356, (1997).

16. L. T. Di Benedetto, T. Dimitrakopoulos, 'Evaluation of a new wall-jet flow-through cell for commercial ion-selective electrodes in flow injection potentiometry', Electroanalysis, **9**, 179 - 182, (1997).

17. C. Hongbo, E. H. Hansen and J. Ruzicka, 'Evaluation of critical parameters for measurements of pH by flow injection analysis', Analytica Chimica Acta, **169**, 209 - 220 (1985).

18. J. Ruzicka and E. H. Hansen, 'Flow Injection Analysis', John Wiley and Sons, New York, 2nd ed., (1988).

19. K. Cammann, 'Working with Ion-Selective Electrodes', Springer-Verlay, Berlin, (1979).

20. M. Valcárcel and M. D. Luque De Castro, 'Flow-Through (Bio)Chemical Sensors', Elsevier, Amsterdam, (1994).

21. T. J. Cardwell, R. W. Cattrall, I. C. Hamilton and P. J. Iles, 'Photo-cured polymers in ion-selective electrode membranes: Part 3 A potassium electrode for flow injection analysis', Analytica Chimica Acta, **204**, 329 - 332, (1988).

22. J. R. Farrell, P. J. Iles and T. Dimitrakopoulos, 'Photocured polymers in ion-selective electrode membranes. Part 5: Photopolymerised sodium sensitive ion-selective electrodes for flow injection potentiometry', Analytica Chimica Acta, **334**, 133 - 137, (1996).

23. J. R. Farrell, P. J. Iles and T. Dimitrakopoulos, 'Photocured polymers in ion-selective electrode membranes. Part 6: Photopolymerised lithium sensitive ion-selective electrodes for flow injection potentiometry', Analytica Chimica Acta, **335**, 111 - 116, (1996).

Chapter Seven: Conclusions

The results presented in this thesis demonstrate the novelty of the FIP systems described. Its various systems can be operated in a totally portable manner with low power consumption, using a six 1.2 Volt Ni-Cd rechargeable battery-pack to run the analog-to-digital converter and the peristaltic pump and can be operated for up to three hours before recharging was required. The system described in this work weighs 2.1 kg. The use of a notebook computer allows for real time plotting of data at remote locations away from conventional laboratories.

There have been numerous FIP systems reported in previous studies that have employed single ISEs [1-3] and multiple ISE array systems [4-12] that are suitable for various applications. However, none of these FIP systems have been incorporated into a portable system that is suitable for FIP measurements outside the laboratory away from mains power supply.

Initially, the electronic design performance was tested with a single Orion iodide ISE as an example of a commercial ISE in the FIP mode. Secondly, a tungsten / tungsten oxide pH electrode was used with the same FIP system. The electrode response observed for the iodide ISE in the FIP mode exhibited near-Nernstian response of -53.8 mV change / activity decade to super-Nernstian response of -67.8 mV change/ activity decade, depending on the carrier and ionic background employed. The optimum log-linear range observed in the FIP mode was between 0.005 mM and 10 mM. The FIP response observed for the iodide ISE represents 80% of the steady-state value and the performance exhibited would be analytically useful for remote-site monitoring.

The tungsten / tungsten oxide coated wire electrode was applied to the portable FIP system as an example of a miniaturised pH electrode. The pH electrode exhibited a sub-Nernstian response of 44.8 ± 0.5 mV change per pH unit over a pH range between 2.2 and 11.0 in the steady-state mode. It was shown that the presence of dissolved oxygen in the universal pH buffer solutions was the reason for the sub-Nernstian response of the tungsten oxide electrode. The electrode exhibited a fast response with 5 seconds peak widths and the FIP response represented 95% of the steady-state value.

The tungsten / tungsten oxide coated wire electrode is robust, easily miniaturised and is a low cost alternative to the glass or liquid polymer membrane based electrodes in common use today. However, for accurate pH measurements in the FIP mode, it was important to account for interferences from other cations (eg. sodium ions) and reducing agents (eg. ascorbic acid) present in the sample of interest.

The possibilities of multi-ion determinations in a portable FIP system were demonstrated using a nitrate, potassium and sodium ISE array. The three ion sensors selected were chosen because of easy commercial availability in the planar design and because of the relatively low cost compared to other commercially available ISEs. The array system was used successfully to determine nitrate, sodium and potassium levels simultaneously in natural mineral water samples, to simulate environmental water analysis at remote-site locations. Optimisation of experimental conditions was required to select the best carrier composition and an appropriate background for the mixed nitrate, sodium and potassium standards in order to minimise the response to interfering ions on the ISEs employed for the FIP measurements at remote-site locations. One of the main problems in an array of ISEs in FIP mode is finding a suitable carrier composition that will have a negligible interference on the ISE array. The use of selective ISEs in the FIP array allows the operator to conduct rapid simultaneous determinations of nitrate, sodium and potassium in aqueous samples, employing a low cost data acquisition system. Furthermore, the ISE array can be operated in a totally portable manner in the FIP mode, whereby fast and precise data can be obtained in a short time span suitable for remote-site monitoring.

The eight-electrode flow cell used in the portable FIP system provides peak heights of high precision and reproducible electrode slopes for the response to silver and, to a certain extent, iodide ions. The optimum injection volume determined for this eight-electrode flow cell was 200 μL. The possibility of either applying eight different sensors or employing the cells-in-series approach makes this portable FIP system a highly attractive analytical instrument for remote site monitoring, and work then was developed for multi-ion arrays based on photo-cured liquid polymer membranes.

There are numerous applications that could be utilised with the multi-sensor flow cell used in the portable flow injection system for remote site monitoring. The design of the analog-

to-digital converter employed in this portable system should allow for liquid polymer membranes selective to different analytes to be applied to each silver substrate. Hence, high resistance electrodes with liquid membranes > 10 MΩ could be used in the flow injection mode. However, the main obstacle to be overcome with this approach was the choice of the carrier solution to be used for FIP measurements, such that the sensitivity and selectivity of the liquid membrane based sensors is not affected.

Photo-cured bisphenol A epoxydiacrylate based membranes were investigated and these membranes exhibited excellent adhesion to the silver substrate making them reliable in flow-through systems. The photo-cured ammonium, hydrogen (pH1), potassium (K2) and nitrate CWEs exhibited reliable response to their respective determinand in the steady-state and FIP modes, each using one of the eight silver electrodes in the multi-electrode flow cell as described previously. The selectivity exhibited by each of these CWEs suggests that these photo-cured CWEs could be applied to a multi-sensor array that would not require any mathematical corrections. The reliability of these CWEs in the FIP mode was demonstrated by the analysis of various water samples for their respective determinand, giving good agreement with comparative analytical methods. Lithium acetate carrier solutions were employed for each of the above-mentioned CWEs in the FIP mode, and will be the obvious choice as a carrier when employing these CWEs in a multi-sensor arrangement.

This study further demonstrated the reliability of photo-cured epoxydiacrylate membrane based CWEs used in a multi-electrode system for FIP measurements. The main advantages of photo-cured epoxydiacrylate membranes include an increased mechanical strength, improved adhesion to metal substrates and faster manufacturing time (< 5 minutes) compared to the traditional PVC membranes (2 days), making photo-cured membranes more suitable for flow-through systems.

Three multi-CWE arrangements presented in Chapter six, namely the ammonium - hydrogen (pH1) CWE array, the calcium (Ca5) - chloride - nitrate - potassium (K2) CWE array, and the ammonium - Ca5 - chloride -pH1 - nitrate - K2 CWE array. Each performed reliably in the FIP mode and accurate analyses of various environmental and drinking water samples was demonstrated. The FIP results obtained with the multi-CWE arrangements were in good agreement with comparative analytical methods. The ideal carrier and ionic

background for all three multi-CWE arrangements was found to be 3 mM lithium acetate. In the case where the pH1 CWE was employed in a multi-electrode array system, the pH of the carrier required to be close to the pH 7.0 to minimise the dispersion of the injected sample zone.

The FIP response observed for each photo-cured CWE used in each of the three multi-CWE arrangements represented up to 85% of the steady-state value, making each of the CWE array systems analytically useful. In each of the multi-CWE arrangements presented in this work, the lithium acetate carrier contained a small amount of the determinand ion (usually 0.0005 mM) in order to automatically condition the CWEs as well as maintaining a stable baseline. Consequently, improved response of the photo-cured based CWEs was achieved.

The excellent selectivity demonstrated by each of the photo-cured CWEs eliminated the need for chemometric type corrections to be applied to each of the multi-CWE arrangements which was an additional advantage of the described FIP system. Therefore, the multi-CWE arrangements used in the portable FIP system described in this work could practically be applied to field measurements at remote locations. An operator would simply need to calibrate the portable FIP system with standard solutions and then test samples on site and store the acquired data on the notebook computer, and then move onto the next site and repeat the procedure. The advantage of the data acquisition program used in this work is that it can display each electrode potential from a given CWE array simultaneously on the notebook's screen and therefore an operator can also monitor the performance of each CWE employed in the field as a diagnostic tool.

7.1 References

1. M. Valcárcel and M. D. Luque De Castro, 'Flow Injection Analysis. Principles and Applications', ed. S. J. Lyle and R. A. Chalmers, Ellis Horwood Ltd., New York, (1987).

2. M. Valcárcel and M. D. Luque De Castro, 'Flow-Through (Bio)Chemical Sensors', Elsevier, Amsterdam, (1994).

3. J. Ruzicka and E. H. Hansen, 'Flow Injection Analysis', 2nd ed., John Wiley and Sons, New York, (1987).

4. A. U. Ramsing, J. Janata, J. Ruzicka and M. Levy, 'Miniaturization in analytical chemistry - A combination of flow injection analysis and ion-selective field effect transistors for determination of pH, and potassium and calcium Ions', Analytica Chimica Acta, **118**, 45 - 52, (1980).

5. A. Sibbald, P. D. Whalley and A. K. Covington, 'A miniature flow-through cell with four-function chemFET integrated circuit for simultaneous measurements of potassium, hydrogen, calcium and sodium ions', Analytica Chimica Acta, **159**, 47 - 62, (1984).

6. J. F. Van Staden, 'Electrodes in series. Simultaneous flow injection determination of chloride and pH with ion-selective electrodes', Analyst, **111**, 1231 - 1234, (1986).

7. T. J. Cardwell, R. W. Cattrall, P. C. Hauser and I. C. Hamilton, 'A multi-ion sensor cell and data-acquisition system for flow injection analysis', Analytica Chimica Acta, **214**, 359 - 366, (1988).

8. K. Cammann, 'Flow injection analysis with electrochemical detection', Fresenius Journal of Analytical Chemistry, **329**, 691 - 697, (1988).

9. B. H. Van Der Schoot, H. H. Van Den Vlekkert, N. F. De Rooij, A. Van Den Berg and A. Grisel, 'A flow injection analysis system with glass-bonded ISFETs for the simultaneous detection of calcium and potassium ions and pH', Sensors and Actuators, **B4**, 239 - 241, (1991).

10. R. J. Forster and D. Diamond, 'Nonlinear calibration of ion-selective electrode arrays for flow injection analysis', Analytical Chemistry, **64**, 1721 - 1728, (1992).

11. F. J. Sáez de Viteri and D. Diamond, 'Determination and application of ion-selective electrode model parameters using flow injection and simplex optimization', Analyst, **119**, 749 - 758, (1994).

12. F. J. Sáez de Viteri and D. Diamond, 'Ammonium detection using an ion-selective electrode array in flow-injection analysis', Electroanalysis, **6**, 9 - 16, (1994).

Appendix 1

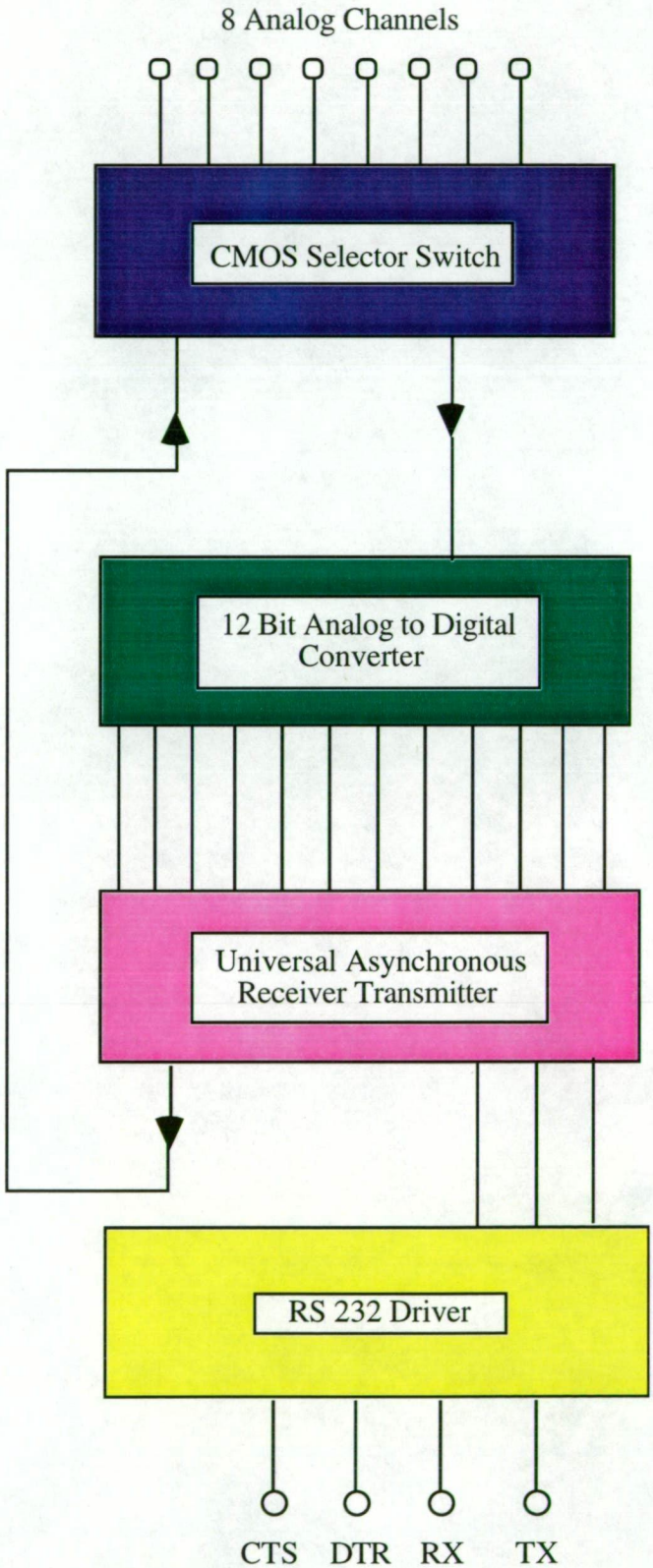
8 Analog Channels
CMOS Selector Switch
12 Bit Analog to Digital Converter
Universal Asynchronous Receiver Transmitter
RS 232 Driver
CTS
DTR
RX
TX

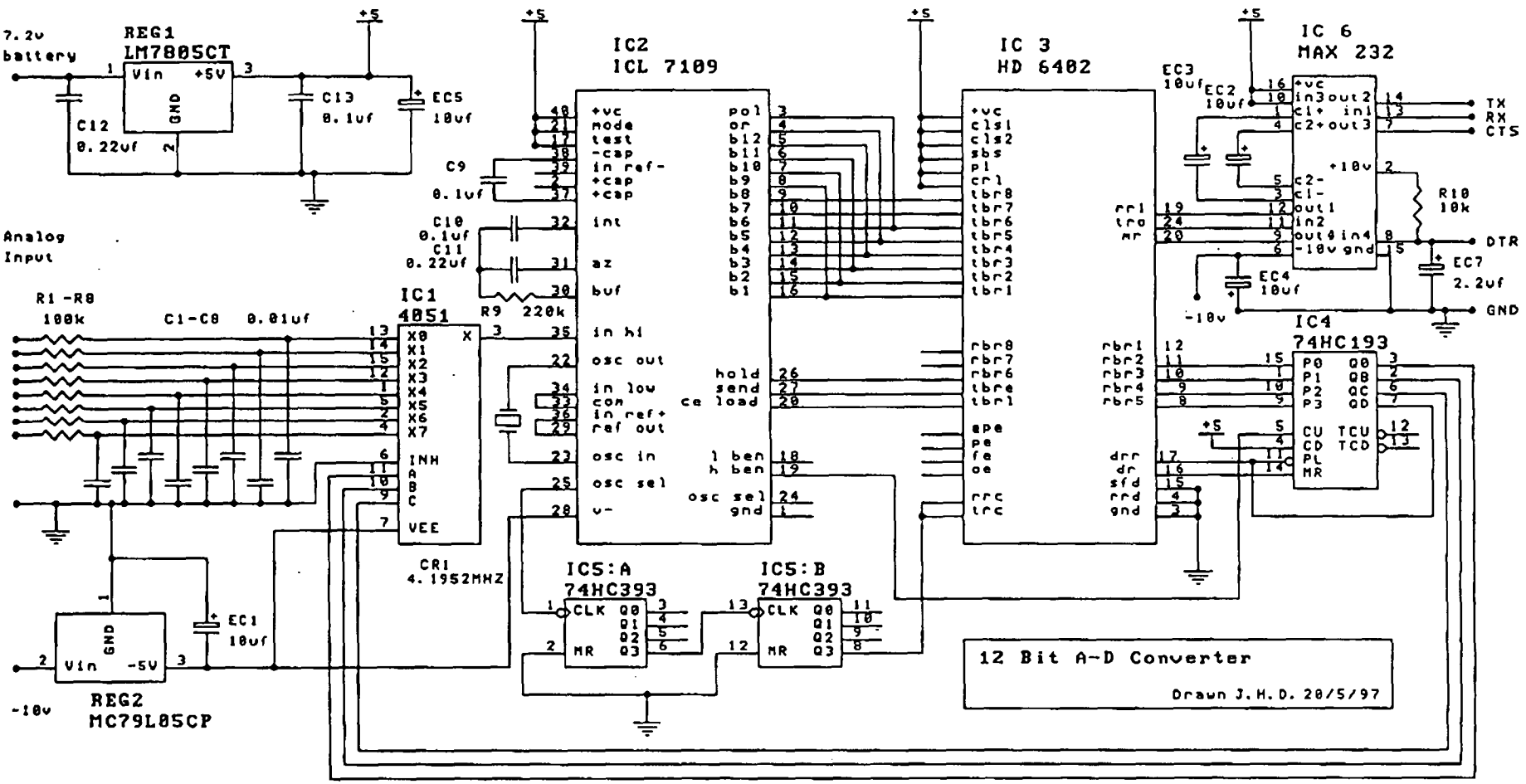
7.2v
battery
REG1
LM7805CT
Vin
+5V
GND
C12
0.22uf
C13
0.1uf
EC5
10uf
+5
IC2
ICL 7109
C9
0.1uf
C10
0.1uf
C11
0.22uf
R9 220k
Analog
Input
R1 -R8
100k
C1-C8 0.01uf
IC1
4051
X0
X1
X2
X3
X4
X5
X6
X7
INH
A
B
C
VEE
CR1
4.1952MHZ
IC 3
HD 6402
IC 6
MAX 232
EC3
10uf
EC2
10uf
+10v
-10v
R10
10k
EC7
2.2uf
EC4
10uf
TX
RX
CTS
DTR
GND
IC4
74HC193
IC5:A
74HC393
IC5:B
74HC393
EC1
10uf
REG2
MC79L05CP
12 Bit A-D Converter
Drawn J.H.D. 20/5/97